

**Groundwater movement in heterogeneous, water-limited, low-relief
landscapes: understanding interactions of geology, topography, and
climate at multiple spatiotemporal scales**

by

Kelly J Hokanson

A thesis submitted in partial fulfillment of the requirements for the degree of

DOCTOR OF PHILOSOPHY

Department of Earth and Atmospheric Sciences

University of Alberta

© Kelly J Hokanson, 2021

Abstract

The low-relief, sub-humid Boreal Plains (BP) region of Canada, is characterized by pond-peatland-forestland complexes underlain by thick glacial deposits, which result in inter-dependent surface water processes and groundwater flow systems with varying spatiotemporal controls. A fundamental framework of climate, geology, and topography was used to better understand and explain the spatiotemporal variability in hydrologic responses and shallow groundwater flow systems in the BP. A 20 year historic hydrometric dataset (e.g., hydraulic head, vertical hydraulic gradients, geochemical signatures, stable water isotope ratios, and climatological data) collected from a pre-existing network of over 850 shallow and deep monitoring wells was supplemented with contemporary measurements and wells. Two primary spatiotemporal scales were examined to create a holistic, variable-scale conceptual model of groundwater movement in the BP: the large scale (e.g., glacial landforms, regional topography, and decadal climate cycles), and the small scale (e.g., individual landcovers, local hummocks, and annual moisture deficits).

At the large spatial scale (i.e., 100 km²) the landscape was delineated into hydrologic response areas (HRAs) based on geologic substrate characteristics (i.e., texture and geologic origin): coarse glaciofluvial outwash, fine-textured hummocky moraine, and clay-till plain. It was found that in the coarse outwash HRA and the hummocky moraine HRA, water tables were recharge (i.e., precipitation) controlled, while in the clay-till plain HRA they are topography controlled. Moreover, groundwater flow (and the controls thereon) is considered “intermediate” in the clay-till plain and “local” in the hummocky moraine; however, the coarse outwash contains multiple scales of flow and is influenced by adjacent HRAs and larger-scale flow systems.

These larger-scale flow systems as well as surface water-groundwater interactions were further explored in the coarse outwash by examining the variability of the relative contributions of groundwater to eleven different lakes. It was demonstrated through the use of isotope hydrology, that landscape position is the dominant control over groundwater contributions to lakes; however, surface water connections were also significant and can short circuit groundwater pathways and confound the isotopic signal. Lakes at low landscape positions with large potential groundwater capture areas had relatively higher and more consistent groundwater contributions and low interannual variability thereon. Isolated lakes high in the

landscape experienced high interannual variability as they have little to no groundwater input to buffer the volumetric or isotopic changes due to evaporation and precipitation.

At the small or local spatial scale, both empirical and numerical modelling approaches were taken. The hydraulic gradients between forested hummocks and adjacent peatlands at sixteen locations, which represent a spectrum of hummock and peatland morphometries, topographic positions, and geologic settings, were monitored over the course of a mesic (non-drought) year. The dominant gradient was found to be from the peatland to the forestland (opposite that of the topographic gradient). Water table depressions under each forested hummock indicate that boreal forestlands are not reliable sources of groundwater recharge, spatially or temporally, which supports previous regional-scale research showing that peatlands are the primary water source for landscape-scale runoff.

Variably saturated numerical modelling was undertaken to better understand the source-sink relationship between forested hummocks and adjacent peatlands and the controls on water table dynamics and groundwater recharge at the hummock scale. Hydraulic conductivity played the largest role in determining groundwater recharge rates. It was shown that the sink or source function of a forested hummock is dependent more on hydrogeologic and morphometric controls than climatic variability, where taller and narrower hummocks served as sources of groundwater and longer flatter hummocks served as sinks.

Glacial depositional landscapes, such as the BP, are highly complex regions with spatially heterogeneous storage and transmission properties and temporally variable recharge potentials, resulting from the delicate, and often tipped, balance between precipitation and evapotranspiration. These studies demonstrate that in regions such as this, smaller-scale heterogeneities in geology and recharge can be a dominant factor over topography, notably in areas with high conductivity or hummocky terrain. Understanding the natural spatial and temporal variability of, and controls on, water table position, groundwater movement, and groundwater recharge under varying physical and climatic scenarios is important, as water security, ecosystem sustainability, and environmental quality become the focus of land management and reclamation efforts.

Preface

K.J. Hokanson was the lead author and investigator, responsible for all major areas of concept formation, analysis, and manuscript composition for all chapters. Data collection was completed under the Hydrology Ecology and Disturbance projects lead by K. Devito and C. Mendoza from 1998 to 2017, and was supplemented for the purposes of this research by K.J. Hokanson. Versions of Chapters 2 and 4 have been published. Versions of Chapters 3 and 5 have been submitted to journals. Co-authors for each publication provided intellectual supervision and editorial comment, unless otherwise stated.

A version of Chapter 2 has been published as: Hokanson K.J., Mendoza C.A., Devito K.J. Interactions between regional climate, surficial geology, and topography: Characterizing shallow groundwater systems in subhumid, low-relief landscapes. *Water Resources Research*. 2019; 55(1):284-97. An early version was also published in conference proceedings as: Hokanson K.J., Mendoza C.A., Devito K.J. 2018. Shallow groundwater systems in sub-humid, low-relief Boreal Plain landscapes: Interactions between glacial landforms, climate and topography. *Proceedings, GeoEdmonton, 71st Canadian Geotechnical and 13th Joint CGS/IAH-CNC Groundwater Conference, Edmonton, September*. Paper 511. 8p.

A version of Chapter 3 has been accepted to *Hydrogeology Journal* as: Hokanson K.J., Rostron B.J., Devito K.J., Hopkinson C., Mendoza C.A. 2021. Landscape controls of surface-water/groundwater interactions on shallow outwash lakes: how long-term groundwater signal overrides interannual variability due to evaporative effects. C Hopkinson processed and provided DEM data.

A version of Chapter 4 has been published as: Hokanson K.J., Peterson E.S., Devito K.J., Mendoza C.A. Forestland-peatland hydrologic connectivity in water-limited environments: hydraulic gradients often oppose topography. *Environmental Research Letters*. 2020; 15 034021. E.S. Peterson provided field assistance and data management.

A version of Chapter 5 has been published as: Hokanson K.J., Thompson C., Devito K., Mendoza C.A. Hummock-scale controls on groundwater recharge rates and the potential for developing local groundwater flow systems in water-limited environments. *Journal of Hydrology*. 2021; 29 126894. C. Thompson provided editorial and methodological assistance.

Acknowledgements

I would like to thank my supervisors, Dr. Carl Mendoza, Dr. Kevin Devito, and Dr. Daniel Alessi for their tireless support. Thank you, Carl, for taking me on as a student, despite the distance. I've learned so much under your direction and am extremely appreciative of your expertise and encouragement to follow my intellectual interests and become a more independent hydrogeologist. Through your mentorship I've grown significantly, both as a scientist and as a professional, and for that I am grateful and forever indebted. Thank you, Kevin, for always pushing the boundaries of what I thought was possible and constantly reminding me to think beyond my immediate scientific circumstances. I am profoundly grateful for both the academic and personal mentorship you've offered me for many years.

This work was funded through a variety of sources, including: Natural Sciences and Engineering Research Council (NSERC) Collaborative Research and Development (CRD) grant with industry partners Syncrude Canada and Canadian Natural Resources (Awarded to Devito and Mendoza); the forWater research network, a pan-Canadian strategic research network; an NSERC postgraduate doctoral scholarship; Queen Elizabeth II Doctoral Scholarship; the Ian McLaren Cook Sr. Graduate Scholarship in Geology from the University of Alberta; Institute of Geophysical Research Roy Dean Hibbs Memorial Graduate Scholarship; Scholarship for Graduate Studies in Hydrogeology from the Canadian National Chapter of the International Association of Hydrogeologists; University of Alberta Northern Research Grant; and the Canadian Meteorological and Oceanographic Society – Weather Research House Doctoral Scholarship.

Thanks to the members and colleagues of the various research groups and projects I've had the pleasure of taking part in. Your assistance in the field and in the lab was instrumental. A special thanks to my fellow PhD student Emily, always ready to listen about my recent misadventures and to share her own.

My love and thanks to my friends and family, both back home in Virginia and here in Canada; you've provided me unwavering support during this long and arduous process (and graciously allowed me to rant about inane and esoteric topics with a smile on your faces). And finally, to my parents, Terry and Neil, and my partner Peter, you've provided unending patience, motivation, stability, and love, without which I wouldn't be where I am today.

Table of Contents

Abstract	ii
Preface	iv
Acknowledgements	v
Table of Contents	vi
List of Tables	x
List of Figures	xi
Chapter 1: Introduction	1
1.1 Background	1
1.2 Thesis objective and format	3
Chapter 2: Interactions between regional climate, surficial geology, and topography: Characterizing shallow groundwater systems in sub-humid, low-relief landscapes	5
2.1 Introduction	5
2.2 Methods	7
2.2.1 Study Site	7
2.2.2 Precipitation.....	7
2.2.3 Hydrological Response Area (HRA) Delineation	8
2.2.4 Hydrogeology	8
2.2.5 Geochemical and Isotopic Compositions:	9
2.3 Results	9
2.3.1 Precipitation.....	9
2.3.2 HRAs and HRA Physical Properties	9
2.3.3 Hydrogeology	10
2.3.4 Long-term Water Levels.....	11
2.3.5 Chemoscapes and Isoscapes	11
2.4 Discussion	12
2.4.1 The Concept of HRAs.....	12
2.4.2 Topography vs. Recharge Controlled Water Tables.....	13
2.4.3 Groundwater-Surface Water Interactions	14
2.4.4 Annual and Interannual Variability	15
2.4.5 Chemoscapes and Isoscapes as Management Tools	15
2.5 Conclusions	16

Chapter 3: Landscape controls on surface water-groundwater interactions on shallow outwash lakes: Long-term groundwater signal overrides interannual variability due to evaporative effects	29
3.1 Introduction	29
3.2 Methods	31
3.2.1 Study Area and Hydrogeology	31
3.2.2 Stable O and H isotope ratios in water	33
3.3 Results and Discussion	34
3.3.1 Groundwater slow systems	34
3.3.2 Long-term isotopic compositions of URSA lakes and groundwater	35
3.3.3 Ic-excess of study lakes	36
3.3.4 Possible effects of lake morphometry on Ic-excess	38
3.3.5 Competing roles for groundwater and surface water	38
3.3.6 Hydrogeological case study: Lakes 17, 16, 5	39
3.4 Conclusions	40
Chapter 4: Forestland-peatland hydrologic connectivity in water-limited environments: hydraulic gradients often oppose topography.....	49
4.1 Introduction	49
4.2 Study Site and Methods.....	51
4.3 Results	53
4.4 Discussion	54
4.5 Conclusions.....	56
Chapter 5: Hummock-scale controls on groundwater recharge rates and the potential for developing local groundwater flow systems in water-limited environments.....	62
5.1 Introduction	62
5.2 Study Area	63
5.2.1 Motivation	63
5.2.2 Study hummock site and field measurements	64
5.3 Numerical Modelling and Statistical Methods	65
5.3.1 General approach	65
5.3.2 Transient variably-saturated model	66
5.3.2.1 Model domain and material properties	66
5.3.2.2 Boundary and initial conditions	67
5.3.3 Scenario testing	68
5.3.3.1 Hummock regimes	68

5.3.3.2	Sink-source dynamics.....	69
5.3.3.3	Relative controls on groundwater recharge.....	69
5.4	Results and Discussion.....	70
5.4.1	Model performance.....	70
5.4.1.1	Comparing observed and simulated water table elevations	70
5.4.1.2	Sensitivity analysis.....	70
5.4.2	Hummock water balance	71
5.4.2.1	Water table elevations and peatland-forestland fluxes	71
5.4.2.2	Groundwater recharge.....	72
5.4.3	Scenario testing: water table elevation and groundwater recharge	73
5.4.3.1	Effects of hydraulic conductivity	74
5.4.3.2	Effects of hummock morphometry	74
5.4.3.3	Effects of climate	76
5.4.4	Sink-source function of hummocks: a conductivity paradox	76
5.4.5	Controls on groundwater recharge.....	77
5.5	Summary and Conclusions	78
Chapter 6: Conclusion: Variable-scale conceptual framework for shallow groundwater systems in the Boreal Plains with complementary proof-of-principle groundwater flow models.....		
		91
6.1	Introduction	91
6.2	Conceptual framework.....	92
6.2.1	Background: Study area geology and climate	93
6.2.2	Space	93
6.2.2.1	Wetlands.....	93
6.2.2.2	Forestlands.....	94
6.2.2.3	Wetland-forestland interactions.....	95
6.2.2.4	Hydrological Response Areas: Physiography and dominant controls.....	96
6.2.3	Time	98
6.2.3.1	Seasonal/Annual.....	98
6.2.3.2	Interannual variability and decadal wet-dry cycles	99
6.3	Proof-of-principle 3D groundwater flow models	100
6.3.1	Model implementation and scenarios.....	100
6.3.2	Model scenarios	101
6.4	Model Results and Discussion.....	101
6.4.1	Hummock water table elevations	101
6.4.2	Evapotranspiration and runoff.....	102

6.4.3 The way forward	103
6.5 Conclusions.....	104
References.....	115
Appendix A	134
Appendix B	137
Appendix C	140

List of Tables

Table 2-1. Topographic characteristics for each hydrologic response area (HRA) at URSA.....	17
Table 3-1: Lake Characteristics.....	42
Table 3-2: Historic Water Budgets for Lake 16.....	47
Table 4-1: Site Characteristics	57
Table 5-1: Calibrated material properties	81
Table 6-1: Material parameters	109
Table A-1: Regression coefficients (R^2) for linear correlations between the shallowest annual WT for each study well vs. climatic indices. Green cells indicate the highest R^2 value for that site.....	136
Table B-1: van Genuchten-Mualem soil hydraulic properties for 1D model.....	138

List of Figures

- Figure 2-1: The (a) surficial geology and (b) ground elevation of the Utikuma Region Study Area (URSA; ~103 km²), and its relative location within (c) Canada and the Boreal Plains ecozone (Marshall et al., 1999), with well locations, and delineated HRAs: Coarse outwash (CO), hummocky moraine (HM), and clay plain (CP). 18
- Figure 2-2: Annual precipitation data and three-year cumulative departure from the mean P (CDM-3) for URSA, before and during the study period. Long-term average annual P (444 mm; 1987-2015) and PET are shown for context. Pre-1998 data were obtained from Alberta Agriculture and Forestry (2018). 19
- Figure 2-3: Generalized geologic cross section along transect A – A' (Figure 2-1), showing the HRA boundaries (dashed lines) and well locations (black numbers indicate sites on the cross section; grey numbers indicate sites off the cross section). Vertical lines represent boreholes. Boreholes that intersect the bedrock (in grey) were collected by the Alberta Research Council, who did not differentiate between materials outside of sand units (Ceroici, 1978; Vogwill, R. 1978). Shallow boreholes (in black), that intersect the surface, were collected as part of this study. 20
- Figure 2-4: Hydraulic conductivity distributions by depth for each HRA. On each box, the central horizontal line indicates the median, the bottom and top edges of the box indicate the 25th and 75th percentiles, respectively; whiskers show the most extreme data not considered outliers (individual black dots). 21
- Figure 2-5: Vertical hydraulic gradients (i_v) along the transect A-A' (Figure 1) for the driest (2003) and wettest (2013) years during the study period. Positive values indicate an upward, discharge gradient. A generalized cross section is shown for context. 22
- Figure 2-6: Time series for water table depth at each site. Blue and red zones indicate representative wet (2013) and dry (2003) years, respectively. Black symbols represent sites on the cross section (Figure 3); grey symbols represent sites off the cross section. Each legend is organized by elevation of site (lowest to highest). Lines connecting data points are shown for visual purposes only and do not infer known data. Dry well data are not shown. 23
- Figure 2-7: Long-term water table elevations measured at wells throughout the study period. Circles and bars denote median and historic range of water table elevation, respectively, at each site. 24
- Figure 2-8: Boxplots of concentrations of major cations and anions in groundwater samples spanning the study period. See Figure 4 for an explanation of the boxplot characteristics. 25
- Figure 2-9: Dual isotope plot of groundwater and surface water samples spanning the study period. The URSA LMWL (dashed line) and URSA LEL (solid line) are shown for context. Size of data points vary for visual purposes only. Dashed regions indicate delineated isoscapes. 26
- Figure 2-10: The line-conditioned (l_c) excess of surface and groundwater stable isotope samples taken at URSA over the study period, with HRA boundaries shown as dashed lines. For sites and ponds not directly on A-A', distances were interpolated. An l_c -excess value close to zero indicates little difference between samples and local P; whereas more negative values indicate higher degrees of

fractionation (evaporation). Not all sites were sampled during both the dry (2003) and wet (2013) year.....	27
Figure 2-11: Basin-scale profile showing (a) ground-surface elevation and (b) depth to bedrock from (c) the Rocky Mountains to the Canadian Shield. URSA is located near the middle of a basinal flow system in an area of low relief with thick unconsolidated substrates.	28
Figure 3-1: Ground elevation of the Utikuma Region Study Area (URSA; main panel) and its relative location within Canada, North America, and the Boreal Plains (BP) ecozone (inset; Marshall et al., 1999), with study lake locations and elevations, delineated potential groundwater capture areas and surficial geology type (Fenton et al., 2013). Bold lines indicate limits of separate flow systems (i.e., the potential groundwater capture area for the lowest lake in that system); finer lines indicate potential groundwater capture area for the lakes positioned higher in each system.	41
Figure 3-2: (a) Dual isotope plot of Utikuma Region Study Area (URSA) precipitation and lake waters with (inset) annual local evaporation lines (LEL) from 1999-2019; (b) dual isotope plot of URSA groundwater sampled from 1999-2019 and (c) a generalized geologic cross-section along transect A-A' (Figure 1) with groundwater $\delta^{18}O$ -excess (sampled from 2000 to 2019) values shown above. Each set of box and whiskers represents one groundwater well or a cluster of wells. The cross section shows the lake and well locations that lie on the transect (black numbers indicate lake ID on the cross section; gray numbers indicate lakes off the cross section). Vertical lines represent boreholes; see Hokanson et al. (2019) for more details.	43
Figure 3-3: Box plot of summer lake $\delta^{18}O$ -excess values. Flow systems are separated by solid black lines and are ordered by landscape position. Winter 2020 samples are shown as well, where each circle represents a single water sample and are not considered in the boxplots.	44
Figure 3-4: Time series of July lake $\delta^{18}O$ -excess in context of cumulative precipitation. Daily precipitation is summed over the year prior to the lake sampling date.	45
Figure 3-5: Relationships between median July $\delta^{18}O$ -excess and (a) groundwater contributing area and (b, c) lake morphometry (area and depth). Lakes considered isolated are not included due to the wide range of summer $\delta^{18}O$ -excess values. Groundwater contributing area only considers coarse surficial geology (Table 1). Marker size is proportionate to lake volume (a) and lake area (b). Lake volume is approximated by multiplying lake area by average depth.	46
Figure 3-6: Lakes 17, 16, and 5 study area with ground surface topography and selected field instrumentation (left; Adapted from Smerdon et al., 2008). Water table contours and groundwater flow direction shown for July 2002. Location of Utikuma Region Study Area and Boreal Plains region in Alberta, Canada, shown on inset. July stable water isotope values for Lakes 17, 16, and 5 for each year of the study period (right) are show in dual isotope space with the LMWL (dashed line) and long-term LEL (solid line) for reference. The further along the LEL (i.e., offset from the LEL-LMWL intersection) the data point lies, the more negative the corresponding $\delta^{18}O$ -excess value. ...	48
Figure 4-1: Annual precipitation (P) data and 3-year cumulative departure from the mean precipitation (CDM-3) for Utikuma Region Study Area (URSA), before and during the study period (left). Long-	

term average annual P (444 mm) and potential evapotranspiration (PET; 517 mm) are shown for context. Daily and cumulative precipitation at URSA for the 2018 hydrologic year (right) 58

Figure 4-2: Topographic profiles of each peatland-forestland pair grouped by hydrologic response area. Vertical exaggeration for all profiles = 20X. Water levels between each well pair are indicated with a line to demonstrate the direction of the gradient but do not infer the location of the water table between wells. For sites where the hummock well was dry (denoted by *), water level is drawn at the bottom of the hummock well. A schematic is shown in the legend to illustrate hummock height (H) and length (L) and water table elevation difference (Δh). CO=coarse outwash; CO-P=perched over coarse; HM=hummocky moraine; CP=clay-till plain; WL = water level..... 59

Figure 4-3: Empirical cumulative distribution functions of the depth to water table (WT) at each well, where ground surface is represented by zero. Wells that were dry are represented by dashed lines, which show the location of the bottom of the screened interval. 60

Figure 4-4: Peatland and forested hummock water table elevations for each site. The dashed line shows the 1:1 relationship, where points to the left of the line show a gradient towards the forested hummock and points to the right of the line show gradients towards the peatland. For sites where the hummock well was dry, a time series of the peatland water table is presented and the bottom of the hummock well is shown for reference. All elevations are relative to 600 m asl. All elevation axes have equivalent scales. 61

Figure 5-1: (a) The location of the Utikuma Region Study Area (URSA) in the Boreal Plains ecoregion (grey); (b) Map showing the study area with transect A-A', well locations, and vegetative and surface water, and relative topographic elevation; (c) The model domain for the study hummock, along transect A-A', showing the hydrogeologic units, observation wells, historic maximum and minimum observed water tables, and boundary conditions. 80

Figure 5-2: Hummock morphometry scenarios A-I. The original study hummock topography is shown in grey for reference, thus Scenario E most closely resembles the study hummock. 82

Figure 5-3: Simulated and observed water table elevations at observation wells WA, WB, and WC for the study hummock over time. Grey circles represent water table observations from an unequilibrated well and were not used in the calibration process. 83

Figure 5-4: Time series (a) of 1 year, 2 year, and 3 year cumulative departures from the long-term mean annual precipitation (CDM), and (b) total precipitation, snowmelt, and recharge at well WA in the study hummock. 84

Figure 5-5: A detailed water balance of the modelled study hummock. (a) cumulative annual recharge at WA, WB, and WC, where negative recharge values represent upflux; (b) cumulative annual fluxes

for the model relative to the surface area of the hummock, where negative values are fluxes out of hummock. Evaporation is composed of interception of rainfall and sublimation of snowfall. 85

Figure 5-6: (a) Storage state at the end of the hydrologic year for the study hummock, and (b) the relationship between annual groundwater recharge at WA for a given hydrologic year compared with the storage state at the end of the previous hydrologic year. 86

Figure 5-7: Water table elevations at WA, WB, and WC in the study hummock. (a) An empirical cumulative distribution function of water table elevations for the entire simulation with (a-inset) corresponding water table configurations within the hummock; (b) a time series of water table elevations and weekly flux from the peatland, where a positive value represents flow from the peatland to the forested hummock, and a negative value represents flow from the forested hummock to the peatland. 87

Figure 5-8: Simulated water table elevations at the top of the slope for the 27 different hummock regimes shown as (left) empirical cumulative distribution functions, and (right) time series. The shapes of each hummock morphometry scenario A to I can be seen in Figure 5-2. The base K, high K, and low K scenarios are shown in grey, green, and red, respectively. The timing and elevation of perched water tables are shown with asterisks in the corresponding K-scenario color. The elevations of the peatland and the ground surface at the top of the hummock are shown for reference in each plot. 88

Figure 5-9: Annual simulated groundwater recharge and hydrologic function of each hummock regime. The shapes of each hummock morphometry scenario A-I can be seen in Figure 5-3. Violin plots show the distributions of annual groundwater recharge values at the top of the hummock for each scenario from 1930 to 2018. The boxplots which overlay them show the distributions of the ratio of annual groundwater recharge and annual available precipitation (precipitation (P) minus evaporation (E)). No overlaps between boxplot notches indicate significant differences at a 95% confidence interval. The base K, high K, and low K scenarios are shown in grey, green, and red, respectively. The long-term hydrologic function of each hummock regime is also indicated by an arrow, where an 'up arrow' indicates that the hummock was a long-term source of water to the adjacent peatland, a 'down arrow' indicates that the hummock was a long-term sink of water to the adjacent peatland, and a 'up arrow/down arrow' pair indicates that the hummock was either a weak sink or weak source or fluctuated between being a sink and source through time. 89

Figure 5-10: Results from the boosted regression tree (BRT) model: (a) Comparison of the annual recharge (as modelled in Hydrus simulations) from all 2D models and annual recharge values predicted by the BRT, and (b) the estimated importance of each predictor variable in predicting annual recharge. All climatic predictor variables are for the hydrologic year. PET = potential evapotranspiration; P = precipitation; K = saturated hydraulic conductivity of upper till. 90

Figure 6-1: Conceptual framework presented in Section 6.2 for various landforms and textures in each of the three main HRAs. Relative AET and lateral GW fluxes are shown with red and black arrows,

respectively. Ranges in water table fluctuations for each land unit are shown with double-sided arrows that are to scale with the vertical axis (metres) on each panel.	105
Figure 6-2: The monthly distribution of P and PET from 1920 to 2020, where the error bars represent standard deviations (upper), and an annual time series of major atmospheric fluxes (lower). CDM-1 and CDM-3 are the one and three year cumulative departure from the long-term mean precipitation, respectively. Sources of precipitation and temperature (used to calculate PET (Hamon, 1963)) data are outlined in Section 5.2.2).....	106
Figure 6-3: Relationships between inputs (rectangles and circles), outputs (bold), and models (diamonds) using MODFLOW with the UZF package. Inset shows a schematic diagram showing the relationship between the one-dimensional saturated-zone flow model (UZF) and saturated flow (MODFLOW) domains (adapted from Niswonger et al., 2006).....	107
Figure 6-4: The three topological scenarios implemented in MODFLOW. (A) many small forested hummocks divided by small peatlands, (B) few large forested hummocks divided by small peatlands, and (C) few large forested hummocks divided by large peatlands. Each scenario is realized with hummocks heights 3 and 11 m above the peatlands. The cross sections have a vertical exaggeration of 30x.....	108
Figure 6-5: Modelled heads observed at the monitoring wells shown in Figure 6-6 for the 24 simulations. The 3 m and 11 m high hummocks are shown by dashed and solid lines, respectively. The color coding (orange, blue, and black) corresponds to the different topological scenarios presented in Figure 6-4.....	110
Figure 6-6: Time series of modelled AET (composed of groundwater ET, vadose zone ET, rejected recharge, interception, and sublimation) for the 24 simulations (left), and time series of outflow from the drains (right). Both fluxes are normalized for the areal extent of the model domains. The 3 m and 11 m high hummocks are shown by dashed and solid lines, respectively. The color coding (orange, blue, and black) corresponds to the different topological scenarios presented in Figure 6-4.....	111
Figure 6-7: The cumulative outflow through the drains for the duration of each simulation. The cumulative fluxes are color –coded by texture. The 3 m and 11 m high hummocks are shown by dashed and solid lines, respectively. Each line is labeled with its corresponding topological scenario (Figure 6-4).	112
Figure 6-8: 6-8: Boxplots showing the distribution of major annual fluxes for each simulation. The 3 m and 11 m high hummocks are shown by dashed and solid boxplots, respectively. AET and drain outflows are shown in green and red, respectively. A final boxplot to the right illustrates the distribution of annual precipitation. A, B, and C refer to the different topological scenarios presented in Figure 6-4.	113
Figure 6-9: Cumulative changes in storage for the vadose (left) and groundwater reservoirs (right). Changes in storage are normalized for the areal extent of the model domains. The 3 m and 11 m high hummocks are shown by dashed and solid lines, respectively. The color coding (orange, blue, and	

black) corresponds to the different topological scenarios presented in Figure 6-4. A red light denotes zero change in storage..... 114

Figure A-1: An example showing the relative correlations between the annual minimum WT positions for (a) well 85 in the CO HRA and (b) well 569 in the HM HRA and the total precipitation for that hydrologic year (P_{ann}), the 2 year cumulative departure from the mean (CDM-2), the 3 year cumulative departure from the mean (CDM-3), and the 4 year cumulative departure from the mean (CDM-4). Linear regression R^2 values for each best-fit line are shown in bold above each subplot.....135

Figure B-1: Observed and simulated volumetric soil water content for the 1D model. Materials and probe depths are annotated on the graph and correspond to the materials and depths in Table B-1... 139

Figure C-1: Results from the sensitivity analysis of major model parameters for the detailed study hummock model showing the effects of (a) anisotropy ratio, (b) soil depth, (c) peatland water table elevation, (d) van Genuchten-Mualem α and n parameters. The lower panel shows the probable dual permeability of the glacial till and the effects of α , n , and K in that context.....142

Chapter 1

Introduction

1.1 Background

Reconciling complex spatial and temporal interactions between scales of hydrologic processes remains a considerable challenge in hydrology, including hydrogeology. The identification of critical scales of hydrological processes and the integration of operational hierarchies is needed for an improved ability to move between such scales (Gentine et al., 2012; Sophocleous, 2002;). Although broad hierarchical frameworks for generalizing water balances of individual land units have been developed (e.g., Rodriguez-Iturbe, 2000), these frameworks have not adequately addressed the problem of cross-scale interactions to explain hydro(geo)logic variability over both time and space. Additionally, most work has emphasized runoff generation and topographically defined basin response to precipitation (Gupta et al., 2012), and there is a notable gap in research concerning variable-scale surface and subsurface hydrologic processes in regions where topography is not the dominant control (Devito et al., 2005b).

Understanding the controls on, and natural variability of, water table depth, and using that understanding to predict changes in water table position and groundwater quality under varying physical and climatic scenarios is important as water security, ecosystem sustainability, and environmental quality become the focus of land management and reclamation efforts. Policies and adaptive management strategies would benefit from an understanding of the interactions that occur among processes operating at micro (e.g., soil profile), small (e.g., hillslope), meso (e.g., glacial landform(s)), and regional (e.g., groundwater divides) spatial scales, and short (e.g., snowmelt, precipitation), intermediate (e.g., seasonal), and long (e.g., multi-year, decadal) time scales.

The Boreal Plains (BP) ecoregion, located in the Western Glaciated Plains, is characterized by pond-peatland-forestland complexes underlain by thick glacial deposits, which result in highly complex groundwater flow systems with varying spatiotemporal controls (Lennox et al., 1988; Lissey, 1971; NWWG, 1988; Winter, 1999). The BP is experiencing unprecedented anthropogenic disturbances, in the forms of climate change, forestry, agriculture, and oil-and-gas operations. The spatial and temporal scales at which Boreal Plains landscape elements are hydrologically connected are not well understood. To successfully manage and adapt to the ongoing disturbances, the critical scales at which key hydrological processes operate need to be identified and explored further.

Deep glaciated deposits groundwater patterns are complex and not solely determined by topography, but rather their hydrogeological setting and climate (Meyboom, 1966; Winter, 2001). The climatic state of a landscape can be best described by the deficit or surplus created by precipitation (P) and evapotranspiration (ET), which primarily manifests itself as groundwater recharge. The spatiotemporal variability of recharge, due to temporal variability in precipitation and spatial variability in ET (due to land and vegetation cover), results in dramatic spatiotemporal changes in saturated zone storage and therefore

water table position and groundwater flow. The variability in saturated zone storage is further exacerbated by the high spatial variability of substrate textures in the BP. Typically, as in humid climates, water predictably flows from topographic highs to topographic lows, and the water table mirrors the surface topography. In the BP, ET often equals or exceeds P, which results in a delicate water balance, neither humid nor arid, where a sub-humid climate creates a general moisture deficit and a propensity for vertical flow, larger than average ET demands, and large, highly variable unsaturated zone storage rather than lateral flow (Bothe and Abraham, 1993; Devito et al., 2005a). Consequently, P, ET, and geology may have a much greater control than topography over local hydrology (Devito et al., 2005b).

Identifying the spatial variability of the scale of groundwater flow yields insights regarding the source and fate of groundwater and the time scales governing water table behavior and groundwater chemical signatures, in addition to indicating the hydrologic connectivity of a given HU to its surroundings. A common approach to characterizing groundwater flow is to implement numerical models, informed by hydrogeological parameters and hydraulic head data (Anderson et al., 2015), which typically assume the water table is equivalent to the topography, where high elevations serve as recharge zones and valleys serve as discharge zones (Cardenas et al., 2007; Freeze and Witherspoon, 1967; Winter 1978; Zijl, 1999). However, the water table rarely mimics topography in the BP (Devito et al., 2012) and the temporal and spatial variability of the water table position are not, yet, well known. Additionally, fixing the water table at any depth will wholly control the distribution and length of groundwater flow paths, discharge zones, and recharge zones (Tóth, 1963). Scale of flow is often thought to be easily compartmentalized into recharge or discharge and local or regional flow zones based on basin topography and the position of hillslopes and rivers; however, this is not the case in regions with low topographic relief, low recharge rates, and complex surficial geology, as in the BP.

While the above relationships between topography and groundwater behavior are operative in areas of high recharge and relief, they are not realistic solutions in low-relief, sub-humid regions like the BP, where the WT does not mirror topography in most areas. At a sedimentary basin scale there is a clear and dominant effect of topography on groundwater flow, where major topographic features (mountains and foothills) serve as groundwater recharge zones and major lowlands are groundwater discharge zone. The BP, however, is located in a generally low relief region with thick (~140 m) unconsolidated substrates. While groundwater flow has been modelled at the regional scale (Tóth, 1978) and hillslope scale (Smerdon et al., 2005; Thompson et al., 2015) in the BP, no previous study has explored shallow groundwater systems at the meso-scale (i.e., multiple pond-forestland complexes within a single regional basin).

The topographically defined watershed is a pervasive concept throughout the hydrological and shallow hydrogeological communities. It is also the primary 'go-to' land management unit for policy makers and developers; hydrological management is founded on catchment and watershed delineation. For example, in Alberta, which comprises a significant portion of the BP, 'Alberta ArcHydro Phase 2', 'Hydrologic Unit Code Watersheds of Alberta', and 'Watersheds of Alberta' are all generated using digital elevation models (DEMs) (AEP, 2018). While they may serve as useful large-scale land units, they do not

necessarily offer insight into hydrologic connections (e.g., sources or sinks of water) at the scale of interest to local operators, forestry planners, reclamation specialists, developers, etc. Additionally, they may not adequately represent the heterogeneity (Devito et al., 2017) that leads to groundwater divides being separate from topographic divides. Such scenarios are present in the glaciated BP and other sub-humid regions, and those boundaries have been shown to vary with geology and climatic stresses at various spatiotemporal scales (Borchardt, 2018; Winter et al., 2003). The purpose of this research is to provide, and validate, an alternative framework for water movement in these challenging regions (i.e., low relief, low recharge, heterogeneous geology) that can be applied over a range of spatiotemporal scales.

1.2 Thesis objective and format

The objective of this thesis was to use a fundamental framework of controls (i.e., climate, geology, and topography) to explain the temporal and spatial variability in hydrologic responses and behaviors in the BP and to develop a variable-scale conceptual model for groundwater movement and groundwater-surface water interactions. Specifically, this thesis explores the following fundamental questions as they pertain to the hydrogeology of the Boreal Plains or similar environments:

1. Where (spatial scale and/or geologic setting) and when (under what climatic conditions) are shallow groundwater systems recharge controlled versus topography controlled?
2. What are the controls on groundwater-surface water interactions in various BP geologic settings?
3. How does hummock texture, hummock morphometry, and long-term and seasonal atmospheric fluxes (i.e., P and ET) affect the water table position in the hummock? Additionally, under what conditions do hummocks serve as significant sources or sinks of groundwater to adjacent wetlands?
4. How does the organization of various landform morphometries and forestland-peatland topologies affect water availability at the landscape scale?

This thesis is presented in “paper format” – each of the chapters is written to stand alone in a form publishable in a journal. This means that each chapter has its introduction and conclusion, and the reader may notice some repetition from previous chapters. Following this introduction, Chapters 2, 3, 4, 5, and 6 present separate studies that focus on specific objectives, utilizing both field and modelling methods:

Chapter 2: To test the influence of interactions between glacial deposit types, climate, and topography on water table position and groundwater flow in the BP, three hydrological response units (HRA) that represent the main glacial depositional types typical of the BP were delineated and characterized. Hydrogeological data at sites that span topographic positions within these HRAs were examined to determine the roles of topography, geology, and climate on hydrogeologic responses and to classify each HRA

as recharge or topography controlled. The potential for HRAs to delineate chemoscapes and isoscapes to provide practical predisturbance hydrogeological benchmarks for developing beneficial land management practices was also explored. A version of this chapter was published in 2019.

Chapter 3: To determine the landscape-scale controls of groundwater-surface water interactions in a coarse-textured glacial outwash setting by using isotopic compositions of lakes, groundwater, and precipitation to explore the relative groundwater contributions to and hydrological interactions between eleven lakes. A version of this chapter was submitted in 2021.

Chapter 4: To test the common conceptualization of topography driven flow and groundwater mounding under mineral hummocks and to examine the hydrogeologic function of forestlands in different HRAs, the hydraulic gradients between peatlands and adjacent forested hummocks were examined at sixteen different locations during one ice-free period. A version of this chapter was published in 2020.

Chapter 5: To identify the role of fine-textured aspen forested hummocks in the generation (or loss) of groundwater and hydrologic connectivity to adjacent peatlands by examining the simulated recharge patterns and sink-source functions of various hummock regimes. Field data were used to develop a variably-saturated flow model, whose morphometry and hydraulic conductivity were systematically altered to further understand the hummock-scale controls on groundwater recharge and water table dynamics. A version of this chapter was submitted in 2021.

Chapter 6: To present a variable-scale conceptual framework that describes water movement in low-relief water-limited landscapes, which incorporates both the findings from previous chapters in this thesis as well as previous work in similar landscapes. The conceptual framework is implemented in large-scale 3D groundwater models as a proof-of-principle to explore the hydrological implications of landform topology, topography, texture and climate.

Chapter 2

Interactions between regional climate, surficial geology, and topography: Characterizing shallow groundwater systems in sub-humid, low-relief landscapes¹

2.1 Introduction

Reconciling complex spatial and temporal interactions between scales of hydrologic processes and integrating operational hierarchies at multiple scales remains a considerable challenge in hydrology and hydrogeology (Gentine et al., 2012; Sophocleous, 2002). Broad hierarchical frameworks for generalizing water balances of individual land units have been developed (Rodriguez-Iturbe, 2000; Winter, 2001); however, these frameworks do not adequately address cross-scale interactions to explain hydro(geo)logic variability over both time and space. Additionally, most work has emphasized runoff generation and topographically defined basin responses to precipitation (P; Gupta et al., 2012); there is a notable gap in research that couples variable-scale surface and subsurface hydrologic processes over both time and space.

The Boreal Plains (BP), located in the Western Glaciated Plains of North America (Figure 2-1), exists in a subhumid climate, where evapotranspiration (ET) often equals or exceeds P, resulting in a delicate water balance with short-term wet-dry climate cycles, a propensity for vertical flow; larger ET demands; and large, highly variable unsaturated zone storage (Bothe and Abraham, 1993; Devito et al., 2005a; Devito et al., 2005b). The BP is characterized by pond-peatland-forestland complexes underlain by thick glacial deposits, which result in interdependent surface water processes and groundwater flow systems with varying spatiotemporal controls (Lennox et al., 1988; Lissey, 1971; National Wetlands Working Group, 1988; Winter, 1999, 2001). In humid climates, water predictably flows from topographic highs to topographic lows, and the water table mimics surface topography (Freeze and Witherspoon, 1967). However, in the thick glaciated deposits of the BP, groundwater flow patterns are not solely determined by topography; the climate and hydrogeological setting may have dominant influences (Meyboom, 1966; Winter, 2001). Temporal variability in P and spatial variability in ET due to land and vegetation cover result in dramatic spatiotemporal changes in saturated zone storage and groundwater recharge rates (Brown et al., 2014; Redding and Devito, 2008). Consequently, at certain spatial scales, P, ET, and subsurface geology can have a greater control than topography over local hydrology (Fan, 2015).

¹ A version of this Chapter has been published:

Hokanson K.J., Mendoza C.A., Devito K.J. Interactions between regional climate, surficial geology, and topography: Characterizing shallow groundwater systems in subhumid, low-relief landscapes. *Water Resources Research*. 2019; 55(1):284-97. doi: 10.1029/2018WR023934.

Due to its wet-dry cycles, complex geology, and low relief, the BP is an ideal setting to develop and test hierarchical frameworks that explain groundwater-surface water interactions at multiple scales. Furthermore, the BP is experiencing unprecedented anthropogenic disturbances in the forms of forestry, agriculture and oil-and-gas operations, and climate change, so understanding hierarchies of hydrological connections and influences is necessary for management and reclamation decisions. The dominant spatial and temporal scales at which BP hydrological processes operate are not well understood; thus, to successfully model, manage, and adapt to ongoing disturbances, processes need to be explored at micro (e.g., soil profile), small (e.g., hillslope), meso (e.g., glacial landform[s]), and regional (e.g., groundwater divides) spatial scales, and short (e.g., snowmelt, P), intermediate (e.g., seasonal), and long (e.g., multiyear) timescales.

Characterization of groundwater flow systems requires identification of the dominant spatial and temporal patterns of groundwater movement, and scales of groundwater flow (Tóth, 2009). The identification of the spatial variability of scale of groundwater flow yields insights regarding the source and fate of groundwater and the hydrologic connectivity of a given landform to its surroundings. Additionally, it can elucidate the timescales governing water table depth and behavior and groundwater chemical signatures. Haitjema and Mitchell-Bruker (2005) identified the different hydrogeological conditions that would affect water table position, and thus scale of groundwater flow, finding that the primary controls on water table position are texture, recharge, and relief. There is a need to determine the relative importance and scale dependence of the three elements of Tóth's (1970) "hydrogeologic environment" in subhumid regions with low-relief and thick heterogeneous deposits: geology, recharge (i.e., climate), and topography. Here I explore the relationships between texture and relief in environments of generally low-recharge compared to most humid environments.

Although regional flow systems have been defined in the BP using regional-scale topographic divides (on the order of 104 km²; Tóth, 1978), smaller intermediate or local flow systems within the regional systems have not been explored and are at a scale where climate (i.e., recharge), and geology could have dominant influences over groundwater movement compared to topography alone. While Tóthian flow (Tóth, 1963) operates in humid regions or at large spatial scales where the water table typically mimics topography, it may be less relevant in subhumid regions or at smaller spatial scales (Haitjema and Mitchell-Bruker, 2005).

Hydrologic response units (HRUs), derived from a combination of soil characteristics, land use, and topography, have been used traditionally to predict runoff (e.g., Arnold et al., 1998; Flügel, 1995; Kirkby and Beven, 1979); however, runoff is very low in the BP (Devito et al., 2017; Redding and Devito, 2008). Thus, I argue it is more suitable to use the hydrogeologic setting to delineate hydrologic response areas (HRAs), which are areas with similar water transmission and storage properties, rather than being defined solely on basin topography. While the disaggregation of the landscape into discrete subregions is helpful, and often necessary, in most modeling scenarios (Becker and Braun, 1999), doing so by only considering surficial characteristics and processes (e.g., basin topography, soil type, vegetation, and surface runoff)

has limited applicability in regions with low-relief and thick substrates, such as the BP. In contrast to HRUs, HRAs are delineated by first considering the depth and texture of the geologic substrate, which in turn control subsurface storage and transmissivity. The concept of HRAs has been used to successfully explain the variation in annual runoff from large (50 to 5,000 km²) BP catchments (Devito et al., 2017); however, they have not been fully characterized at smaller, more practical scales for describing shallow groundwater flow patterns. These operational scales are applicable to common management units for determining, for example, recommended forest management practices, reconstructed landscape designs, and road placement (Jeglum et al., 2003).

To test the influence of interactions between glacial deposit types, climate, and topography on water table position and groundwater flow in the BP, I delineate and characterize three HRAs that represent the main glacial depositional types typical of the BP, and I analyze 19 years of hydrogeological data at sites that span topographic positions. I hypothesize that topography (i.e., elevation or relief) alone cannot be used to predict water table position and that geology (texture) and climate (recharge) will have an overriding influence at local to mesoscales. To evaluate the spatial and temporal variability of shallow groundwater flow systems, I use four major measures: magnitude and frequency of water table fluctuation, vertical hydraulic gradients (i.e., recharge vs. discharge), geochemical signatures, and stable water isotope ratios. I also evaluate the potential for HRAs to delineate chemoscapes and isoscapes to provide practical predisturbance hydrogeological benchmarks for developing beneficial land management practices.

2.2 Methods

2.2.1 Study Site

This study was conducted along a 70-km transect at the Utikuma Region Study Area (URSA; 56°N, 115°W), located 370 km north of Edmonton, Alberta, in the BP ecozone of Canada (Figure 2-1c). The climate is subhumid with historic annual potential ET (517 mm; Bothe and Abraham, 1993) often exceeding the historic average annual P (481 mm; Marshall et al., 1999). The region is characterized by low topographic relief and thick (45 to 240 m) heterogeneous glacial substrates that can be characterized largely as glaciofluvial, glaciolacustrine, or moraine deposits, all overlying the Smoky Group, a Cretaceous marine shale (Vogwill, 1978). Previous research at URSA includes several multiyear ecohydrological and hydrogeological studies spanning 1998 to present (Devito et al., 2016).

2.2.2 Precipitation

P data were collected throughout the study period (1999 to 2017) using two to three tipping bucket rain gauges adapted for snowfall by using antifreeze in the reservoirs. Due to the strong effect of antecedent moisture conditions on hydrologic response in the BP (Devito et al., 2005a), the 3-year cumulative departure from the mean P (CDM-3) was calculated using the recent long-term mean P (444 mm; Figure 2-2; 1987 to 2015) to identify wet and dry states. The CDM-3 was used because it offered the best correlation to

groundwater levels over the study period (Appendix A). Consequently, it acts to capture lag or memory in the interactions between P (i.e., rainfall and snowmelt) and water table (WT) fluctuations.

2.2.3 Hydrological Response Area (HRA) Delineation

Three main HRAs were delineated along the study transect at URSA (Figure 2-1). The HRAs are based on surficial geology: coarse outwash (CO), hummocky moraine (HM), and clay-till plain (CP). The HRA bounds were determined from units delineated in the Alberta Geological Survey surficial geology mapping (Fenton et al., 2013; Figure 2-1), following Devito et al. (2017), to represent the broad spatial differences in local relief, storage potential, and transmission characteristics (Devito et al., 2017; Winter, 2001). Fenton et al. (2013) utilized genetic and geomorphic modifiers (e.g., texture, genesis, topographic relief, thickness, and lithology) in their surficial geology schema, which were subsequently reclassified into the three HRAs. The first delineation was between coarse and fine materials (coarse = gravel, sand, sandy-gravel, silty-sand, silty-gravel; fine = silt, clay, sand-silt-clay, sandy-silt, sandy-clay, silty-clay, clayey-silt). If no texture classification was available (Atkinson et al., 2014; Fenton et al., 2013) fluvial, glacial-fluvial, eolian, and littoral glacio-lacustrine landforms were combined for coarse, and the remaining landforms were considered fine. All coarse-textured surficial geologic units were classified as CO HRA, while fine-textured surficial geologic units were further defined as either HM or CP HRAs. All nonsandy stagnant ice moraines and moraines with hummocky geomorphic classes were classified as HM HRA. The CP HRA consisted of fine-textured units that are defined as lacustrine, distal glacio-lacustrine, and thrust moraine landforms. Organic deposits (i.e., peatlands) were assumed to be underlain by fines and were therefore classified the same as the adjacent fine HRA but classified as CO if >75% of the perimeter is surrounded by coarse-textured landforms. Isolated pockets less than 1 km wide of different geology were incorporated into larger HRAs. Mesoscale topography was used to constrain an HRA to the study area.

2.2.4 Hydrogeology

At 24 sites, a total of 24 wells (0.051-m diameter polyvinyl chloride pipe) and 15 piezometers (0.025- to 0.051-m diameter polyvinyl chloride pipe) were installed in mineral uplands to depths ranging from 2 to 38 m at various local and regional topographic positions in all three HRAs (Figure 2-1). Sites were chosen to be representative of forested mineral uplands and therefore do not capture areas such as riparian zones, ecotones, or ephemeral wetlands. Wells were screened for the entirety of the well; piezometer screens were 0.2 to 2 m long and entirely below the water table. Where the substrate would collapse into the borehole, typically in saturated coarse material, wells and piezometers were driven into the native substrate. Otherwise, the borehole annulus was filled with a sandpack to 0.25 to 0.5 m above the screen, sealed with bentonite chips, and backfilled with cuttings. Installations began in 1998, and most were completed by 2003. Once the wells and piezometers were installed, water levels were typically measured at least once a year, in late July, from 2000 to 2017.

Stratigraphy of the unconsolidated substrate was logged at each borehole, where the texture was assessed by hand and periodically confirmed using particle size analysis (Redding, 2009; Smerdon et al.,

2005). Supporting information, including depths to bedrock and aquifers, was provided by the Alberta Research Council (Ceroici, 1979; Pawlowicz and Fenton, 2002a, 2002b; Vogwill, 1978). Vertical hydraulic gradients were calculated between the piezometer and the water table measured at 14 primary, nested, monitoring sites along the main transect (Figure 2-1). Horizontal saturated hydraulic conductivity (K) was estimated at 185 monitoring sites (295 total measurements). At wells and piezometers, the Hvorslev (1951) method was used; for shallow depths (<1 m below ground surface) above the water table, a Guelph Permeameter (Redding, 2009; Reynolds and Elrick, 1986) was used. Elevations and topography were obtained from LiDAR data sets collected in 2008.

2.2.5 Geochemical and Isotopic Compositions:

Groundwater was sampled and analyzed for a suite of major anion and cation concentrations, including Mg^+ , Ca^{2+} , Na^+ , K^+ , Cl^- , SO_4^{2-} , CO_3^{2-} , and HCO_3^- . Electrical conductivity (EC) of groundwater and surface water was measured in both the field and lab using a conductivity probe.

Additionally, surface water and groundwater were sampled for stable $^{18}O/^{16}O$ and $^2H/H$ ratios, while P (rain and snow) was sampled throughout the study period to establish a local meteoric water line (LMWL). Pond water samples obtained throughout the summer seasons were used to create a local evaporation line (LEL; Gibson et al., 1993). Rainwater was collected using a collector specifically built to prevent fractionation (Gröning et al., 2012). Results are expressed as per mil difference (‰), relative to Vienna Standard Mean Oceanic Water in both a dual-isotope space and as the line-conditioned excess (Ic-excess). The Ic-excess describes the deviation from the LMWL (Landwehr and Coplen, 2006), a locally relevant metric, as opposed to the global meteoric water line, which is used in calculating deuterium excess (Dansgaard, 1964). All isotopic and hydrochemical analyses were performed at BASL laboratory, University of Alberta, Edmonton, AB, Canada (<http://www.biology.ualberta.ca/basl/>).

2.3 Results

2.3.1 Precipitation

Mean annual P for the study period (1999 to 2017) was 423 mm, with the highest and lowest annual P occurring in 2016 (537 mm) and 2001 (257 mm), respectively (Figure 2-2). However, using the CDM-3, 2013 was chosen as a representative “wet” year, with a CDM-3 of +177 mm, and 2003 chosen as a representative “dry” year, with a CDM-3 of -343 mm.

2.3.2 HRAs and HRA Physical Properties

The three main HRAs delineated along transect A-A' at URSA (CO, HM, and CP) are shown in Figure 2-1. All data shown in this study are exclusively from these HRAs. The entire elevation range of the three HRAs is 87 m (630 to 719 m above sea level). The CO HRA has the largest elevation range, while the HM and CP HRAs have slightly more limited ranges (Table 2-1). The average slope of both the CO and HM HRAs (1.43% and 1.30%, respectively) is appreciably higher than the CP (0.56%), which is similar to

the average slope of the three HRAs (0.79%). Additionally, through observed water table configurations and sediment layering, a transition zone has been identified within the CO HRA, near the border of the HM HRA, where a clay layer overlying sand leads to several perched ponds and peatlands. This area is labeled “CO-Perched” and is further explained below. The CP HRA is considerably larger than both the CO and HM HRAs, primarily due to the extensive nature of glaciolacustrine clays and their associated peatlands.

2.3.3 Hydrogeology

The depth to the shale bedrock in the northwest of URSA in the CO HRA ranges from 80 to 120 m, from 90 to 100 in the HM HRA, and from 90 to 150 m in the CP HRA (Figure 2-3). The CO HRA in the northwest is the start of a sand/gravel aquifer that extends below the CO-Perched area and HM HRA and tapers off under the CP HRA to the southeast. The CO HRA is predominantly sands and gravels, interbedded with small, spatially discontinuous, silt lenses. The CO-Perched transition lies on the eastern boundary of the CO HRA and has a laterally unconfined water table but is confined vertically by layers of low permeability clay overlying unsaturated coarse-textured sediments approximately 12 m above a water table in the underlying sand aquifer. Ponds and peatlands in lower topographic regions exist in the sand and gravel as discharge or flow-through systems that intersect the water table, while the ponds and peatlands in higher topographic regions tend to be underlain with finer textured silts and clayey silts. The HM HRA is predominantly silty hummocks underlain by clay and clay till, with small peatlands and ponds underlain with gyttja and clay. The CP HRA consists of extensive peatlands surrounding low-relief silt-clay hummocks and ponds underlain by clay.

Field measurements show that the mineral K varies by 7 orders of magnitude across URSA; however, K is more tightly constrained within each HRA (Figure 2-4). The CO HRA has a geometric mean K of 4.6×10^{-5} m/s, and the HM and CP HRAs have geometric mean K values of 1.4×10^{-6} and 4.2×10^{-7} m/s, respectively. Overall, the CO HRA has higher K, but the difference is most notable at shallow and intermediate (<5-m) depths. The CO (including CO-Perched) and HM HRAs all exhibit higher K values at very shallow (<1-m) depths. The CP HRA has the least variability in K, where most boreholes exclusively intersected lacustrine clay. At sites deeper than 1 m, K values in the HM HRA are similar, ranging from 6.0×10^{-9} to 2.5×10^{-7} m/s (interquartile range), while the K values in the CO and CP HRAs decrease with depth. The K values for deep sites (i.e., in the sand aquifer below the clay confining beds) in the CO-Perched area show the disparity in conductivity between underlying sand (3.3×10^{-6} m/s) and the overlying silt and clay (1.3×10^{-8} m/s).

Along the transect there were near negligible vertical hydraulic gradients in the CO HRA but strong recharge gradients in the HM HRA (Figure 2-5). In the CP HRA, near negligible to slight positive (discharge) vertical gradients were present in the “valley” of the transect (~35 km) trending to strongly negative (recharge) gradients on the plateau of the CP HRA. The vertical gradients trended with overall regional topography and vertical distance to the upper sand aquifer. Considering both the wettest and driest years, within the CO and HM HRAs vertical gradients did not follow the absolute elevation of the wells (R^2

[correlation coefficient] = 0.55 and $R^2 = 0.10$, respectively); however, in the CP HRA this was not the case ($R^2 = 0.87$). Vertical gradients in the HM and CO HRAs were not particularly sensitive to climate and did not vary between the wettest and driest years (i.e., 2013 and 2003, respectively). Gradients in the CP HRA were generally less negative in the wettest year, than in the driest year.

2.3.4 Long-term Water Levels

In the CO HRA, water table fluctuations varied greatly in both magnitude and frequency between sites, with some sites (i.e., sites 8 and 9) exhibiting highly stable water levels and others (i.e., sites 10 and 64) responding strongly to interannual climate variability over the study period (Figure 2-6). Additionally, during the dry year (2003), which had the lowest CDM-3 but an average annual P, most sites (i.e., sites 1, 4, 5, 10, 12, and 85) exhibited their lowest water table levels. Sites that did not show a water table decline leading up to 2003 were generally stable through the entire study period. Within the CO HRA, beneath the CO-Perched area, water table elevations were stable and not influenced by either long- or short-term climate. Both the HM and CP HRA well sites showed high seasonality (i.e., annual peaks) at most sites.

At the scale of the entire URSA, WT positions generally appear to follow ground surface topography (as denoted by the 1:1 line in Figure 2-7); however, this relationship does not necessarily hold at the scale of individual HRAs. The magnitudes of water table fluctuations over the study period showed differing patterns within each HRA (Figure 2-7). Within the CP HRA, the site with the largest water table fluctuation was located at the highest topographic position, and sites at lower elevations had smaller fluctuations, and the water table position generally followed ground surface topography (as denoted by the 1:1 line in Figure 2-7). This pattern was not evident at the HM or CO HRAs, where there was a strong departure from the 1:1 line and the magnitude of fluctuations was not related to topographic position. Two distinct water tables were evident at the CO-Perched sites. The relationships, in the case of the CP HRA, or lack thereof, in the case of CO and HM HRAs, between topographic position and water table fluctuation magnitude closely follow trends regarding topography and vertical hydraulic gradients (Figure 2-5).

2.3.5 Chemoscapes and Isoscapes

Groundwater at all three HRAs showed the same hydrochemical facies: alkaline earths (Ca^{2+} and Mg^{+}) exceed alkalis (Na^{+} and K^{+}). For the major cations (Mg^{+} , Ca^{2+} , Na^{+} , and K^{+}) and anions (Cl^{-} , SO_4^{2-} , CO_3^{2-} , and HCO_3^{-}), there was a general pattern of concentrations between HRAs: $\text{CO} < \text{CO-Perched} < \text{HM} < \text{CP}$ (Figure 2-8). EC measured in the wells and ponds followed the same general trend, with ponds and wells in the CP and HM HRAs having generally higher EC than those in the CO HRA. Across URSA, ponds had lower EC values than groundwater. Pond EC ranged from 120 to 800 $\mu\text{S}/\text{cm}$ in the HM and CP HRA and from 15 to 360 $\mu\text{S}/\text{cm}$ in the CO HRA. There was no significant difference in EC between ponds in the CO HRA and CO-Perched area. Groundwater ECs in the HM and CP HRAs were similar and ranged from 530 to 5500 $\mu\text{S}/\text{cm}$. Groundwater ECs in the CO HRA and CO-Perched area were significantly lower and ranged from 20 to 1,000 $\mu\text{S}/\text{cm}$ and from 140 to 1,250 $\mu\text{S}/\text{cm}$, respectively. At this meso (HRA) scale there was no apparent relationship between interannual climate variability and groundwater chemistry.

The LMWL (Eq. 2.1) and LEL (Eq. 2.2) for URSA were found to be:

$$\delta^2\text{H} = 7.25 \cdot \delta^{18}\text{O} - 11.37 \quad (\text{adjusted } R^2 = 0.97) \quad [2.1]$$

$$\delta^2\text{H} = 4.12 \cdot \delta^{18}\text{O} - 66.34 \quad (\text{adjusted } R^2 = 0.93) \quad [2.2]$$

Ponds in each HRA follow the URSA LEL, while groundwaters in each HRA occupy different spaces in the dual-isotope space (Figure 2-9). Groundwater samples from the CP and HM HRAs follow the LMWL, while groundwater samples from the CO HRA deviate from the LMWL and more closely follow the LEL (Figure 2-9). This indicates that groundwater in the fine-textured HRAs is meteorically sourced and has not undergone kinetic fractionation, whereas there is more spatial variability in groundwater-surface water interaction in the CO HRA.

The Ic -excess values at URSA (Figure 2-10) show that the individual evaporative signatures of both ponds and groundwater correlated very well with climate extremes; highly evaporative signatures generally correspond with the driest year (2003) and vice versa. However, on a year-to-year basis there was not a strong relationship. Ponds generally showed a strong evaporative signature with a high degree of interannual variability. Groundwater samples showed significantly less interannual variability. In the HM and CP HRAs there was a strong separation of groundwater and pond signatures, suggesting there is little to no hydraulic communication between the glacial substrate and neighboring ponds and that groundwater primarily has an atmospheric origin with little opportunity for evaporation. This recharge signature corresponded well with vertical hydraulic gradients (Figure 2-5), where in the HM and CP HRAs there were generally strong negative vertical hydraulic gradients and Ic -excess excess values near zero (i.e., meteoric water). In contrast, the CO HRA had several sites that showed a mixing signature between the ponds and groundwater, specifically at 2 km (site 10; Figure 2-3), 10 km (site 3), and 16 km (site 11) on Figure 2-3. Site 11 is in the CO-Perched area and warrants further investigation because it represents water in the sand aquifer overlain by low permeability clays; however, sites 10 and 3 are both proximal to stagnant ice moraine geologic units. They were also the CO HRA sites that experienced the greatest water table variability over time.

2.4 Discussion

2.4.1 The Concept of HRAs

This study clearly demonstrates the limited influence topography has on water table position in the BP. While there is a strong relationship between topography and water table behavior in regions of high recharge and appreciable relief, this is not a realistic a priori assumption in low-relief, subhumid regions like the BP. At a sedimentary basin scale, from the Rocky Mountains to the Canadian Shield, there is a clear and dominant effect of topography on groundwater flow: major topographic features (mountains and foothills) serve as groundwater recharge zones and major lowlands (e.g., Athabasca oil sands) are groundwater discharge zones (cf. Hitchon, 1969). Additional systems in deep, bedrock aquifers are driven

by erosional rebound and past tectonic compression (Bachu, 1999; Garven, 1989). However, URSA and the BP as a whole are in a generally low-relief region with thick (on the order of hundreds of metres) unconsolidated substrates (Figure 2-11) with shallow groundwater systems that are largely isolated from these deep bedrock systems. While basin-scale gravity-driven flow on a geologic timescale (Tóth, 1978) and hillslope-scale fluxes (Smerdon et al., 2005; Thompson et al., 2015) have been simulated in the BP, no previous study has explored shallow groundwater systems at the mesoscale (i.e., multiple pond-peatland-forestland complexes within a single regional basin). Here I show that at intermediate spatiotemporal scales, groundwater flow systems cannot be defined by topography alone but are defined by a hierarchy of long-term climate (subhumid), geology, short-term climate (CDM-3), and topographic relief.

By delineating HRAs based on geologic substrate characteristics (i.e., texture and origin), the physiographic characteristics within the HRA become dominant factors. When addressing URSA as a whole, the spatial variability of slope and relief is lost; however, by delineating HRAs, distinctive patterns of topography are apparent (Table 2-1). HRAs do not account for regional topographical boundaries (e.g., groundwater divides), but they do emphasize the importance of smaller scale relief (e.g., hummocks and swales) within the HRA. The BP is an extremely low-relief region, and, as such, determining groundwater flow patterns becomes a difficult task (except for at the regional geologic scale) without intensive site-specific investigation. This study shows that HRAs are a useful way of discretizing the landscape into areas with predictable hydrogeologic characteristics and shallow groundwater flow patterns (or lack thereof) in a landscape that otherwise would be too flat and heterogeneous to use traditional methods like HRUs. Finally, while HRUs are common, they necessarily emphasize surficial or local-scale processes; HRAs, however, allow for multiple scales of interaction and flow and help the user identify critical scales.

2.4.2 Topography vs. Recharge Controlled Water Tables

In the CP HRA, vertical hydraulic gradients and water table fluctuations illustrate that topography is the primary control over water table position and scale of groundwater flow, which follows surface topography very well. Sites in the higher elevations (i.e., high water table fluctuations and strong recharge gradient) have more localized controls than sites at lower elevations with more stable water tables and more tempered hydrologic controls (i.e., less localized controls). In the CP HRA the characteristic length of the relief is very large, and therefore, the effects of topography and substrate texture dominate over local-scale controls such as recharge and ET (Haitjema and Mitchell-Bruker, 2005).

Substrates of the HM HRA are similar to those found in the CP HRA; however, the HM HRA has a wider range in K; the local relief and slope are appreciably greater (Table 2-1 and Figure 2-2); and water table position, water table fluctuation, and vertical hydraulic gradients do not follow topography (Figures 2-4 and 2-5). The site at the highest elevation in the HM HRA (site 19) has the deepest (relative to the ground surface) and most stable water table of all the HM HRA sites. Traditionally, areas with pronounced relief, like the HM HRA, typically have dominant local flow systems (i.e., water flowing from local highs to adjacent

lows). However, in the HM HRA this only occurs at select sites during wet years with the highest water table conditions (Figure 2-6). These sites show water table behaviors characteristic of local control, and as such, the effects of recharge and ET are the dominant controls, overwhelming the effects of local and mesoscale topography (Haitjema and Mitchell-Bruker, 2005).

The CO HRA substrates, in contrast to the CP and HM HRAs, are predominantly high K sands and gravels with little to no vertical gradient. In the CO-Perched sites, there are two clearly distinguishable water tables: one in the underlying sand aquifer and one perched on the overlying silt and clay layers. Except at the lowest elevations in the CO HRA, the water table does not follow local topography and generally exhibits very small (relative to CP and HM HRAs) water table fluctuations over time (Figure 2-5) due to its high K/recharge ratio. Because the relief in the CO is low relative to its hydraulic conductivity, the ground elevation of a hummock may belie its true topographic position in a pond dominated glacial outwash (Kratz et al., 1997). With largely flat water tables in a coarse-textured setting with relatively low recharge rates and high K (Haitjema and Mitchell-Bruker, 2005), pond-to-pond flow, flowing through shallow, focused parts of the landscape, is the most probable groundwater flow path (Smerdon et al., 2005) and as such could be a better metric of landscape position than simply ground surface elevation alone. With this perspective in mind, a pattern becomes clear where sites located at intermediate pond elevation locations have the largest water table fluctuations and pond isotopic signatures, and sites at the lowest pond elevations have the most moderated or minimal water table fluctuations. However, isotopic data indicate that at most elevations, flow is primarily vertical with little to no lateral hydraulic communication between landforms. The highest elevation (and therefore perched, at URSA) sites are also highly moderated due to the shallow confining layer, while the deep water table (under the confining layer) is likely regionally controlled.

The above characterizations can be categorized taking a “Tóthian approach” (Tóth, 1963). Groundwater flow (and the controls thereon) is considered “intermediate” in the CP HRA and “local” in the HM HRA; however, the CO HRA contains multiple scales and is influenced by adjacent HRAs and larger-scale flow systems.

2.4.3 Groundwater-Surface Water Interactions

While recharge-controlled water tables tend to be dominated by horizontal flow (Haitjema and Mitchell-Bruker, 2005), the isotopic data show a general lack of lateral hydrologic connectivity and bulk water movement in the BP. This is likely due to the general water deficit and lack of regional or mesoscale gradients needed to drive appreciable lateral groundwater flow. The general separation of groundwater and pond Ic-excess indicate that there could be limited water movement between groundwater and surface water, specifically from ponds to groundwater. Recharge in this region, albeit small, most likely isolates the forested uplands from surface water bodies or larger flow systems (Winter et al., 2003). Alternatively, it may be that either any pond water that does flow to mineral forestlands is taken up by vegetation and does not affect groundwater isotopic signatures or the volume of any groundwater that does flow to ponds is insufficient to affect pond isotopic signatures. Additionally, because BP pond budgets are dominated by P

and ET, even in ponds that are considered “groundwater fed,” groundwater contributes only <20% to 30% of the total pond budget (Shaw et al., 1990; Smerdon et al., 2005). While relatively small groundwater fluxes to ponds can have considerable effects on nutrient budgets (LaBaugh et al., 1995; Plach et al., 2016; Schuster et al., 2003), the strong fractionating effects of pond evaporation overwhelm the short-term isotopic mass balance without site-specific characterization (Gibson et al., 2002), especially during the summer months (Cui et al., 2018).

2.4.4 Annual and Interannual Variability

The generally low recharge rates in the BP, which are a product of the long-term subhumid climate, are a primary control over water table position and groundwater flow in the BP and make the landscape sensitive to annual and interannual variability of climate. The relative control that topography has on WT position and groundwater flow is highly dependent on recharge rates (Goderniaux et al., 2013), which in this case are generally low but vary when multiyear deficits or surpluses accumulate. Consequently, the CDM-3 is a good indicator of the interannual effects of climate (Figure 2-6; supporting information), where the lowest water tables occurred in 2003 (lowest CDM-3), even though this year had an average annual P. However, the differences in WT position in 2003 (lowest CDM-3) and 2013 (highest CDM-3) within a given HRA were not as great as the differences seen between HRAs. Overall, the CO-Perched sites were least affected by multiyear climate signals, while the HM and CO HRA sites were more sensitive. In the CO-Perched HRA, the deep water table reflects deep storage that is unaffected by surface fluxes like ET and P, while the shallow water table is perched on low conductivity layers with very low storage. In the HM HRA, the water table more closely follows topography during wet periods, both annually and interannually. Although CP HRA sites show high seasonality, they do not appear responsive to cumulative climatic wetting or drying. No significant relationship between groundwater chemistry and climate was observed in this study.

2.4.5 Chemoscapes and Isoscapes as Management Tools

Establishing a geochemical and isotopic “baseline” with a quantification of an area’s natural variability is an important prerequisite when managing a landscape, either predisturbance or postdisturbance (Edmunds et al., 2003). Here I provide basic chemoscapes and isoscapes in the context of HRAs as both (1) a guideline for the natural spatiotemporal variability of groundwater geochemical and isotopic signatures in a predisturbance environment and (2) an example to demonstrate the importance of understanding and interpreting other hydrogeological data while considering surficial geological heterogeneity and scale of groundwater flow.

I observed striking differences in both EC (section 3.5) and major ion concentrations (Figure 2-8) between HRAs at URSA. The characterization of typical BP groundwater chemoscapes (i.e., salinity, with major ion concentrations and compositions, and spatiotemporal variability) provides stakeholders with the appropriate information to set goals and measures for evaluating the success for large-scale reconstruction

efforts, such as in the oil-sands region of Canada (BGC Engineering Inc, 2010), or for small-scale reclamation efforts, such as well pad or road reclamation (MacKenzie and Renkema, 2013).

Isoscapes, expressed in the dual-isotope space and as $\delta^{13}C$ -excess, demonstrate the importance of having an a priori understanding of geological and climatological heterogeneity before interpreting results of large-scale spatial sampling campaigns. Synoptic isotope sampling has become a popular method of characterizing major hydrologic fluxes and fates; however, they are rarely contextualized regarding groundwater processes (Scheliga et al., 2017). Here I show that in a highly heterogeneous landscape, groundwater isoscapes persist through time in each HRA. However, synoptic sampling campaigns should not be interpreted across HRAs, but only within them. Due to the spatiotemporal variability of groundwater-surface water interactions and processes, individual isotopic signatures cannot be taken at “face-value” and applied to a wide spatial extent, without first considering the climatic and geologic context. Nevertheless, isoscapes are a useful tool for elucidating HRA-scale controls over groundwater flow and groundwater-surface water connectivity in the context of additional hydrogeological data.

2.5 Conclusions

It has been shown previously that the dominant fluid potential in any part of a regional basin is essentially the fluid potential at the topographic surface; in other words, groundwater flow and water table position are topographically driven. In glaciated landscapes and regions with low-recharge, smaller-scale heterogeneities in geology and recharge can be a dominant factor over topography, notably in areas with high conductivity or hummocky terrain. Glacial depositional landscapes are highly complex regions with spatially heterogeneous storage and transmission properties and temporally variable recharge potentials, resulting from the delicate, and often tipped, balance between P and ET. The use of HRAs to evaluate hydrogeological characteristics of the typical glacial landforms found in the BP provides a convenient and holistic way of discretizing the landscape into subunits with unique hydrogeological properties and water table conditions. While small catchment or HRU delineation has been a dominant focus in the hydrology community, often relying on surface topography as a first-order control, I stress the need to consider subsurface characteristics and processes, especially in landscapes with low recharge and low relief.

This increased understanding of underlying processes and controls provides the framework for better understanding the effects of disturbance and the hydrologic function of both undisturbed and reclaimed landscapes. In the midst of unprecedented development in the BP there is an urgent need for engineered, constructed, and reclaimed landscapes that are predictable and operable from hydrogeological and hydrological perspectives. Such landscapes will be composed of native glacial materials. The results of this study provide managers and stakeholders with an understanding of the dominant controls on hydrological processes at a more useful operational scale, the scale between the basin scale and the hillslope scale. These results indicate that managers should consider the complex interactions of topography, recharge, and texture when planning and managing disturbed and reconstructed landscapes and that they are more spatially and temporally variable than previously thought.

Table 2-1. Topographic characteristics for each hydrologic response area at URSA

		Slope (%)	Elevation (m asl)			Area (km ²)
		Mean	Min	Max	Range	Total
HRA	CO	1.43	656	719	63	160
	HM	1.30	642	690	48	95
	CP	0.56	630	669	39	610
All	URSA	0.79	630	719	87	865

Note. URSA = Utikuma Region Study Area; HRA = hydrologic response area; CO = coarse outwash; HM = hummocky moraine; CP = clay-till plain; asl = above sea level.

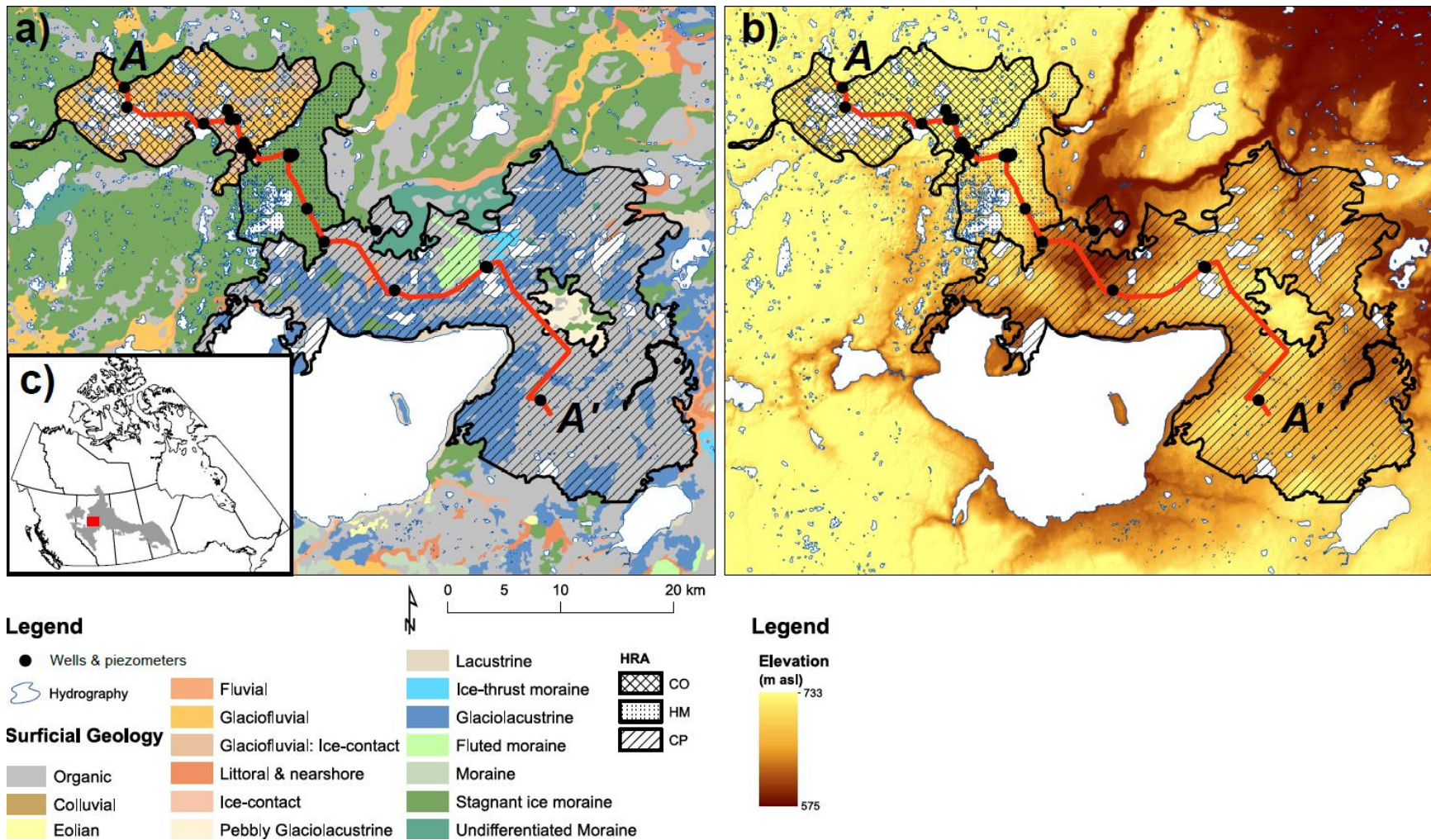


Figure 2-1: The (a) surficial geology and (b) ground elevation of the Utikuma Region Study Area (URSA; ~103 km²), and its relative location within (c) Canada and the Boreal Plains ecozone (Marshall et al., 1999), with well locations, and delineated HRAs: Coarse outwash (CO), hummocky moraine (HM), and clay plain (CP).

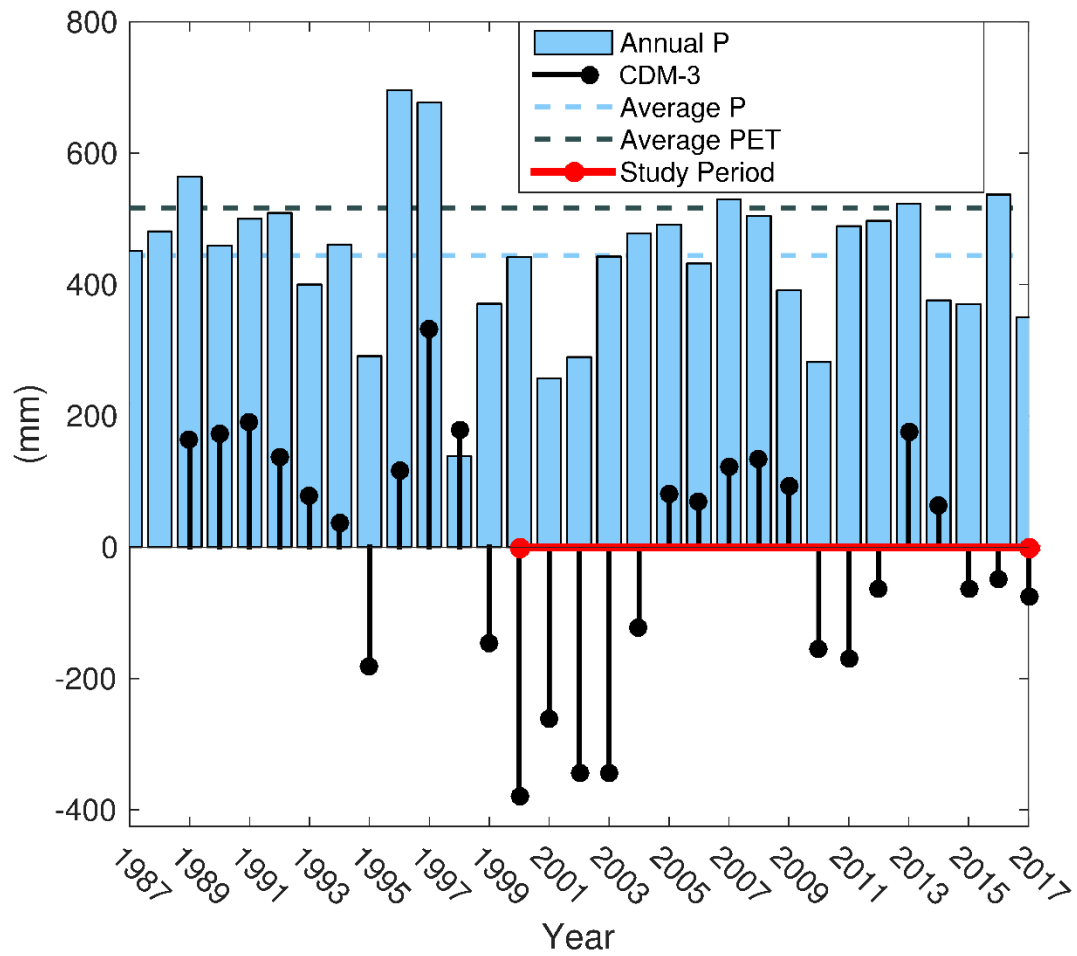


Figure 2-2: Annual precipitation data and three-year cumulative departure from the mean P (CDM-3) for URSA, before and during the study period. Long-term average annual P (444 mm; 1987-2015) and PET are shown for context. Pre-1998 data were obtained from Alberta Agriculture and Forestry (2018).

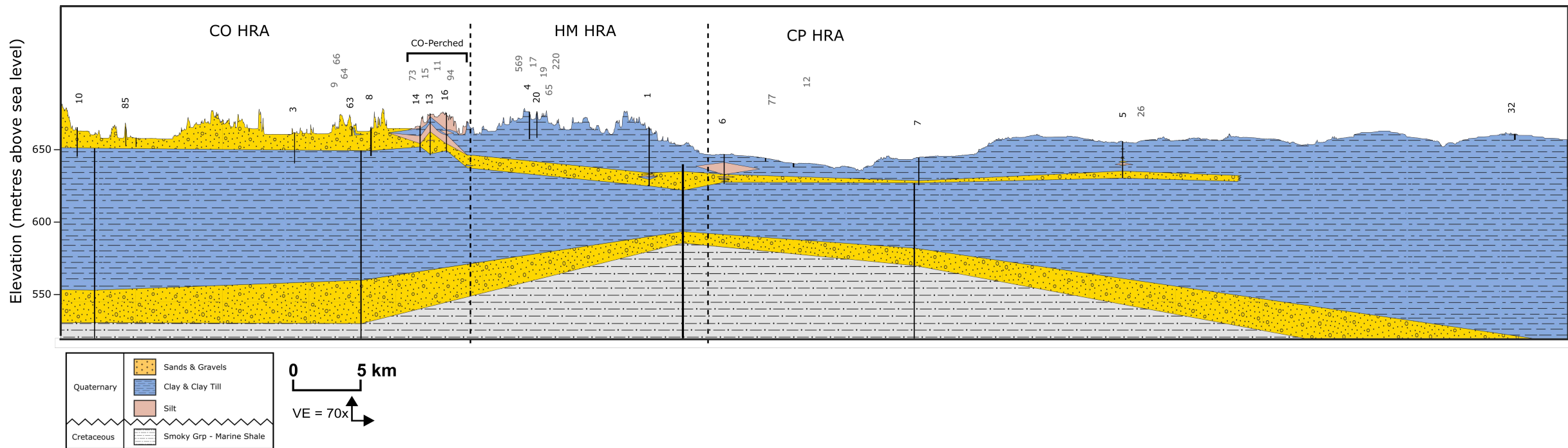


Figure 2-3: Generalized geologic cross section along transect A – A' (Figure 2-1), showing the HRA boundaries (dashed lines) and well locations (black numbers indicate sites on the cross section; grey numbers indicate sites off the cross section). Vertical lines represent boreholes. Boreholes that intersect the bedrock (in grey) were collected by the Alberta Research Council, who did not differentiate between materials outside of sand units (Ceroici, 1978; Vogwill, R. 1978). Shallow boreholes (in black), that intersect the surface, were collected as part of this study.

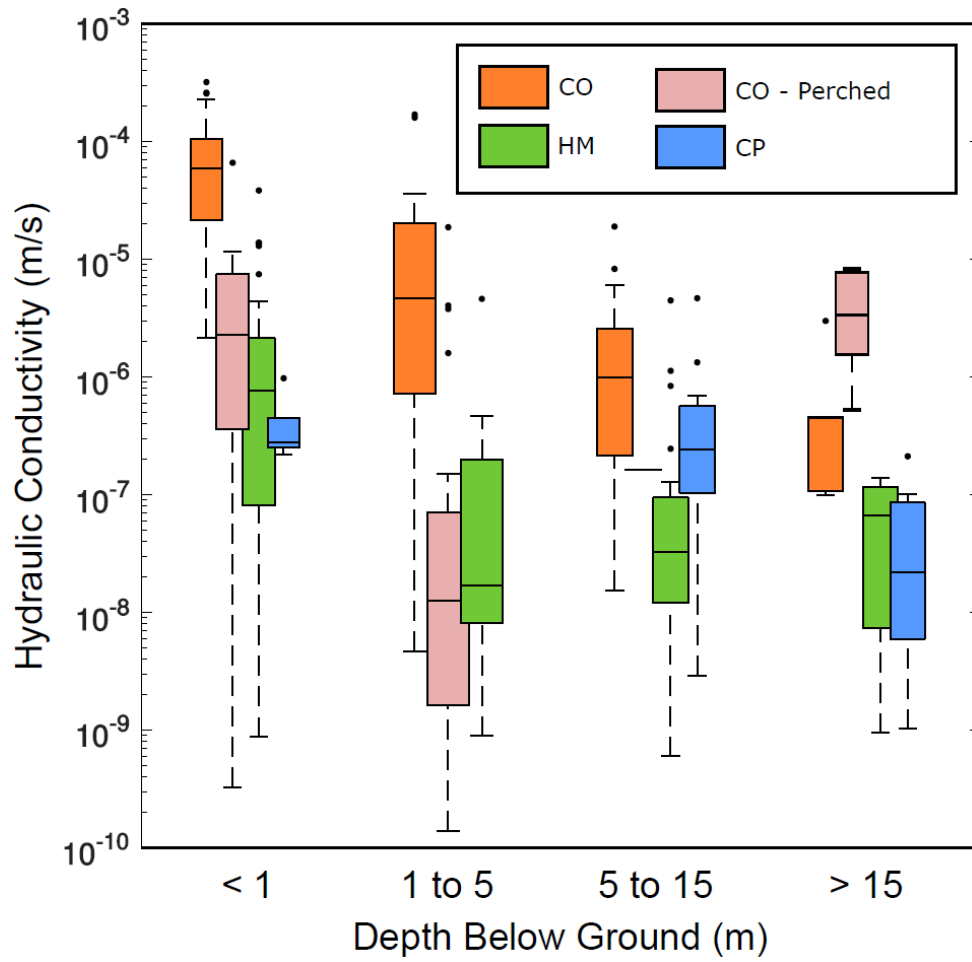


Figure 2-4: Hydraulic conductivity distributions by depth for each HRA. On each box, the central horizontal line indicates the median, the bottom and top edges of the box indicate the 25th and 75th percentiles, respectively; whiskers show the most extreme data not considered outliers (individual black dots).

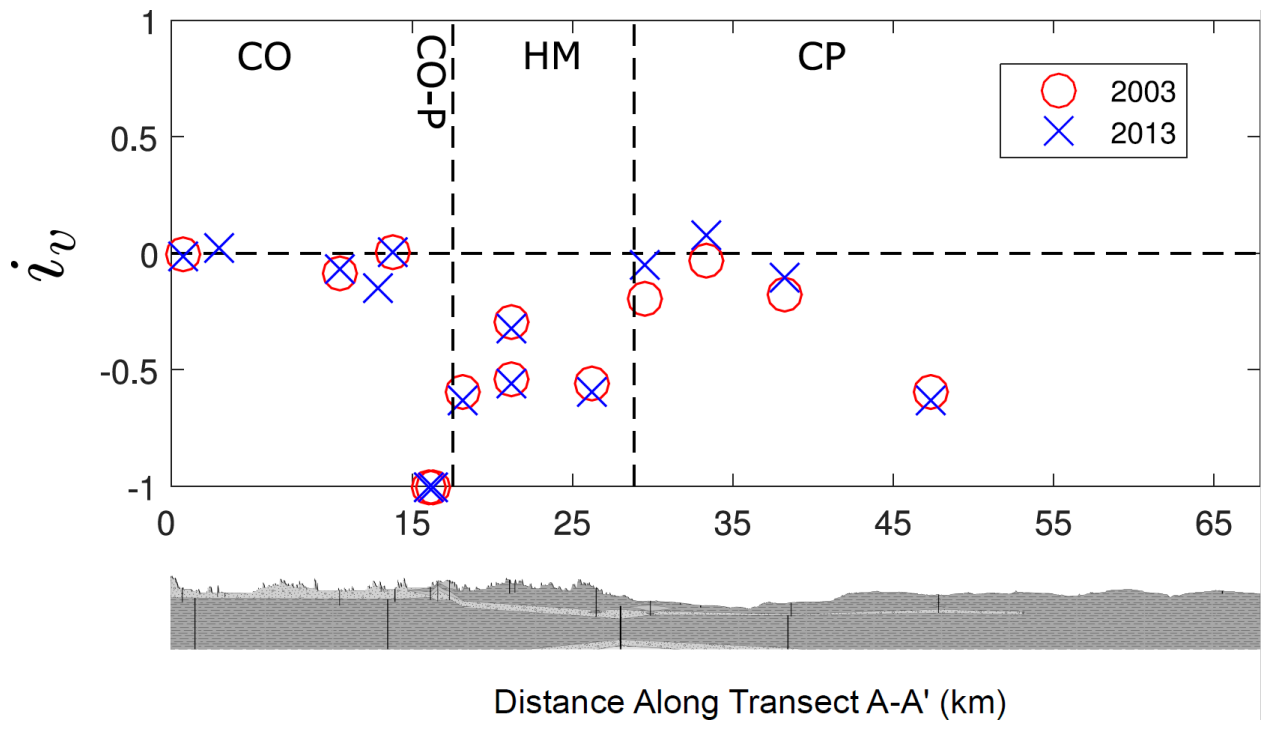


Figure 2-5: Vertical hydraulic gradients (i_v) along the transect A-A' (Figure 1) for the driest (2003) and wettest (2013) years during the study period. Positive values indicate an upward, discharge gradient. A generalized cross section is shown for context.

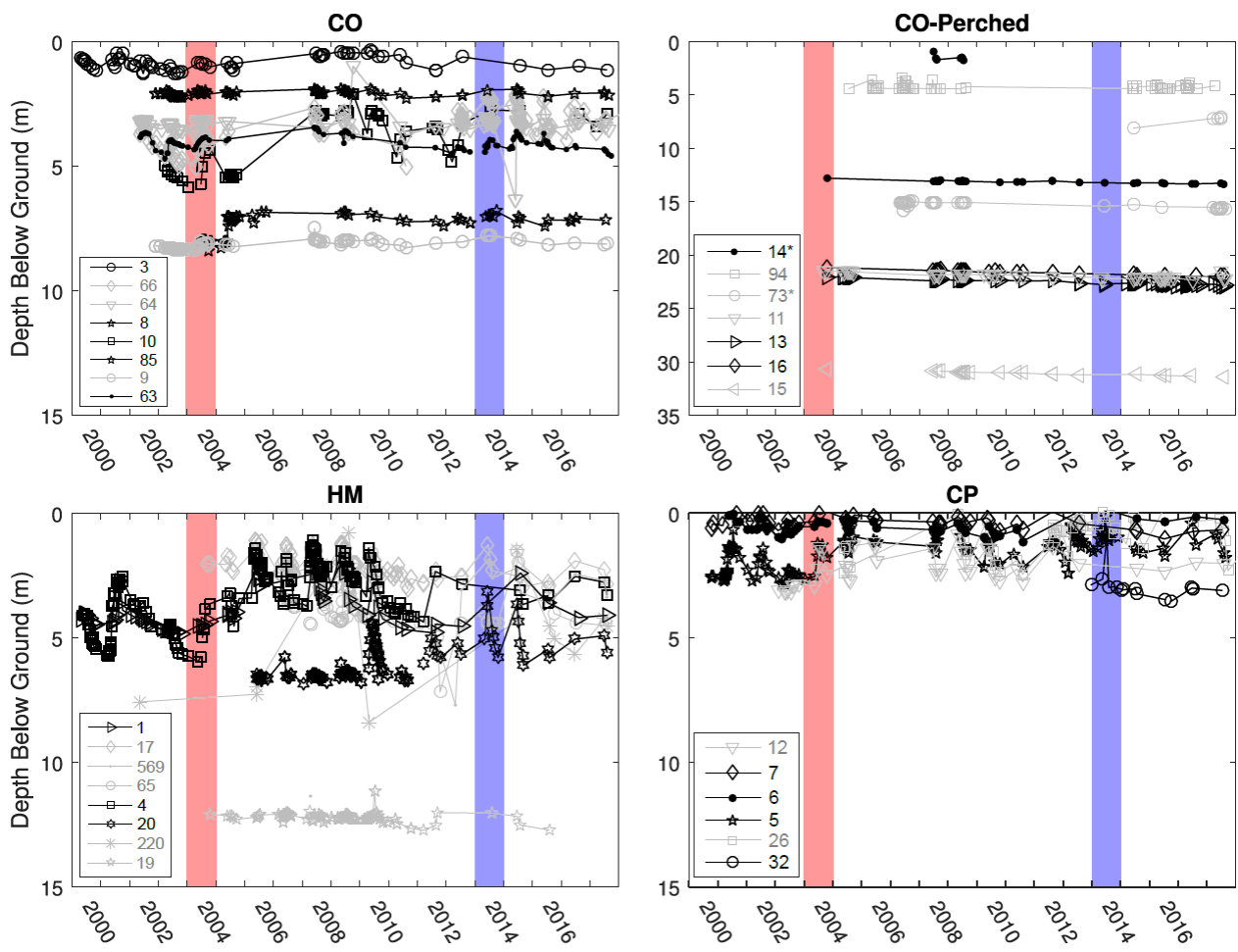


Figure 2-6: Time series for water table depth at each site. Blue and red zones indicate representative wet (2013) and dry (2003) years, respectively. Black symbols represent sites on the cross section (Figure 3); grey symbols represent sites off the cross section. Each legend is organized by elevation of site (lowest to highest). Lines connecting data points are shown for visual purposes only and do not infer known data. Dry well data are not shown.

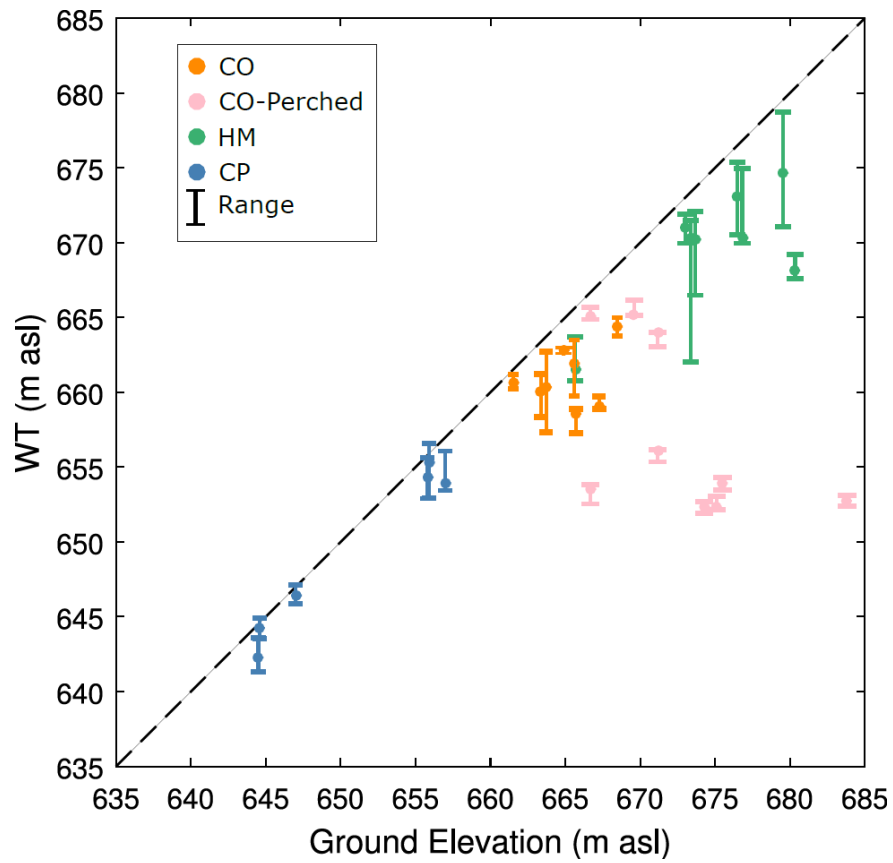


Figure 2-7: Long-term water table elevations measured at wells throughout the study period. Circles and bars denote median and historic range of water table elevation, respectively, at each site.

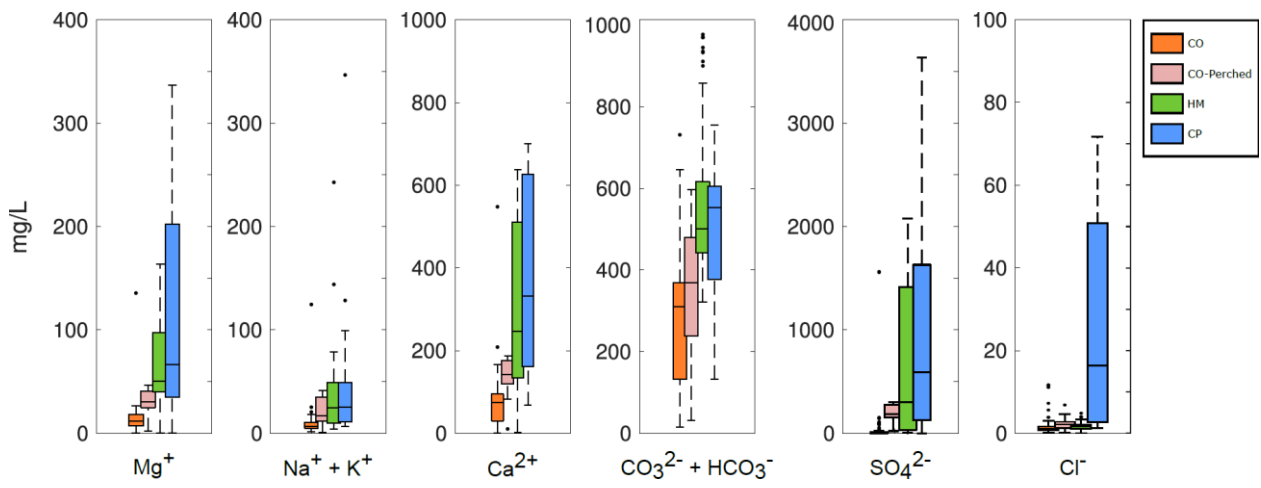


Figure 2-8: Boxplots of concentrations of major cations and anions in groundwater samples spanning the study period. See Figure 2-4 for an explanation of the boxplot characteristics.

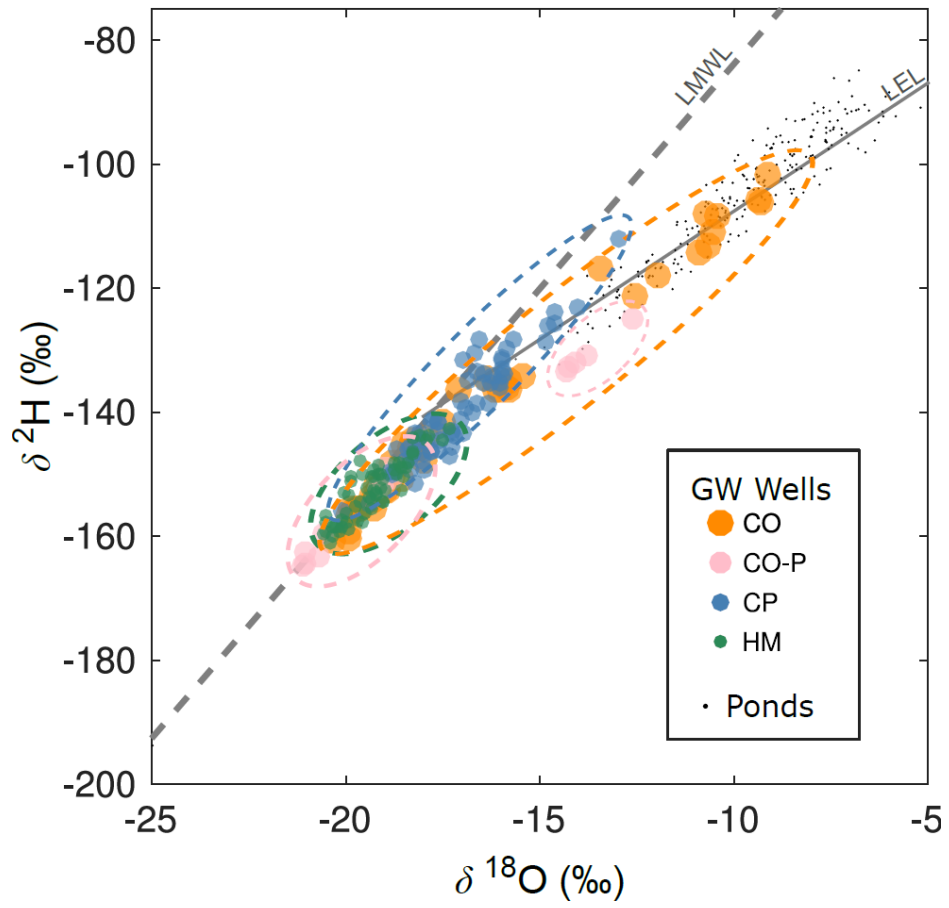


Figure 2-9: Dual isotope plot of groundwater and surface water samples spanning the study period. The URSA LMWL (dashed line) and URSA LEL (solid line) are shown for context. Size of data points vary for visual purposes only. Dashed regions indicate delineated isoscapes.

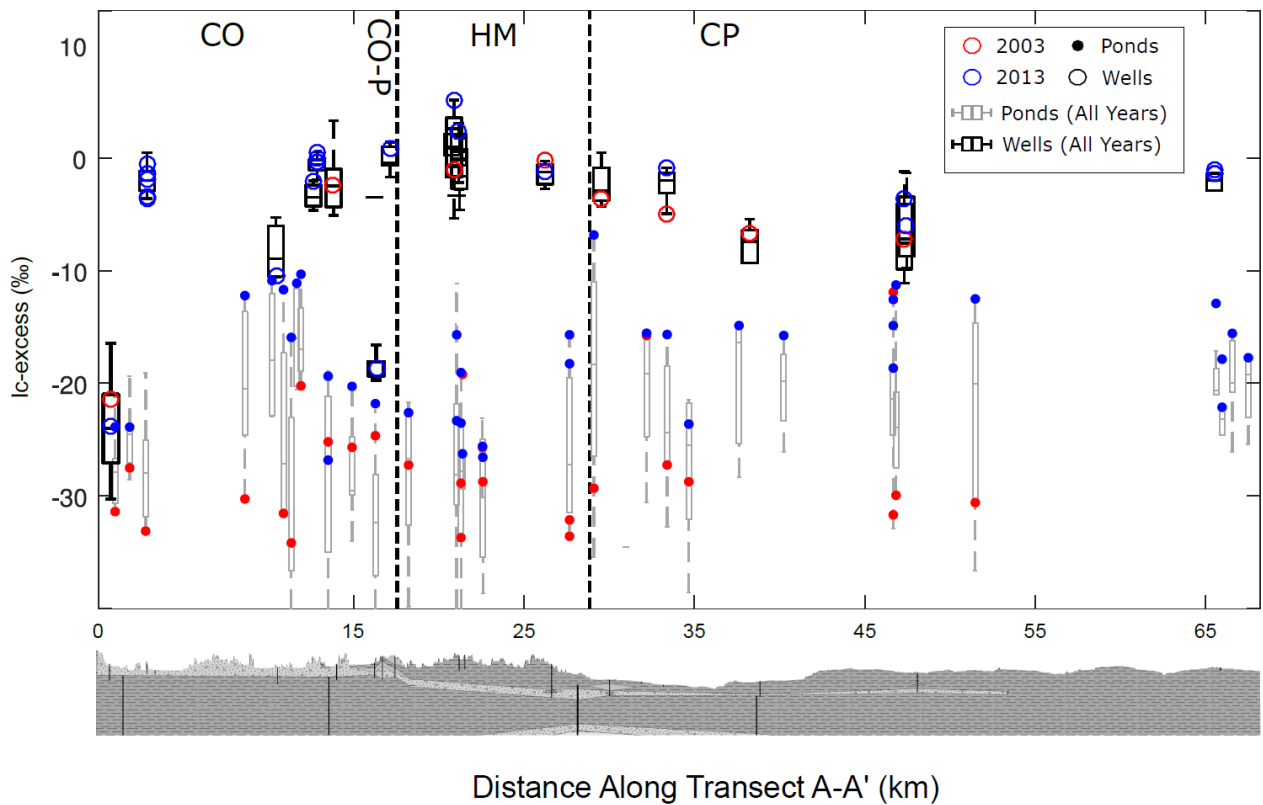


Figure 2-10: The line-conditioned (l_c) excess of surface and groundwater stable isotope samples taken at URSA over the study period, with HRA boundaries shown as dashed lines. For sites and ponds not directly on A-A', distances were interpolated. An l_c -excess value close to zero indicates little difference between samples and local P; whereas more negative values indicate higher degrees of fractionation (evaporation). Not all sites were sampled during both the dry (2003) and wet (2013) year.

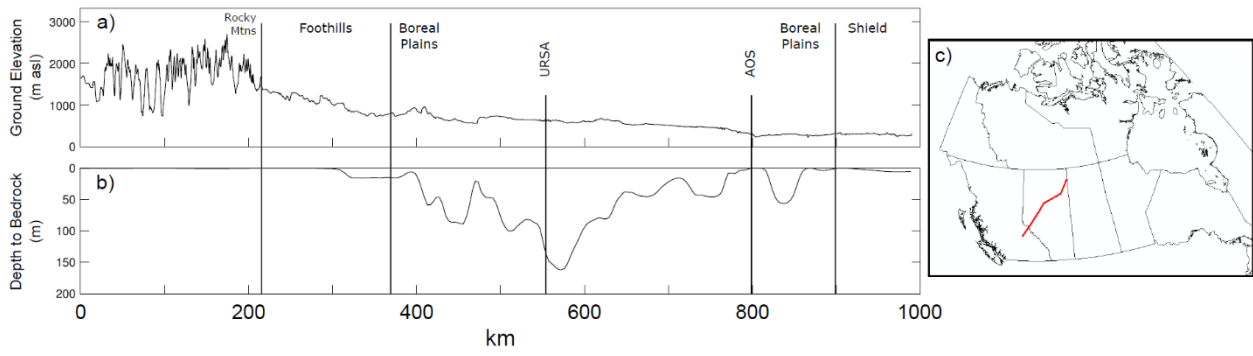


Figure 2-11: Basin-scale profile showing (a) ground-surface elevation and (b) depth to bedrock from (c) the Rocky Mountains to the Canadian Shield. URSA is located near the middle of a basinal flow system in an area of low relief with thick unconsolidated substrates.

Chapter 3

Landscape controls on surface water-groundwater interactions on shallow outwash lakes: Long-term groundwater signal overrides interannual variability due to evaporative effects

3.1 Introduction

Shallow lakes in the sub-humid climate of Canada's Boreal Plains (BP) exist in a fine balance between precipitation and evaporation. However, in coarse-textured landscapes, the connection to larger-scale groundwater flow systems may buffer these lakes from most precipitation-deficit conditions and can decrease a lake's sensitivity to anthropogenic impacts, both of which are common in the BP region of Canada (Arnoux et al., 2017; Smerdon et al., 2005). Yet, although groundwater influxes to lakes, even at low rates, are often important to both hydrologic and nutrient budgets, the process is poorly understood and often ignored (LaBaugh et al., 1995; Plach et al., 2016; Rosenberry et al., 2015; Schuster et al., 2003).

The BP is characterized by numerous shallow lakes and lake-wetland complexes underlain by thick glacial deposits, which result in interdependent surface water processes and groundwater flow systems with varying spatiotemporal controls (Lennox et al., 1988; Lisse, 1971; National Wetlands Working Group, 1988; Winter, 1999, 2001). These shallow lakes act as important ecological, biodiversity, and biogeochemical hotspots (Beklioglu et al., 2016; Cheng et al., 2017), and are critical for continental waterfowl populations (Blancher and Wells 2005; Mack and Morrison, 2006; Slattery et al. 2011), indigenous traditional uses and recreational activities (Parlee et al., 2012). The sub-humid climate, where evapotranspiration often equals or exceeds precipitation, results in a delicate water balance with large evaporative demands (Bothe and Abraham, 1993; Devito et al. 2005a, 2005b). The BP also experiences multi-year wet and dry cycles, with the potential for increases in frequency and extremes of multi-decadal drought cycles with climate change (Bonsal et al., 2013; Ireson et al., 2015; Mwale et al., 2009). During these extended dry periods some isolated shallow lakes dry out completely, while other lakes, better connected to groundwater sources, are permanent fixtures in the landscape (Smerdon et al., 2005; Thompson et al., 2017). Impacts of climate and geology on surface water-groundwater interactions are largely unknown and are difficult to predict due to the large interannual variability in precipitation and evaporation and subsequent variability in shallow lake water budgets observed in this region (Devito et al., 2012; Ireson et al., 2015). The hydrology, biogeochemistry, and ecology of boreal shallow lakes are at an ever increasing risk to impacts due to anthropogenic activity, such as forestry, oil and gas, agriculture, increased wildfire frequency and magnitude, and climate change (ESTR, 2014; Ireson et al., 2015; Schindler, 1998). Shallow lakes, especially those with large catchments areas, have been shown to be particularly sensitive to eutrophication, salinization, and alkalinization as anthropogenic and climatological impacts effects these lakes (Tammelin and Kaupilla, 2018).

The role of groundwater is an important factor in determining lake permanence and resilience to change. Although groundwater flow is much slower than surface flow, the area of interaction between a lake and an adjacent groundwater flow system is large and the flow is usually more uniform, which results in appreciable volumes of water entering and/or leaving a lake on an annual basis (Freeze and Cherry, 1979; Tóth, 1999). Understanding and anticipating surface water-groundwater interactions and dynamics for these lakes are essential for forecasting water quantity and quality in the BP; however very few lakes in this region are gauged, monitored, or sampled. Consequently, techniques and frameworks to evaluate surface water-groundwater connectivity are needed to better predict lake sensitivity and response to climate change.

There have been many intensive studies in the BP on singular lakes or connected lake systems (e.g., Ferone and Devito, 2004; Gibson et al., 2002, 2015, 2016; Riddell, 2008; Shaw and Prepas, 1980; Smerdon et al., 2005, 2008; Thompson et al., 2015); however, these studies have focused on a single lake, deeper lakes, or purely isolated or headwater lakes. The long-term dynamics and patterns of surface water-groundwater interactions with shallow BP lakes are not well studied. While it has been shown that there is minimal lateral subsurface hydrologic connectivity through fine-textured mineral substrates in the BP, there is evidence of local to large-scale groundwater connectivity in coarse-textured landscapes (Chapter 2; Devito et al., 2017; Ferone and Devito, 2004; Smerdon et al., 2005). Coarser-textured substrates tend to have deeper water tables and higher rates of groundwater recharge to provide base flows during dry periods (Devito et al., 2017; Haitjema and Mitchell-Bruker, 2005; Smerdon et al., 2008;).

Extensive research conducted in the glacial outwashes of the American Midwest shows that lake-groundwater connectivity can be dynamic and operate at different scales resulting in variable groundwater contributions to lakes (Cherkauer and Zager, 1989; Jaquet, 1976; Kenoyer and Anderson, 1989; Krabbenhoft et al., 1990; Krabbenhoft and Webster et al., 1995; LaBaugh, 1986; LaBaugh et al., 1997; Siegel and Winter, 1980; Winter, 1986). Studies in northern Wisconsin showed that landscape position had a strong control on groundwater contribution within the same flow system, where lower lakes had the highest contributions from groundwater (Kratz et al., 1997; Webster et al., 1996). Additionally, lakes that received greater contributions from groundwater were more resistant to drought, had higher biodiversity, and higher concentrations of base cations. However, the annual precipitation (i.e., potential groundwater recharge) at these Wisconsin lakes is up to 50% higher and the lakes are much deeper than in the BP. In such humid regions groundwater flow is characteristically driven by topography and flow is therefore more predictable and temporally stable than in the BP, where the water table is often not a subdued replica of surface topography (Chapter 2).

In the sub-humid climate of the BP, evaporation is commonly the largest component of lake water budgets (Devito et al. 2005a; Smerdon et al., 2005; Thompson et al., 2015). Accordingly, the onset and duration of evaporation is an important control on lake stage. Precipitation and groundwater inputs are therefore critical fluxes for shallow lake water level maintenance. Although local-scale groundwater flow systems adjacent to lakes can be both temporally and spatially dynamic, lakes positioned low in regional-scale flow systems may have more temporally stable groundwater flow (Webster et al., 1996).

The objective of this study was to evaluate and compare the relative groundwater contributions to eleven lakes located in a coarse-textured glaciofluvial outwash in the sub-humid BP to determine the landscape controls of lake-groundwater interactions. Annual mid-summer stable O and H isotope ratios over eight consecutive years were used for the analysis. Specifically, I aim to determine if (i) the spatial patterning between lake summer stable water isotope ratios was temporally persistent, (ii) lake landscape position controls interannual variability of isotopic ratios, and (iii) lakes lower in their respective flow system do indeed have greater groundwater contributions. Alternatively, (iii-a) I test whether lakes with lower area-to-depth ratios are merely systematically associated with less evaporative influence on the isotopic mass balance leading to similar conclusions regarding groundwater inputs, albeit through a different mechanism. I expect that isotopic compositions of lakes positioned lower in the landscape will indicate relatively large non-evaporative water inputs from groundwater with low interannual variability, while those of lakes with higher landscape positions will indicate more evaporative effects with notably higher interannual variability.

3.2 Methods

3.2.1 Study Area and Hydrogeology

The Utikuma Region Study Area (URSA; 56°N, 115°W) is located 370 km north of Edmonton, Alberta, in the BP ecozone of Canada (Figure 3-1, inset). The climate is sub-humid with historic annual potential ET (517 mm; Bothe and Abraham, 1993) often exceeding the historic average annual P (481 mm; Marshall et al., 1999). The region is characterized by low topographic relief and thick (45 to 240 m) heterogeneous glacial substrates overlying the Smoky Group, a marine shale of Cretaceous age (Vogwill, 1978). This study focuses on eleven lakes on a coarse-textured glaciofluvial outwash that are shallow, cold polymictic lakes, but vary in landscape position, potential groundwater contributing area and lake area.

While all eleven lakes are in the coarse outwash, there is some variation in texture within the outwash and can be separated into 4 distinct systems. Three lakes (7, 11, and 19) are located at the transition between coarse outwash deposits and a fine-textured hummocky stagnant ice moraine; they have closed basins with no channelized inflows. Lake 19 is in silt rich glacial fluvial material deposited on a thick low-permeability clay layer 12 m above the regional water table in the underlying sand aquifer, which is part of the coarse outwash (Chapter 2). Lake 19 has been shown to have limited to no local groundwater input and the water budget is controlled by precipitation and evaporation (Riddell, 2008). Lakes 7 and 11 have both disintegration moraine and glacial fluvial ice-contact deposits near the basin and in the surface topographic catchments. Based on surficial geology maps (Fenton et al., 2013) and elevation, it is suspected that Lakes 7 and 11 are functionally similar to Lake 19; however, no deep wells are situated adjacent to the lakes to confirm this.

Lakes 208, 206, and 201 are in a region with clean, well-sorted sands. Lake 206 has first order channelized inflow from a local catchment with mixed disintegration moraine and glacial fluvial deposits. There are no channelized surface connections between Lakes 206 and 201 or 208, but diffuse flow through wide peatlands occurs at Lake 201 and 208 outlets. Lake 206 is adjacent to fine-textured

hummocky stagnant ice moraine deposits; however, boreholes confirm that it is not perched on fine-textured sediment and is well connected to the coarse outwash.

Lakes 1, 17, 16, 5, and 2 are located between the two regions (i.e., the low permeability clays in the eastern region of the study area and the clean sands in the western region) and are characterized by sands and gravels with notable laterally discontinuous silt lenses. No surface outflow or channelized inflow is visible between lakes 1, 17, 16 and 5. Diffuse flow through wide alluvial fens occurs at the outflow area of Lake 16. Diffuse flow and occasional channelized flow through a fen wetland connect an upstream lake to the north with Lake 1. Surface flow is present from Lake 5 to Lake 2, and channelized outflow is visible at Lake 2. All near surface lateral diffuse inflow or outflow in wetlands and channelized flow have been historically or are currently influenced by beaver activity. Lake 19, and presumably Lakes 11 and 7, which are perched on fine textured sediment, contribute recharge to the underlying coarse sand aquifer which connects Lakes 17, 16, and 5; however, they are hydraulically separate from the adjacent groundwater flow system.

All the lakes examined are within a 50 km² study area and are therefore subject to similar weather and climate conditions (Devito et al., 2016). Disregarding the possible effects of wind sheltering due to surrounding vegetation, precipitation and evaporation fluxes have been assumed similar amongst the lakes. The primary dissimilarities between these lakes are therefore variable groundwater-surface water interactions and lake morphometry (i.e., area and depth). Daily precipitation amounts were collected throughout the study period (2012 – 2019) using two to three tipping bucket rain gauges adapted for snowfall using an antifreeze reservoir. Lake area was determined from air photos. Multiple lake depth measurements were taken by boat or during ice cover during average climatic conditions (i.e., mesic conditions, not during prolonged drought or deluge; Kevin Devito and Samantha Leader, unpublished data). Lake volume was approximated as the product of lake area and average lake depth, which is a reasonable representation for the purpose of comparing lakes within the same region (Hayashi and van der Kamp, 2000).

Landscape position was determined for each lake following the approach of Kratz et al. (1997) and Webster et al. (1996), which considers the relative location of each lake within their local hydrologic flow system in addition to the topographic elevation. Given a specific locale, landscape position should provide a method for predicting lake responses to drought, water quality, and ecological viability for aquatic communities (Kratz et al., 1997). Lake elevation and potential groundwater capture areas were determined from a DEM (Montgomery et al., 2019).

Groundwater flow systems were estimated for the study area using regional topographic relief, and further informed by previous studies (Chapter 2; Riddell, 2008; Smerdon et al., 2005). Potential groundwater capture areas for each lake were determined by delineating flow systems using regional highs and lows. The high permeability substrates and low groundwater recharge typical of this BP outwash result in water tables that may not mimic local topography and extend far beyond the local hillslopes adjacent to each lake (Winter, 2003). Regional-scale ridges and valleys were used to constrain the groundwater capture areas and local topographic highs (i.e., 5 to 10 m relief) were disregarded. Delineating groundwater flow systems in high permeability, low relief, locally hummocky

regions such as this can be difficult. The groundwater contributing area to lakes in this type of terrain and geology most certainly extends beyond local surface watersheds and changes through time (Winter et al., 2003). Consequently, it is assumed that the flow system extents (Figure 3-1) are conservative estimates. Additionally, the focus is on the position of lakes within each flow system and comparisons within flow systems where possible.

3.2.2 Stable O and H isotope ratios in water

As part of the Hydrology, Ecology and Disturbance (HEAD) long-term research and monitoring project in URSA (Devito et al., 2016), precipitation (n = 696), lakes (n = 759), and groundwater wells (n = 614) were sampled throughout the year for stable O and H isotope ratios in water from 1999 to 2019. Precipitation samples were collected at three different meteorological stations (Figure 3-1). Rain was sampled using collectors specifically built to prevent fractionation, either that of Gröning et al. (2012) or using mineral oil to prevent evaporation from the collector, while snow samples were collected as soon after snowfall as possible as described in Clark and Fritz (1997). Due to the remote nature of the study sites, the rain collectors captured multiple storm events before being sampled and therefore the resultant local meteoric water line (LMWL) is not weighted. Sampled groundwater wells ranged from 0.5 to 5.5 m below the ground surface; details regarding groundwater well installation and sampling are outlined in Chapter 2.

For this study, the eleven study lakes were sampled between day-of-year (DOY) 184 and 193 annually from 2012 to 2019 for stable isotope ratios of O and H in water. Water samples were collected at a depth of 20 to 40 cm from the lake surface (Sass et al., 2007). All lakes are polymictic and well mixed. Each yearly sampling campaign was completed within a 2 or 3 day period. Therefore, on a year-to-year basis, the lakes were “ice-free” and free to evaporate for comparable periods of time each year. Lakes that could be safely accessed by snowmobile (19, 206, 201, 208, 17, 16, 5, 2, 1) were sampled on March 20, 2020, near the end of the winter lake ice season. During this winter campaign, samples were collected from the top and bottom of the water column as well as near the bottom of the lake ice. Ice thickness was uniform (51.5 ± 5.2 cm) between lakes.

Measured isotope ratios are given in per mil (‰), relative to Vienna Standard Mean Ocean Water (VSMOW), in both a dual-isotope space and as the line-conditioned excess (lc-excess). All isotopic analyses were performed at BASL laboratory, University of Alberta, Edmonton, AB, Canada (<http://www.biology.ualberta.ca/basl/>).

The influences of evaporation and sources of water to a lake can be inferred using a secondary isotope-derived parameter, line-conditioned excess (Esquivel-Hernandez et al., 2018; Landwehr and Coplen, 2006; Sprenger et al., 2017). Line-conditioned excess is a locally relevant metric, compared to the global meteoric water line, which is used in calculating deuterium excess (Dansgaard, 1964). Line-conditioned excess is defined as:

$$\text{lc-excess} = \delta^2\text{H} - a\delta^{18}\text{O} - b \quad [3.1]$$

where a and b are the slope and intercept of the LMWL, respectively (Landwehr and Coplen, 2006). The $\delta^{18}O$ -excess describes the offset of a water sample from the LMWL in dual isotope space, where a negative $\delta^{18}O$ -excess value is indicative of evaporative fractionation. If a body of water, such as a lake, is initially formed by meteoric water (i.e., precipitation), it will plot directly on the LMWL and have an $\delta^{18}O$ -excess value of zero. If that lake is allowed to freely evaporate, the lighter isotopologues of water will preferentially escape through the process of kinetic fractionation and the lake water will plot below the LMWL and have a negative $\delta^{18}O$ -excess value.

Due to the shallow nature of the lakes studied here, they receive shallow poorly mixed groundwater, the isotopic signature of which can vary temporally and spatially. Additionally, the volume, precipitation input, groundwater outflow, and isotopic composition of boreal lakes may experience high variability due to summer convective storms, seasonal ice cover, and evaporation-induced fractionation; therefore, I do not perform a transient or steady state isotopic mass balance (Gibson et al., 2002; Krabbenhoft et al., 1994). Rather, I use long-term spatial trends to compare differences in isotopic compositions to infer relative groundwater contributions to the study lakes.

3.3 Results and Discussion

3.3.1 Groundwater flow systems

Four separate hydrologic flow systems were delineated for this study. Groundwater flow is from areas and lakes at higher elevations to lakes at lower elevations within the same flow system without significant groundwater exchange between flow systems, were identified for the purpose of this study: (1) isolated Lakes 11, 7, and 19, which are at the highest landscape positions, are isolated from groundwater inputs and have no visible surface inputs; (2) the western groundwater flow system, where Lake 206 is in the highest position and Lakes 201 and 208 are in similar positions; (3) the eastern groundwater flow system, where Lake 17 is in the highest position and Lake 2 is the lowest; and (4) a central groundwater flow system, where Lake 1 is in a low position before the flow systems joins the western system at Lake 2 (Table 3-1).

Conceptualized groundwater contributing areas for each lake are shown in Figure 3-1. Within these areas the gross groundwater flow is assumed to be from high elevations to low elevations. Due to the coarse texture of the outwash sediments, the contributing area for lakes low in the flow system are large and extend well beyond local ridges (Winter, 2003). Alternatively, the potential groundwater capture areas are small for lakes located near the upper ends of flow systems. Potential groundwater contributing areas were calculated (Table 3-1); however, these boundaries extend, for some lakes, into regions with fine-textured sediments (i.e., predominately silts and clays). Due to their low hydraulic conductivity (Chapter 2) these fine-textured regions most likely do not generate appreciable groundwater flow when compared to the high-conductivity coarse-textured outwash; areal estimates both with and without estimated areas of fine-textured sediments are shown in Table 3-1.

3.3.2 Long-term isotopic compositions of URSA lakes and groundwater

The LMWL for URSA derived from the long-term precipitation samples collected from 1999-2019 (Figure 3-2) is defined as:

$$\delta^2\text{H} = 7.25 \cdot \delta^{18}\text{O} - 11.4 \text{ ‰} \quad (\text{R}^2 = 0.98) \quad [3.2]$$

The slope of the URSA LMWL is lower than that of the global meteoric water line (GMWL; $\delta^2\text{H} = 8 \cdot \delta^{18}\text{O} + 10 \text{ ‰}$) of Craig (1961) and is similar to that of Mildred Lake (200 km NE of the URSA) in the Athabasca Oil Sands area of Alberta ($\delta^2\text{H} = 7.20 \cdot \delta^{18}\text{O} - 10.3 \text{ ‰}$; Baer et al., 2016). Rain at URSA has more isotopic variability than snow, with the $\delta^{18}\text{O}$ of rain ranging from -22.2 to -10.2 ‰ and snow ranging from -26.0 to -19.3 ‰, which represent the 5th and 95th percentiles, respectively.

Lake waters at URSA, which includes samples from over 30 lakes across URSA sampled over the same period (i.e., 1999 – 2019) plot on a local evaporation line (LEL), defined by:

$$\delta^2\text{H} = 4.41 \cdot \delta^{18}\text{O} - 63.3 \text{ ‰} \quad (\text{R}^2 = 0.91) \quad [3.3]$$

The long-term LEL has a slope of 4.41, similar to studies in nearby regions in central and northern Alberta (Gibson et al., 2016; 2019). The intersection of the LEL and the LMWL can be used as an estimate of the weighted mean isotopic composition of annual precipitation, which is often assumed to be the isotopic composition of input to the lake (Gibson et al., 1993; Paulsson and Widerlund, 2020). However, this may not be true for non-headwater lakes where the primary input could be groundwater. Here, the intersection falls approximately between the composition of rain and snow, tending towards rain ($\delta^{18}\text{O} \approx -18 \text{ ‰}$; $\delta^2\text{H} \approx -142 \text{ ‰}$; Figure 3-2a). The slope of the LEL showed high interannual variability and ranged from as low as 3.4 ($\text{R}^2 = 0.89$; $n = 42$) in 2017 and as high as 4.7 ($\text{R}^2 = 0.83$; $n = 52$) in 2012 (Figure 3-2a inset). This variability usually reflects the interannual variability of temperature, humidity, and wind over the evaporation season (Gibson et al., 1993) and may be influenced by strong seasonality of evaporation and ice coverage of lakes (Gibson et al., 2008). Just as the slope of the LEL varied year-to-year, so did the intercept with the LMWL as the weighted mean annual isotopic composition of precipitation changed year-to-year. The intercept varied by approximately 4 ‰ and ranged from -19 to -15 ‰ in $\delta^{18}\text{O}$ space.

For the most part, the isotopic ratios of the groundwater near the study lakes in the glacial outwash (Figure 3-2b) plot directly on the LMWL, meaning the groundwater is of meteoric origin and has not undergone evaporative fractionation. There are, however, some exceptions where wells intersect groundwater that was recharged directly from an adjacent lake and shows a fractionated signature and plots on the LEL; these cases are discussed in a later section. The isotopic composition of the groundwater at the outwash tends more towards that of snow and shoulder season (i.e., early spring and late fall) rain.

While the groundwater samples plot on the LMWL, there is considerable spread. This is evidence of the local and episodic nature of groundwater recharge typical of the BP. Most precipitation (50% to 60%) falls during summer months when vegetation is active and potential evapotranspiration is at its peak, therefore most groundwater recharge in the BP occurs outside of the growing season and

is the product of snow melt and late season storms (Smerdon et al., 2008; Thompson et al., 2015). Deeper groundwater, representing regional groundwater flow systems would be old and well mixed, and thus temporally uniform (Tóth, 2009). Studies which utilize lake isotopic mass balances or end member mixing analyses yield the best results when groundwater is uniform and well mixed, usually clustered at the intersection of the LEL and the LMWL (e.g., Arnoux et al., 2017; Gibson et al., 2019; Krabbenhoft et al., 1990; Petermann et al., 2018;); however, this is often assumed, yet may be untrue. Groundwater, especially shallow groundwater, is not well mixed and varies isotopically in both time and space (Figure 3-2b). In many studies the groundwater is either not sampled or not sampled extensively, either spatially or temporally (e.g., Jones et al., 2010; Shi et al., 2017; Zuber, 1983).

3.3.3 Ic-excess of study lakes

Due to the high interannual variability of the URSA LEL (slope and intercept) and groundwater isotopic ratios in the outwash, it is difficult to determine the starting composition or the composition of the inflow for the study lakes on an annual or sub-annual basis. While this variability makes creating an accurate mass balance difficult, the relative influence of evaporation in lakes can be inferred by using (Ic-excess (Equation 1; Landwehr and Coplen, 2006)), where a negative value indicates evaporative fractionation. Because both groundwater and precipitation at URSA plot along the LMWL, the Ic-excess parameter is more informative than $\delta^2\text{H}$ or $\delta^{18}\text{O}$ alone since it describes the offset of a water sample from its original meteoric composition, regardless of the variability due to seasonality along the LMWL (Esquivel-Hernández et al., 2018; Sprenger et al., 2017). Lakes with the smallest offset from the LMWL will have the highest (i.e., closest to zero) Ic-excess values and represent lakes whose water balance is least affected by enrichment due to evaporative fractionation. These lakes are generally more flushed by meteoric-sourced water (i.e., groundwater inflow and outflow). Conversely, lakes with large offsets from the LMWL will have low, more negative Ic-excess values and will represent lakes whose water balance is dominated by evaporative fractionation and have little to no external sources of water (Gibson et al., 2016). While there are characteristic temporal changes in lake Ic-excess due to the annual variations in the balance between precipitation and evaporative fractionation (Gibson et al., 1993), groundwater input can buffer these changes, where lakes with little or no groundwater input rely entirely on precipitation to mitigate volumetric losses and isotopic enrichment due to evaporation.

Variations in Ic-excess of the eleven study lakes in the coarse-textured glaciofluvial outwash are shown in Figures 3-3 and 3-4. As landscape position decreases and groundwater contributing area increases, the Ic-excess values generally increase (Table 3-1). This is evident within both the western (Lakes 206, 201, and 208) and eastern (Lakes 17, 16, 5, and 2) flow systems as a function of landscape position, and between flow systems as a function of groundwater contributing area (Figure 3-5a). This increase is due to progressively larger volumes of groundwater, of meteoric origin, being contributed to the lakes through the permeable substrate of the outwash (Cheng and Anderson, 1994; Smerdon et al., 2005; Townley and Davidson, 1988; Winter et al., 2003). The isolated lakes (11, 7, and 19) had a much wider distribution of Ic-excess and showed the greatest evaporative enrichment. Lakes 11, 7, and 19 had Ic-excess values as low as -41.9‰, -49.9‰, and -38.8‰, respectively.

Within each flow system (Table 3-1; Figure 3-4) there is notable temporal persistence in the relationships of annual lake lc-excess values. For every year in the eastern flow system, the relative order of lake lc-excess is in ascending order: Lake 17, 16, 2, and 5. In the western flow system, the lc-excess of Lake 201 is consistently higher than Lake 206. Lakes 208 and 201 are very similar and track together over time. Lake 1, which is in its own central flow system but similar landscape position to Lakes 2 and 5 regularly has an lc-excess between both lakes.

The persistence in the pattern of lake lc-excess is also present during the winter sampling in March 2020 (Figure 3-3). The lakes were sampled near the end of the ice-over period to test whether the spatial pattern of lc-excess values described above was present after the formation of ice and whether continued influxes of groundwater without the presence of evaporative fractionation would further raise the lc-excess values of the lake water. Heavy isotopologues of water are preferentially incorporated into ice as it forms, thereby decreasing the $\delta^2\text{H}$ and $\delta^{18}\text{O}$ values of the underlying lake water (i.e., resulting in increased lc-excess values), mimicking the effect of groundwater inputs to the lake. The shallow lakes, except for possibly the deepest, Lake 17, can be assumed well mixed during the ice-off season; however, isotopic stratification through fractionation may be common during winter ice-over. The lc-excess of the winter lake ice was similar to or lower than under-ice water samples, as expected (Figure 3-3). Most lakes did not show significant stratification, although Lakes 16 and 2 exhibited notable differences in lc-excess values between the top and bottom of the water column. Lake 1 showed a slight difference. Due to the fractionation that takes place during ice formation it is expected that water just below the ice would be isotopically lighter than deeper lake water but, interestingly, the water sampled at the bottom of the lakes is even lighter. If the stratification were purely due to ice creation, isotopically lighter water (i.e., less negative lc-excess) would be located at the top of the column and isotopically heavier water (i.e., more negative lc-excess) at the bottom (Krabbenhof, 1990); however, the opposite trend is seen at Lakes 16, 2, and 1. Both the “reverse stratification” at Lakes 16, 2, and 1 and the lack of stratification at the remaining lakes could be the result of isotopically light groundwater discharging to the lake throughout the winter. More rigorous sampling is required to confirm this hypothesis.

The region has low annual precipitation (~444 mm/yr) with significant variability between years, which in turn affects the annual isotopic signatures and water balances of these BP shallow lakes (Figure 3-4). The greatest disparity between interannual variability in lc-excess can be seen when comparing the isolated lakes (11, 7, and 19) with the more connected lakes that are part of larger flow systems. Isolated lakes had the largest interannual variability, with lc-excess values ranging from -50 ‰ to -12 ‰ over the course of the study period, and had an average interquartile range (IQR) of 12.7 ‰. The annual summer lc-excess values of the isolated lakes had a strong linear correlation with the cumulative annual precipitation (i.e., precipitation accumulated over the previous year from the sampling date) ($R^2 = 0.69$; $p < 0.001$). Without groundwater to buffer them the isolated lakes are virtually exclusively controlled by precipitation and evaporation, and due to their shallow nature and overall low volume, small amounts of precipitation would have large controls over the isotopic mass balance. These findings support previous studies that show that Lake 19, which is located high in the landscape, had only ~20 mm of shallow lateral inflow during the 2005 and 2006 hydrologic years (Riddell, 2008). In

contrast, the more connected lakes had less interannual variability and the annual values were not correlated with precipitation ($R^2 = 0.18$). Lakes in the eastern flow systems (17, 16, 5, 2, 1) appear to have similar interannual variability (Average IQR = 6.3 ‰) over the study period, and do not appear to vary systematically with topographic position. The western lakes (206, 201, 208) have the least interannual variability (Average IQR = 3.9 ‰). This is likely due to the difference in geology between the western lakes, which are in an area with clean, uniform, high conductivity sands that promotes steady hydraulic conditions. The eastern lakes, in contrast, have notable heterogeneity in the form of sands and gravels interbedded with silt lenses, the latter of which can result in transient lateral groundwater connectivity.

3.3.4 Possible effects of lake morphometry on $\delta^{18}O$ -excess

Lake volume has a direct effect on the isotopic mass balance, and therefore on the amount of groundwater or precipitation necessary to maintain lake levels and less evaporative isotopic compositions. Deeper lakes are less sensitive to volumetric and concentration changes for a given evaporation or precipitation event when compared to shallower lakes with the same surface area. As an alternative explanation to groundwater inputs being the primary mechanism for lake maintenance, deeper, larger lakes could simply be less sensitive to evaporative fractionation and merely be maintained by precipitation in this landscape. However, this study has both a large lake (Lake 17; $\sim 6 \times 10^6 \text{ m}^3$) with very little groundwater contributing area and very low $\delta^{18}O$ -excess (-26.7 ‰) and a small lake (Lake 1; $\sim 2.5 \times 10^5 \text{ m}^3$) with a large groundwater contributing area and relatively high $\delta^{18}O$ -excess (-15.9 ‰). If lake morphometry were a controlling factor (i.e., lakes with larger areas and shallower depths are associated with greater evaporative influences) there would be a negative correlation between $\delta^{18}O$ -excess and the lake area/depth ratio (Yang et al., 2018). At the study lakes where it was hypothesized that groundwater was a controlling factor for $\delta^{18}O$ -excess, the opposite is true; there is a weakly positive correlation ($R^2 = 0.25$). The pattern of $\delta^{18}O$ -excess appears to be independent of lake morphometry (Figure 3-5b and 3-5c).

3.3.5 Competing roles for groundwater and surface water

There are varying degrees of interaction between surface water and groundwater in this glaciofluvial outwash. Due to the local sub-humid climate, lakes act as 'evaporation windows' on groundwater and can influence isotopic compositions in both groundwater outflow and downstream lakes by re-introducing fractionated (i.e., lake-affected) water back into the flow system, which has the potential to then discharge to down-gradient lakes (Gat and Bowser, 1991). This is evident in both groundwater and lake water samples at the URSA outwash. The groundwater is mostly isotopically uniform and similar to that of meteoric waters (Figure 3-2). However, wells on the southwest side of Lake 206 (green symbols on Figures 3-2b and 3-6) and the well between Lakes 5 and 2 (black symbols on Figures 3-2b and 3-6), show evaporatively fractionated water.

Groundwater sampled adjacent to Lake 206 is isotopically heavier when compared to other groundwater, although less so than Lake 206 itself. This is a result of water in Lake 206 mixing with ambient groundwater recharged from meteoric water. There is also evidence for lake water being affected by other 'upstream' lakes, in a "chain of lakes effect" (Gat and Bowser, 1991). Lake 2 has a

lower $\delta^{13}C$ -excess value relative to its landscape position. Although it is in the lowest landscape position for its respective flow system, Lake 2 has a lower $\delta^{13}C$ -excess than Lake 5, which is up-gradient and has a correspondingly smaller potential groundwater contributing area (Figure 3-3). Lake 2 is one of only two lakes in this study to have surface inflow, where a semi-permanent stream flows from Lake 5 to Lake 2 most years (Table 3-1; Figure 3-1). Both groundwater and surface water flowing from Lake 5 to Lake 2 are isotopically heavier due to the fractionation that took place in Lake 5. Consequently, while the sources of inflow to the remainder of the lakes are either precipitation or groundwater, both of which have a meteoric origin, Lake 2 receives both slightly fractionated groundwater and fractionated lake water from Lake 5.

Synoptic isotope sampling has become a popular method of characterizing major hydrologic fluxes, sources, and fates. The data presented here, however, demonstrate the need for both surface and groundwater processes to be contextualized together and that their interactions may vary in both space and time.

3.3.6 Hydrogeological case study: Lakes 17, 16, 5

Previous works by Smerdon et al. (2005, 2008, 2012) have provided a comprehensive hydrogeological model and understanding of the hydrologic controls on Lakes 17, 16, and 5. These studies included intensive monitoring of hydrometric instruments and complimentary numerical modelling to quantify the components of the water balance for Lake 16 (Table 3-2). Groundwater moves from southeast to northwest at an average horizontal gradient of 0.002 (Figure 3-6; Smerdon et al., 2008). For Lake 16, and most other lakes in the Boreal Plain, precipitation and evaporation are the dominant influx and outflux, respectively, on an annual basis (Ferone and Devito, 2004; Smerdon et al., 2005; Thompson et al., 2017). It was shown for Lake 16 for two consecutive years that the groundwater components were consistent, contributing 230 and 222 mm/yr during the 2002 and 2003 hydrologic years, respectively. Groundwater discharge to the lake was temporally consistent throughout the year and was the dominant influx between November and April, when evaporation is limited due to low temperatures and/or ice cover. Lake 16 is 2.4 m lower than Lake 17 and 1.8 m higher than Lake 5. The stages at Lakes 17, 16, and 5 showed progressively less variability as their landscape position decreased.

Lake 17 was shown to have little to no input from groundwater sources and to be sensitive to annual precipitation as a primary input, while Lakes 16 and 5 are progressively lower in the topographic gradient and therefore capture more groundwater flow. Lake 17 was most sensitive to annual precipitation and evaporation. Figure 3-6 shows the groundwater flow directions around Lake 16, illustrating the position of the lakes within a larger flow system (Smerdon et al., 2008). The isotope data for Lakes 17, 16, and 5 presented here expand on and fully support the findings of Smerdon et al. (2005, 2008), where $\delta^{13}C$ -excess is progressively less negative as the landscape position decreases (i.e., from Lake 17 to 16 to 5) in one groundwater flow system (Figure 3-3). This pattern, irrespective of interannual climate variation, is exceedingly stable through time (Figure 3-6). These principles of lake landscape position, potential groundwater contributing area, and spatial changes in isotopic concentrations are

expanded on, both spatially and temporally, and supported by the isotopic data presented for the non-isolated lakes (17, 16, 5, 2, 1, 208, 201, 206) in this study.

3.4 Conclusions

Eleven shallow boreal lakes were sampled annually for eight years. Stable O and H isotope ratios indicate that lakes with lower landscape positions and associated larger potential groundwater contributing area had relatively larger groundwater inputs. This is the first study to show that the spatial pattern of long-term groundwater signals amongst lakes in the same flow system overrides the seasonal evaporative effects on stable water isotopic compositions of these shallow boreal lakes. In other words, the spatial variability of $\delta^{18}O$ -excess between lakes within the same groundwater flow systems persisted through time, despite interannual variability due to climate-driven evaporative losses. This work demonstrates the feasibility of using $\delta^{18}O$ -excess to qualitatively compare water sources of lakes within flow systems; future work in this complex environment should focus on performing isotopic mass balances to quantify groundwater inputs and impacts on $\delta^{18}O$ -excess of lake water over time. Isolated lakes high in the landscape experience much higher interannual variability because they have little to no groundwater input to buffer the volumetric or isotopic changes due to evaporation and precipitation. Landscape position within coarse outwash landscapes is a strong predictor for relative groundwater input; however, surface water connections can short circuit groundwater pathways and confound the signal. Due to the highly heterogeneous glacial substrates present in the Boreal Plain it can be difficult to interpret between flow systems; a conceptual understanding of the system's surface and subsurface hydrology is therefore required. A strong conceptual model and thorough understanding of potential water sources and fates is required to explain the spatial heterogeneity in groundwater and surface water isotopic compositions at local and regional scales.

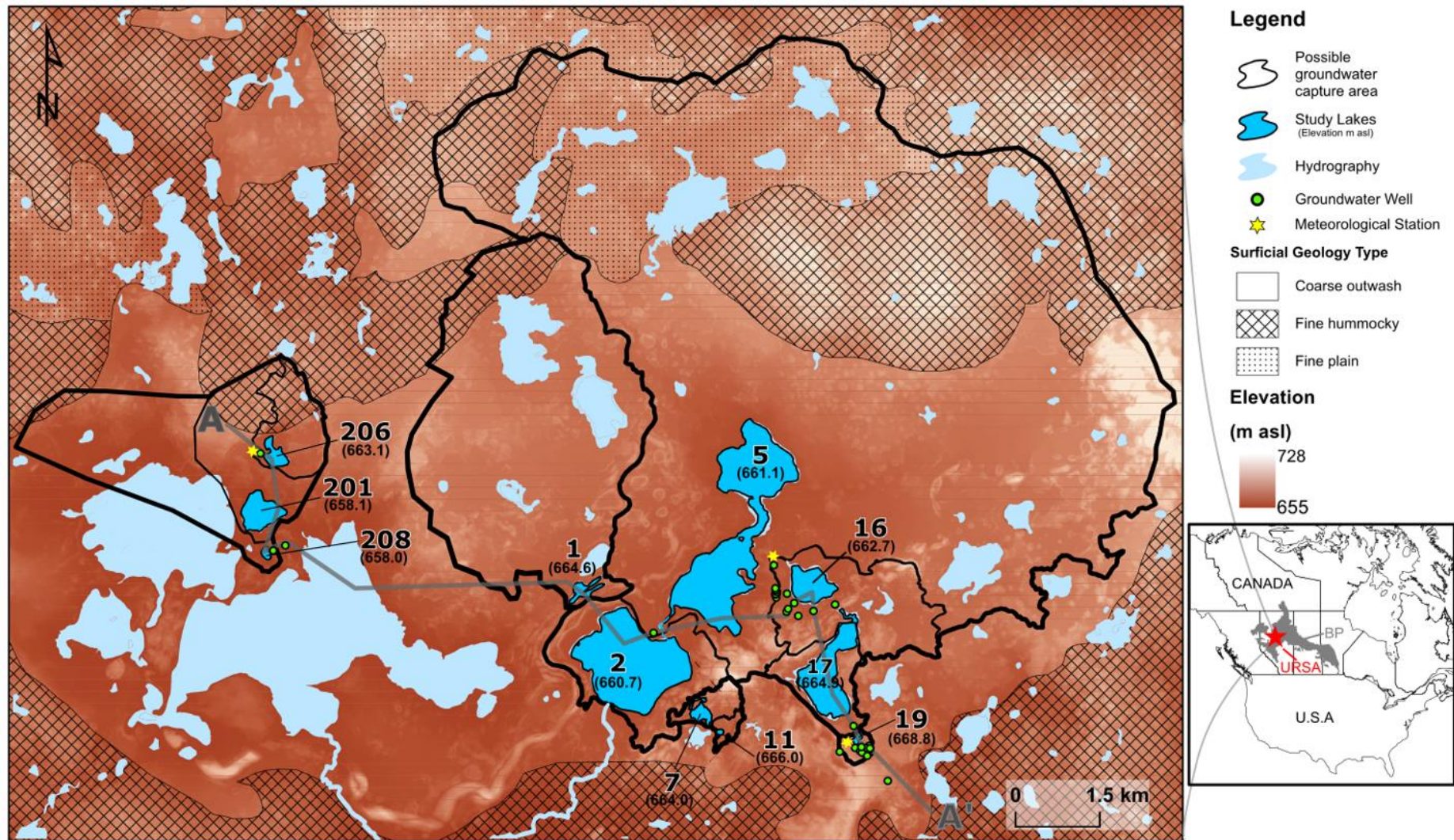


Figure 3-1: Ground elevation of the Utikuma Region Study Area (URSA; main panel) and its relative location within Canada, North America, and the Boreal Plains (BP) ecozone (inset; Marshall et al., 1999), with study lake locations and elevations, delineated potential groundwater capture areas and surficial geology type (Fenton et al., 2013). Bold lines indicate limits of separate flow systems (i.e., the potential groundwater capture area for the lowest lake in that system); finer lines indicate potential groundwater capture area for the lakes positioned higher in each system.

Table 3-1: Lake Characteristics

	Lake	Mean Depth (m)	Area (km ²)	Surficial Geology	Dominant Surrounding Landscape	Elevation (m asl)	Surface Water Inputs?	Total Groundwater Capture Area (km ²)	Coarse* Groundwater Capture Area (km ²)	Landscape Position Rank
Isolated lakes	11	1.5	0.01		Wetland	666.0	No	0.2	0.2	High
	7	1.6	0.03	Perched on fines	Forestland	664.0	No	0.8	0.8	High
	19	1.8	0.04		Forestland	668.8	No	0.3	0.3	High
Western flow system	206	2.8	0.14	Uniform sands	Forestland	663.1	No	1.8	1.03	High
	201	2.6	0.38		Mixed	658.1	No	5.2	3.5	↓
	208	1.3	0.04		Wetland	658.0	No	11.2	9.3	Low
Eastern flow system	17	5.3	1.10	Sands & gravels with silt lenses	Forestland	664.9	No	1.9	1.9	High
	16	1.8	0.47		Wetland	662.7	No	6.2	6.2	
	5	3.1	3.20		Wetland	661.1	No	94.2	51.4	↓
	2	3.9	2.40		Wetland	660.7	Yes	99.1	56.3	Low
Central flow system	1	2.3	0.110	Sands & gravels with silt lenses	Wetland	664.6	Yes	19.8	17.84	Low

Flow systems are separated by lines.

*Course groundwater capture area refers only to the capture area composed of coarse outwash deposits

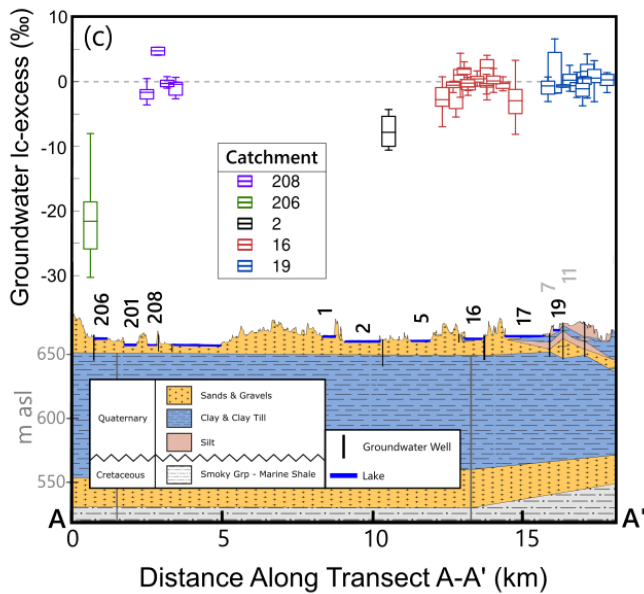
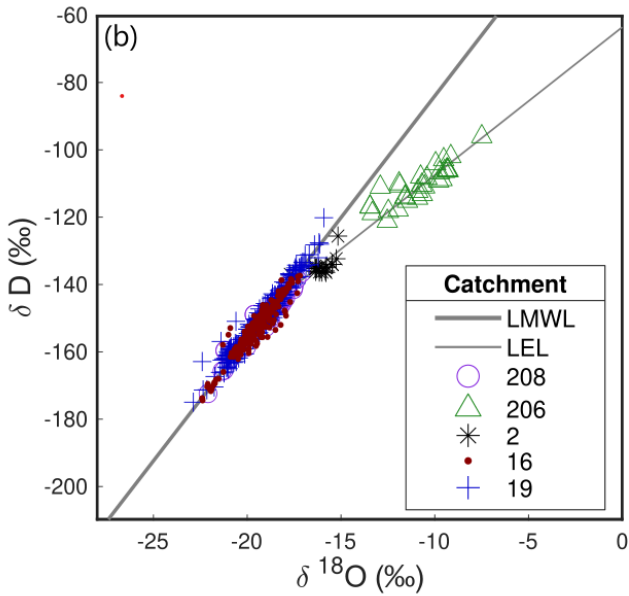
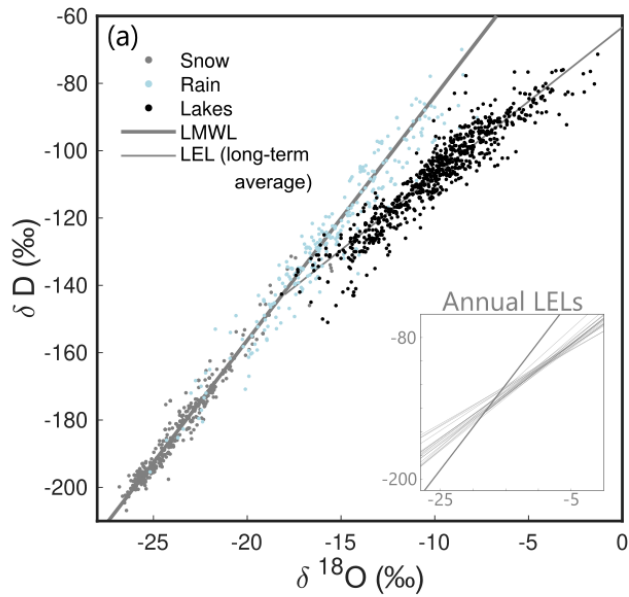


Figure 3-2: (a) Dual isotope plot of Utikuma Region Study Area (URSA) precipitation and lake waters with (inset) annual local evaporation lines (LEL) from 1999-2019; (b) dual isotope plot of URSA groundwater sampled from 1999-2019 and (c) a generalized geologic cross-section along transect A-A' (Figure 1) with groundwater δ -excess (sampled from 2000 to 2019) values shown above. Each set of box and whiskers represents one groundwater well or a cluster of wells. The cross section shows the lake and well locations that lie on the transect (black numbers indicate lake ID on the cross section; gray numbers indicate lakes off the cross section). Vertical lines represent boreholes; see Hokanson et al. (2019) for more details.

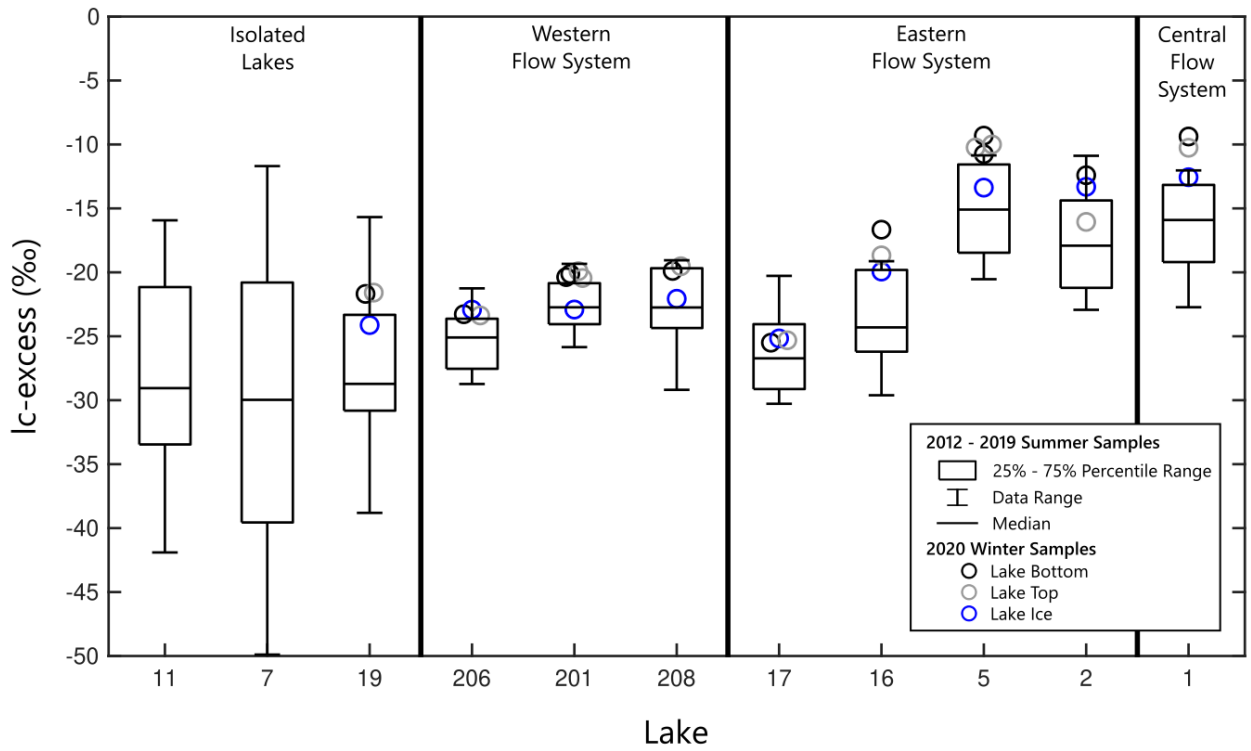


Figure 3-3: Box plot of summer lake Ic-excess values. Flow systems are separated by solid black lines and are ordered by landscape position. Winter 2020 samples are shown as well, where each circle represents a single water sample and are not considered in the boxplots.

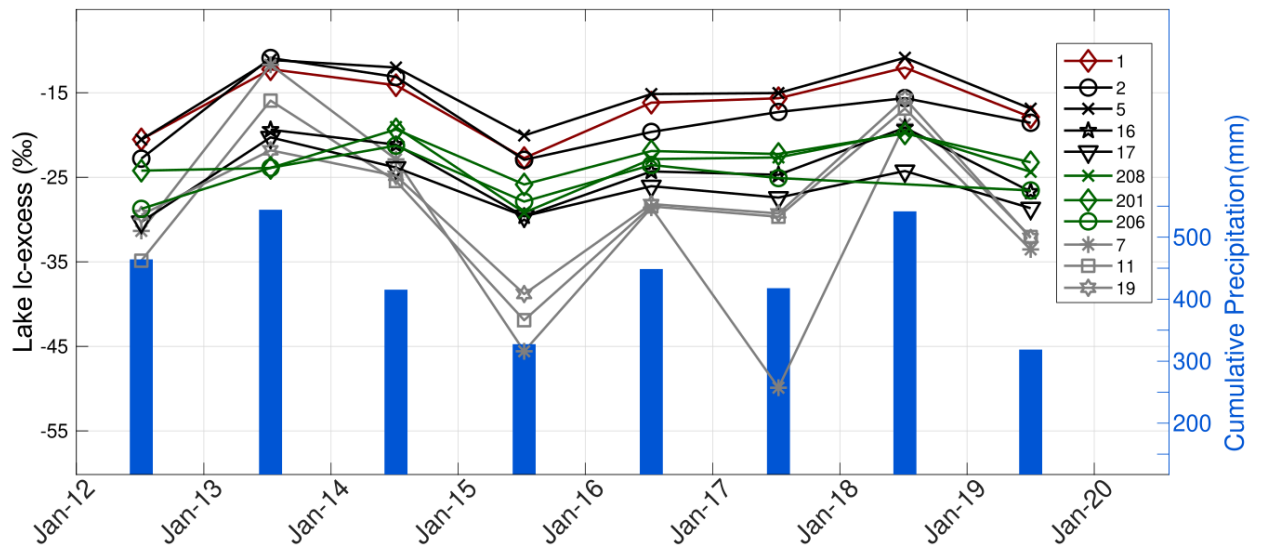


Figure 3-4: Time series of July lake Ic-excess in context of cumulative precipitation. Daily precipitation is summed over the year prior to the lake sampling date.

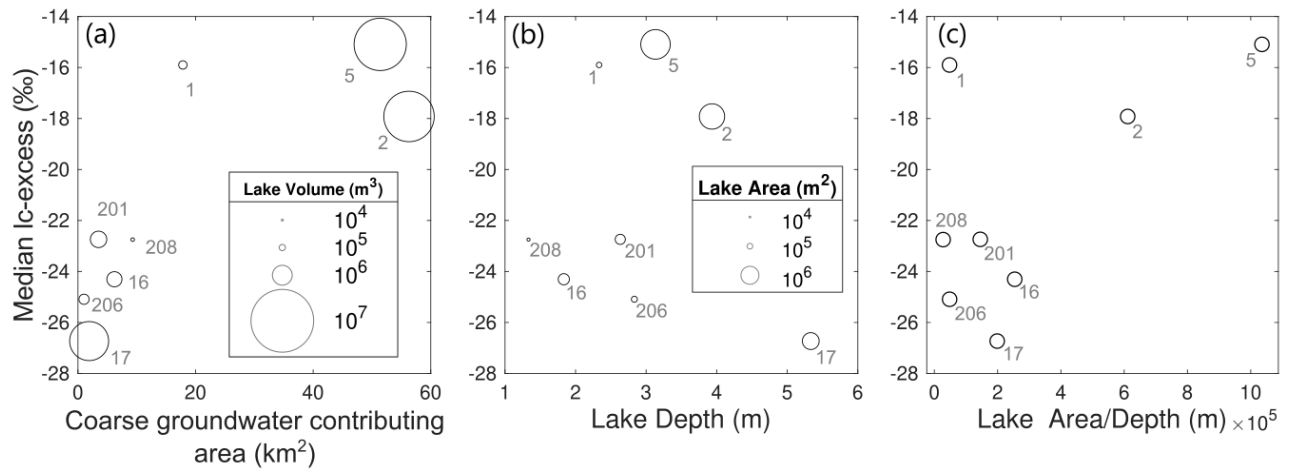


Figure 3-5: Relationships between median July Ic-excess and (a) groundwater contributing area and (b, c) lake morphometry (area and depth). Lakes considered isolated are not included due to the wide range of summer Ic-excess values. Groundwater contributing area only considers coarse surficial geology (Table 1). Marker size is proportionate to lake volume (a) and lake area (b). Lake volume is approximated by multiplying lake area by average depth.

Table 3-2: Historic Water Budgets for Lake 16

Budget Component (mm)	2002	2003
Evaporation	339	450
Precipitation	286	366
Groundwater In	233	221
Groundwater Out	34	27
Surface Water Out	297	116
Surface Water In	--	--
Change in Lake Storage	-104	+35

(from Smerdon et al., 2005)

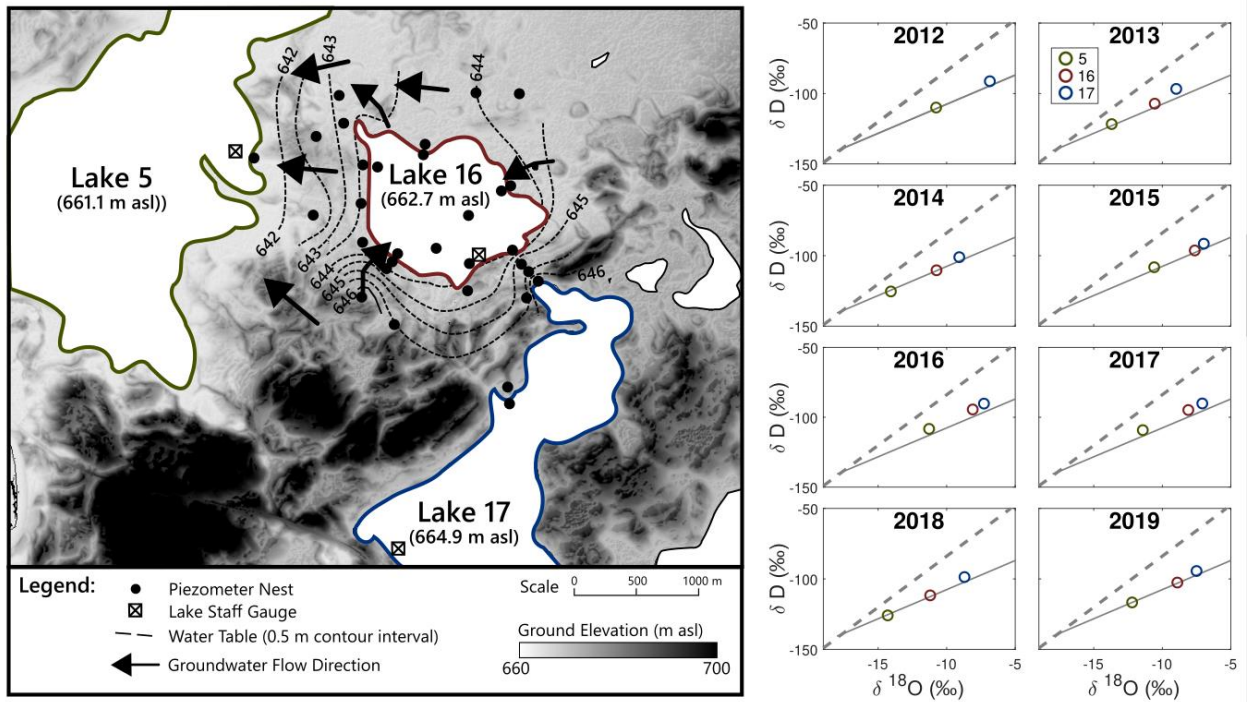


Figure 3-6: Lakes 17, 16, and 5 study area with ground surface topography and selected field instrumentation (left; Adapted from Smerdon et al., 2008). Water table contours and groundwater flow direction shown for July 2002. Location of Utikuma Region Study Area and Boreal Plains region in Alberta, Canada, shown on inset. July stable water isotope values for Lakes 17, 16, and 5 for each year of the study period (right) are shown in dual isotope space with the LMWL (dashed line) and long-term LEL (solid line) for reference. The further along the LEL (i.e., offset from the LEL-LMWL intersection) the data point lies, the more negative the corresponding I_c -excess value.

Chapter 4

Forestland-peatland hydrologic connectivity in water-limited environments: hydraulic gradients often oppose topography²

4.1 Introduction

A widely accepted approach in both conceptual and numerical models of groundwater flow is to assume that the water table is a subdued replica of topography (e.g., Cardenas, 2007; Hubbert, 1940; Tóth, 1963). The topography-driven paradigms underpinning this water table configuration generally perform best in humid, high-relief regions or for large regional groundwater systems (Gleeson et al., 2011); however, water table configurations are also controlled by climate (recharge) and geology (Freeze and Witherspoon, 1967; Haitjema and Mitchell-Bruker, 2005; Tóth, 1970). Therefore, topography may not be a first-order control in water-limited regions or those with low relief (Chapter 2; Devito et al., 2005b; Winter, 1999). These regions are globally prevalent (e.g., Southern Australia, Western Canada, Western Siberia, Central Europe, Northern China, The Great Hungarian Plain) and are considered to be hydrologically vulnerable to anthropogenic activity, including climate change. However, the intricate, highly non-linear interactions between climate, geology, and topography are difficult to predict (Condon and Maxwell, 2015; Jackson et al., 2009; Jobbágy and Jackson, 2004).

Tóth (1963) first analytically demonstrated the relationship between topography and groundwater flow systems (i.e., local, intermediate, regional) and groundwater fluxes (i.e., recharge and discharge). Furthermore, he demonstrated that with decreasing topographic relief the relative prominence of local flow systems (flow in which the recharge area is directly adjacent to its discharge area) also decreases. Despite this, local groundwater flow systems can be important components of the hydrological cycle, affecting surface or near surface processes such as solute transport, pond and wetland water and chemical budgets, and landform hydrologic connectivity (Tóth, 2009). The spatiotemporal presence or absence of local flow systems (i.e., groundwater mounding under local topographic highs) is primarily controlled by net recharge (Haitjema and Mitchell-Bruker, 2005), where regions with low recharge tend to have greater spatial variability in groundwater-surface water interactions (Schaller and Fan, 2009).

The sink-source function (i.e., groundwater recharge or discharge) of a landscape unit and its proclivity to change through time is crucial to the regional water balance in complex water-limited, low-relief environments. The Boreal Plains ecozone, located in the Western Glaciated Plains of North America, is such an environment. It is characterized by thick, unconsolidated, heterogeneous substrates and a sub-humid climate, where potential evapotranspiration often equals or exceeds precipitation, manifesting as a regionally sub-humid climate with multi-year wet and dry cycles (Mwale

² A version of this chapter has been published:

Hokanson K.J., Peterson E.S., Devito K.J., Mendoza C.A. Forestland-peatland hydrologic connectivity in water-limited environments: hydraulic gradients often oppose topography. *Environmental Research Letters*. 2020; 15:034021. doi: 10.1088/1748-9326/ab699a.

et al., 2009). Hydrogeology in the Boreal Plains is made even more complex by the presence of peatlands. While previous regional-scale studies have shown that runoff from large catchments is positively associated with peatland coverage (Devito et al., 2017; Gracz et al., 2015; van der Velde et al., 2013), little is known about the spatiotemporal variability of or controls on hummock-scale processes or landform connectivity that control it. Nonetheless, identifying the spatiotemporal hydrologic behaviors of the smaller land units that make up larger runoff source areas is an important aspect of “scaling-up” in order to predict landscape scale runoff responses (Jensco et al., 2009).

Most previous studies concerning water table dynamics in undisturbed landscapes have focused on high relief, humid regions with shallow water tables and/or hydrogeologic settings that promote predictable and steady local-scale flow systems (Goodbrand et al., 2019; Jensco et al., 2009; Prancevic and Kirchner, 2019). Consequently, there is a general lack of understanding regarding the spatiotemporal distribution of groundwater recharge and discharge zones in more complex and dynamic landscapes. Thick unconsolidated sediments, low relief, and a water-limited climate result in interdependent surface water and groundwater processes with varying spatiotemporal controls (Lissey, 1971; Winter, 1999, 2001). Traditional conceptualizations of water tables as subdued replicas of topography necessarily require that recharge and discharge zones are primarily fixed in space and dependent solely on topography. Alternatively, in heterogeneous low-relief regions, slight changes in the interannual climatic water balance or variations in vegetative cover can shift, or even switch, recharge and discharge zones through time. For example, a forested hummock may act as a source (i.e., groundwater recharge) during water surplus and subsequently become a water sink (i.e., subsurface discharge) during a water deficit when evapotranspiration exceeds precipitation (Heuperman, 1999).

The Boreal Plains are experiencing unprecedented anthropogenic and natural disturbance, including climate change, oil and gas operations, and wildfire. As a consequence, boreal peatlands and forestlands are a primary focus of both reclamation and reconstruction efforts (Wytrykush et al., 2012; Daly et al., 2012). While the notion of topography-driven flow between forested uplands and peatlands is common and is often implied in conceptual site models (e.g., Holden, 2006; Ireson et al., 2015; Ketcheson et al., 2017; Nwaishi et al., 2015), it may not always be a realistic representation of boreal hydrology. It is well understood that peatlands maintain fairly stable internal water table depths, even in dry continental settings and under drought conditions, by limiting evaporation through a system of autogenic processes. For example, water table depth is involved in negative feedback loops with peat deformation (e.g., Morris et al., 2011), moss surface resistance (e.g., Price et al., 2009), and moss productivity (e.g., Thompson and Waddington, 2008). I refer readers to the review paper by Waddington et al. (2015) for more detailed descriptions. Despite this, there is a general lack of knowledge concerning the controls on, and spatiotemporal patterns of, external hydraulic gradients from forested hummocks to adjacent wetlands (Dimitrov et al., 2015; Price et al., 2005; Redding and Devito, 2008). It is conventionally assumed, but not widely monitored, that in sub-humid boreal environments water moves from forestlands to wetlands during average, non-drought conditions (Ketcheson et al., 2016). The intricate mosaic of forestlands and peatlands overlying thick heterogeneous glacial deposits typical of the Boreal Plains results in highly spatially variable evapotranspiration rates, subsurface hydraulic

properties, and surface topographic gradients; all of which influence the hydrologic function of each land unit.

Through understanding these dynamic and complex environments we increase our ability as hydro(geo)logists to conceptualize groundwater and surface water movement and availability across a spectrum of geologies and climates by identifying primary controls in each landscape that may surpass those attributed to topography alone. To address this key knowledge gap and to test the common conceptualization of topography driven flow and groundwater mounding under hummocks, the hydraulic gradients between peatlands and adjacent forested hummocks were analyzed at sixteen sites. Peatland-forestland pairs were purposefully selected to represent a spectrum of unconsolidated deposit types typical of those blanketing the boreal regions of the Western Glaciated Plains, forested hummock morphometries, and regional topographic position.

Previous work by Devito et al., (2005b, 2012) has challenged the topographically defined catchment and the practice of assuming that the water table conforms to topography, and as a result introduced the idea of a 'topography last' hierarchical classification to identify the major controls over hydrological regions. Their work focused on concepts related to the dominant roles that climate (i.e., P and ET) and vertical fluxes have in regions with deep soils and large water storage potential. Following this, Chapter 2 showed at the intermediate scale in the BP that the roles of climate and geology can have a greater effect than topography on water table position and variability. This study is a direct empirical test of these ideas at the hummock scale over a large and heterogeneous spatial extent.

4.2 Study Site and Methods

The Utikuma Region Study Area (URSA; 56°N, 115°W) is located 370 km north of Edmonton, Alberta, in the Boreal Plains ecozone of Canada. The region is characterized by low topographic relief and thick (45 to 240 m) heterogeneous glacial substrates overlying Cretaceous marine shale (Vogwill, 1978). The climate is considered sub-humid, with long-term precipitation and potential evapotranspiration averaging 444 mm and 517 mm, respectively (Chapter 2; Marshall et al., 1999). The primary sources of precipitation are short duration convective-cell storms, which occur during the summer months when evapotranspiration is highest (Brown et al., 2014; Devito et al., 2005a).

The study region can be divided into three major hydrological response areas (HRAs): coarse outwash (CO), hummocky moraine (HM), and lacustrine clay-till plain (CP), which were thoroughly characterized in Chapter 2. The CO HRA contains areas of fine substrates with perched water tables overlying coarse sediments; perched over coarse (CO-P). These HRAs can be further discretized into hydrological units (HU): forestlands, peatlands, and open water. Forested hummocks are characterized by mixedwoods dominated by trembling aspen (*Populus tremuloides*), while the peatlands have a sparse canopy of black spruce (*Picea mariana*) and tamarack (*Larix* sp.). Peatlands are comprised of peatland mosses, with organic accumulations ranging from 2 to 5 metres with hydraulic conductivity values ranging from 10^{-4} to 10^{-6} m/s in the top two metres (Lukenbach et al., 2017). For each HRA, considering the CO-P region independent of CO, four hummock–peatland pairs were chosen to represent a spectrum of hummock morphometries and topographic positions (peatland elevation). Over

the 70 km long transect encompassed by this study, the peatland elevations have a range of 30 m, which is typical of the low relief of the Boreal Plains (Chapter 2). Peatland areas range from 0.5 ha to greater than 100 ha. All hummocks have forest stands dominated by aspen (*Populus tremuloides*), except for CO-d, which is primarily jack pine (*Pinus banksiana*).

Precipitation data were collected throughout the 2018 hydrologic year (November 1, 2017 to October 31, 2018) using two tipping bucket rain gauges in separate HRAs. The gauges were adapted for snowfall in winter months by using antifreeze reservoirs and data were validated with manual gauges. To place this study period in context of the long-term climate and to account for the strong effect of antecedent moisture conditions on hydrologic response in the Boreal Plains, the 3-year cumulative departure from the mean precipitation (CDM-3) was calculated using the recent long-term mean precipitation (444 mm; 1987 to 2015) and preceding three annual precipitation values (Chapter 2).

To characterize the hydrologic function of each HU and to determine the direction of the water table gradient between HUs, a single monitoring well (0.0381 - 0.051 m diameter polyvinyl chloride pipe) was located at each HU at each site (32 wells). Peatland wells were screened over the entirety of the well, while forestland wells were either screened over the entirety of the well or had solid casing extending from the top of the well to 1 m below the ground surface. In all cases the screened interval spanned the water table for the duration of the study. All wells were instrumented with pressure transducers (Solinst, Georgetown, Ontario, Canada; Northern Widget LLC, Minneapolis, Minnesota, USA), which recorded water levels at thirty-minute intervals during the ice-off period of 2018 (mid-May to mid-October) and were barometrically compensated using the closest barometric pressure transducer (Solinst). To validate the transducer readings, levels were also measured manually three times: Spring (mid-May), summer (mid-July), and fall (mid-October). Water table elevations were determined by coupling the water level data to survey data of the tops of the well casings collected using a theodolite or a digital water level (Smart Leveler, Smyrna, Tennessee, USA; ± 0.00254 m). Pressure transducers were damaged at two sites (CO-P-d, CP-d); in which case only manual water levels are presented. The absolute difference in water table elevations (Δh) and gradient direction are presented in lieu of true gradients because variable distances between forestland-peatland wells would have an undue influence on the magnitude of calculated gradients.

The hydraulic conductivity (K) of the mineral substrate in each hummock was estimated using the Hvorslev (1951) method, either at the primary hummock well or at a nearby, representative well. Values presented are geometric means of three tests, where both rising and falling head slug tests were used. Topographic profiles of the ground surface were obtained from LiDAR datasets collected in 2008 and were used to obtain metrics to characterize the morphometry of each hummock, specifically the height (H; elevation above adjacent peatland) and length (L; distance between peatlands).

4.3 Results

For the 2018 hydrologic year, precipitation totaled 498 mm and 467 mm in the CP and CO-P HRAs, respectively (Figure 4-1), which are averaged to 483 mm to represent all URSA. Overall the 2018 hydrologic year was considered 'mesic,' or average, in terms of both annual precipitation and the CDM-3. In the context of the long-term climate at URSA (Figure 4-1), 2018 was only 39 mm above the long-term average annual precipitation and the CDM-3 from the mean was +38 mm.

Measured K values of the hummocks (Table 4-1) are generally highest in the CO HRA (3.7×10^{-6} to 1.5×10^{-4} m/s) and lowest in the HM HRA (5.7×10^{-10} to 1.3×10^{-7} m/s). Conductivities of the CP and CO-P hummocks range from less than 1×10^{-9} to 6.1×10^{-7} m/s and 1.8×10^{-9} to 7.9×10^{-9} m/s, respectively. Profiles through each site (Table 4-1; Figure 4-2) show the wide range of forested hummock morphometries sampled. The length/height ratio (L/H) for the hummocks range from 15 to 195 m/m, where a small L/H indicates a tall narrow hummock (e.g., CO-d) and a large L/H indicates short broad hummock (e.g., HM-c). Overall, the L/H values are reflective of the texture of each HRA (e.g., clay-rich sediments limit the height of hummocks at the time of glacial deposition), where CO and CP have the lowest and highest L/H values, respectively.

Seasonal water table fluctuations within each HU are included in Figure 4-3. Peatlands showed little variability in water table position over the study period, both within (temporal variation over the study period at one well) and between sites, regardless of peatland topographic position (Table 4-1). Forested hummocks, however, exhibited much more variability. Water tables in the CP HRA were the shallowest and had high variability within sites, but the least variability between sites. The CO HRA sites had the least variability within and the most variability between sites, with water table depths ranging from ~2.9 to ~7.7 m below ground surface. Water tables in the HM HRA were at intermediate depths (~4 m) with high seasonal variability.

Hydraulic gradients were opposite to the topographic gradient, directed from the peatland towards the adjacent forested hummock, at 14 of the 16 sites (Figures 4-2 and 4-4) indicating the presence of a groundwater depression beneath the hummock. Maximum and minimum water table elevation differences (Δh) are shown in Table 4-1. A negative Δh indicates that the peatland water table was above that of the forested hummock. At three hummock sites (CO-P-b, CO-P-c, HM-c) the water table was below the screened interval of the well for the duration of the study; however, the wells were drilled to a sufficient depth to imply that the water table was below that of the peatland and therefore to infer the direction of the gradient. Only two sites (CP-a, HM-b) had gradients towards the peatland for the majority of the study period. At Site CP-c, the gradient was towards the peatland for only 50 days (~30% of the study period). The CO sites had the lowest magnitude difference in water table elevations while the HM had the highest. The only forested hummock dominated by pine (CO-d), which was also one of the sandiest, had an essentially flat water table. I attribute the small difference in water table elevations at CO-d to isolated mounding within the peatland.

4.4 Discussion

I show that traditional topography-driven approaches to groundwater flow do not function in this complex water-limited environment, even in mesic, non-drought years. In peatland and forest hydrology there is a silent but prevalent assumption that water flows from highs to lows, even in sub-humid, low-relief areas. This paradigm presents itself in conceptual site models (e.g., Nwaishi et al., 2015), assumptions for subsurface water flow between boreal forests and peatlands in numerical models (e.g., Dimitrov et al., 2014), and in new approaches for peatland construction following large-scale disturbances (e.g., Price et al., 2010). I demonstrate that the development of the groundwater mounding required to drive flow from topographic highs is both spatially and temporally infrequent in low-recharge settings like the Boreal Plains. Under mesic climate conditions, the typical water table configuration between peatlands was depressed, rather than mounded. These observed conditions necessarily require 'negative recharge' (i.e., upflux) which clearly exceeds 'positive recharge' from precipitation in these sub-humid environments, even in non-drought years. The spatial pervasiveness of groundwater depressions illustrate that negative net recharge is more of a rule rather than an exception in the Boreal Plains.

Where traditional hydrogeological paradigms would predict that groundwater mounding would be greatest (and ubiquitous) in areas of low permeability and undulating topography (Haitjema and Michell-Bruker, 2005), I find those areas (HM HRA) are most prone to deep groundwater depressions. In these cases, the low K and specific yield values found in fine-textured HRAs (i.e., CP, HM, CO-P; Thompson et al., 2015), exaggerates the negative (however slight) net recharge required to form these depressions, which further limits the generation of lateral flow. Chapter 2 supports this lack of lateral groundwater flow, where isotopic and hydrogeologic data showed that flow was primarily vertical with little to no lateral hydrologic connectivity and bulk water movement. In cases where there was a noticeable elevation difference between peatlands (HM-a,d and CO-P-c,d), the groundwater within the hummock was controlled by the relative topographic positions of the peatlands. The water table behavior was independent of the hummock morphometry and therefore did not rise with the surface topography between the peatlands. It instead was dependent on the position of each peatland, further demonstrating the hydrogeologic influence peatlands have on the larger environment. In the singular pine sand hummock (CO-d), the water table was, in effect, flat. Additionally, its high hydraulic conductivity, short length, and highly sandy texture means there is little capability for groundwater mounding to occur, regardless of recharge rate (Haitjema, 1995). Previous work by Smerdon et al., (2008) demonstrated that in high K settings, height above the water table was a primary control on groundwater recharge rates, where deeper water tables experienced higher overall recharge rates. These characteristics, coupled with the low transpirative demands of pine, likely make CO-d, and similar sites, key sources of groundwater recharge in the Boreal Plains.

In this study, hydraulic potentials, which drive groundwater flow, are not primarily controlled by topography or gravity, but by plant uptake. In the Boreal Plains, forestlands have higher ET rates and deeper rooting depths (up to 3 m; Debyle and Winokur, 1985) than peatland ET rates and peatland black spruce rooting depths (< 0.5 m; Lieffers and Rothwell, 1987). This disparity of evapotranspiration rates between boreal forestlands and peatlands has been shown through regional-scale studies (Devito

et al., 2017; Hwang et al., 2018; Prepas et al., 2006), catchment-scale studies (Devito et al., 2005a), and stand-scale studies (Barker et al., 2009; Barr et al., 2012; Brown et al., 2010; Brown et al., 2014; Petrone et al., 2007). These ET patterns coupled with the internal water-conserving mechanisms characteristic of boreal peatlands are the primary processes governing the hydraulic gradients, which are typically away from peatlands. These results demonstrate these features in almost all scenarios (hummock morphometry, substrate texture, topographic position), even in a non-drought year. This study was conducted during mesic climate conditions, meaning the annual precipitation was close to the long-term average and the CDM-3 was close to zero (i.e., no multi-year water deficit or surplus). Additional work is being conducted to determine the climatic conditions required to induce groundwater mounding under various hydrogeological conditions.

Water table depressions are well studied in the fields of dryland agriculture and afforestation (Jobbágy and Jackson, 2004; Tóth et al., 2014) and groundwater overexploitation (e.g., Changming et al., 2001); however, study of the controls and thresholds governing naturally occurring depressions has largely focused on near-shore or riparian vegetation (e.g., Meyboom, 1966; Winter and Rosenberry, 1995). While traditional approaches from regions where P is greater than PET may correctly presume mounding, to adequately represent reality in water-limited environments, more emphasis needs to be placed on the roles that soil storage and evapotranspiration play in the water budget (Redding and Devito, 2008). I show that even between two peatlands with stable water tables, vertical fluxes due to ET from the forested hummock are strong enough to create water table depressions. Research in arid environments or those with salinization problems (e.g., afforested grasslands) already emphasize vertical fluxes due to vegetation as the principal component of water budgets in low-relief areas (Allison et al., 1994; Jobbágy and Jackson, 2004); however, research and applications in climate transitional zones like the Boreal Plains have not yet adopted this as a primary approach and topography is usually considered as the first-order control on saturated subsurface water flow (Dimitrov et al., 2014).

Work by Devito et al. (2017), Gibson et al. (2002), Prepas et al., (2006), which are all large-scale catchment studies, showed that long-term boreal catchment runoff was positively related to peatland cover and negatively related to deciduous forest cover. This study demonstrates the water table elevations and hummock-scale storage patterns and processes responsible for these trends, which has not been shown previously. Hummock-scale processes have large implications for catchment-scale runoff generation (Jensco et al., 2009), and local flow generation in both natural and reconstructed landscapes (Lukenbach et al., 2019). This work represents a crucial advance in the research needed to understand these multi-scale processes and their distribution in space and time.

Currently there are unprecedented efforts being put towards total landscape reconstruction following megaprojects (e.g. open-pit mining) in water-limited boreal environments, where regulatory requirements mandate that landscapes be reconstructed and returned to a self-sustaining, pre-disturbance capability (Government of Alberta, 2018). Understanding hummock-scale processes and water table dynamics in natural systems is a necessary step in the planning and evaluating constructed and reclaimed landscapes (Devito et al., 2012). Consequently, there is an urgent need for hydrologic frameworks and models that accurately identify the major controls on water movement. This study

serves to demonstrate that in most scenarios forested hummocks are not reliable sources of groundwater to adjacent peatlands, and should not be constructed with the intent of acting as such.

The Boreal Plains ecozone of Canada is a water-limited environment, where potential evapotranspiration often equals or exceeds precipitation. Due to this delicate balance, the Boreal Plains and other similar landscapes have been identified as regions of high hydroecologic sensitivity to anthropogenic disturbances, such as agriculture, forestry, and climate change (Bergengren et al., 2011; Ireson et al., 2015), which can easily tip this balance. Thompson et al. (2017) used numerical simulations of a Boreal Plains catchment to show that water levels in aspen-forested hillslopes may be reduced by 0.5 to 1 m due to the effects of climate change. Additionally, it is predicted that temperature-driven increases in evapotranspiration will exceed any small increases in precipitation due to climate change (Wang et al., 2014), which may serve to increase the temporal and spatial persistence of the hydraulic gradients or groundwater depressions presented here.

4.5 Conclusions

This is the first study to demonstrate the spatial pervasiveness of water table depressions between boreal peatlands. Traditional topography-driven approaches assume hummocks are sources of water (i.e., groundwater mounding) for local flow systems (Ketecheson et al., 2016); however, I show that even in non-drought conditions, local flow from hummocks to adjacent wetlands is spatially infrequent. Realistic conceptualizations of hydraulic fluxes are necessary to predict landscape hydrologic responses, especially in areas susceptible to climate change or other anthropogenic disturbances. Additionally, in the expanding field of landscape reconstruction after large-scale disturbances (Cooke and Johnson, 2002), immature wetlands and landscapes constructed with the intent that they be maintained by recharge from hummocks (Wytrykush et al., 2012) may not succeed in the most prevalent conditions of this climate (dry to mesic), unless located in a stable larger-scale groundwater discharge zone.

The sink-source function of forested hummocks in water-limited environments is not as simplistic as traditional topography-driven approaches would indicate. Forested hummocks do not steadily provide water to adjacent peatlands, and are not stable sources of recharge to the larger landscape. Regardless of how accurate, or indeed conservative, recharge or hydrophysical property estimates are, predictions of water table position will fail in these landscapes if conceptual and numerical models continue to be developed around the anticipation of water table mounding (Haitjema and Michell-Bruker, 2005). There is a clear need to shift away from 'topography-first' approaches in large parts of the boreal and veritably all sub-humid and low-relief regions.

Table 4-1: Site Characteristics

HRA	Site	Peatland	Forested Hummock					Δh max	Δh min
		Elevation	K	Height H	Length L	$\frac{L}{H}$			
		(m asl)	(m/s)	(m)	(m)	(m/m)			
CO	a	663	2×10^{-4}	4.2	190	45	-0.65	-1.10	
CO	b	665	2×10^{-5}	10.1	190	19	-1.00	-1.50	
CO	c	663	4×10^{-6}	2.1	102	49	-0.05	-0.35	
CO	d	658	7×10^{-5}	9.7	145	15	-0.05	-0.20	
CO-P	a	673	3×10^{-9}	5.7	850	148	-1.20	-2.75	
CO-P	b	673	8×10^{-9}	2.1	115	55	-0.35	-0.60	
CO-P	c	675	2×10^{-9}	0.7	140	196	-1.40	-1.90	
CO-P	d	675	6×10^{-8}	0.4	125	313	-0.15	-1.15	
HM	a	677	1×10^{-7}	2.2	130	58	-1.85	-2.75	
HM	b	671	8×10^{-9}	5.5	380	69	3.15	1.30	
HM	c	672	6×10^{-10}	2.4	228	94	-1.90	-2.45	
HM	d	664	7×10^{-8}	1.4	180	128	-1.80	-3.05	
CP	a	655	6×10^{-7}	1.2	135	110	1.00	-0.05	
CP	b	657	$< 1 \times 10^{-9}$	1.1	130	114	-0.15	-0.45	
CP	c	644	1×10^{-7}	1.2	145	116	1.00	-0.40	
CP	d	659	$< 1 \times 10^{-9}$	0.9	45	49	0.00	-0.30	

Note. HRA = Hydrologic response area; CO = coarse outwash; CO-P = perched over coarse; HM = hummocky moraine; CP = clay-till plain. Δh values are rounded to the nearest 5 cm.

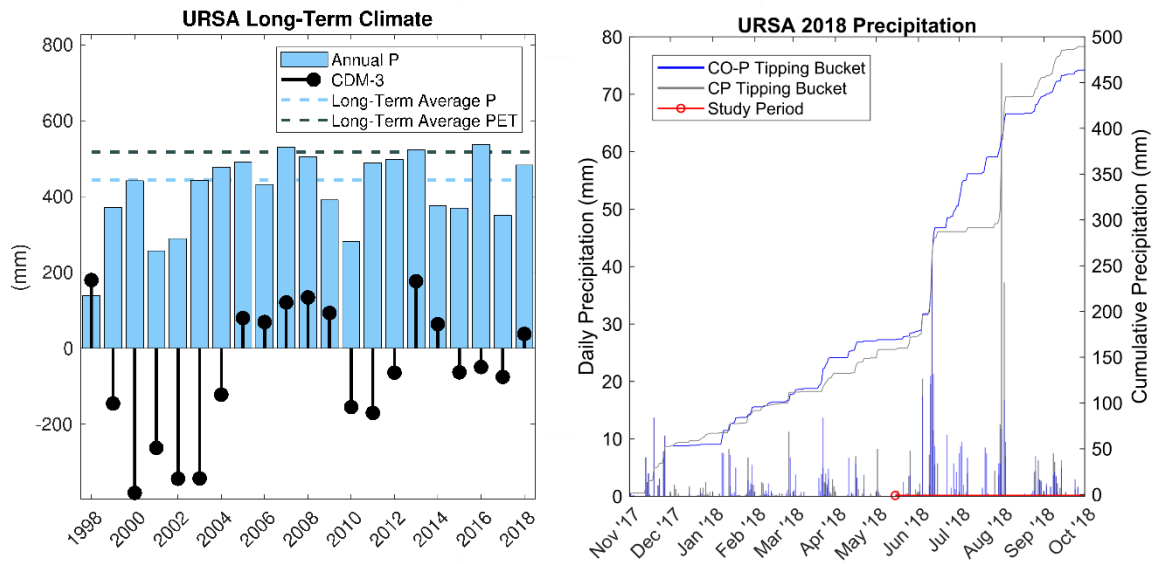


Figure 4-1: Annual precipitation (P) data and 3-year cumulative departure from the mean precipitation (CDM-3) for Utikuma Region Study Area (URSA), before and during the study period (left). Long-term average annual P (444 mm) and potential evapotranspiration (PET; 517 mm) are shown for context. Daily and cumulative precipitation at URSA for the 2018 hydrologic year (right)

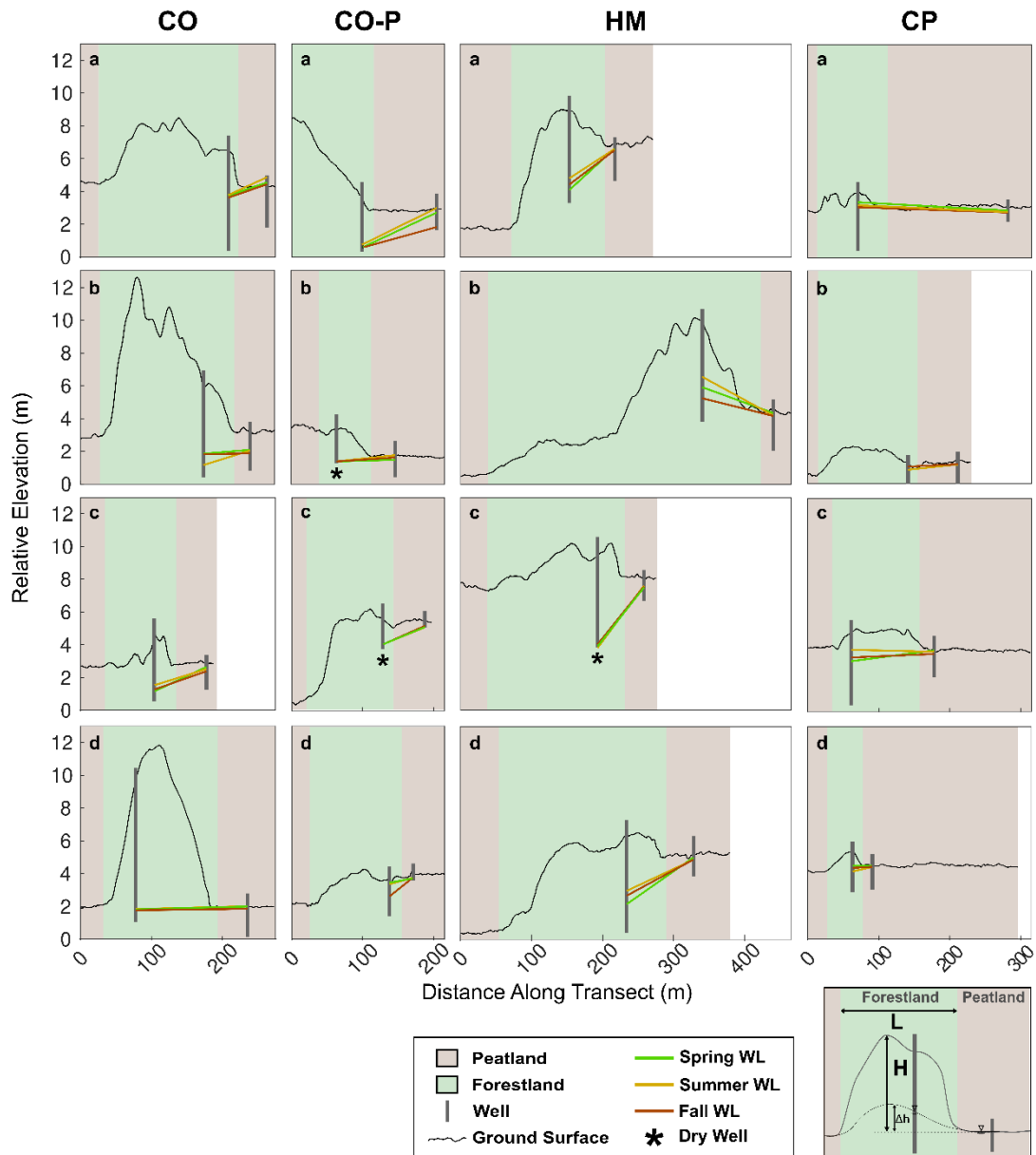


Figure 4-2: Topographic profiles of each peatland-forestland pair grouped by hydrologic response area. Vertical exaggeration for all profiles = 20X. Water levels between each well pair are indicated with a line to demonstrate the direction of the gradient but do not infer the location of the water table between wells. For sites where the hummock well was dry (denoted by *), water level is drawn at the bottom of the hummock well. A schematic is shown in the legend to illustrate hummock height (H) and length (L) and water table elevation difference (Δh). CO=coarse outwash; CO-P=perched over coarse; HM=hummocky moraine; CP=clay-till plain; WL = water level

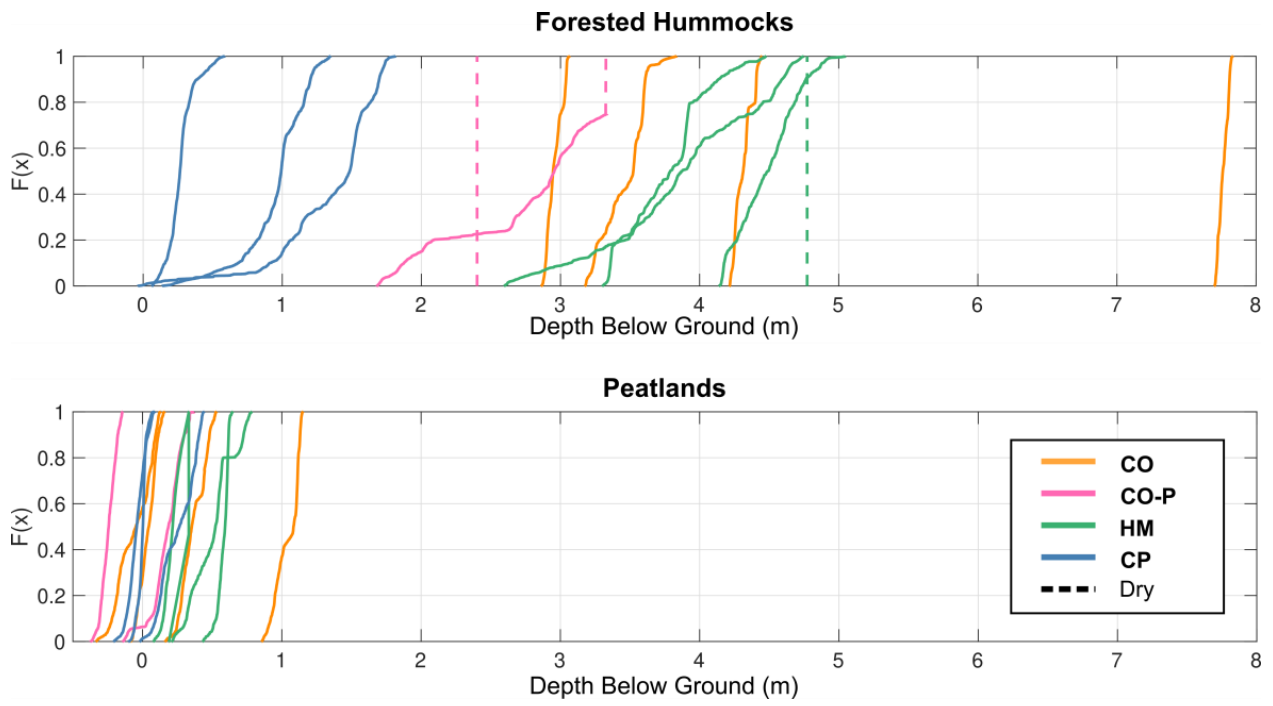


Figure 4-3: Empirical cumulative distribution functions of the depth to water table (WT) at each well, where ground surface is represented by zero. Wells that were dry are represented by dashed lines, which show the location of the bottom of the screened interval.

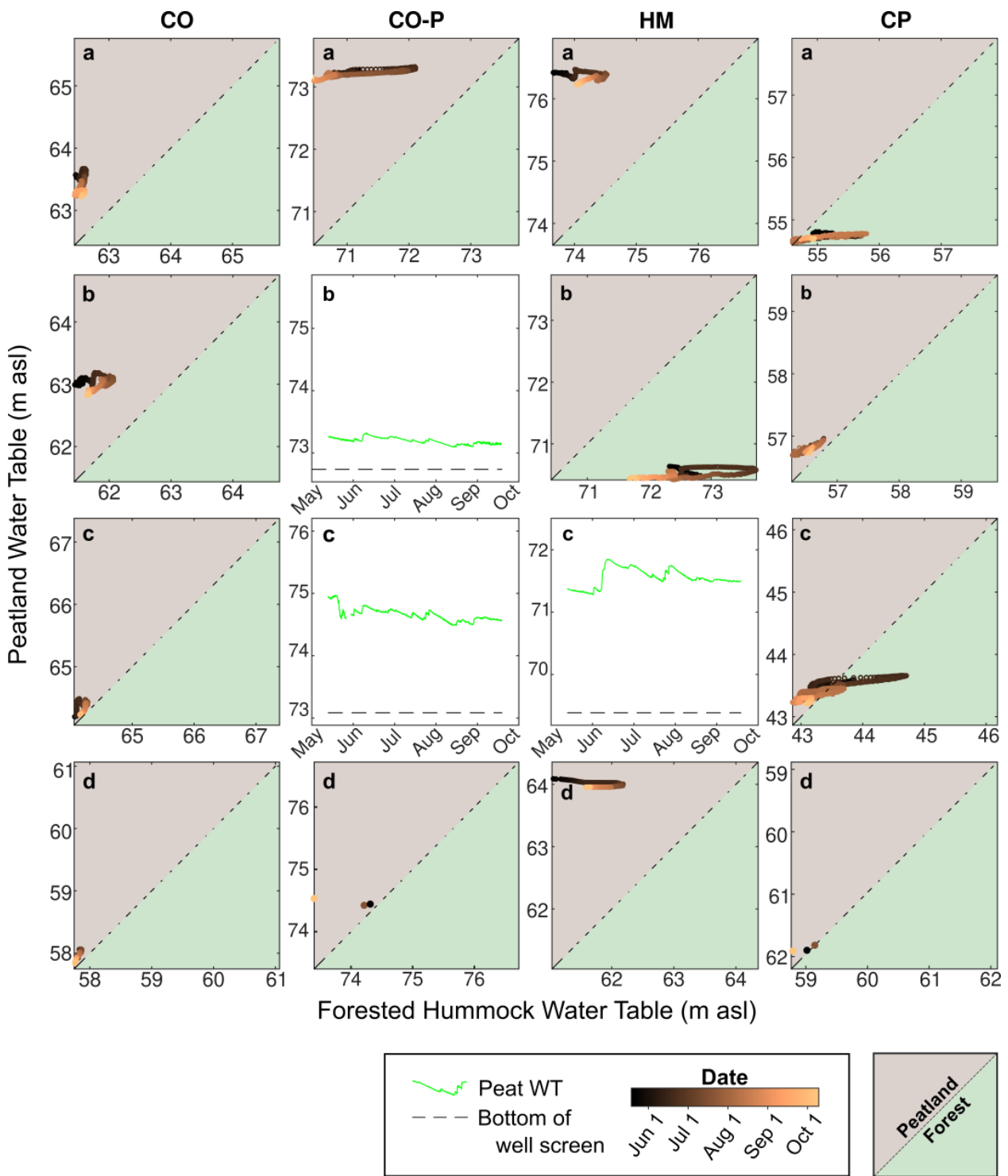


Figure 4-4: Peatland and forested hummock water table elevations for each site. The dashed line shows the 1:1 relationship, where points to the left of the line show a gradient towards the forested hummock and points to the right of the line show gradients towards the peatland. For sites where the hummock well was dry, a time series of the peatland water table is presented and the bottom of the hummock well is shown for reference. All elevations are relative to 600 m asl. All elevation axes have equivalent scales.

Chapter 5

Hummock-scale controls on groundwater recharge rates and the potential for developing local groundwater flow systems in water-limited environments³

5.1 Introduction

The Canadian Boreal Plains are dominated by aspen mixedwood forests, shallow lakes, and peatlands. The intrinsic variability in water storage of these land covers in conjunction with the sub-humid climate causes large interannual variability in runoff generation and hydrological connectivity at local to landscape scales. Local groundwater flow systems (i.e., flow in which the recharge area is above and directly adjacent to its discharge area) are necessary to hydrologically link forested hummocks with adjacent peatlands or ponds, and subsequently create runoff from the landscape. However, the development of groundwater mounds beneath hummocks, which is required to generate local groundwater flow systems, is both spatially and temporally infrequent in low-relief and low-recharge settings like the Boreal Plains (Chapter 4). Thus, identifying the spatiotemporal controls on groundwater mounding is crucial to understanding the climatic and geological conditions required for landscape connectivity and runoff generation at larger, regional scales. This insight is becoming increasingly important as water security, ecosystem sustainability, and environmental quality become the focus of land management, reclamation, and reconstruction efforts. For large parts of North America, forestlands are the primary source of landscape-scale runoff; however, in the Boreal Plains it has been shown that sparsely vegetated, coarse glacial outwashes and peatlands are the primary water producing landforms (Chapter 4; Barr et al. 2012; Devito et al., 2017; Smerdon et al., 2007). Nevertheless, large parts of the Boreal Plains are characterized by fine-textured glacial deposits, with aspen mixedwood forests. Thus far, the hydrologic function of fine-textured (i.e., silts and clays) forested hummocks has not been adequately defined for sub-humid regions.

Water tables in low-relief, water-limited environments are generally not topographically controlled, and therefore local groundwater flow systems are scarce (Chapter 2; Haitjema and Mitchell-Bruker, 2005; Tóth, 1963). Rather, these systems are recharge controlled, meaning water table positions are more dependent on transient recharge events than the gravity driven flow of more stable topographically controlled water tables. Groundwater recharge, an essential process by which a downward flux of water enters groundwater storage (Healey, 2010), is controlled by complex interactions between precipitation (both timing and magnitude), evaporation to the atmosphere and transpiration by vegetation, interception of precipitation by the canopy, soil water retention properties, and depth to the water table (Wang et al., 2009, 2015; Turkeltaub et al., 2015; Carrera-Hernandez et

³ A version of this Chapter has been published:

Hokanson K.J., Thompson C., Devito K., Mendoza C.A. Hummock-scale controls on groundwater recharge rates and the potential for developing local groundwater flow systems in water-limited environments. *Journal of Hydrology*. 2021; 29 126894.

al., 2011; Smerdon et al., 2008; Healey, 2010). Although it is an important component in groundwater systems and is vital to understanding subsurface water movement and availability, recharge is difficult to measure and the relative importance of these controlling factors are poorly understood (Healey, 2010).

Through a combination of field observations and numerical modelling, this study identifies the role of aspen forested hummocks in the generation (or loss) of groundwater and hydrologic connectivity to adjacent peatlands by examining the simulated recharge patterns and sink-source functions of various hummock regimes in the Boreal Plains. A silty clay loam hummock located in the BP is used to develop and calibrate a numerical model to better understand the spatiotemporal dynamics of recharge, water table position, and lateral flow between the forestland and adjacent peatland. The calibrated model is then used for scenario testing to further understand the controls on recharge and forestland-peatland interactions. Specifically, I test the effects of altering the height, length, and hydraulic conductivity of the forested hummock under both wet and dry climatic periods.

5.2 Study Area

The Utikuma Region Study Area (URSA; 56°N, 115°W) is located 370 km north of Edmonton, Alberta, in the Boreal Plains ecozone of Canada (Figure 5-1a). The region is characterized by low topographic relief and thick (45 to 240 m) heterogeneous glacial substrates that can be characterized as glaciofluvial, glaciolacustrine, or moraine deposits, all overlying the Smoky Group, a Cretaceous marine shale (Vogwill, 1978). The climate is sub-humid, with long-term potential evapotranspiration (PET; 517 mm/yr) exceeding long-term precipitation (P; 444 mm/yr; Marshall et al 1999). All annual values reported in this study refer to the hydrologic year (November 1 to October 31). Wetter years, where P exceeds PET, occur on an approximately 10 to 25 year cycle (Mwale et al., 2009). The primary modes of precipitation (i.e., 50 – 60%) are short duration convective-cell storms, which occur during the summer months when evapotranspiration is highest (Devito et al 2005b; Brown et al 2014). Previous research at URSA has included several multi-year ecohydrological and hydrogeological studies (Devito et al., 2016). Previous work by Smerdon et al. (2005, 2008) and Carrera-Hernandez et al. (2011) focused on water table and recharge dynamics in coarse textured materials in the Boreal Plain. This study focuses on water table and recharge dynamics in the fine-textured hummocky moraine regions of URSA. These glacial landforms are characterized by silty clay loam hummocks underlain by clays and clay tills, where shallow (i.e., 1 to 15 m below the surface) mineral hydraulic conductivity ranges from 1×10^{-9} to 1×10^{-6} m/s (Chapter 2; Thompson et al., 2015).

5.2.1 Motivation

Numerous forested hummocks have been monitored since 2000 as part of the larger URSA long-term observation network (Devito et al., 2016). The hummocks are dominated by trembling aspen (*Populus tremuloides*) and are adjacent to peatlands. The peatlands have fairly stable water elevations (± 0.5 m above or below the peat surface; Chapter 4; Thompson et al., 2015); however, the hummocks exhibit very different water table configurations. All of the monitored hummocks at URSA are located in the same 100 km² region, so are subject to the similar annual weather patterns (e.g., P, PET). Nevertheless, through the various studies conducted at URSA, it is evident that no simple metric (annual

P, multi-year cumulative P-PET, saturated hydraulic conductivity, etc.) is a good predictor for water table elevation or potential mounding within the hummocks. Hummocks with similar storage potential (i.e., height of hummock above the adjacent peatland) may have very different water table behavior over time (Chapter 4; Devito, unpublished data). For example, two hummocks with similar textures will exhibit extremely different water table patterns, where one might exhibit groundwater mounding above the adjacent peatland every year and the other might only wet up once or twice over twenty years. Consistent groundwater mounding (i.e., the generation of groundwater via recharge and subsequent flow away from the hummock) is required for hummocks to act as a hydrologic ‘sources’ of water; and while it is often assumed that local topographic highs, like hummocks, act as sources of water to the larger landscape, it has been shown that this is not the case for many hummocks in the BP (Chapter 4).

An instrumented hummock was selected to develop and calibrate a variably-saturated two-dimensional numerical model to simulate observed water table behavior and concomitant recharge rates. This particular study hummock was part of a larger modelling effort by Thompson et al. (2015, 2017, and 2018), who examined the hydrological effects of climate and aspen harvesting. However, while Thompson et al. focused on peatland, pond, and riparian hydrologic dynamics, here I focus on the groundwater hydrology of the mineral hummock itself. This work uses a numerical model to examine the controls (hummock morphometry, hydraulic conductivity, and annual atmospheric fluxes) over recharge, water table position, and forestland-peatland hydrologic interactions in fine-textured, sub-humid, glacial environments.

5.2.2 Study hummock site and field measurements

The study hummock is in the catchment of Pond 40 at URSA (Petroni et al., 2016; Thompson et al., 2015), and is part of a pond-peatland-forested hummock complex (Figure 5-1b). Lake 40 and its catchment are located on a regional high which functions as a regional recharge zone with strong vertical gradients (Chapter 2; Ferone and Devito, 2004). The hummock is separated from Lake 40 by a 50 m wide peatland, above which the mineral hummock rises approximately 6 m. The study hummock and those around it are characterized by Gray Luvisolic soils (Soil Classification Working Group, 1998) developed from disintegration moraine deposits, which are typically silt-rich but spatially heterogeneous, with zones of high clay or sand content (Fenton 2013; Redding and Devito, 2008). The A soil horizon is typically 0.1 m thick and the B horizon typically only extends 0.5 m to 0.7 m below the ground surface (Redding and Devito, 2008). Boreholes indicate an extremely heterogeneous glacial landscape with evidence of sand and clay lenses in largely silty clay loam hillslopes (Chapter 2; Thompson et al., 2015; Vogwill, 1978).

The water table elevation in the hillslope was monitored, from 2004 to 2018, at three monitoring wells: near the crest of the hummock (WA), mid-slope (WB), and at the toe of the slope (WC; Figure 5-1c). These water levels were recorded both manually (i.e., water level tape) and remotely (i.e., pressure transducers with dataloggers, Solinst). Hydraulic conductivity of the glacial substrate and upper soil layers were estimated using slug tests and a Guelph Permeameter, respectively. These data have been reported previously (Redding et al., 2011; Thompson et al., 2015, 2018). The Lake 40 catchment was

clear-cut during the winters of 2007 (north side of Lake 40) and 2008 (south side of Lake 40). Thompson et al. (2018) studied the hydrological impacts of this harvest and compared them with an adjacent reference catchment. They found that aspen harvesting had limited impacts on groundwater levels beyond the initial post-harvest years due to the rapid recovery of aspen evapotranspiration and high soil-moisture storage capacity of the native glacial materials (Thompson et al., 2018).

Depending on the seasonal and interannual climatic conditions, the water table exhibits periods with groundwater mounds (i.e., the water table is above the adjacent peatland) and periods with groundwater depressions (i.e., the water table is below the adjacent peatland). The water table elevation near the top of the hummock (WA; Figure 5-1c) ranges from approximately 1.5 m below the adjacent peatland to more than 3 metres above the peatland, while the water table in the peatland varies less than 0.5 m in a given year and remains within 0.5 m above or below the peat surface (Thompson et al., 2015).

Daily P data were collected from 1999 to 2018 at URSA using two to three tipping bucket rain gauges adapted for snowfall by using anti-freeze in the reservoirs. Historic daily P was taken from the Fort McMurray CS Weather Station (WMO 71585; 56.65°N, 111.21°W) from 1944 to 1999 and at the Fort McMurray Weather Station (WMO 2581; 56.73°N, 111.38°W) from 1920 to 1943, the closest maintained weather stations to URSA with the most continuous data (Environment Canada, 2019). Daily average temperature from 1921 to 2018 was also obtained from the Fort McMurray weather stations (Environment Canada, 2019). Precipitation expressed as cumulative departure from the long-term mean annual P (CDM) is used in some analyses. The CDM was calculated by (a) creating a daily time series of annual P (a moving sum of daily P with a window of 365 days), (b) subtracting the long-term annual mean P (444 mm) from the moving sum of annual precipitation values, resulting in a daily time series of moving window one-year departures from the mean (CDM-1), and (c) accumulating the resulting departures over a period of either two, or three years (CDM-2, CDM-3). This approach of moving window cumulative departures has the advantage of showing both long-term cumulative trends in moisture deficit or surplus as well as short-term effects, such as large melt or storm events (Smail et al., 2019).

5.3 Numerical Modelling and Statistical Methods

5.3.1 General approach

The surficial geology at the study site is highly heterogeneous; however, the model was constructed as a simplified representation with homogeneous layers to capture the essential hydraulic characteristics and behavior of the system, yet still be applicable to a range of hummock scenarios. This generalization inevitably reduces the accuracy of the transient hydraulic heads predicted by the model; however, and more importantly, it allows for the model to later be applied to different hummock morphometries without being limited by idiosyncratic, site-specific features, such as a buried sand lens.

A two-dimensional profile from the hillslope crest to the peatland was chosen to represent the system (Figures 5-1b and 5-1c). This domain is consistent with the conceptual flow field, where lateral flow is from the crest of the hummock to the peatland, or vice versa.

Observed water table elevations along the primary study hummock were used to calibrate the model, which represents the integrated responses to recharge rates, root-water uptake, and lateral fluxes between the peatland and hummock. The calibrated model was then modified for scenario testing to represent other hummock regimes, by increasing or decreasing the available storage vertically and laterally away from the peatland (i.e., hummock height and length), and changing the transmission properties of the hummock substrate (i.e., hydraulic conductivity). This approach allows for the identification of the major controls or thresholds governing water table behavior, recharge, and the development of local groundwater flow systems.

5.3.2 Transient variably-saturated model

Due to the sub-humid nature of the Boreal Plain region, P/PET is close to unity, meaning small changes in either P or ET have large effects on infiltration, vadose zone storage, root-water uptake and, ultimately, recharge. Variably-saturated conditions are therefore fundamental to understanding the entire system. To simulate both saturated and unsaturated conditions, transient two-dimensional simulations were carried out in HYDRUS-2D, which is a finite element model for simulating the movement of water in variably-saturated media by solving the Richard's equation with a sink term for root-water uptake (Version 2.05; Šimůnek et al., 2006). The soil water retention curve and the unsaturated hydraulic conductivity function were modelled using the van Genuchten–Mualem constitutive relationships (Mualem, 1976; van Genuchten, 1980).

5.3.2.1 Model domain and material properties

The model domain extends laterally from the middle of the peatland to the crest of the hummock, and vertically from the crest of the hill to 26 m depth (Figure 5-1c). The finite-element mesh was discretized such that a version of this appendix was published in:

Hokanson K.J., Thompson C., Devito K., Mendoza C.A. Hummock-scale controls on groundwater recharge rates and the potential for developing local groundwater flow systems in water-limited environments. *Journal of Hydrology*. 2021; 29 126894. at the upper layers have vertical and horizontal nodal spacing of approximately 0.15 m and 0.45 m, respectively. The nodal spacing gradually increases with depth so that the lowest part of the domain has vertical and horizontal nodal spacing of approximately 0.8 m and 4 m, respectively.

Four primary hydrogeologic units were included in the model: peat, forest floor, soil, and glacial till (Table 5-1; Figure 5-1c). The peatland is represented by two model materials, a less dense fibric peat and a denser sapric peat. Fibric peat is found at the surface and is least decomposed and least dense, and sapric peat is found at the bottom and margins of peatlands and is more decomposed and denser. The soil horizons are represented by two model layers: a 10 cm thick forest floor layer representing the LFH (litter, fibric, humic) materials, and a soil layer representing the A and B horizons. The C horizon and underlying glacial till are simplified to a single extensive glacial till unit, which has the same soil hydraulic parameters, but is discretized into 3 layers (upper, mid, and lower till), where the saturated hydraulic conductivity decreases with depth (Table 5-1).

The soil hydraulic properties of the forest floor, soil, and glacial till were informed by field measurements and previous modeling efforts (Redding and Devito, 2008, 2011; Thompson et al., 2015,

2018) before being calibrated. An anisotropy ratio ($K_x:K_z$) of 30:1, which represents one and a half orders of magnitude contrast, was applied for all materials except the peat, which had an anisotropy ratio of 10:1, and the forest floor, which was isotropic. Due to the impact they have on recharge, the soil hydraulic properties for the forest floor and soil layers were calibrated using a separate, but complementary 1D modelling approach utilizing measured soil water content over two winter-summer cycles (see Appendix B for further details on the 1D model construction and calibration).

5.3.2.2 Boundary and initial conditions

The upper surface of the model represents the aspen forestland, the peatland, and the transition between the two (Figure 5-1c). Net P, consisting of daily fluxes of throughfall (i.e., rain not intercepted by vegetation) and snow melt after sublimation, and root-water uptake were applied to the surface of the model composed of the aspen forestland and the narrow peatland-forestland transition and peatland margin, represented here by sapric peat. Daily P was considered rain on days with average air temperature greater than 0°C; it was then applied directly to the surface of the model after accounting for interception. Otherwise, it was considered snow and accumulated on the surface. To determine snowmelt, a simple degree-day melting model was applied (NRCS, 2004). Evaporation was removed from the daily precipitation externally from the model in the forms of rain interception and snow sublimation. Free water evaporation from the soil surface was assumed to be negligible (Blanken et al., 2001), and therefore not considered. A constant daily canopy interception of 0.5 mm in the spring and 2 mm following full leaf out was applied to the daily rain data (Thompson et al., 2015), and 13% of snow water equivalent was removed from melting snow to account for snow sublimation (Pomeroy et al., 1998).

Daily PET was determined using the Hamon (1963) method. Daily potential transpiration (T_p) was partitioned from daily PET using the leaf area index (LAI) of the hummock vegetation via the Beer-Lambert Law (Ritchie, 1972). The initiation of leaf emergence and time until the full-leaf period was determined by the cumulative degree-day (D) method, where leaf emergence begins when the sum of D exceeds 69 degree-days, prior to which LAI is zero. A fully-leafed canopy, during which LAI is 4.5 and incorporates the aspen canopy and shrub subcanopy (Little-Devito, unpublished data), is assumed when the sum of D reaches 316 degree days (Barr et al., 2004). Between leaf emergence and full leaf out, LAI increased linearly. The senescence of boreal aspen has been found to be primarily controlled by decreased daylight hours, therefore the initiation and completion of leaf senescence was set to the same calendar day of year, 226 and 259, respectively, for every year (Barr et al., 2004; Sutton and Price 2020). To simulate the limited effects of aspen harvesting, T_p was reduced to $0.7 \cdot T_p$ for the first post-harvest year and returned to full T_p by the 7th post-harvest year consistent with Thompson et al. (2018).

Previous studies have shown that fine, shallow, lateral roots primarily exploit resources (water and nutrients), while deep, large diameter roots are responsible for structural stability (Block et al., 2006; Strong and La Roi, 1983). Snedden (2013) found that, along a hillslope at the URSA, aspen root mass was most concentrated in the top 0.2 to 0.3 m of the soil profile. Root-water uptake was therefore concentrated in the upper 0.3 m of the hillslope in the model domain.

The peatland was represented by a constant pressure head boundary ($\Psi = -0.3$ m), which represents a stable water table 0.3 m below the surface of the peatland middle; the implications of this are explored in the sensitivity analysis. A constant head boundary ($h = 662$ m asl; $\Psi = 11$ m) was applied to the base of the model to simulate connection with the deeper, regional groundwater flow system. This implementation is supported by deep piezometers in the area, which show little to no seasonal or inter-annual variability in hydraulic head (Chapter 2; Thompson et al., 2015). This lower boundary condition resulted in a downward head gradient of ~ 0.4 , similar to the vertical gradients reported in Chapter 2 for the same catchment. No-flow boundary conditions were applied to the lateral edges of the domain.

Representative initial conditions were obtained by allowing the model to spin up, from hydrostatic conditions, using observed climate data for the 10 years prior to the period of interest. Ten years was deemed more than sufficient, as any period greater than 5 years resulted in equivalent model results.

5.3.3 Scenario testing

5.3.3.1 Hummock regimes

Once calibrated, the model domain was modified to represent a spectrum of forested hummock 'regimes,' with differing combinations of hydraulic conductivity, hummock height, and hummock length. The topography of the study hummock was simplified and adjusted to represent these hummock morphometries. The ground surface elevation (Z) leading away from the peatland was represented by a sine function:

$$Z = A \cdot \sin^E(B \cdot X) \quad [5.1]$$

where X is the distance into the hillslope, away from the peatland, A is the vertical distance from the peatland to the top of the hummock (i.e., hummock height), B controls the distance from the peatland edge to the hummock crest (i.e., hummock length), and E controls the concavity.

To focus on the controls of hummock morphometry on water table position and recharge, E was held constant at a value of 2. Hummock height, A , was set to 2, 6, and 10 m, and B was set to 0.0118, 0.018 and 0.038 (which translates to hummock lengths of approximately 45, 85, and 135 m, respectively), for a total of 9 different hummock morphometry combinations (Figure 5-2). Of these nine morphometric scenarios (A through I), Hummock E most closely resembles the morphometry of the study hummock used to calibrate the numerical model (Figure 5-1c).

Three hydraulic conductivity (K) scenarios were tested by varying the base K in the glacial till units: 'base K ' (the same conductivities as the study hummock; Table 5-1), 'high K ' (K values increased by an order of magnitude), and 'low K ' (K values decreased by an order of magnitude). The combinations of the three heights, three lengths, and three conductivity scenarios result in 27 unique hummock regimes. These parameters were chosen to approximate the range of hummock characteristics (morphometry and hydraulic conductivity) observed in the field across the glaciated western Boreal Plains (Chapter 4).

Simulations were run from 1930 to 2018, after a ten-year spin-up period (1920-1930), and did not include a reduction in T_p due to harvesting.

5.3.3.2 Sink-source dynamics

The long-term sink or source function for each hummock regime was assessed by examining the water fluxes to and from the adjacent peatland. If, by the end of the 88-year simulation period, more than $90 \text{ m}^3/\text{m}$ (i.e., approximately $1 \text{ m}^3/\text{m}/\text{yr}$) of water was sourced to the peatland from the hummock, or to the hummock from the peatland, it was deemed a long-term source or sink of water, respectively. If the function switched or fluctuated, or was otherwise very small, throughout the simulation and therefore the end/net value was less than $90 \text{ m}^3/\text{m}$ in either direction, it was deemed a 'weak sink/source'. In this 2D representation of a 3D hillslope, $1 \text{ m}^3/\text{m}$ represents 1 m^3 flowing across the peatland-forestland interface per metre along the interface.

5.3.3.3 Relative controls on groundwater recharge

The simulated annual recharge rates (88 years for each of 27 regimes; $n = 2376$) were then used to train a boosted regression tree (BRT) ensemble to evaluate the relative importance of the morphometric, hydrogeological, and climatic controls on the model results. BRTs create hundreds to thousands of regression trees (in this case, predicting groundwater recharge), which are produced forward and stage-wise by re-weighting residuals from previous trees. The final BRT model is a linear combination of all the created trees that can be conceptualized as a regression model where each term is a tree (Elith et al., 2008), from which I can estimate each predictor variable's importance by averaging the relative importance or influence of the variables over the collection of trees (De'ath, 2007). BRTs are valuable because they do not assume normality or stationarity, they ignore non-informative predictors, can accept both numeric and categorical predictors, are unaffected by outliers, are not prone to overfitting due to correlated or redundant predictors, and are efficient at modelling non-linear relationships (De'ath, 2007; Dormann et al., 2013; Elith et al., 2008). Not only do BRTs build predictive regression models, they can provide insight to the relative importance of each predictor variable, which are used here to determine which hummock-scale parameters influence recharge the most.

Although BRTs are a relatively new machine learning method, they have been successfully applied in previous hydrogeological studies, such as: developing frameworks for groundwater nitrate models (Nolan et al., 2015), aquifer salinity (Knierim et al., 2020), groundwater spring mapping (Chen et al., 2020) and examining the relative controls of climate and geology on basin water yield (Sun et al., 2019). The BRT analysis here was performed in MATLAB using the Machine Learning Toolbox, where a ten-fold cross validation process was used to evaluate the performance of the BRT model and to prevent overfitting (Babiyak, 2004; Kohavi, 1995). The hyperparameters of the BRT (e.g., leaf size, number of trees) were optimized to improve the accuracy and further prevent the overfitting of the developed BRT model similar to that of Lou et al. (2016).

5.4 Results and Discussion

5.4.1 Model performance

5.4.1.1 Comparing observed and simulated water table elevations

Simulated transient water table elevations were compared with measured water table elevations at three monitoring wells along the study hummock hillslope: WA (n = 2277), WB (n = 111), and WC (n = 87; Figure 5-3). For WA, only the continuous data set, which was resampled at a daily time step, was used as it was seen to be more reliable than the manual well measurements. Considering all synchronous water table observations and model predictions (n = 2475), 89% of observations were within 1 m of one another, and 73% of observations were within 0.5 m. Because I greatly simplified the hydrogeology of the hummock, perfectly modelling the minutia of water table dynamics was never an expectation. Nevertheless, by visually examining the transient simulation results, it appears that the model is adequately representing the basic hydrologic functions of the hummock.

In general, the characteristics of the water table hydrographs (e.g., peaks, rising limb, and recession) in the hillslope were well represented by the model (Figure 5-3). Seasonal and interannual trends were also well-represented by the model. In most years, winter periods show a gradual increase in water table elevation in the modelled data that is absent in the observed data. This is an expected artefact of the numerical model since HYDRUS does not simulate ice or frozen groundwater in the peatland or riparian zones, which may lead to increased lateral subsurface flow from the peatland to the hillslope during winter periods. The timing of the spring water table rise, which is the result of snowmelt infiltration, is, for the most part, accurate. However, for some years it is early by several weeks and is a limitation of the simplistic degree-day melting approach implemented here. The rate of melt, and therefore potential recharge, is dependent on snowpack size and density, which can delay melt (Bartlett et al., 2006).

The observed water table elevations at the WA monitoring well were considerably lower in the first three years of observational data (2006, 2007, and 2008) when compared to the remainder of the time series (2009 to 2019). This discrepancy may be due to several factors; for example, the monitoring well at WA (installed in 2006) had not reached equilibrium with the surrounding fine-textured substrate, or, as Redding et al. (2008) noted, periodic freeze-melt cycles can result in concrete frost which inhibits virtually all snowmelt infiltration. Alternatively, a buried lens of contrasting material could have a threshold effect on water table response, which was not explored here.

5.4.1.2 Sensitivity analysis

This model builds on the work of Thompson et al. (2015, 2018), which contains a detailed sensitivity analysis and emphasizes the role of the lake and peatland. This work, however, focuses on the water table position in the mineral hummock. Consequently, the sensitivity analysis reflects these different objectives.

Changing the lower boundary condition, peatland hydraulic conductivity, and the range between saturated and residual water content of the till was found to have minimal impacts on the model

results. Changing the soil thickness (increase resulted in a decrease in recharge), the anisotropy ratio (increase resulted in lower water tables), and the till unsaturated flow parameters had disproportionate effects at the upper slope of the hummock (WA), where the vadose zone is thickest, compared to the mid-slope (WB) and toe of slope (WC) regions. However, changing the elevation of the fixed water table in the peatland (decrease resulted in lower water tables) had a stronger effect on the water table position in the lower portions of the hummock and a negligible effect in the upper slope. The detailed sensitivity analysis can be found in Appendix C.

5.4.2 Hummock water balance

During the 88-year simulation, the dominant annual fluxes in the hummock water budget were P and evapotranspiration (the sum of evaporation, composed of interception and sublimation, and root-water uptake), which had annual mean values of 443 and 385 mm/yr, respectively over the entire modelling period. Annual precipitation, snowmelt, recharge, and CDM-1, CDM-2, and CDM-3 for the modelling period are shown in Figure 5-4. All major budget components are plotted in Figure 5-5 for a ten-year period (hydrologic years 1961 to 1970), which contains some of the highest (186 mm; 1970) and lowest (35 mm; 1965) recharge rates.

P is partitioned into evaporation, infiltration, and runoff (Figure 5-5b), the latter of which is the residual of P, evaporation, and infiltration. For the entirety of the model run, there was little to no surface runoff at the top of the hillslope; however, during spring melt and high intensity summer storms there was intermittent runoff at the toe of the slope, which on an annual basis had a median value of 18 mm/yr and is most correlated with precipitation that occurred prior to full leaf out of the aspen ($R^2 = 0.61$). While most years had relatively low runoff values, only during especially wet periods (i.e., precipitation prior to full leaf out exceeds 230 mm) annual runoff exceeded 85 mm/yr. Large runoff events have been recorded in aspen dominated catchments in the BP, but are infrequent and may only occur every 10 to 20 years (Devito et al., 2005a).

The cumulative change in storage became relatively large (i.e., 75 to 150 mm) in April or May of each year but by the end of the hydrologic year was starting to decline (Figure 5-5b); however, most years ended with an appreciable storage surplus or deficit. When compared to the average long-term storage in the hummock, the maximum end-of-year storage deficit was -84 mm, and the maximum end of year storage surplus was +83 mm (Figure 5-6a). The middle 68% (i.e., \pm one standard deviation) of the end of year storage difference ranged from -40 mm to +40 mm. This indicates that the system does not 'reset' itself each year and there are opportunities for multi-year impacts on water levels or recharge. That is, when the change in storage does not return to zero it may have a disproportionate effect on the next year's recharge as a product of precipitation. Such behaviour is contrary to the very common assumption that the annual change in storage is zero, which can lead to either under or overestimation of other parameters in a water balance study (Han et al., 2020; Devito et al., 2005b).

5.4.2.1 Water table elevations and peatland-forestland fluxes

The hydrographs for all three wells showed seasonal peaks and associated recessions in response to annual spring melt; however, the hydrographs at WB and WC had earlier peaks and quicker

recessions than those at WA. A time series of the simulated water table elevations at the three monitoring wells for a selected five-year period (1960 – 1965) are shown in Figure 5-7b. The water table exhibited a similar pattern on an annual basis, where the annual spring melt (usually in mid-April) would cause the water table to rise and the subsequent onset of transpiration from the aspen forest land would both retard recharge and draw down the water table, reaching a minimum elevation in the late summer or early fall. Throughout the simulation, the water table elevation at the top of the hummock (WA) was more dynamic than at the mid slope (WB) and toe of slope (WC) positions; however, the water table lower on the hummock were deeper, and lower than the peatland for longer durations. Water table configurations representing the 5%, 50%, 95%, and 99% percentile ranks are shown with empirical cumulative distribution functions for water table elevations for each well in Figure 5-7a. While the trends in the hydrographs were the same along the hillslope, the timings were not in sync. At the toe and mid slope locations (WC and WB, respectively), the hydrographs would peak and start to decline much earlier than at the crest of the hummock (WA). Water table behaviour of this kind is controlled by the thickness of the unsaturated zone above the water table.

Only the 90th and 95th percentiles (Cases C and D in Figure 5-7a) have water tables that truly follow topography. The 5th and 50th percentiles (Cases A and B in Figure 5-7a) show a water table extending from the peatland laterally into the hummock, where at the toe and mid slope there is a notable depression for large parts of the year. This water table depression is caused by groundwater upflux due to root-water uptake (i.e., transpiration), which in turn generates a gradient for groundwater to flow into the depression from the peatland and, later in year, from upslope near WA (Figure 5-7b). Fluxes of water between the peatland and the forested hummock are transient and vary from year to year and are dependent on water table elevations at the toe of the slope (Figures 5-5b and 5-7b). On a daily basis, the directions of the flow of water between the peatland and hummock was almost evenly split, where the direction of flow was towards the hummock approximately 49% of the time. However, especially during spring snow melt, the magnitude of the fluxes was larger when flow was from the hummock to the peatland and on an annual basis the median peatland flux was 13 mm away from the hummock.

5.4.2.2 Groundwater recharge

Daily recharge was calculated at each location along the hummock (i.e., WA, WB, WC) and was either positive, to represent downward flow of water that intersects the water table, or negative, to represent upflux or upward flow of water away from the water table into the unsaturated zone, usually due to root-water uptake and redistribution under capillary action (Figure 5-5a). The spatial distribution of recharge patterns along the hillslope was generally organized into the classic Tóthian unit basin (Tóth, 1962), where at the top of the hummock (WA) there was generally positive recharge throughout the year and at the bottom of the hummock (WC) there was predominantly upflux. This upflux was usually due to root-water uptake; however, when water tables at the mid and toe of the slope were especially high (e.g., hydrologic years 1961 and 1970 in Figure 5-5a), WC acted as a groundwater discharge zone and upflux through the land surface was the result. The mid slope (WB) showed greater temporal variability than either WA or WC, with recharge dominating in the snow melt season and upflux dominating once transpiration began during leaf out of the aspen forest. During most years, WA

received the most recharge, followed by WB and WC. This is due to the depth of the water table below the ground surface and the thickness of the unsaturated zone, where percolating water has the greatest probability of 'escaping' the rooting zone before it can transpire. Cross-correlation analyses indicate that there is an average 26-day lag time between daily P and recharge at WA, whereas the lag times for WB and WC average only 1 day.

Total precipitation applied to the forested hummock, which is a combination of throughfall and snow melt after sublimation, ranged from 187 to 605 mm/yr, while recharge at the crest of the hummock (WA) ranged from only 15 mm to 200 mm (Figure 5-4a). Notably, there was no strong correlation between annual recharge and annual precipitation ($R^2 = 0.16$), annual snowmelt ($R^2 = 0.28$), or P-PET ($R^2 = 0.15$). However, there was a stronger relationship between annual recharge and the sum of the previous two years total precipitation ($R^2 = 0.48$) and the two-year departure from the long-term mean (CDM-2; $R^2 = 0.56$). This is mostly likely a consequence of the control exerted by the state of the hummock storage (i.e., deficit or surplus) at the end of the previous year. If a hydrologic year begins under storage deficit conditions: (a) the water table itself is likely lower and transit times through the vadose zone will be longer, (b) the low soil moisture in the vadose zone reduces the effective hydraulic conductivity, and (c) increased available storage must be filled before recharge can commence (Han et al., 2008; Wossenyeleh et al., 2020). Figure 5-6b shows the relationship between recharge and the storage state at the beginning of the hydrologic year (i.e., at the end of the previous hydrologic year); this relationship makes it clear that the previous hydrologic year has a dominant influence on the current year's recharge rate, regardless of current atmospheric fluxes.

5.4.3 Scenario testing: water table elevation and groundwater recharge

The 27 hummock regimes presented here test the effects of hummock morphometry (height and length) and hydraulic conductivity on water table elevation and recharge. The general water table behaviour, fluctuations, frequency of groundwater mounding, and recharge rates were evaluated for each scenario and were measured at the top of each respective hummock, similar to WA observation point at the study hummock.

Previous studies have focused on plot-scale controls on recharge, such as van Genuchten parameters α and n , rooting depth, and depth of forest floor material (e.g., Lukenbach et al., 2020; Wang et al., 2009; Naylor et al., 2016), or on regional-scale controls, such as climate, topography, and geology (Healy et al., 2010; Hajjema and Mitchell-Bruker, 2005). However, there is a noticeable lack of studies that examine the hierarchy of controls over water table configurations and recharge at the hillslope or hummock scale and how variations therein affect regional hydrology (Appels et al., 2015; de Vries and Simmers, 2002). Hillslopes are, nonetheless, the building blocks and fundamental units of larger-scale hydrologic systems. They serve as local topographic highs and are a key scale for the generation and determination of local groundwater flow and discharge patterns systems and therefore all groundwater flow accumulation for intermediate scale systems.

When comparing the annual recharge rates to either previous studies in the same region or to other regions in the world, it is important to note that the recharge rates reported here are for the top of the hummock (in a similar position to WA in the study hummock; Figure 5-1c). Water that infiltrates at

the top of the hummock has the highest probability of escaping the aspen rooting zone and becoming recharge, and therefore represents the upper limits of groundwater recharge for a given hummock.

5.4.3.1 Effects of hydraulic conductivity

Within a single hummock morphometric scenario (i.e., hummocks A - I; Figure 5-2), lower K conditions (i.e., decreasing the K of the glacial till by a factor of 10) generally acted to increase the elevation and the flashiness, or seasonal variability, of the water table (Figure 5-8). In the smaller hummocks (short and narrow; e.g., hummock G), low-K conditions delayed the hydrograph peak most years. Additionally, in the smaller hummocks, during years with lower-than-average snowmelt, the late spring hydrograph peak was very muted as the annual melt was held in storage and subsequently removed from the domain by root-water uptake. During years with average or greater spring snow melt, the hydrograph peaks were similar in magnitude between the low- and base-K conditions. Conversely, in the large hummocks (tall and long; e.g., hummock C), low-K conditions resulted in consistently higher water tables. Low-K conditions also appeared to amplify interannual patterns (e.g., the dry period from 1940 to 1955) where there are prolonged periods of low or high water tables due to climatic conditions (discussed below). Between hummocks, the effects of changing K were more amplified the larger the hummock was.

High-K conditions (i.e., increasing the K of the glacial till by a factor of 10) had similar effects in all hummocks, where the general elevations of the water tables were lowered, seasonal fluctuations were amplified, and the interannual fluctuations were dampened. In all cases, the high-K scenarios resulted in water tables with elevations similar to that of the peatland. This is due to increased root-water uptake and increased lateral distribution of water within the hummock, which results in a generally flat water table as the higher K substrates cannot support a steep gradient over such a short distance. For the shorter hummocks (i.e., 2 and 6 m high), the longer the hummock was, the deeper the water tables were under high-K conditions.

Temporarily perched water tables were a frequent phenomena in the low K scenarios (Figure 5-8) and resulted from high precipitation events quickly saturating the soil and top of the till, while the underlying till remained unsaturated; however, these conditions only lasted for a few days before the saturated front dispersed through the soil profile or was taken up by the aspen.

Changing the K had dramatic effects on the annual recharge rates for all the hummocks, where high-K scenarios increased the median annual recharge by an average of 150% and low K conditions decreased the median annual recharge by an average of 70% (Figure 5-9). Annual recharge rates under low-K conditions did not have very much interannual variability; however, under high-K conditions the spread was considerably larger.

5.4.3.2 Effects of hummock morphometry

The effects of hummock morphometry on both water table elevation and recharge can be seen in Figures 5-8 and 5-9, respectively. Hummock height and length have strong synergistic effects where increases in both height and length result in elevated water tables and increased recharge. However, increasing only one parameter does not cause an increase in either water table elevation or recharge.

For example, an especially tall and narrow hummock (hummock A) does not have appreciably higher water table elevations compared to a shorter hummock of the same length (hummock G). Increasing the length while keeping the height the same (e.g., from hummock D to F) reduces the recharge and promotes groundwater depressions beneath the hummock. The increased hummock height and narrow length promote increased flux to and from the peatland and the short later distance does not promote the development of high hydraulic gradients, so the propensity for groundwater mounding is low. Conversely, the tallest and longest hummock (C) has the highest recharge rates and most elevated water tables while hummock I which is both short and long has the lowest recharge rates and water tables. The variation in recharge between tall and short hummocks and long and narrow hummocks mirrors the spatial variability of recharge along the slope (i.e., distance and elevation from the peatland) in the study hummock (Figure 5-5a).

The actual annual recharge rates (violin plots in Figure 5-9) had high interannual variability, especially under base and high K conditions, due to large variability in annual precipitation (Figure 5-4); however, the ratio of recharge to available net precipitation (i.e., precipitation after interception and sublimation; recharge/P) showed much less variability between years and allows for more robust comparisons between hummock regimes regardless of annual precipitation conditions (box plots in Figure 5-9). When examining only the base K conditions, the median recharge/P ratios ranged from as low as 0.04 (hummock I) to as high as 0.42 (hummock C), which have the longest hummock length tested. Both absolute and variability in recharge /P ratios were higher in the taller hummocks. This supports previous findings, which show that increasing the unsaturated zone thickness also increases the probability of recharge. Smerdon et al. (2008), who performed 1D models of outwash sands and gravels, found a threshold height of 4 m above the water table is required for reliable recharge. Lukenbach et al. (2019), who performed 2D simulations of forest floor material over tailings sand in a reclaimed mining landscape, found a similar threshold of only 2 m above the water table. Additionally, I show that both distance and elevation along a hummock are key factors in controlling recharge in these water-limited environments (Figures 5-5a and 5-9). Therefore, the common practice in saturated groundwater flow modelling of applying a uniform recharge rate across similar land units could result in gross over or underestimations of actual recharge through space in small or mesoscale models/systems.

Although only the effects of hummock length and height were explicitly tested here, there is an opportunity to examine the effects of topography on potential recharge. The study hummock has a subtly undulating ground surface topography (Figure 5-1c) and, when this surface was simplified by smoothing, this undulation was removed. The hummock scenario that most closely resembles the study hummock is hummock E (Figure 5-2). Under the same geologic and atmospheric conditions, the study hummock had a median annual recharge rate of 89 mm/yr (± 45 mm; standard deviation) and hummock E only had a median annual recharge rate of 57 mm/yr (± 13 mm). Hummock E had both significantly less recharge ($p < 0.001$) and a much less interannual variability. The variation in ground surface elevation in the study hummock creates a depression that allows for focused recharge before it leaves the system as runoff. These various forms of relief on a single hillslope in the form of both microtopography and mesotopography (e.g., on the scales of centimeters and tens of metres,

respectively), have been shown to focus infiltration and enhance recharge (Appels et al., 2015, 2017; Le et al., 2014; Thompson et al., 2010).

5.4.3.3 Effects of climate

Across all 27 hummock regimes, there were notable temporal patterns in water table elevations, regardless of morphometry or conductivity, that are attributed to interannual precipitation patterns (Figures 5-4a and 5-8). Notably, there were extended periods with lower-than-normal water tables (e.g., from about 1940 to 1950 and from about 1998 to 2005) and higher-than-normal water tables (e.g., from about 1955 to 1965 and from about 1975 to 1980) present in each hummock regime.

These wet and dry periods align very well with the CDM-2 and CDM-3 precipitation indices; however, on an annual basis (e.g., annual P or CDM-1) there is little correlation in most cases. For example, in 2000 the simulated recharge total at the study hummock was 41 mm (Figure 5-4), which represents the 16th percentile of annual recharge, and the water table elevations were far below average; however, the annual P was 442 mm, which would be considered an average year (i.e., long-term mean annual P is 444 mm; Figure 5-4). While the CDM-1 was essentially zero for that year, the CDM-2 and CDM-3 were approximately -80 mm and -250 mm, respectively. This further highlights the role that multi-year storage deficits or surpluses play in modulating annual atmospheric fluxes. These multi-year water deficits and surpluses have large implications for both land management and research approaches. Common time-scales for site investigations, environmental assessments, or even scientific research efforts, are on the order of one to several years; however, climate cycles in the BP are on the order of 15 years (Figure 5-4a; Mwale et al., 2006). Consequently, results and implications from any site investigation must be put into long-term climatic context through understanding of relationships and processes, such as those developed here.

5.4.4 Sink-source function of hummocks: a conductivity paradox

The sink-source relationship between the forested hummock and adjacent peatland is dependent not on the magnitude of recharge, but on the water table position within the hummock which drives lateral hydraulic gradients between the land units (Figure 5-8). The long-term hydrologic function (i.e., sink or source to the adjacent peatland) was affected by all three tested parameters (i.e., hummock length, height, and hydraulic conductivity) by varying degrees.

Hydraulic conductivity had the greatest effect, whereby in all but the largest hummock (C), high K conditions resulted in the hummock being a long-term sink. Moreover, hummock C alternated between being a sink and a source depending on climatic conditions and was therefore classified as a weak sink/source. Although dramatically increased recharge may be present under the high-K scenarios (Figure 5-9), the increased K also allows for increased lateral redistribution of water within the hummock and permits more water to be available for root-water uptake by the aspen forest. It is also important to note that the K values presented here do not represent the full range of K present in the glaciated BP region of Canada, but a range of K representative of fine-textured moraine deposits. The paradox of relatively increased K conditions (e.g., $K_z = 1 \times 10^{-7}$ m/s) resulting in a hummock with elevated recharge rates while also acting as a hydrologic sink would not arise under high K conditions

(e.g., $K_z = 1 \times 10^{-4}$ m/s) in a sand hummock. The latter would have especially high recharge rates while also acting as a hydrologic source because water would percolate quickly to a low water table below the rooting zone and flow laterally to adjacent land units.

Hummock height had less control over the sink-source function of the hummock, by which hummocks of similar length but varying height had similar sink-source functions based on hydraulic conductivity regardless of height (e.g., hummocks A, D, G; Figure 5-9). Interestingly, while the longest hummocks F and I were sinks in all cases, the longest and tallest hummock C was either a long-term source (low and base K) or weak sink/source (high K). The longer the hummock, the larger and/or more persistent the groundwater depression caused by root-water uptake can become, resulting in a long-term sink of water from the landscape. However, at some threshold height (e.g., 10 m above the peatland; hummock C) a sustained gradient provides a consistent source of water to neighboring land units.

It is common to conceptualize the water table as a subdued replica of surface topography, where water flows from topographic highs to topographic lows. This concept is also widely applied to peatland hydrology, where the assumption of peatlands being 'fed' water by adjacent forestlands through topography-driven flow is ubiquitous (Chapter 4). However, as I show here, the sink-source function of a hummock in a sub-humid landscape is highly sensitive to both hydrogeological properties and hummock morphometry. The sink-source function of a land unit and its proclivity to change through time is crucial to understanding the regional water balance, both now and in the future, in water-limited environments. It has been shown at the basin scale, that peatlands and forestlands have important, but competing, roles in influencing surface and subsurface hydrological systems, both through empirical observations (Devito et al., 2017) and numerical models (Hwang et al., 2018). Peatlands, despite existing in a water-deficit environment, have lower actual evapotranspiration rates than forestlands (Barker et al., 2009; Devito et al., 2005a, 2017; Petrone et al., 2007; Prepas et al., 2006), which when coupled with the internal water-conserving feedback mechanisms typical of boreal peatlands (Waddington et al., 2015), makes them primary water sources to the larger landscape in the BP. Forested hummocks, which at the basin-scale average don't provide as much water as peatlands, may be important at the local-scale. Future work is needed to explore the thresholds and implications that various landscape topologies and topographies may have on intermediate and regional groundwater and surface water systems.

5.4.5 Controls on groundwater recharge

The modelled annual recharge rates from each hummock regime over the 88-year simulation were used to train a boosted regression tree (BRT) to examine and rank the relative importance of each of the tested hummock parameters (hummock height, hummock length, and glacial till hydraulic conductivity), as well as several annual climatic variables (potential evapotranspiration (PET), total precipitation prior to full leaf out, throughfall, and snowmelt). The overall performance of the final trained and fitted BRT model can be seen in Figure 5-10a, which had an RMSE of 17 mm and an R-Squared of 0.96. There was no pronounced under or overestimation of annual recharge and the model performed well over the range of hummock regimes tested here. The relative predictor importance can be seen in

Figure 5-10b, where it is clear that, in fine-textured landscapes, hydrogeologic and morphometric factors exerted far more influence than annual climatic variables. The hydraulic conductivity had, by far, the greatest effect on annual recharge, followed by hummock height and length, which had equal importance. These patterns are evident, but not entirely obvious, in Figure 5-9, where the greatest disparity in annual recharge can be seen between K scenarios, and that hummock height and length appear to have a synergistic effect. Of the climatic variables, snow melt was most important followed by throughfall. These results confirm observations from several empirical and modeling studies from the same region, which showed that surficial geology had a larger control over hydrological responses than climate or topography (Chapter 2) and that annual recharge is mostly sourced from spring melt (Smerdon et al., 2008; Thompson et al., 2015). The BRT machine learning method was used here to explore the relative importance of each hydrogeological and climatic variable; however, its successful implementation and high prediction confidence makes it clear that it has the potential to be a valuable tool in predicting hydrological responses to highly non-linear and interdependent processes in complex landscapes such as the Boreal Plains.

When looking at the timing of the hydrographs from the top of both the study hummock and the various hummock regimes (Figures 5-3, 5-7b, 5-8) as well as the cumulative recharge along the study hummock (Figure 5-5a), it is surprising that snowmelt or precipitation prior to full leaf did not have significantly higher estimated importance when compared to throughfall. This is likely because, while the timing of the annual hydrograph indicates recharge sourced from spring snow melt, there is a low correlation between the actual magnitude of recharge and the magnitude of the spring melt due to the effects of antecedent storage deficits or surpluses (Figure 5-6b).

5.5 Summary and Conclusions

The controls on the spatiotemporal variability of water table elevation, recharge, and the sink-source function of fine-textured forested hummocks were explored using a two-dimensional variably-saturated flow model. In addition to a site-specific model, which was created to simulate a study hummock in the Boreal Plains region of Canada with over 13 years of collected hydrogeologic observations, 27 generic model domains were created to represent a range of hummock morphometries and hydraulic conductivities. I found that, between hummocks, geology and morphometry had a greater control over recharge rates than annual atmospheric fluxes. Specifically, high conductivity values and larger hummock heights resulted in greatly elevated recharge rates; however, higher hydraulic conductivity values and longer hummock lengths also allowed for more root-water uptake, had a greater propensity for water table depressions, and resulted in the hummock acting as a hydrologic sink. Taller hummocks with lower conductivity values tended to act as hydrologic sources. Within a single hummock regime, the magnitude of recharge and water table elevation responses were poorly correlated with annual atmospheric fluxes due to the strong residual effects of storage deficits and surpluses within the hummock; however, the timing of water table hydrographs (both observed and simulated) indicate that the bulk of recharge is sourced from spring melt. Recharge and water table elevation did correlate well with both two- and three-year cumulative departure from the long-term mean annual precipitation.

This study demonstrates that both recharge rates and the sink-source function of fine-textured forested hummocks are highly dependent on and sensitive to geology and morphometry of the hummock. In heterogeneous glacial landscapes, recharge is therefore highly variable in space and time. Additionally, while the magnitude of recharge and water table elevation are less sensitive to annual atmospheric fluxes, they are markedly affected by the decadal wet-dry cycles typical of the Boreal Plains climate. Improving our understanding of the spatial and temporal variation of recharge and water table elevation will promote better management practices and assist in planning for the future.

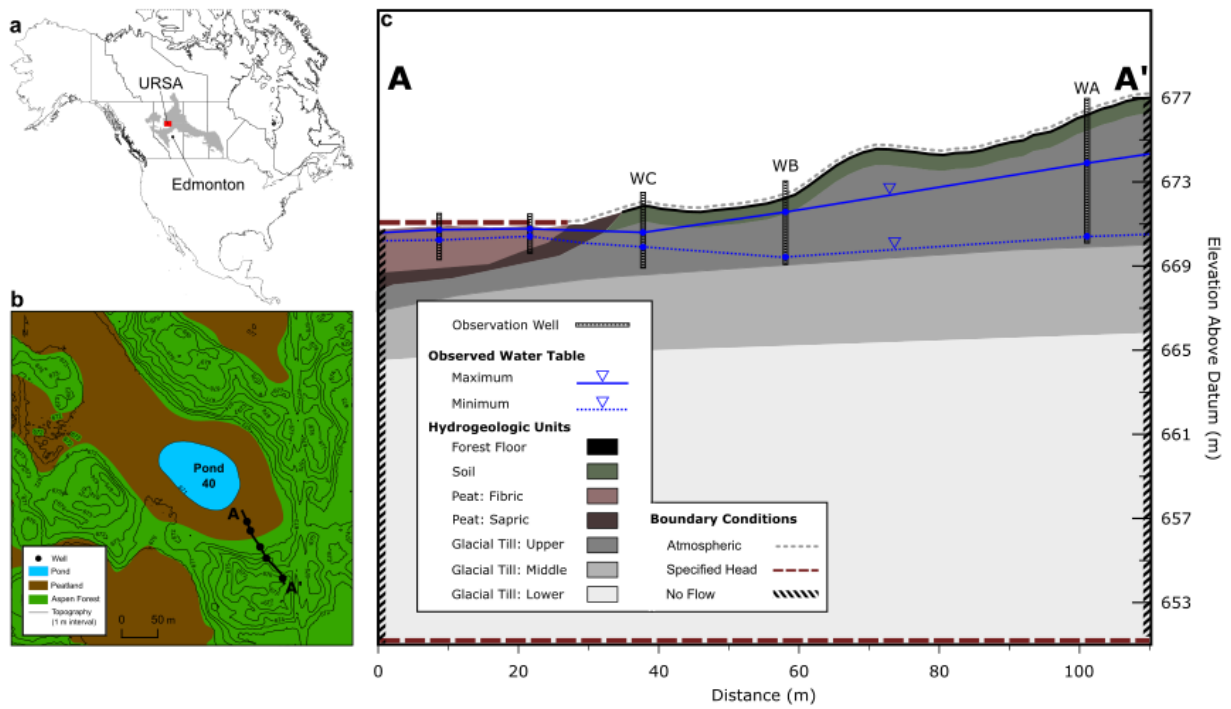


Figure 5-1: (a) The location of the Utikuma Region Study Area (URSA) in the Boreal Plains ecoregion (grey); (b) Map showing the study area with transect A-A', well locations, and vegetative and surface water, and relative topographic elevation; (c) The model domain for the study hummock, along transect A-A', showing the hydrogeologic units, observation wells, historic maximum and minimum observed water tables, and boundary conditions.

Table 5-1: Calibrated material properties

	$\Theta_s - \Theta_r$ (-)	α (1/m)	n (-)	Kz (m/s)	Anisotropy Ratio (Kx:Kz)
Forest Floor	0.84	13	1.9	1.8×10^{-4}	1:1
Soil	0.4	0.8	1.37	9.3×10^{-7}	30:1
Peat:					
Fibric*	0.89	0.8	1.9	2.8×10^{-4}	10:1
Sapric*	0.61	0.3	1.6	9.9×10^{-8}	10:1
Glacial Till:					
Upper	0.25	0.3	1.31	7×10^{-8}	30:1
Mid	0.25	0.3	1.31	7×10^{-9}	30:1
Lower	0.25	0.3	1.31	7×10^{-10}	30:1

* Obtained from CLASS hydraulic parameterization scheme (Letts et al., 2000).

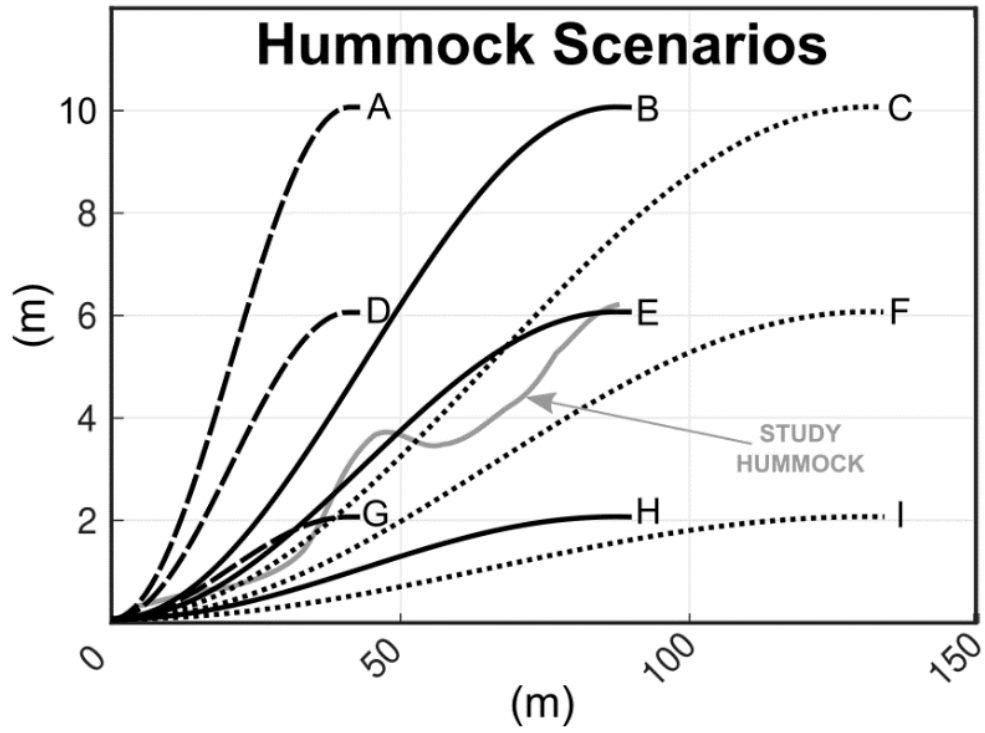


Figure 5-2: Hummock morphometry scenarios A-I. The original study hummock topography is shown in grey for reference, thus Scenario E most closely resembles the study hummock.

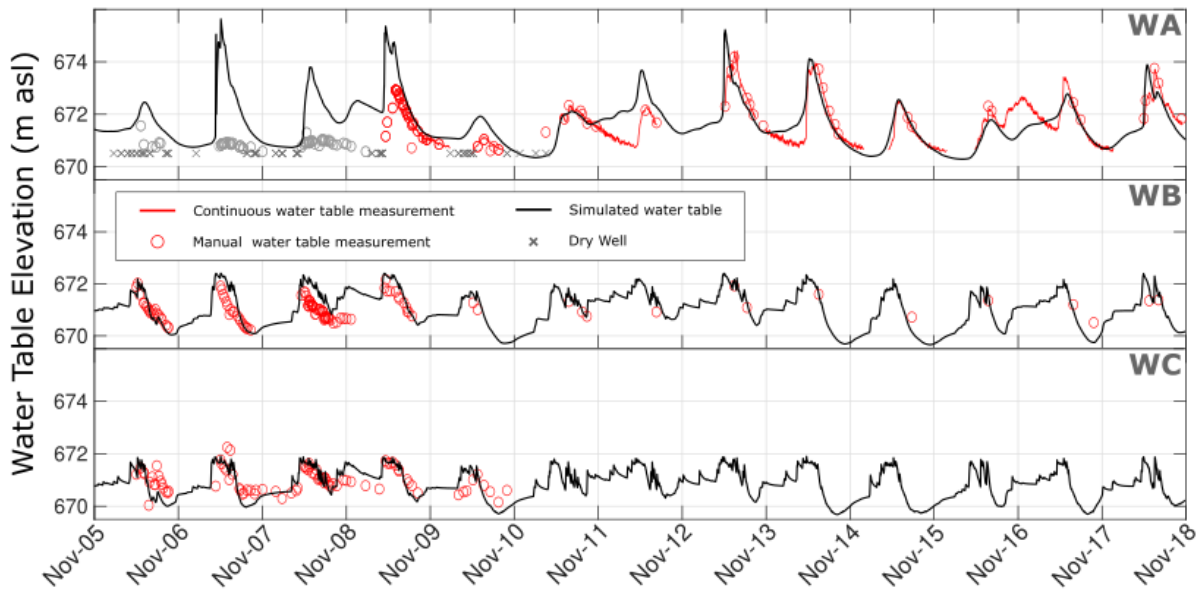


Figure 5-3: Simulated and observed water table elevations at observation wells WA, WB, and WC for the study hummock over time. Grey circles represent water table observations from an unequibrated well and were not used in the calibration process.

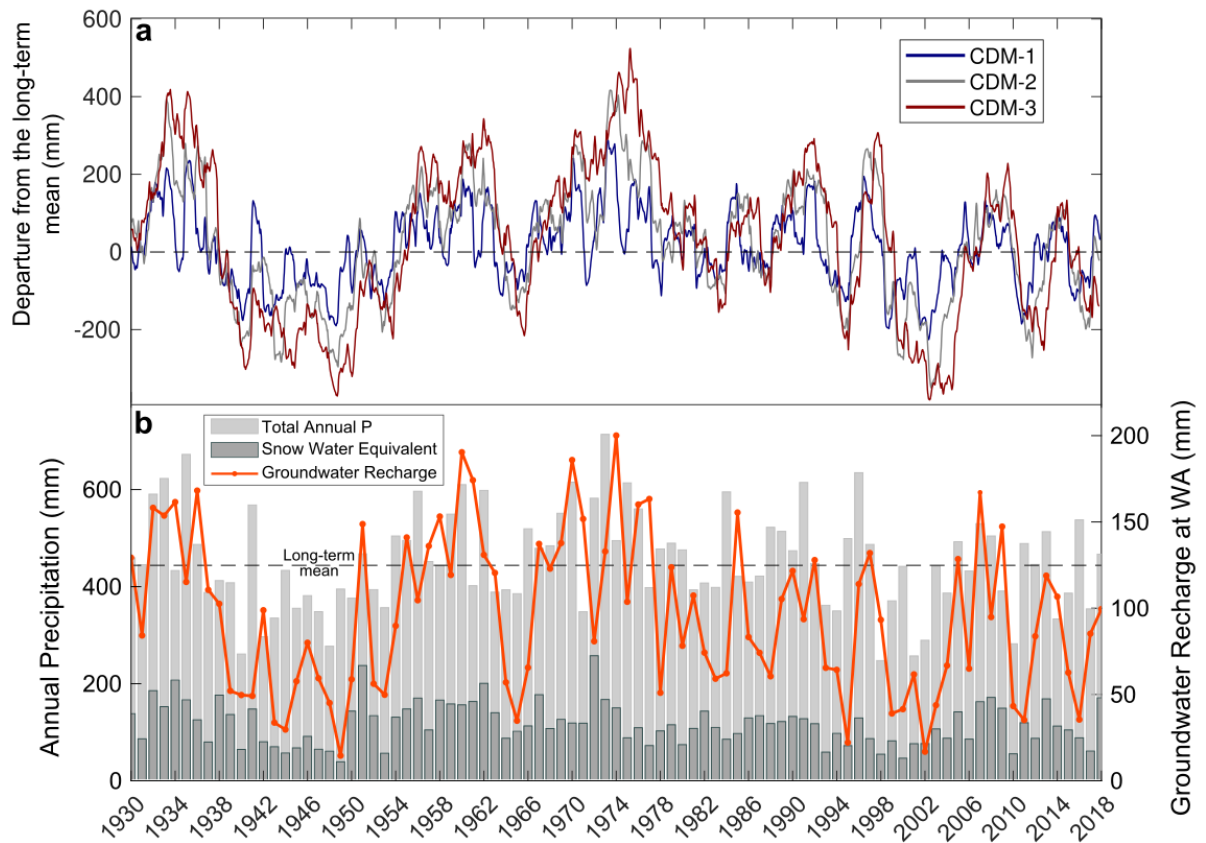


Figure 5-4: Time series (a) of 1 year, 2 year, and 3 year cumulative departures from the long-term mean annual precipitation (CDM), and (b) total precipitation, snowmelt, and recharge at well WA in the study hummock.

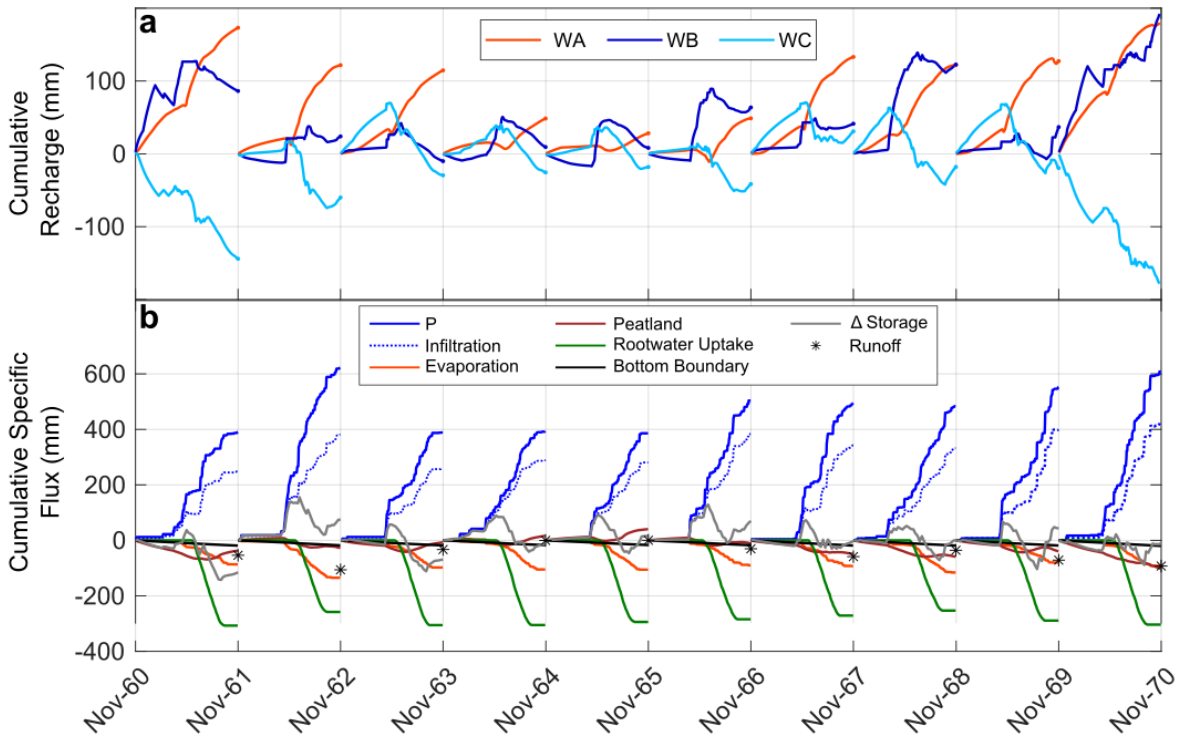


Figure 5-5: A detailed water balance of the modelled study hummock. (a) cumulative annual recharge at WA, WB, and WC, where negative recharge values represent upflux; (b) cumulative annual fluxes for the model relative to the surface area of the hummock, where negative values are fluxes out of hummock. Evaporation is composed of interception of rainfall and sublimation of snowfall.

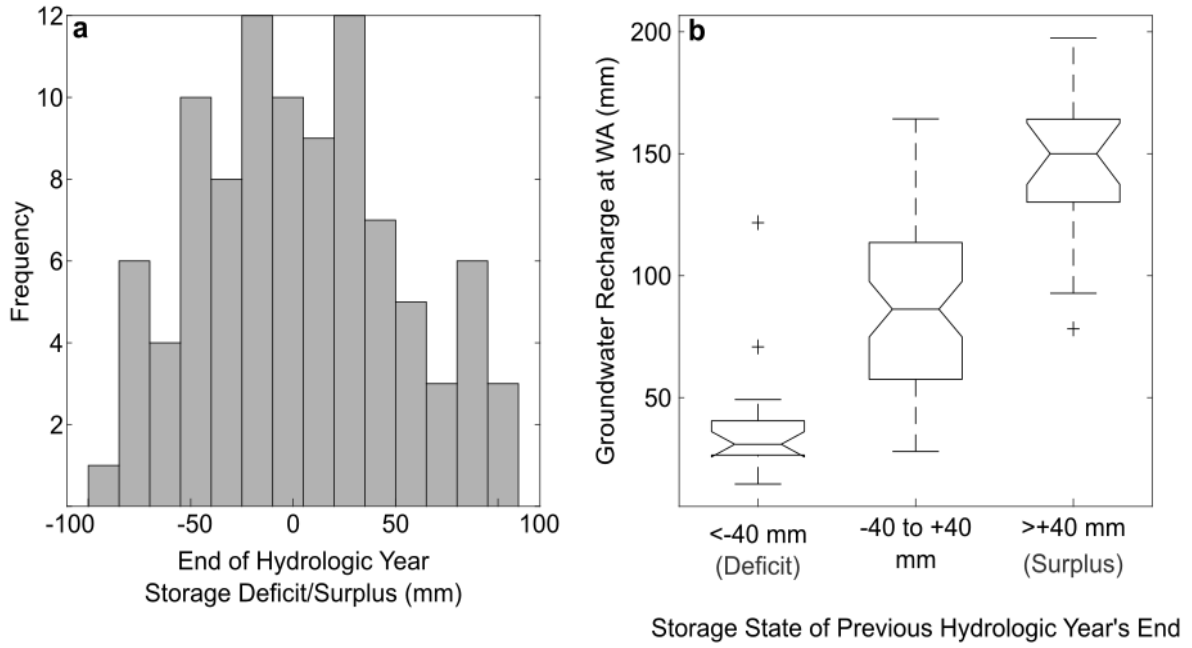


Figure 5-6: (a) Storage state at the end of the hydrologic year for the study hummock, and (b) the relationship between annual groundwater recharge at WA for a given hydrologic year compared with the storage state at the end of the previous hydrologic year.

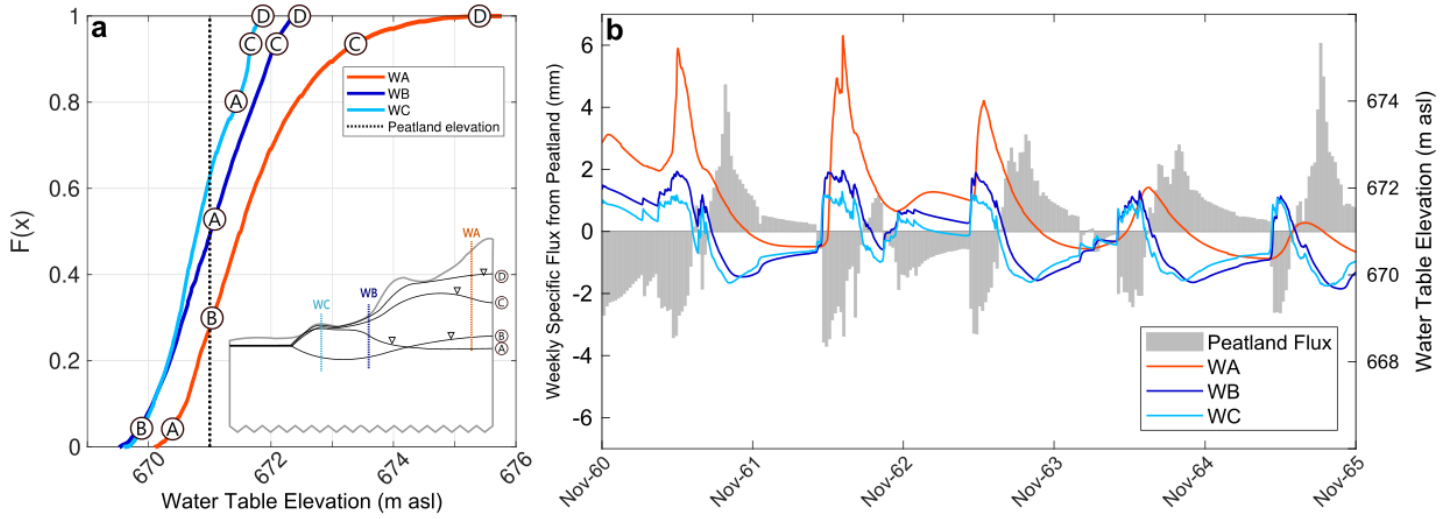


Figure 5-7: Water table elevations at WA, WB, and WC in the study hummock. (a) An empirical cumulative distribution function of water table elevations for the entire simulation with (a-inset) corresponding water table configurations within the hummock; (b) a time series of water table elevations and weekly flux from the peatland, where a positive value represents flow from the peatland to the forested hummock, and a negative value represents flow from the forested hummock to the peatland.

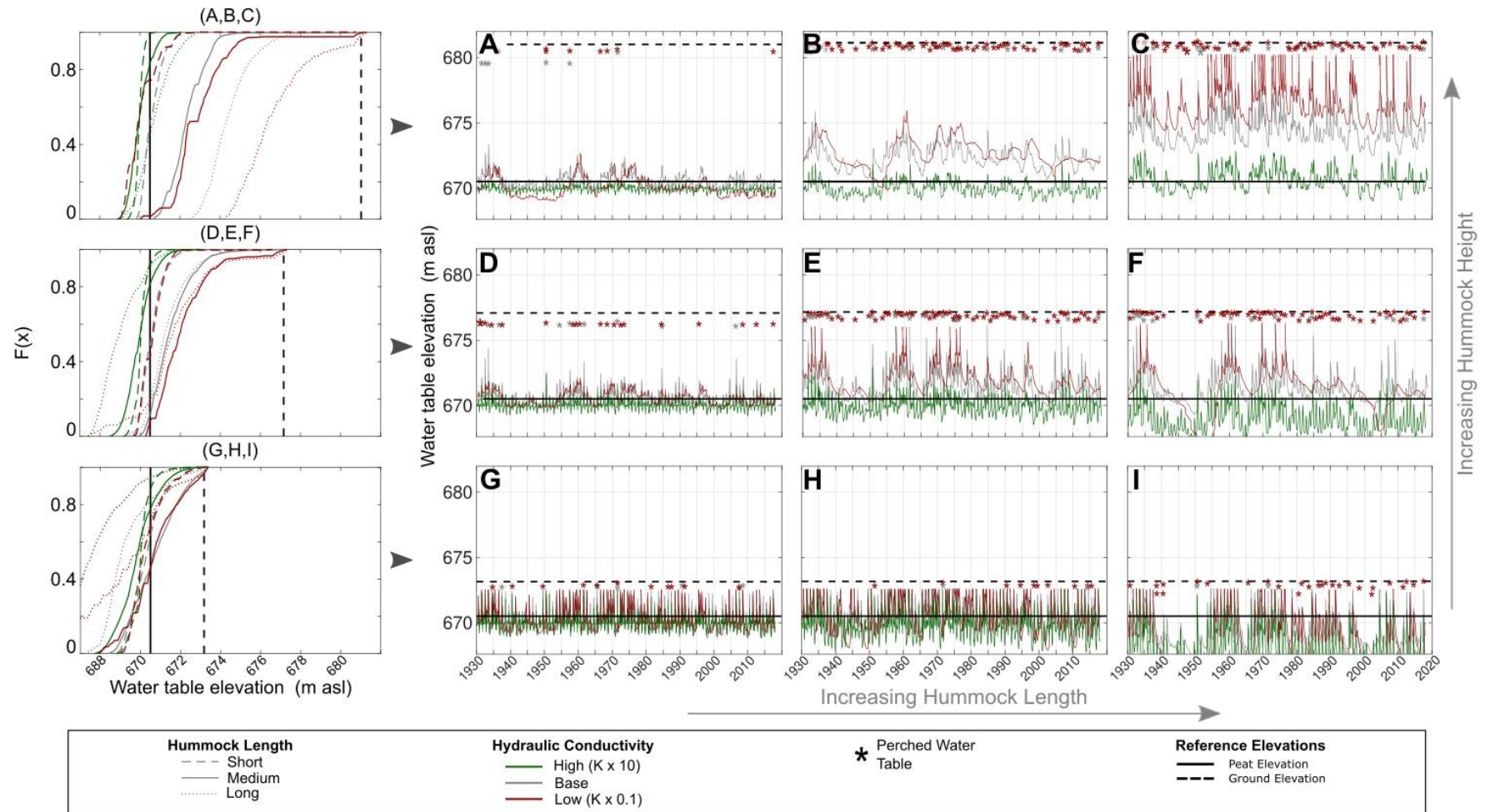


Figure 5-8: Simulated water table elevations at the top of the slope for the 27 different hummock regimes shown as (left) empirical cumulative distribution functions, and (right) time series. The shapes of each hummock morphometry scenario A to I can be seen in Figure 5-2. The base K, high K, and low K scenarios are shown in grey, green, and red, respectively. The timing and elevation of perched water tables are shown with asterisks in the corresponding K-scenario color. The elevations of the peatland and the ground surface at the top of the hummock are shown for reference in each plot.

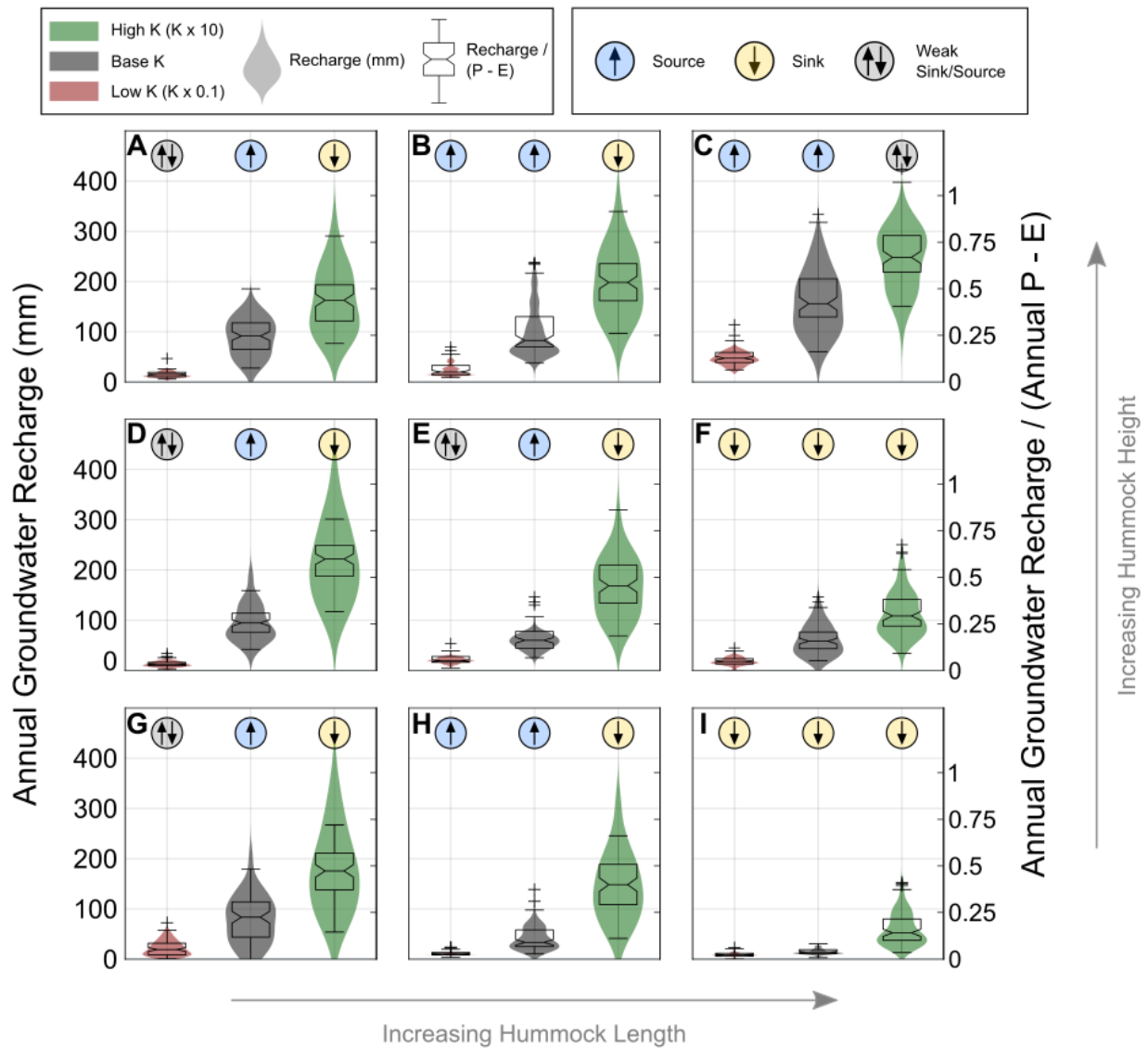


Figure 5-9: Annual simulated groundwater recharge and hydrologic function of each hummock regime. The shapes of each hummock morphology scenario A-I can be seen in Figure 5-3. Violin plots show the distributions of annual groundwater recharge values at the top of the hummock for each scenario from 1930 to 2018. The boxplots which overlay them show the distributions of the ratio of annual groundwater recharge and annual available precipitation (precipitation (P) minus evaporation (E)). No overlaps between boxplot notches indicate significant differences at a 95% confidence interval. The base K, high K, and low K scenarios are shown in grey, green, and red, respectively. The long-term hydrologic function of each hummock regime is also indicated by an arrow, where an 'up arrow' indicates that the hummock was a long-term source of water to the adjacent peatland, a 'down arrow' indicates that the hummock was a long-term sink of water to the adjacent peatland, and a 'up arrow/down arrow' pair indicates that the hummock was either a weak sink or weak source or fluctuated between being a sink and source through time.

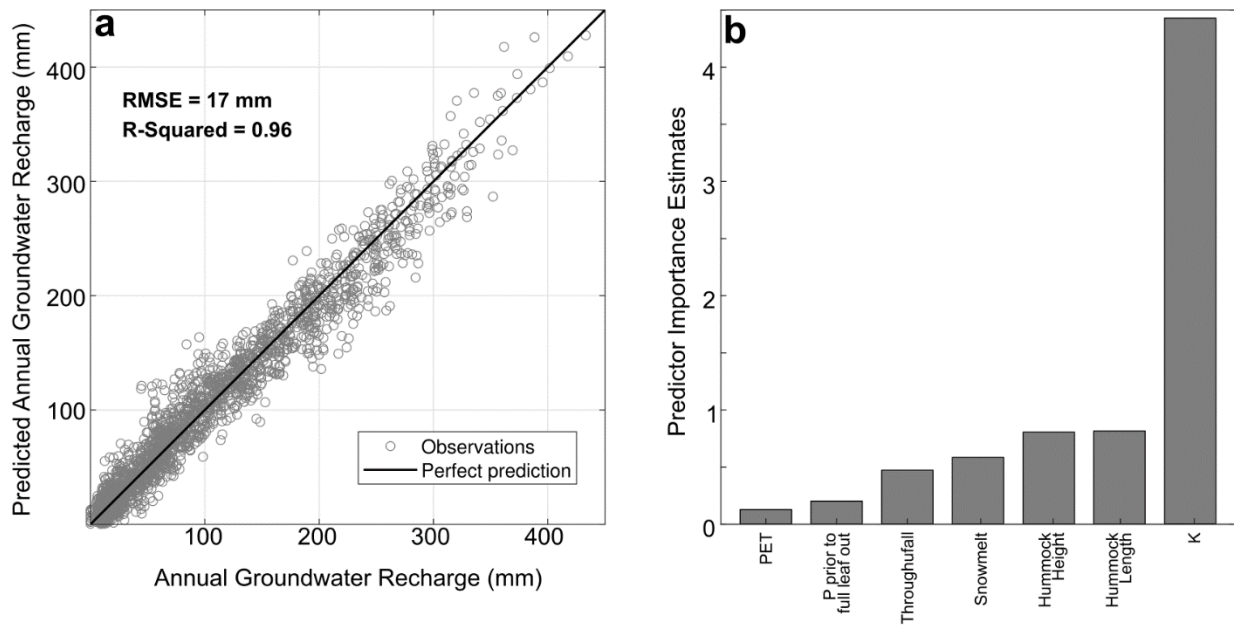


Figure 5-10: Results from the boosted regression tree (BRT) model: (a) Comparison of the annual recharge (as modelled in Hydrus simulations) from all 2D models and annual recharge values predicted by the BRT, and (b) the estimated importance of each predictor variable in predicting annual recharge. All climatic predictor variables are for the hydrologic year. PET = potential evapotranspiration; P = precipitation; K = saturated hydraulic conductivity of upper till.

Chapter 6

Conclusion: Variable-scale conceptual framework for shallow groundwater systems in the Boreal Plains with complementary proof-of-principle groundwater flow models

6.1 Introduction

The primary goal of this thesis was to use a fundamental framework of climate, geology, and topography to explain the temporal and spatial variability in hydrologic responses and behaviors and to develop a variable-scale conceptual model for groundwater movement and groundwater-surface water interactions in the BP. This was achieved in part by meeting the first 3 Objectives described in Chapter 1. Specifically:

Chapter 2 defines, tests, and characterizes the concept of hydrologic response areas (HRA) as a way of discretizing the BP landscape into areas with predictable hydrogeologic characteristics and shallow groundwater flow patterns (or lack thereof) in a landscape that otherwise is too flat and heterogeneous to use traditional methods like topographically defined catchments. Three HRAs were identified based on geologic substrate characteristics (i.e., texture and geologic origin): coarse glaciofluvial outwash (CO), fine-textured hummocky moraine (HM), and clay-till plain (CP). It was found that in the coarse outwash HRA and the hummocky moraine HRA, water tables are recharge (i.e., precipitation) controlled, while in the CP HRA they are topography controlled. In the CP HRA the characteristic length of the relief is very large, and therefore, the effects of topography and substrate texture dominate over local-scale controls such as recharge and ET. The HM HRA shows water table behaviors characteristic of local control and, as such, the effects of recharge and ET are the dominant controls, overwhelming the effects of local and mesoscale topography. In the CO HRA, the scale of flow and controls thereon are influenced by HRAs and a site's position relative to larger-scale flow systems.

While minimal groundwater-surface water interactions are evident in fine-textured landscapes, there was evidence of significant groundwater-surface interactions in the high conductivity CO HRA. Chapter 3 focuses on the spatial controls that govern the groundwater-surface interactions in various flow systems in the CO HRA. It was shown that landscape position is the dominant control over groundwater contributions to lakes; however, surface water connections are also significant and can short circuit groundwater pathways and confound the isotopic signal. Lakes at low landscape positions with large potential groundwater capture areas have relatively higher and more consistent groundwater contributions and low interannual variability thereon. Isolated lakes high in the landscape experience high interannual variability as they have little to no groundwater input to buffer the volumetric or isotopic changes due to evaporation and precipitation.

Chapter 4 explores the subsurface connectivity between forestlands and peatlands at various HRAs and topographic settings. It was found that during a mesic year (i.e., a year with average precipitation and antecedent moisture conditions) the dominant gradient is from peatlands to adjacent forestlands, opposite of the topographic gradient, regardless of texture and topography. Water table depressions under the forested hummocks indicate that Boreal Plains forestlands are not reliable sources of groundwater recharge, either spatially or temporally. One large, fine-textured hummock had persistent groundwater mounding throughout the study period and, as such, was the initial focus of Chapter 5.

In Chapter 5 a silty clay loam hummock was used to develop and calibrate a variably-saturated flow model to better investigate the dynamics of recharge, water table position, and lateral flow between the forested hummock and adjacent peatland. Scenario testing (achieved by increasing and decreasing the hydraulic conductivity by an order of magnitude and altering the hummock height and length) provided further understanding of the controls that hydraulic conductivity and hummock morphometry exert on recharge and forestland-peatland interactions. Hydraulic conductivity plays the largest role in determining groundwater recharge rates. The sink or source function of a forested hummock in the BP is dependent more on hydrogeologic and morphometric controls than climatic variability, where taller and narrower hummocks serve as sources of groundwater and longer flatter hummocks serve as sinks. Decadal wet-dry cycles played a larger role in modulating water tables than seasonal, short-term precipitation trends.

This chapter presents a variable-scale conceptual framework that describes water movement in low-relief water-limited landscapes. The framework incorporates findings from previous chapters as well as previous work in these and similar landscapes. This conceptual framework is then used to develop several representative “proof-of-principle” 3D groundwater models, wherein various configurations and proportions of peatlands and forestlands are modelled and the generated runoff rates and water table hydrographs are presented. These results are intended to provide probable hydrologic outcomes for various landscape scenarios, meeting Objective 4 as described in Section 1.4.

6.2 Conceptual framework

Previous research by Devito et al. (2005b, 2012) showed that traditional hydrological paradigms (e.g., precipitation-runoff relationships, topographically defined catchments) do not operate in complex water-limited landscapes with deep unconsolidated substrates and low topographic relief. Adding to that complexity is the mosaic of land covers (e.g., shallow lakes, peatlands, forestlands), geology (e.g., glacial deposit type), and the decadal wet and dry cycles typical of the BP, which represent differences in water supply, demand, and storage in both space and time. Devito et al., (2017) found that the runoff efficiency (the ratio of runoff to precipitation) was highly variable and ranged from 0.01 to 0.27 for a wide range of Boreal Plains (BP) catchments. Additionally, they found complex interactions between underlying glacial deposit texture (e.g., coarse sand, fine silt), overlying soil-vegetation land cover (e.g., lake, peatland, forestland), and regional slope. Similarly, Hwang et al. (2018) found that, at the basin-

scale, forestlands and peatlands have significant and, more importantly, competing roles in surface-subsurface hydrologic systems. Devito et al. (2005b) presented a “topography last” hierarchical classification of factors that generalized the dominant controls on water cycling and appropriate scales of interaction; however, there is a need for a comprehensive variable-scale framework that describes hydrogeological behaviour in these challenging regions, that operates at both small and large spatiotemporal scales, and can be applied to land management, forestry and reclamation design, and policy development.

Most research used to create this framework was part of the HEAD (Hydrology, Ecology, and Disturbance) research programs at the Utikuma Region Study Area (URSA; Devito et al., 2016), which is located approximately 370 km north of Edmonton, Alberta, in the Boreal Plains ecozone of Canada (56°N, 115°W). Additional studies from similar environments are also used to gain insight into relevant patterns and processes, but this does not represent a comprehensive literature review. The framework is summarized in Figure 6-1, where various landform combinations, textures, and topographic ranges are shown with major hydrologic fluxes illustrated in relative terms.

6.2.1 Background: Study area geology and climate

The western Boreal Plains landscape is comprised of glacial sediments that range from 80 to 240 m thick (Pawlowicz and Fenton, 2002b), that overlie the Smoky Group, a Cretaceous marine shale (Vogwill, 1978). Glacial sediment types or landforms vary from fine-textured landforms (e.g., lacustrine, stagnant ice moraine) to coarse-textured landforms (e.g., glaciofluvial, eolian) with inherent heterogeneity in the form of lenses of contrasting texture, all of which reflect the advance and retreat of the Laurentide Ice Sheet during the last glaciation (Late Wisconsin; Paulen et al., 2006). Fenton et al. (2013) utilized genetic and geomorphic modifiers (e.g., texture, genesis, topographic relief, thickness, and lithology) in their surficial geology schema, which can be subsequently delineated as coarse or fine materials (Chapter 2). Fine-textured sediments in this region have saturated hydraulic conductivity (K) values ranging from 10^{-6} to 10^{-9} m/s, while coarse-textured sediments have saturated hydraulic conductivity (K) values ranging from 10^{-3} to 10^{-6} m/s (Chapter 2).

The climate is sub-humid, with long-term potential evapotranspiration (PET; 517 mm/yr) exceeding long-term precipitation (P; 444 mm/yr; Marshall et al 1999). Wetter years, where P exceeds PET, occur on an approximately 10 to 25 year cycle (Mwale et al., 2009). The actual evapotranspiration (AET) from a given landform is dependent on the available water as well as the vegetative cover (if any) and represents water lost to the atmosphere, either by evaporation of free water or transpiration through plants. The ratio of AET and P (AET/P) is a helpful metric used evaluate whether a given landform is generally under surplus (AET/P < 1) or deficit (AET/P > 1) water conditions and whether it acts a water source or sink, respectively.

6.2.2 Space

6.2.2.1 Wetlands

Terrestrial (i.e., non-standing water) wetlands, such as peatlands (bogs, fens) and mineral swamps are common features in the glaciated plains. Peatlands maintain fairly stable internal water

table depths, even in dry continental settings and under drought conditions, by limiting evaporation through a system of autogenic processes. For example, water table depth is involved in negative feedback loops with peat deformation (e.g., Morris et al 2011), moss surface resistance (e.g., Price et al 2009), and moss productivity (e.g., Thompson and Waddington 2008). The review paper by Waddington et al (2015) provides more detailed descriptions. Peatlands are typically forested with black spruce, which have shallow rooting depths (<0.5 m; Lieffers and Rothwell, 1987), which further limits transpiration during periods with low water tables. The AET/P ratios reported for boreal peatlands indicate they are a net source of water: 0.625 (Petroni et al., 2007), 0.87 and 0.76 (Brown et al., 2010), 0.85 (Barr et al., 2012), 0.6 (Wu et al., 2010). Peatlands transmit and supply water to lakes, streams, and adjacent forestlands following wet periods, such as snow melt and rain events, and act to conserve water during periods of drought (Devito et al., 2017; Gibson et al., 2002; Gracz, Moffett, Siegel, & Glaser, 2015; Tetzlaff et al., 2009; Thompson et al., 2015, 2017, 2018).

In contrast, open water wetlands (e.g., aquatic or marsh wetlands, lakes), which have standing water, exhibit AET rates at or above P, and act as net sinks of water (Nijssen & Lettenmaier, 2002; Petroni et al., 2007). Reported AET/P ratios are almost always above unity: 1.18, 1.2 (Smerdon et al., 2005), 1.6 (Petroni et al., 2007), 1.14, 1.2 (Ferone and Devito, 2004), 1.10, 1.26 (Riddell, 2008), 1.78 (median), 1.28 to 2.57 (range; Gibson et al., 1998), 1.36 (median), 0.95 to 2.15 (range; Gibson et al., 2010), 1.5, and 1.33 (Nijssen and Lettenmaier, 2002). The annual AET of an open water wetland decreases as the proportion of open water gets smaller and as the ice-free period decreases. High AET in open-water wetlands can be expected in both coarse-textured (Smerdon, Devito, & Mendoza, 2005) and fine-textured (Ferone & Devito, 2004; Petroni et al., 2007) landscapes. Precipitation and evaporation dominate the water balances of lakes, but the degree of groundwater interaction varies with landscape texture. Lakes that are isolated from groundwater (both mineral and riparian wetland) inputs can go dry during prolonged drought periods; however, lakes with large proportions of contributing wetland area are well moderated and exhibit the least variability.

6.2.2.2 Forestlands

The soil and vegetation present in forestlands typical of the BP varies depending on the underlying surficial geology. Fine-textured sites (e.g., silt and clay loams) are characterized by boreal mixedwoods, where a closed canopy aspen (*Populus tremuloides*) forests dominates in early successional stages, and white spruce (*Picea glauca*) and balsam fir (*Abies balsamea*) become more common with stand age. Coarse-textured, well-drained sites are largely dominated by pine (*Pinus banksiana*; Bridge and Johnson, 2000).

The primary implication of the forest cover type and substrate texture is the relative amount of AET associated with each cover and the ability of the landform to transmit water to adjacent land units. Aspen and mixedwood stands have considerably higher AET rates than pine stands. Previous studies have shown that aspen stands have AET/P ratios of 1.13, 1.87 (Amiro et al., 2006), 0.93 (Barr et al., 2012), 1.13, 1.33 (Brown et al., 2014), 0.99 (Barr et al., 2007), 1.12, and 0.98 (Nijssen and Lettenmaier, 2002). Alternatively, Jack Pine stands have been observed to have much smaller AET/P ratios of 0.86, 0.59 (Amiro et al., 2006), 0.58 (Barr et al., 2012), 0.69, 0.62 (Moore et al., 2000), 0.61, and 0.52 (Nijssen

and Lettenmaier, 2002). The annual AET from a forest stand is controlled primarily by the moisture state of the mineral substrate the forest is rooted in and varies through time. Due to the lower hydraulic conductivity and poorer drainage, more water is available for root-water uptake in fine-textured aspen-dominated forestlands, and therefore they usually act as net water sinks. Aspen and mixedwood stands remove most of the precipitation over the long term in the BP (Barr et al., 2012; Devito et al., 2017; Devito, Creed, & Fraser, 2005) and have been shown to hydraulically redistribute water from adjacent wetland units (Depante et al., 2019), which can lead to AET far exceeding P. Conversely, due to the high hydraulic conductivity and well-drained conditions of sandy substrates, less water is available for pine forests and more water is transmitted away from sandy forested hummocks towards adjacent land units, and they therefore tend to act as net sources of water to the larger landscape (Devito et al., 2017; Redding and Devito, 2011; Smerdon et al., 2008).

In addition to the texture and vegetative cover, the morphometry (i.e., shape) of a forested hummock also has significant effects on its sink-source function. In both fine and coarse-textured landforms, the height of the hummock above the water table has a strong controlling factor over groundwater recharge rates. Carrera-Hernandez et al. (2012), Lukenbach et al. (2019), and Smerdon et al. (2008) all found that for a primarily sandy profile or hummock, a threshold greater than about 2 to 4 m above the water table was required for reliable groundwater recharge year-to-year. Chapter 5 shows a similar threshold of greater than 6 m for fine-textured hummocks, although it was also shown to be highly sensitive to soil hydraulic properties. The topographic profile also plays a large role in groundwater recharge, where depression-focused recharge can drastically increase recharge rates and create temporary or persistent groundwater mounds, whereas a smooth hillslope has less recharge and increased root-water uptake (Chapter 5; Appels et al., 2017; Winter, 2001).

Nevertheless, the sink-source function of a forested hummock is not only dependent on the magnitude of recharge, but on the water table position within the hummock, which governs the direction and magnitude of groundwater flow away from or towards the hummock. The water table position is controlled both by groundwater recharge and the hummock texture (the ability for the material to support a gradient), but also by root-water uptake from the vegetation. If root-water uptake exceeds groundwater recharge, a water table depression will occur driving the hydraulic gradient, and therefore flow, towards the forestland. The longer and shorter the hummock, the larger and more persistent the groundwater depression may become resulting in a long-term sink of water (Chapter 5); however, the absolute dimensions required for a forested hummock to be a consistent source of water is dependent on its texture, where sandy hummocks can be smaller and still act as sources.

6.2.2.3 Wetland-forestland interactions

The degree to which water moves between land units is driven by both the hydraulic conductivity of the substrate (e.g., high-K sand or low-K silt) and the water table position in neighboring land units. The lateral communication in a forestland-lake complex is driven primarily by the stage of the lake and subsequently moderated by the conductivity of the hummock. In coarse-textured landscapes there is increased hydraulic communication between groundwater and lakes, and lakes act as 'evaporation windows' whereby groundwater is preferentially drawn towards the lake basins as the

stage declines and then lost to evaporation (Smerdon 2005; Townley and Davidson, 1988; Winter, 2003). In fine-textured landscapes, lakes receive and lose very little water to mineral groundwater systems and instead exchange water with more conductive peatlands, the degree of which depends on the regional physiography (Ferone & Devito, 2004; Thompson, 2019) and is discussed in the following section.

Because peatlands generally have stable water tables, water movement between forestlands and peatlands is primarily controlled by the water table elevation in the forestland, which is in turn controlled by groundwater recharge and root-water uptake, then further moderated by the conductivity of the hummock. In high-K sandy settings with few fines, pine is the dominant vegetation, which results in high recharge rates as rainfall quickly percolates through the rooting zone and thick unsaturated zone and joins the water table. There is little to no upflux due to root-water uptake and although the hydraulic gradient is small due to the high-K substrates, it is away from the forestland and moves potentially large volumes of water. As the texture of the forestlands become finer (lower K), aspen becomes more dominant, groundwater recharge decreases, and upflux due to root-water uptake increases as it becomes more difficult for water to move past the unsaturated zone. This can result in groundwater depressions where the hydraulic gradient is opposing the topographic gradient and water moves into the forestland; however, the volume of water is limited by the hydraulic conductivity of the forestland substrates.

6.2.2.4 Hydrological Response Areas: Physiography and dominant controls

Hydrological response areas (HRA) are areas with similar water transmission and storage properties (Chapter 2). In regions where there is a strong relationship between topography and water table behavior (i.e., regions with high recharge and appreciable relief), the landscape is discretized into catchments, which are usually delineated solely by surface topography. In contrast, HRAs are delineated by first considering the depth and texture of the geologic substrate, which in turn control subsurface storage and transmissivity. By delineating based on the geologic substrate characteristics (i.e., texture and origin), the physiographic and topological characteristics (e.g., proportions, types, and connectivity of landforms, scale of topographic relief, slope etc.) within the HRA become dominant factors. HRAs do not account for regional topographical boundaries (e.g., groundwater divides), but they do emphasize the importance of smaller scale relief (e.g., hummocks, plains, swales) within the HRA. The HRA type will inherently determine the hydrological function and importance of the individual land units discussed above and will help identify spatiotemporal scales of interest. Four primary HRA types, based on surficial geology typical of the BP have been studied thoroughly characterized in the URSA: clay-till plain (CP), hummocky moraine (HM), coarse outwash (CO), and perched over coarse (CO-P). The CP HRA consists of silt-clay hummocks underlain by clay. The HM HRA is characterized by predominantly by silty clay loams, which can have zones of high clay or sand content, underlain by clays and clay tills. CO HRAs are predominantly sands and gravels, which can be interbedded with small, spatially discontinuous silt lenses. CO-P HRAs are located at some transitions between coarse and fine glacial substrates, where a clay layer overlying deep extensive sands and gravels leads to perched, laterally unconfined hydrologic systems (Chapter 2; Devito et al., 2012; Riddel, 2008).

In CP HRAs regional topography and slope are the primary controls over water table position and scale of groundwater flow. Sites at higher elevations have greater water table fluctuations are strong vertical recharge gradients and have more localized controls than sites at lower elevations, which have more stable water tables; however, water table fluctuations across a CP HRA is very limited compared to other HRAs due the very low hydraulic conductivity and relief. The characteristic length of the relief is very large and therefore the effects of topography and substrate texture dominate over local-scale controls such as recharge and ET. Peatlands are expansive, interconnected, and generate their own shallow flow systems. These are essentially independent from the mineral subsurface, and usually terminate in lakes or fens. This supply of shallow subsurface flow is crucial to the maintenance and permanence of the lakes on CP HRAs.

While the substrate textures found in the HM HRAs are very similar to those in the CP HRAs, the physiography and topology, and therefore the controls on hydrology, can be very different. As the characteristic length of the relief becomes shorter (i.e., more hummocky than gently sloping), peatlands become more isolated and less connected and the cumulative contributing area for lakes becomes smaller. The local relief and slope are appreciably greater and water table position, water table fluctuations, and vertical gradients do not follow topography. The hummocky terrain exhibits water table behaviors characteristic of local control and, as such, the effects of recharge and ET are the dominant controls, which overwhelm the influence of local and mesoscale topography and result in the most dynamic water tables in space and time. The water table dynamics in individual forestlands are primarily governed by the morphometry, or shape, of the hummock. HM HRAs have small geographically isolated peatlands and lakes surrounded by forested hummocks. Peatlands usually surround lakes in depressions between forested hummocks but can also occur in depressions at the top of hummocks. Riparian peatlands in this landscape act as a buffer by conserving water and counterbalancing the high ET of the lakes and aspen forests; however, they are not expansive and well connected like those found in CP HRAs and therefore peatland discharge to lakes may be insufficient and cannot sustain lakes during prolonged drought conditions (Thompson et al., 2015, 2017).

The CO HRAs, which are predominately high K sands and gravels can have large regional relief but little to no vertical hydraulic gradient. Except at the lowest elevations amongst low-K silty hummocks, the water table does not follow local topography and generally exhibits largely flat water tables with very small fluctuations over time. At higher elevations, (i.e., the tops of flow systems), water tables tend to be deeper and exhibit large water table fluctuations in response to seasonal and interannual variations in P and AET. Forestlands dominate with smaller geographically isolated lakes and peatlands are typically underlain with finer silts, clayey silts, and gyttja. Peatlands in this setting are susceptible to more dynamic, and sometimes very low, water tables as they lose water to the adjacent forestlands at rates greater than those in other hydrogeological settings. At lower elevations (i.e., at the bottom of flow systems), water tables are more moderated and lakes have considerably greater groundwater inputs and are therefore more stable. The bottoms of flow systems (regional lows) are characterized by expansive networks of peatlands and lakes usually well connected with and interacting with large-scale flow systems. Water tables and lake stages tend to be less dynamic and more tempered by regional flow.

Groundwater flow (and the controls thereon) can be considered “topography controlled” in the CP HRAs with intermediate-scaled controls, and “recharge controlled” in the HM HRAs with local-scaled controls. While the CO HRAs are generally “recharge controlled,” they can contain multiple scales of flow and be influenced by adjacent HRAs and relation to larger-scale flow systems.

6.2.3 Time

6.2.3.1 Seasonal/Annual

One of the key aspects of the Boreal Plains hydrologic cycle and water balance is the synchronicity of P and ET on a seasonal basis (Figure 6-2). The primary modes of precipitation (i.e., 50 – 60%) are short duration convective-cell storms, which occur during the summer months when evapotranspiration is highest (Devito et al 2005; Brown et al 2014). This leaves little available water on an annual basis. Snowmelt and spring storms, which represents approximately 25% of average annual precipitation, occur during the cooler months before the growing season, when evapotranspirative demand is at a minimum (Figure 6-2; Marshall et al., 1999) and are the primary sources of groundwater recharge (Chapters 3 and 5; Smerdon et al., 2008; Thompson et al., 2015). Water tables in all but the clay-rich hummocks rise in response to this recharge pulse and decline throughout the late summer in response to increasing transpiration rates, lack of recharge, and redistribution of groundwater; although the timings and magnitudes vary based on texture and antecedent moisture conditions. The deeper the water table, the more dampened the spring recharge signal will be as most of the water is stored in the thick vadose zone (Smerdon et al., 2008). Annual water table hydrographs show flashier and larger fluctuations in finer textured landforms when compared to coarse-textured landscapes under similar recharge scenarios due to the large capillary fringes found there (Gillham, 1984). In lower K, clay-rich forestlands with deep water tables, there can be little to no movement of the water table annually or year-to-year. Alternatively, during large infiltration events (e.g., spring snowmelt, or large late season storms), temporary perched water tables may form near to the top of the soil profile, and slowly dissipate as it removed by transpiration.

The shallow groundwater systems present at and around lakes and wetlands in both coarse and fine landscapes are subject to seasonal flow reversals, whereby spring recharge creates groundwater mounds leading to groundwater flow into the lake or wetland, and by late summer that mound will dissipated through ET and lake or wetland water is now recharging the groundwater in that area (Chapter 5; Anderson and Munter, 1981; Smerdon et al., 2005).

Seasonal ice formation and melt can play a large role in the water balance and water movement in the BP. Concrete frost, or ice lenses, can prevent the infiltration and percolation of snowmelt, which instead forms runoff and loses its potential to form groundwater recharge (Redding, 2009). While the meteorological conditions required for concrete frost are common it usually only occurs at sites low canopy cover, where periodic warm temperatures cause snowmelt which infiltrates and refreezes (Proulx and Stein, 1997). Concrete frost is usually patchy and discontinuous in forestlands, still allowing for vertical flow within the forest land unit (Price and Hendrie, 1983; Redding and Devito, 2011), where some frozen soil conditions can actually enhance infiltration rates of snowmelt (Gray et al., 1985; Kalef, 2002). Only wetlands appear to have consistent and continuous concrete frost or ice lenses resulting

in lateral runoff generation (Redding and Devito, 2011). By preventing the infiltration of snowmelt, ice lenses in peatlands create high water tables, which support higher ET and runoff rates in the spring (Brown et al., 2010; Thompson 2019). Early and elevated ET rates can create and enhance water deficit conditions, leading to restricted water exchange between lakes and peatlands. Consequently, lakes that are reliant on contributions from peatlands may be susceptible to drying out during ice-rich years, but this hasn't been explored thoroughly (Thompson 2019). Annual lake and open water wetland evaporation rates are determined by the onset and duration of ice cover, which essentially eliminates evaporation of lake water.

6.2.3.2 Interannual variability and decadal wet-dry cycles

The long-term variability occurs at two primary temporal scales: on the order of two to three years (interannual) and on the order of 10 – 15 years (decadal); however, they are governed by very different processes.

Groundwater recharge and water table elevation in forestlands, in both fine and coarse settings, are poorly correlated with annual atmospheric fluxes (i.e., P, PET, P – PET. CDM-1). There are, however, stronger relationships with the sum of the previous two or three years total P and the two (CDM-2) or three (CDM-3) year cumulative departure from the long-term mean (Section 5.2.2). This is a consequence of the control exerted by the state of the hummock storage (i.e., deficit or surplus) at the end of the previous year (Chapter 5). If a hydrologic year begins under storage deficit conditions: (a) the water table itself is likely lower and transit times through the vadose zone will be longer, (b) the low soil moisture in the vadose zone reduces the effective hydraulic conductivity, and (c) increased available storage must be filled before recharge can commence (Han et al., 2008; Wossenyeleh et al., 2020). Wet or dry conditions are not always evident when examining time series of annual P. For example, in 2003 water tables across URSA were far below average; however, the annual P was 442 mm, which would be considered an average year (i.e., long-term mean annual P is 444 mm). While the CDM-1 was essentially zero for that year, the CDM-2 and CDM-3 were evident of extremely dry conditions and were approximately -156 mm and -213 mm, respectively (Figure 6-2). Interannual storage deficits likely play a larger role in coarser textured landscapes (Chapter 2), where a decrease in soil moisture leads to a steep decline in unsaturated hydraulic conductivity. Time-lagged responses also play a large role in delaying groundwater recharge associated with moisture surplus conditions in coarse settings where there are especially deep water tables (e.g., ~10 m deep; Smerdon et al., 2008).

The BP is characterized by wet-dry cycles, where wet ($P > PET$) periods occur approximately every 10 – 15 years, but these cycles can have periods of 4, 8, 11, and 25 years, usually depending on influences like El Nino Southern Oscillation and Pacific Decadal Oscillation (Mwale et al., 2006). These wet-dry cycles are responsible for the largest variability or fluctuations in water levels in all land cover and geology types. While peatlands are usually resilient to the short-term water deficits and show little variation in their water levels, they can be susceptible to long-term drought conditions. Isolated lakes and peatlands can completely dry out during dry periods and peatlands can experience prolonged flooding during wet periods. The wet-dry periods are evident when examining annual P – PET time

series, however they are amplified or compounded when examining the CDM-3 (Figure 6-2), which takes in to account the carry over effects that storage has in the BP.

6.3 Proof-of-principle 3D groundwater flow models

While the probable hydrologic function of a given land unit is described by the above conceptual framework, the hydrological function of an entire landscape composed of multiple land units is also controlled by the organization (e.g., proportions, types, and connectivity) of those land units. To demonstrate the effects that landcover topology, topography, texture, and climate have at the landscape scale, several simplified 3D groundwater flow models were created.

6.3.1 Model implementation and scenarios

These models are created as generalized “proof-of-principle” models where principles presented in the conceptual framework (Section 6.2) are applied and tested at a landscape scale. To simulate the varying effects that topography, topology, texture, and climate have on landscape runoff, the timing and magnitude of groundwater recharge must be adequately simulated. Traditionally, in humid climates, transient groundwater recharge is applied directly to the water table, where, recharge is calculated external to the groundwater model by subtracting evapotranspiration and runoff from precipitation. This approach assumes that unsaturated zone processes have a negligible influence on overall groundwater flow (Hunt et al., 2008; Romano et al, 1999). However, as shown in Chapter 5, in sub-humid regions unsaturated zone processes are important for moderating the timing and magnitude of groundwater recharge and AET (actual evapotranspiration).

Fully coupled models that use the Richard’s equation (e.g., the HYDRUS model utilized in Chapter 5) are computationally demanding and are generally impractical for transient watershed-scale models. To provide a simplified model domain that is easily manipulated and can simulate general hydrologic system behaviours for long simulation periods, MODFLOW-2005 (Harbaugh, 2005) was used in conjunction with the Unsaturated-Zone Flow (UZF) Package (Niswonger et al., 2006). The UZF package simulates vertical unsaturated flow by approximating the 1D Richard’s equation with kinematic waves and considers the effects of rejected recharge (i.e., infiltration excess) and unsaturated zone ET. Figure 6-3 shows the model structure and the interactions between MODFLOW and the UZF package. See Niswonger et al. (2006) for a detailed explanation.

For all simulated scenarios, a rectangular domain is used with a regional slope of 0.3%. Uniform horizontal nodal spacing of 50 m is used, with 3 layers of variable thickness. A high conductivity peat channel along the centre of the model has branches between forested hummocks (Figure 6-4). The lower boundary and the sides of the model domain are no-flow boundaries. High conductance drains are located at the topographical low end of the model domain and in the high K peat channel. These drains serve as an outlet for flow in the model and measure runoff. The outlet drains have an elevation equal to the land surface elevation; the peat channel drains are set at an elevation 15 cm above the peat surface.

Net P, consisting of daily fluxes of throughfall (i.e., rain not intercepted by vegetation) and snow melt after sublimation, and potential transpiration (i.e., root-water uptake) were applied to the surface of the model. Evaporation is considered to be the sum of interception and sublimation, which are both calculated outside of the MODFLOW model. Daily net P and PET were calculated in a manner similar to the method explained in Chapter 5 (Section 5.3.2.2); however, PET is modulated for each landcover type (i.e., aspen forest, pine forest, and black spruce dominated peatland) as described in Section 6.2.2.2. The models were allowed to ‘spin-up’ for twenty years before the simulations began.

6.3.2 Model scenarios

A total of 24 simulations are considered here. Three topologies are tested: (A) many small hummocks with small well connected peatlands, (B) few large forested hummocks with small well-connected peatlands (C) few large forested hummocks with large well-connected peatlands. Two topographic scenarios are tested: hummock heights of 3 and 11 m above the adjacent peatlands. Four forestland textures are tested: silt loam and silt clay, which represent the soils in fine-textured HRAs, and sand loam and sand, which represent the soils in coarse-textured HRAs. All soil parameters are taken from Rawls et al. (1982). Potential transpiration is applied to represent aspen forests on the sand loam, silt loam, and silt clay; reduced potential transpiration is applied to represent pine forests on the sand models. These various scenarios and parameters are described in Figure 6-4 and Table 6-1.

To evaluate the various scenarios, several metrics are compared: hummock water table elevations, AET, and runoff. Hummock water table elevations are recorded at the observation wells shown in Figure 6-4. AET is composed of unsaturated zone ET, groundwater ET, interception, and snow sublimation for the entire model domain. Rejected recharge (i.e., infiltration excess runoff) is also lumped with AET and represents between 3 and 20% of AET. Considering rejected recharge as AET is a reasonable presumption as the UZF framework prevents the presence of a separate forest floor and B soil horizons, which would most likely retain most if not all of rejected recharge before it became actual runoff. Runoff is considered any water that leaves the model through the drains.

6.4 Model Results and Discussion

6.4.1 Hummock water table elevations

The water table elevations, and controls thereon, in the hummocks (recorded at the monitoring wells in Figure 6-4) are similar to the results shown in Chapter 5 (Figure 5-8). The major control on water table elevation and range is texture, while the strongest control on “flashiness” (i.e., the hydrograph response to the annual spring recharge signal) is hummock height (i.e., unsaturated zone thickness; Figure 6-5). The silt loam has the most dynamic and elevated water tables, while the silt clay has the least responsive. The silt loam has annual hydrograph peaks in response to the spring recharge signal on the order of 2 m in the shorter hummocks, but in the taller hummocks, the primary signal was in response to the long term wet-dry cycles (Section 6.2.3.2, Figure 6-2), which were on the order of 4 m. The silt clay hummocks exhibit flat, unresponsive water tables in the taller hummocks; however, in the 3 m high hummocks there are slight (~0.4 cm) water table responses to the long term wet-dry cycles. When compared to the other materials, the sand hummocks show muted hydrograph responses to both

annual and interannual precipitation trends and have moderated water table responses to the spring recharge signal and wet-dry cycles, which are on the order of 0.3 m and 1 m, respectively. The sand loam exhibits water table behaviours similar to the silt loam; however, they were more moderated and only had a range of approximately 2 m.

Hummock length (i.e., distance between peatlands) alone does not play as large of a role as the entire topology of the system. Both topological scenarios B and C (Figure 6-4) have hummock lengths of 550 m, but the hummocks in B are separated by peatlands with a width of 100 m and the hummocks in C are separated by peatlands with a width of 250 m. Consequently, the wider peatlands of C can transmit more water away from the hummocks, which is subsequently routed to the drains, and results in lower water tables in C hummocks when compared to B hummocks (Figure 6-5). This expands on the results of Chapter 5, which shows that hummock length, in conjunction with hummock height, is a key factor in determining the hydrologic role of a forested hummock. In that modelling scenario, the peatland is represented by a fixed head.

6.4.2 Evapotranspiration and runoff

Texture again plays the largest role in controlling AET and runoff. Sand, which was used to represent pine barrens in coarse-textured glacial outwashes, has the lowest modelled AET and the highest runoff (i.e., outflow from the drains) rates (Figure 6-6, 6-7, 6-8). Coarse-textured pine barrens have the lowest hydraulic gradients between forestlands and peatlands (Chapter 4), but due to their low AET rates and high hydraulic conductivity, they serve as key sources of groundwater recharge and runoff in the BP region (Devito et al., 2017). The sand loam and silt loam had the highest AET rates, due to the optimal water retention properties for root water uptake, and therefore the lowest runoff rates. Silt loam textures, typical of the HM HRA are generally poor sources of water; however, as shown here (Figures 6-6 and 6-8) have very large interannual variability in runoff (Devito et al., 2017).

For the most part, there is no appreciable differences in the magnitude of AET between various topological scenarios. However, hummock height does play a large role in both the source and magnitude of AET and magnitude of annual runoff. For the sand, sand loam, and silt loam the 11 m high hummocks had much greater unsaturated zone AET than groundwater AET, and vice versa for the 3 m high hummocks. This is due to a more pronounced effect of deeper rooting zones at the toe of the hummocks along the forestland-peatland interface and shallower water tables in the shorter hummocks (Section 5.4.3.2). Except for the sand, the shorter hummocks have slightly lower AET rates and higher runoff rates (Figure 6-7 and 6-8) due to decreased storage in the unsaturated zone (Figure 6-9). The sand hummocks have the highest hydraulic conductivity values and therefore, the taller the hummock the higher the likelihood that infiltrated water will become recharge and subsequently drain away from the hummock into the peatlands and leave through the drains. Therefore, the relationship between hummock height and runoff is reversed for the sand models.

Similar to the hydrographs, scenario C (wider peatlands) simulations have higher runoff rates than B (narrow peatlands; Figure 6-7) in all textures except sand, illustrating the importance of peatlands in transmitting water through and away from landscapes. There was no substantial difference in runoff for the topological or topographic scenarios for the sand loam textures; however, for the silt loam the narrow

hummock scenario (Figure 6-4 A) had the highest runoff for both hummock heights. Because silt loam has poor drainage properties and low hydraulic conductivity, narrow hummocks can reduce the time it takes for water in the hummock to reach the peatland and be removed from the model.

Similar to the results presented in previous chapters, annual runoff rates are also poorly correlated with annual P, but better correlated with CDM-3. For example, scenario B (Figure 6-4) with sand as the primary material and hummocks with a height of 11 m had a weak relationship between annual runoff and CDM-1 ($R^2 = 0.13$), but a much stronger correlation between annual runoff of CDM-3 ($R^2 = 0.66$; Figure 6-2). Changes in storage also correlate with various frequencies of precipitation metrics. The taller hummocks display larger and longer fluctuations in groundwater storage similar to CDM-3, while the shorter hummocks and the unsaturated zones exhibit smaller and more erratic fluctuations in storage, similar to CDM-1 (Figure 6-2 and 6-9).

6.4.3 The way forward

The proof-of-principle models presented here are simplified but serve to demonstrate the major concepts and processes outlined in Section 6.2. They are the beginnings of larger scale 3D implementations of the conceptual framework; however, there are marked limitations and future work is needed to fully realize the landscape-scale hydrological implications of various topological, topographical, textural, and climatic scenarios. The topological scenarios used here (Figure 6-4) are conspicuously artificial. Natural and varied topologies can be gleaned from natural systems, or those intended for reclaimed and reconstructed landscapes, to better mimic the physiography and landscapes of interest. For example, it is unlikely that all peatlands present should be connected to a single drainage point; this naturally results in inflated runoff rates. Lakes should also be incorporated into the models, as they are important and persistent hydrologic sinks within the landscape (Smerdon, 2007; Thompson, 2019). Here, as water tables rise above the peat surface, they are not subject to open water evaporation rates, which further reduces AET rates and inflates runoff rates.

The forestland-peatland interface has been shown to be a dynamic and important transition zone (Dimitrov et al., 2015). At the toe of forested hummocks, root water uptake from forest vegetation can create groundwater depressions, which can have a large effect on the sink-source function and AET rates of forestlands (Chapter 5). The shape of the base of the hummocks presented here are convex (Figure 6-4) rather than concave (Figure 5-2), which reduces the influence of the interface vegetation and results in lower AET rates. Low, flat hummocks were sinks of water in the simulations presented in Chapter 5 (Figure 5-9), which contrasts with the modelling presented here, where narrow and short hummocks had higher runoff rates and lower AET. Additionally, the transition of substrate properties (i.e., soil water characteristic curve and saturated hydraulic conductivity) and vegetation (e.g., rooting depth and root water uptake) in the forestland-peatland interface is difficult to measure and model, but nonetheless plays an important role in water transmission and storage. Suitable parameterization of these interfaces for real-world scenarios will be necessary to adequately represent site-scale models and their water balances.

The substrates simulated here are homogeneous; however, discrete units of contrasting material can play large roles in promoting or preventing recharge and runoff. Clay lenses can help

maintain perched peatlands at topographic highs (Riddell, 2008), while eskers can increase recharge and maintain lake levels during drought (Smerdon et al., 2011). Incorporating these features into both large and small-scale models, as well as seeking them out for field studies, could prove insightful as to their importance in landscape scale water storage or transmission.

6.5 Conclusions

Low-relief, sub-humid, glacial depositional landscapes such as found on the BP, are highly complex regions with spatially heterogeneous storage and transmission properties, and variable recharge and ET potentials. As explained in the variable-scale conceptual model and demonstrated in the proof-of-principle flow models, water table behaviour, ET rates, and runoff are controlled by a hierarchy of, and interactions between, long-term climate (i.e., sub-humid, $P \leq PET$), texture (i.e., geology and consequently vegetation), topography (i.e., regional-scale physiography and local-scale hummock morphometry), and short-term climate (i.e., wet-dry cycles, and CDM-3); however, the specific order of controls is dependent on the hydrogeological setting. The modelling results shown here demonstrate the dominant role that texture plays in storage dynamics, AET fluxes, and runoff generation, while peatland-forestland topology can help or hinder the transmission of water.

The studies presented in this thesis demonstrate both the complexity and sensitivity of BP groundwater systems to small perturbations in land cover type, vegetation, and atmospheric conditions. As the BP is home to unprecedented and ever increasing disturbances in the forms of climate change, forestry, agriculture, and oil and gas operations, shifts in precipitation and temperature regimes, forestry road development, and open pit mining will drastically affect shallow groundwater systems. The framework developed in this thesis can be a useful tool to help researchers and managers consider the complex interactions of landform topology, topography, texture, and climate when planning and managing both disturbed and undisturbed landscapes, as well as constructing new landscapes.

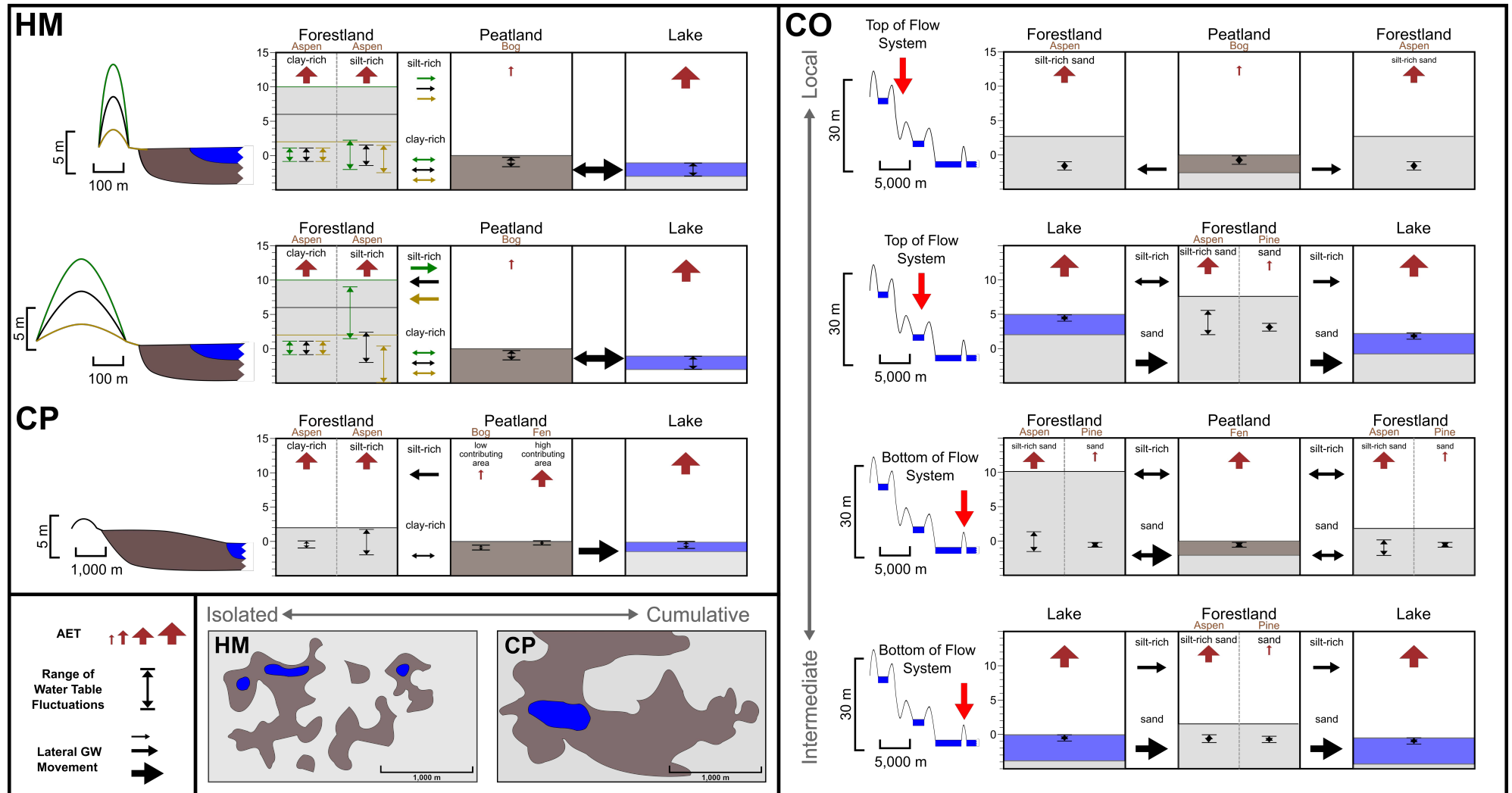


Figure 6-1: Conceptual framework presented in Section 6.2 for various landforms and textures in each of the three main HRAs. Relative AET and lateral GW fluxes are shown with red and black arrows, respectively. Ranges in water table fluctuations for each land unit are shown with double-sided arrows that are to scale with the vertical axis (metres) on each panel.

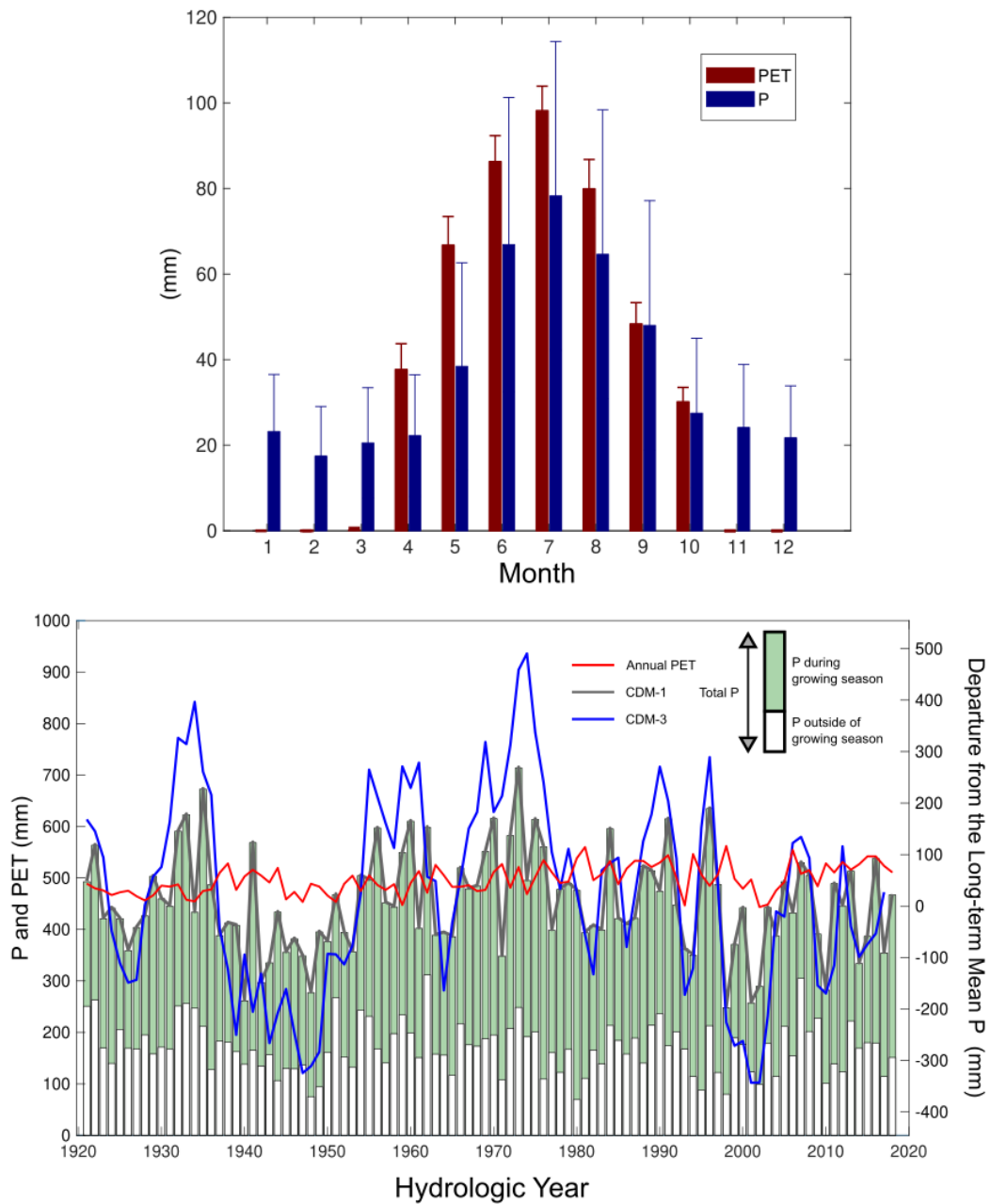


Figure 6-2: The monthly distribution of P and PET from 1920 to 2020, where the error bars represent standard deviations (upper), and an annual time series of major atmospheric fluxes (lower). CDM-1 and CDM-3 are the one and three year cumulative departure from the long-term mean precipitation, respectively. Sources of precipitation and temperature (used to calculate PET (Hamon, 1963)) data are outlined in Section 5.2.2).

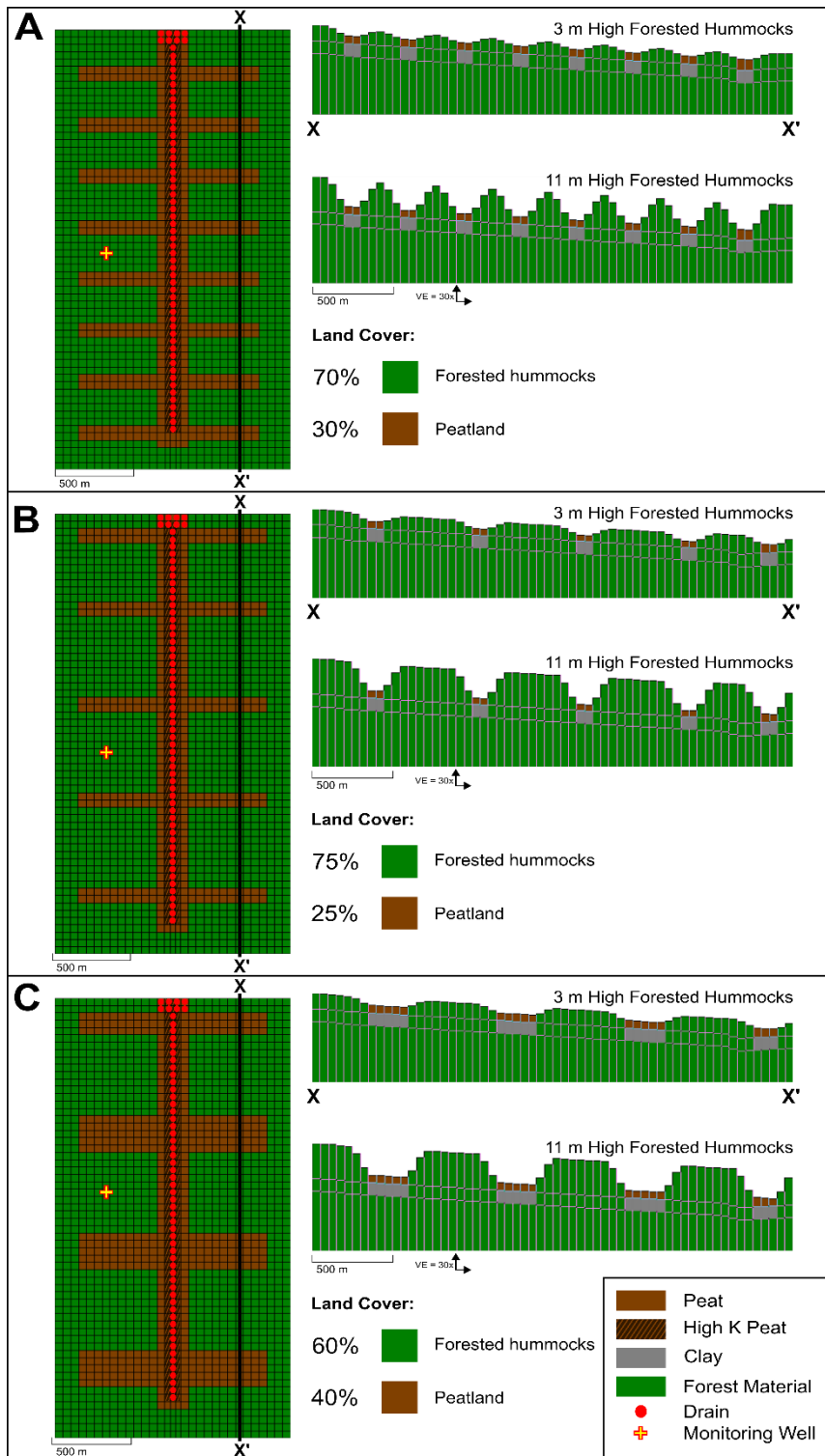









Figure 6-4: The three topological scenarios implemented in MODFLOW. (A) many small forested hummocks divided by small peatlands, (B) few large forested hummocks divided by small peatlands, and (C) few large forested hummocks divided by large peatlands. Each scenario is realized with hummocks heights 3 and 11 m above the peatlands. The cross sections have a vertical exaggeration of 30x.

Table 6-1: Material parameters

		K _{xy} (m/d)	K _z (m/d)	S _s (1/m)	S _y	θ _{sat}	θ _{ext}	θ _{resid}	Brooks- Corey ε	Forest Type	Rooting Depth (m)	
	Peat		3.4	1.02	1x10 ⁻²	0.4	0.88	0.03	0.02	3	Black Spruce	0.4
	High K Peat		12	12	1x10 ⁻²	0.65	0.93	0.03	0.01	3	Black Spruce	0.4
	Confining Clay		0.001	0.001	1x10 ⁻⁴	0.06	0.47	--	--	--	--	
Forest Materials:												
Coarse	Sand		5	1.5	1x10 ⁻⁴	0.32	0.44	0.03	0.02	3	Pine	3.25
	Sand Loam		0.62	1.86	1x10 ⁻⁴	0.28	0.45	0.09	0.04	6	Aspen	3.25
Fine	Silt Loam		0.16	0.049	1x10 ⁻⁴	0.2	0.5	0.13	0.02	8	Aspen	3.25
	Silt Clay		0.02	0.011	1x10 ⁻⁴	0.17	0.4	0.25	0.06	10	Aspen	3.25

Note: K = hydraulic conductivity; S_s = Specific Storage; S_y = Specific Yield; θ_{sat} = saturated water content; θ_{ext} = extinction water content, below which root water uptake ceases; θ_{resid} = residual water content; Brooks-Corey ε = Brooks-Corey epsilon, which is related to the pore-size distribution.

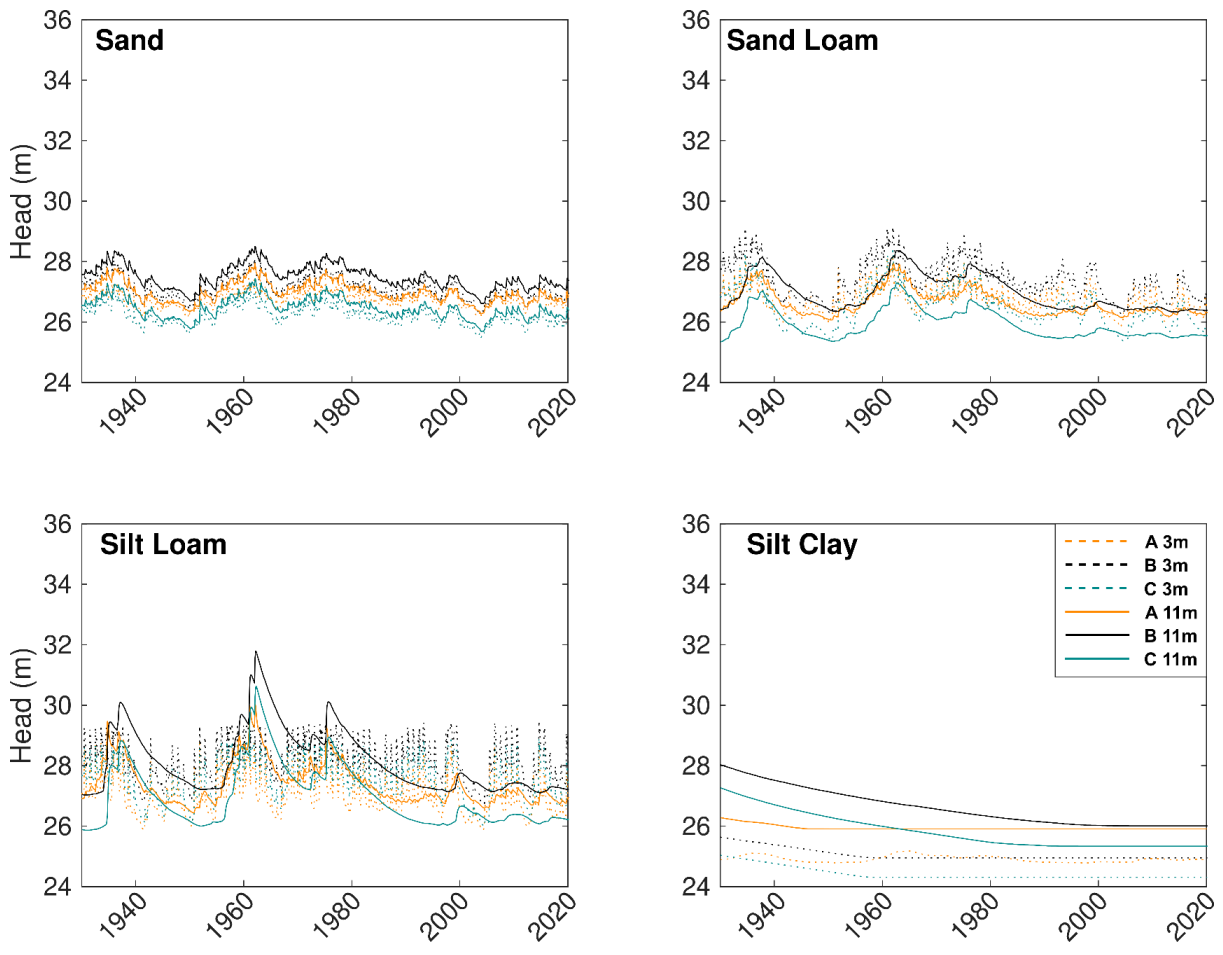


Figure 6-5: Modelled heads observed at the monitoring wells shown in Figure 6-6 for the 24 simulations. The 3 m and 11 m high hummocks are shown by dashed and solid lines, respectively. The color coding (orange, blue, and black) corresponds to the different topological scenarios presented in Figure 6-4.

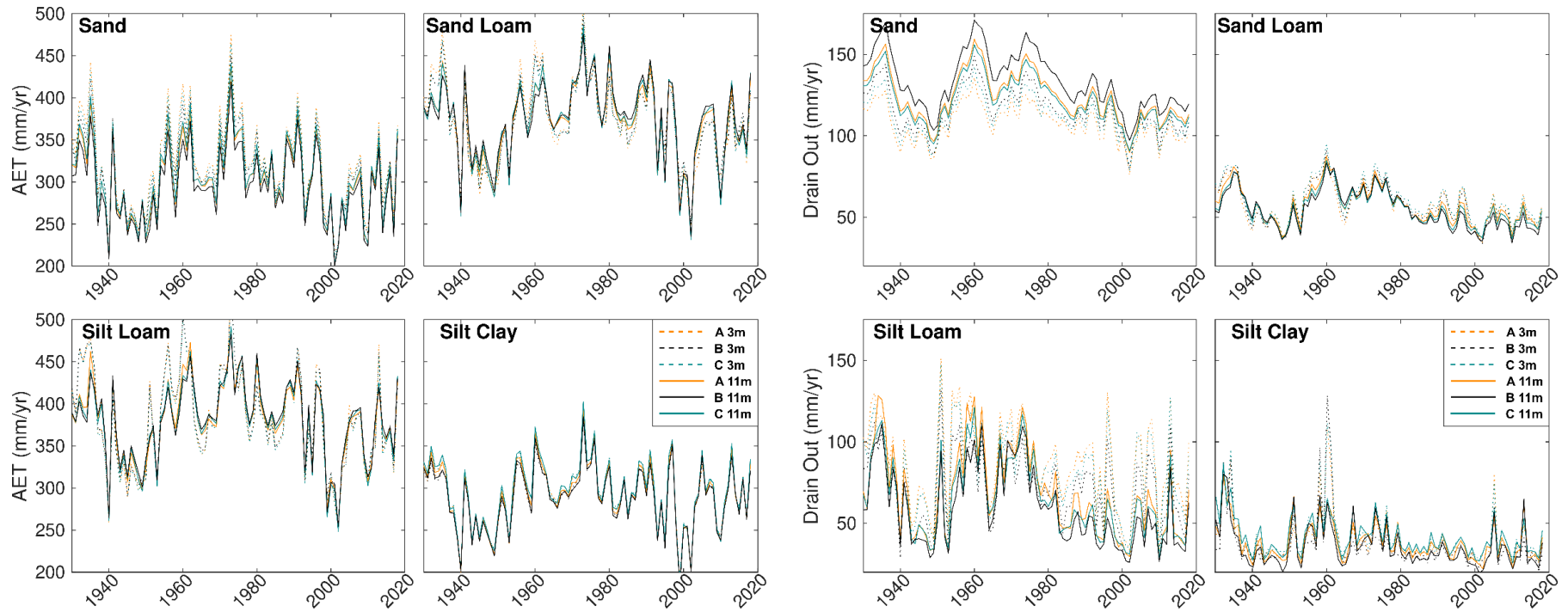


Figure 6-6: Time series of modelled AET (composed of groundwater ET, vadose zone ET, rejected recharge, interception, and sublimation) for the 24 simulations (left), and time series of outflow from the drains (right). Both fluxes are normalized for the areal extent of the model domains. The 3 m and 11 m high hummocks are shown by dashed and solid lines, respectively. The color coding (orange, blue, and black) corresponds to the different topological scenarios presented in Figure 6-4.

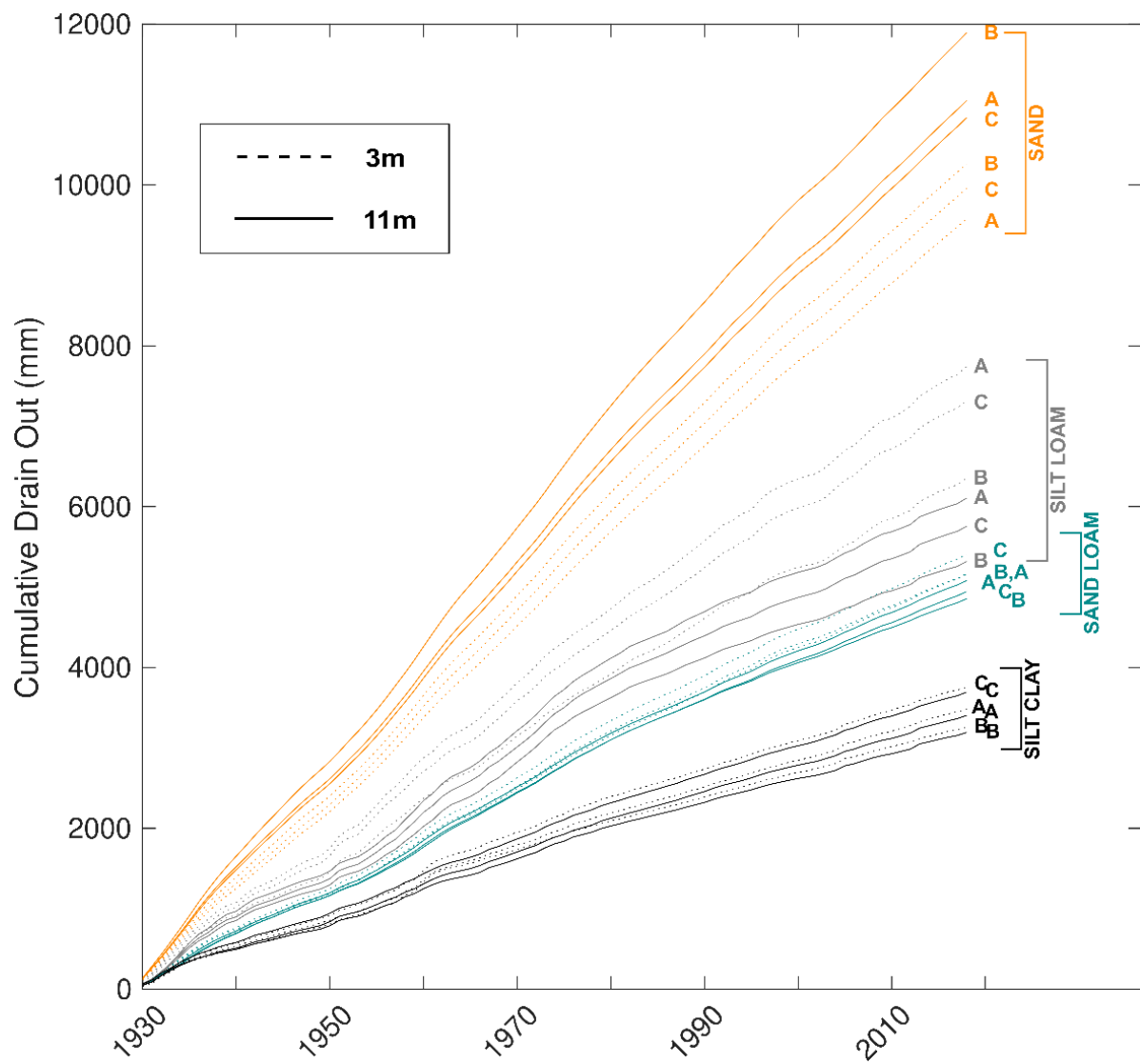


Figure 6-7: The cumulative outflow through the drains for the duration of each simulation. The cumulative fluxes are color-coded by texture. The 3 m and 11 m high hummocks are shown by dashed and solid lines, respectively. Each line is labeled with its corresponding topological scenario (Figure 6-4).

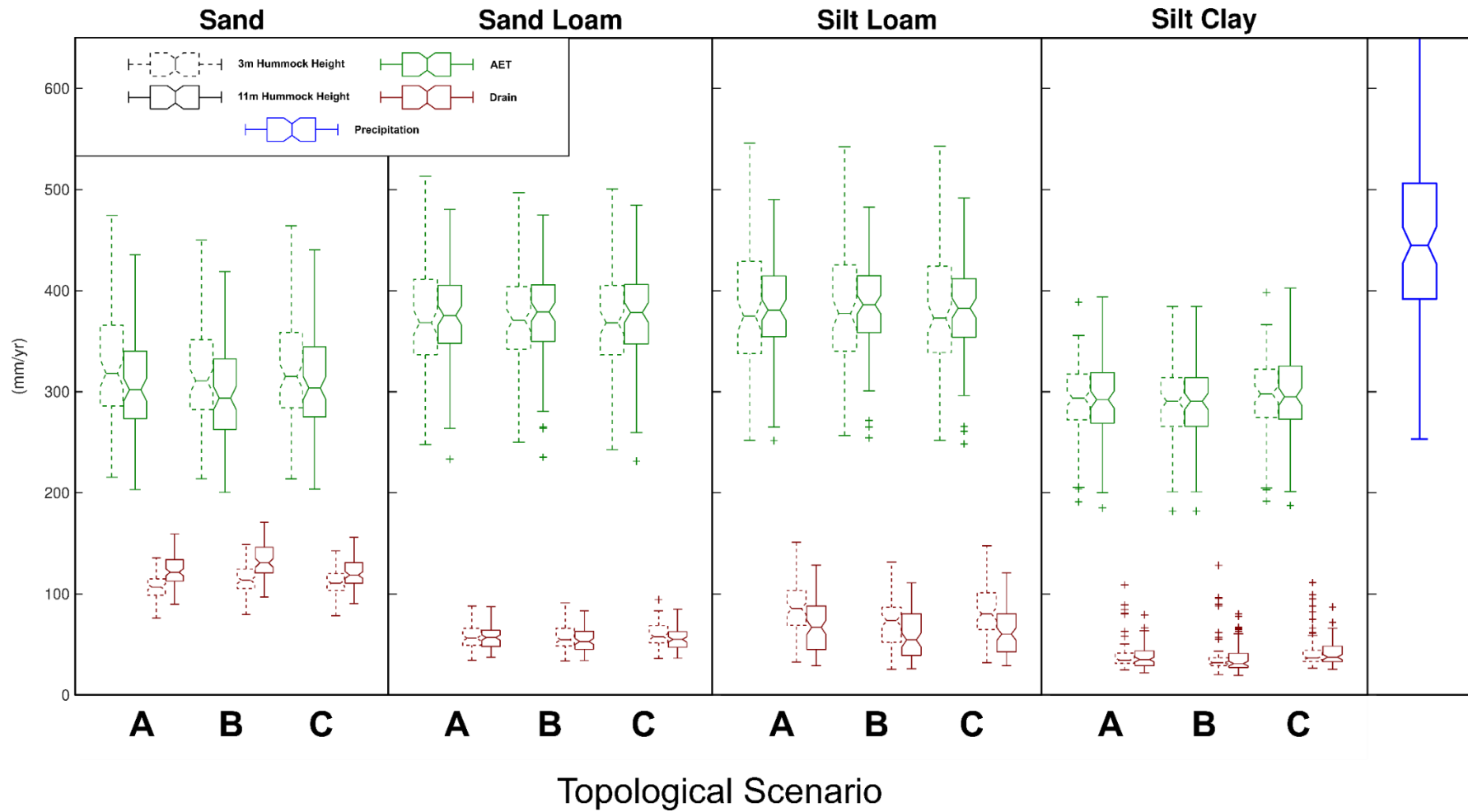


Figure 6-8: Boxplots showing the distribution of major annual fluxes for each simulation. The 3 m and 11 m high hummocks are shown by dashed and solid boxplots, respectively. AET and drain outflows are shown in green and red, respectively. A final boxplot to the right illustrates the distribution of annual precipitation. A, B, and C refer to the different topological scenarios presented in Figure 6-4.

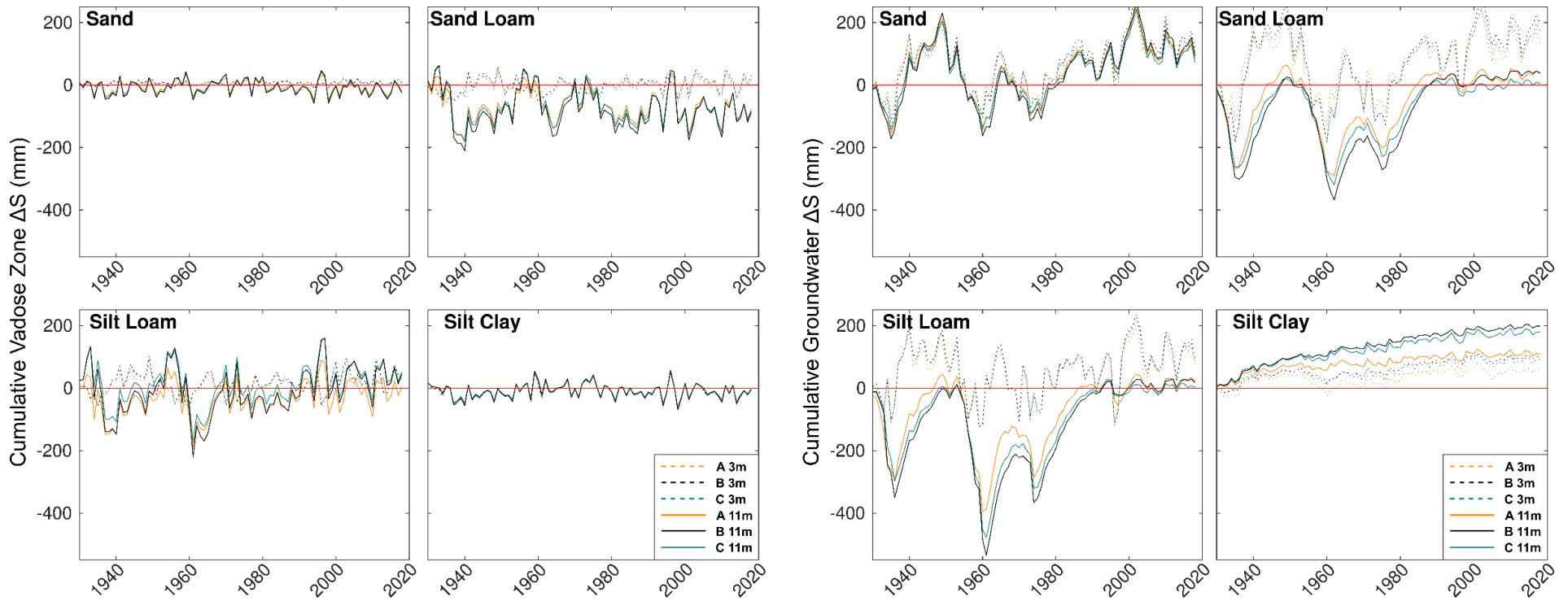


Figure 6-9: Cumulative changes in storage for the vadose (left) and groundwater reservoirs (right). Changes in storage are normalized for the areal extent of the model domains. The 3 m and 11 m high hummocks are shown by dashed and solid lines, respectively. The color coding (orange, blue, and black) corresponds to the different topological scenarios presented in Figure 6-4. A red light denotes zero change in storage.

References

- Alberta Agriculture and Forestry. 2018. Historic Alberta Weather Station Data, Alberta Climate Information Service. Retrieved January 20, 2018, from <https://agriculture.alberta.ca/acis/alberta-weather-data-viewer.jsp>
- Allison GB, Gee GW, and Tyler SW. 1994. Vadose-zone techniques for estimating groundwater recharge in arid and semiarid regions. *Soil Science Society of America Journal*, 58(1), 6-14. doi: 10.2136/sssaj1994.03615995005800010002x
- Amiro BD, Barr AG, Black TA, Iwashita H, Kljun N, McCaughey JH, Morgenstern K, Murayama S, Nesic Z, Orchansky AL, Saigusa N. 2006. Carbon, energy and water fluxes at mature and disturbed forest sites, Saskatchewan, Canada. *Agricultural and forest meteorology*. 136(3-4):237-51, doi: 10.1016/j.agrformet.2004.11.012.
- Anderson MP, Munter JA. 1981. Seasonal reversals of groundwater flow around lakes and the relevance to stagnation points and lake budgets. *Water Resources Research*. 17(4):1139-50, doi: 10.1029/WR017i004p01139.
- Anderson MP, Valley JW. 1990. Estimating groundwater exchange with lakes: 1. The stable isotope mass balance method. *Water Resources Research*, 26(10), 2445-2453. doi: 10.1029/WR026i010p02445.
- Appels WM, Graham CB, Freer JE, and McDonnell JJ. 2015. Factors affecting the spatial pattern of bedrock groundwater recharge at the hillslope scale. *Hydrological Processes*, 29(21), pp.4594-4610, doi: 10.1002/hyp.10481.
- Appels, W.M., Bogaart, P.W., and van der Zee, S.E., 2017. Feedbacks between shallow groundwater dynamics and surface topography on runoff generation in flat fields. *Water Resources Research*, 53(12), 10336-10353, doi: 10.1002/2017WR020727.
- Arnold JG, Srinivasan R, Muttiah RS, and Williams JR. 1998. Large area hydrologic modeling and assessment part I: model development 1. *Journal of the American Water Resources Association*, 34(1), 73-89, doi: 10.1111/j.1752-1688.1998.tb05961.x.
- Arnoux M, Gibert-Brunet E, Barbecot F, Guillon S, Gibson J, Noret A. 2017. Interactions between groundwater and seasonally ice-covered lakes: Using water stable isotopes and radon-222 multilayer mass balance models. *Hydrological Processes*, 31(14), 2566-2581, doi: 10.1002/hyp.11206.
- Atkinson N, Utting DJ, and Pawley SM. 2014. Landform signature of the Laurentide and Cordilleran ice sheets across Alberta during the last glaciation. *Canadian Journal of Earth Sciences*, 51(12), 1067-1083, doi: 10.1139/cjes-2014-0112.
- Babyak MA. 2004. What you see may not be what you get: a brief, nontechnical introduction to overfitting in regression-type models. *Psychosomatic medicine*, 66(3), pp.411-421.

Bachu S. 1999. Flow systems in the Alberta Basin: Patterns, types and driving mechanisms. *Bulletin of Canadian Petroleum Geology*, 47(4), 455-474, doi: 10.35767/gscpgbull.47.4.455.

Barker CA, Amiro BD, Kwon H, Ewers BE, and Angstmann JL. 2009. Evapotranspiration in intermediate-aged and mature fens and upland black spruce boreal forests. *Ecohydrology*, 2(4), 462-471, doi: 10.1002/eco.74.

Barr AG, Black TA, Hogg EH, Kljun N, Morgenstern K, and Nesic Z. 2004. Inter-annual variability in the leaf area index of a boreal aspen-hazelnut forest in relation to net ecosystem production. *Agricultural and forest meteorology*, 126(3-4), pp.237-255, doi: 10.1016/j.agrformet.2004.06.011.

Barr AG, Van der Kamp G, Black TA, McCaughey JH, and Nesic Z. 2012. Energy balance closure at the BERMS flux towers in relation to the water balance of the White Gull Creek watershed 1999–2009. *Agricultural and Forest Meteorology*, 153, 3-13, doi: 10.1016/j.agrformet.2011.05.017.

Bartlett PA, MacKay MD, and Versegny DL. 2006. Modified snow algorithms in the Canadian land surface scheme: Model runs and sensitivity analysis at three boreal forest stands. *Atmosphere-Ocean*, 44(3), pp.207-222, doi: 10.3137/ao.440301.

Becker A. and Braun P. 1999. Disaggregation, aggregation and spatial scaling in hydrological modelling. *Journal of Hydrology*, 217(3-4), 239-252, doi: 10.1016/S0022-1694(98)00291-1

Beklioglu M, Meerhoff M, Davidson TA, Ger KA, Havens K, Moss B. 2016. Preface: Shallow lakes in a fast changing world. *Hydrobiologia*, 778(1), 9-11. doi: 10.1007/s10750-016-2840-5.

Bergengren JC, Waliser DE, and Yung YL. 2011. Ecological sensitivity: A biospheric view of climate change. *Climatic Change*, 107(3-4), 433, doi: 10.1007/s10584-011-0065-1.

BGC Engineering Inc. 2010. Review of Reclamation Options for Oil Sands Tailings Substrates. OSRIN Report No. TR-2, 0-59, Vancouver, BC: BGC Engineering, doi: 10.7939/R3SB6Q .

Blancher PJ, Wells JV. 2005. The boreal forest region: North America's bird nursery. Canadian Boreal Initiative.

Blanken PD, Black TA, Neumann HH, Den Hartog G, Yang PC, Nesic Z, and Lee X. 2001. The seasonal water and energy exchange above and within a boreal aspen forest. *Journal of Hydrology*, 245(1-4), pp.118-136, doi: 10.1016/S0022-1694(01)00343-2.

Block RMA, Van Rees KCJ, and Knight JD. 2006. A review of fine root dynamics in Populus plantations. *Agroforestry Systems*, 67(1), pp.73-84, doi: 10.1007/s10457-005-2002-7.

Bonsal BR, Aider R, Gachon P, Lapp S. 2013. An assessment of Canadian prairie drought: past, present, and future. *Climate Dynamics*, 41(2), 501-516, doi: 10.1007/s00382-012-1422-0.

Bothe RA, Abraham C. 1993. Evaporation and evapotranspiration in Alberta 1986 to 1992 addendum. Surface Water Assessment Branch, Technical Services and Monitoring Division, Water Resources Services, Alberta Environmental Protection.

Brown SM, Petrone RM, Chasmer L, Mendoza C, Lazerjan MS, Landhäusser SM, Silins U, Leach J, and Devito KJ. 2014. Atmospheric and soil moisture controls on evapotranspiration from above and within a Western Boreal Plain aspen forest. *Hydrological Processes*, 28(15), pp.4449-4462, doi: 10.1002/hyp.9879.

Brown SM, Petrone RM, Mendoza C, and Devito KJ. 2010. Surface vegetation controls on evapotranspiration from a sub-humid Western Boreal Plain wetland. *Hydrological Processes: An International Journal*, 24(8), pp.1072-1085, doi: 10.1002/hyp.7569.

Cardenas MB. 2007. Potential contribution of topography-driven regional groundwater flow to fractal stream chemistry: Residence time distribution analysis of Tóth flow. *Geophysical Research Letters*, 34(5), doi: 10.1029/2006GL029126.

Carrera-Hernández JJ, Mendoza CA, Devito KJ, Petrone RM, and Smerdon BD. 2011. Effects of aspen harvesting on groundwater recharge and water table dynamics in a subhumid climate. *Water Resources Research*, 47(5), doi: 10.1029/2010WR009684.

Carsel RF and Parrish RS. 1988. Developing joint probability distributions of soil water retention characteristics. *Water resources research*, 24(5), pp.755-769, doi: 10.1029/WR024i005p00755.

Ceroici WJ. 1978. Hydrogeological map of the Peerless Lake area, Alberta. Map 123. Alberta Research Council, Edmonton, Alberta, Canada.

Changming L, Jingjie Y, and Kendy E. 2001. Groundwater exploitation and its impact on the environment in the North China Plain. *Water International*, 26(2), 265-272, doi: 10.1080/02508060108686913.

Chen W, Zhao X, Tsangaratos P, Shahabi H, Ilia I, Xue W, Wang X, and Ahmad BB. 2020. Evaluating the usage of tree-based ensemble methods in groundwater spring potential mapping. *Journal of Hydrology*, 583, p.124602, doi: 10.1016/j.jhydrol.2020.124602.

Cheng FY, Basu NB. 2017. Biogeochemical hotspots: Role of small water bodies in landscape nutrient processing. *Water Resources Research*, 53(6), 5038-5056, doi: 10.1002/2016WR020102.

Cheng X, Anderson MP. 1994. Simulating the influence of lake position on groundwater fluxes. *Water Resources Research*, 30(7), 2041-2049, doi: 10.1029/93WR03510.

Cherkauer DS, Zager JP. 1989. Groundwater interaction with a kettle-hole lake: relation of observations to digital simulations. *Journal of Hydrology*, 109(1-2), 167-184, doi: 10.1016/0022-1694(89)90013-9.

Clark ID and Fritz P. 1997. Environmental isotopes in hydrogeology. CRC press.

Condon LE, and Maxwell RM. 2015. Evaluating the relationship between topography and groundwater using outputs from a continental-scale integrated hydrology model. *Water Resources Research*, 51(8), 6602-6621, doi: 10.1002/2014WR016774.

Cooke JA and Johnson MS. 2002. Ecological restoration of land with particular reference to the mining of metals and industrial minerals: A review of theory and practice. *Environmental Reviews*, 10(1), 41-71, doi: 10.1139/a01-014.

Craig H. 1961. Isotopic variations in meteoric waters. *Science*, 133(3465), 1702-1703, doi: 10.1126/science.133.3465.1702.

Cui J, Tian L, and Gibson JJ. 2018. When to conduct an isotopic survey for lake water balance evaluation in highly seasonal climates. *Hydrological Processes*, 32(3), 379-387, doi: 10.1002/hyp.11420.

Daly C, Price JS, Rezanezhad F, Pouliot R, Rochefort L, Graf M. 2012. Initiatives in oil sand reclamation: considerations for building a fen peatland in a post-mined oil sands landscape. In: Vitt D., Bhatti J.S. (Eds.), *Restoration and Reclamation of Boreal Ecosystems - Attaining Sustainable Development*, Cambridge University Press, New York, pp. 179-201

Dansgaard W. 1964. Stable isotopes in precipitation. *Tellus*, 16(4), 436-468, doi: 10.3402/tellusa.v16i4.8993.

De Vries JJ and Simmers I. 2002. Groundwater recharge: an overview of processes and challenges. *Hydrogeology Journal*, 10(1), pp.5-17, doi: 10.1007/s10040-001-0171-7.

De'ath G. 2007. Boosted trees for ecological modeling and prediction. *Ecology*, 88, 243–251, doi: 10.1890/0012-9658(2007)88[243:BTFFEMA]2.0.CO;2.

DeByle NV and Winokur RP. 1985. *Aspen: ecology and management in the western United States*. USDA Forest Service General Technical Report RM-119. Rocky Mountain Forest and Range Experiment Station, Fort Collins, Colo. 283 p., 119.

Depante M, Morison MQ, Petrone RM, Devito KJ, Kettridge N, Waddington JM. 2019. Hydraulic redistribution and hydrological controls on aspen transpiration and establishment in peatlands following wildfire. *Hydrological Processes*. 33(21):2714-28, doi: 10.1002/hyp.13522.

Devito KJ, Creed IF, Fraser CJD. 2005a. Controls on runoff from a partially harvested aspen-forested headwater catchment, Boreal Plain, Canada. *Hydrological Processes: An International Journal*, 19(1), 3-25, doi: 10.1002/hyp.5776.

Devito K, Creed I, Gan T, Mendoza C, Petrone R, Silins U, Smerdon B. 2005b. A framework for broad-scale classification of hydrologic response units on the Boreal Plain: is topography the last thing to consider? *Hydrological processes*, 19(8), 1705-1714, doi: 10.5558/tfc2016-017.

Devito KJ, Hokanson, KJ, Moore PA, Kettridge N, Anderson AE, Chasmer L, Hopkinson C, Lukenbach M, Mendoza C, Morissette J, Peters D, Petrone R, Silins U, Smerdon B, Waddington J. 2017. Landscape controls on long-term runoff in subhumid heterogeneous Boreal Plains catchments. *Hydrological Processes*, 31(15), 2737-2751, doi: 10.1002/hyp.11213.

Devito KJ, Mendoza C, Petrone RM, Kettridge N, and Waddington JM. 2016. Utikuma Region Study Area (URSA)–part 1: hydrogeological and ecohydrological studies (HEAD). *The Forestry Chronicle*, 92(1), 57-61, doi: 10.5558/tfc2016-017.

Devito KJ, Mendoza C, Qualizza C. 2012. Conceptualizing water movement in the Boreal Plains. Implications for watershed reconstruction. Synthesis report prepared for the Canadian Oil Sands Network for Research and Development, Environmental and Reclamation Research Group. 164p.

Dimitrov DD, Bhatti JS, and Grant RF. 2014. The transition zones (ecotone) between boreal forests and peatlands: Ecological controls on ecosystem productivity along a transition zone between upland black spruce forest and a poor forested fen in central Saskatchewan. *Ecological Modelling*, 291, 96-108, doi: 10.1016/j.ecolmodel.2013.11.030.

Dormann CF, Elith J, Bacher S, Buchmann C, Carl G, Carre G, ... Lautenbach S. 2013. Collinearity: A review of methods to deal with it and a simulation study evaluating their performance. *Ecography*, 36, 27–46, doi: 10.1111/j.1600-0587.2012.07348.x.

Edmunds WM, Shand P, Hart P, and Ward RS. 2003. The natural (baseline) quality of groundwater: a UK pilot study. *Science of the Total Environment*, 310(1-3), 25-35, doi: 10.1016/S0048-9697(02)00620-4.

Elith J, Leathwick JR, and Hastie T. 2008. A working guide to boosted regression trees. *Journal of Animal Ecology*, 77, 802–813, doi: 10.1111/j.1365-2656.2008.01390.x.

Environment Canada. 2019. Climate Data Online, Fort McMurray, AB. Retrieved from https://climate.weather.gc.ca/historical_data/search_historic_data_e.html

Esquivel-Hernández G, Sánchez-Murillo R, Quesada-Román A, Mosquera GM, Birkel C, Boll J. 2018. Insight into the stable isotopic composition of glacial lakes in a tropical alpine ecosystem: Chirripó, Costa Rica. *Hydrological processes*, 32(24), 3588-3603,. doi: 10.1002/hyp.13286.

ESTR Secretariat. 2014. Boreal Plains Ecozone evidence for key findings summary. *Canadian Biodiversity: Ecosystem Status and Trends 2010, Evidence for Key Findings Summary Report No. 12*. Canadian Councils of Resource Ministers. Ottawa, ON. 106 p.

Fan, Y. 2015. Groundwater in the Earth's critical zone: Relevance to large-scale patterns and processes. *Water Resources Research*, 51(5), 3052-3069, doi: 10.1002/2015WR017037.

Fenton MM, Waters EJ, Pawley SM, Atkinson N, Utting DJ, McKay K. 2013. Surficial geology of Alberta. Map 601. Alberta Geological Survey, Edmonton, Alberta, Canada.

Ferone JM and Devito KJ. 2004. Shallow groundwater–surface water interactions in pond–peatland complexes along a Boreal Plains topographic gradient. *Journal of Hydrology*, 292(1-4), pp.75-95, doi: 10.1016/j.jhydrol.2003.12.032.

Flügel WA. 1995. Delineating hydrological response units by geographical information system analyses for regional hydrological modelling using PRMS/MMS in the drainage basin of the River Bröl, Germany. *Hydrological Processes*, 9(3-4), 423-436, doi: 10.1002/hyp.3360090313.

Freeze RA and Witherspoon PA. 1967. Theoretical analysis of regional groundwater flow: 2. Effect of water-table configuration and subsurface permeability variation. *Water Resources Research*, 3(2), 623-634, doi: 10.1111/j.1936-704X.2012.03105.x

Freeze RA, Cherry JA. 1979. *Groundwater*. Prentice-Hall, Englewood Cliffs, NJ

Garven G. 1989. A hydrogeologic model for the formation of the giant oil sands deposits of the Western Canada sedimentary basin. *American Journal of Science*, 289(2), 105-166, doi: 10.2475/ajs.289.2.105

Gat JR, Bowser CJ. 1991. The heavy isotope enrichment of water in coupled evaporative systems. *Geochemical Society Special Publication: Stable Isotope Geochemistry*, 3, pp. 159-168

Gentine P, Troy TJ, Lintner BR, and Findell KL. 2012. Scaling in surface hydrology: Progress and challenges. *Journal of Contemporary Water research and education*, 147(1), 28-40, doi: 10.1111/j.1936-704X.2012.03105.x.

Gibson JJ, Birks SJ, Edwards TWD. 2008. Global prediction of δ_A and $\delta^2\text{H}-\delta^{18}\text{O}$ evaporation slopes for lakes and soil water accounting for seasonality. *Global biogeochemical cycles*, 22(2) GB2031, doi: 10.1029/2007GB002997.

Gibson JJ, Birks SJ, Moncur M. 2019. Mapping water yield distribution across the South Athabasca Oil Sands (SAOS) area: Baseline surveys applying isotope mass balance of lakes. *Journal of Hydrology: Regional Studies*, 21, 1-13, doi: 10.1016/j.ejrh.2018.11.001.

Gibson JJ, Birks SJ, Yi Y, Moncur MC, McEachern PM. 2016. Stable isotope mass balance of fifty lakes in central Alberta: Assessing the role of water balance parameters in determining trophic status and lake level. *Journal of Hydrology: Regional Studies*, 6, 13-25, doi: 10.1016/j.ejrh.2016.01.034.

Gibson JJ, Birks SJ, Yi Y, Vitt D. 2015. Runoff to boreal lakes linked to land cover, watershed morphology and permafrost thaw: a 9-year isotope mass balance assessment. *Hydrological Processes*, 29(18), 3848-3861, doi: 10.1002/hyp.10502.

Gibson JJ, Edwards TWD, Bursley GG, Prowse TD. 1993. Estimating Evaporation Using Stable Isotopes: Quantitative Results and Sensitivity Analysis for Two Catchments in Northern Canada: Paper presented at the 9th Northern Res. Basin Symposium/Workshop (Whitehorse/Dawson/Inuvik, Canada-August 1992). *Hydrology Research*, 24(2-3), 79-94, doi: 10.2166/nh.1993.0015.

Gibson JJ, Prepas EE, McEachern P. 2002. Quantitative comparison of lake throughflow, residency, and catchment runoff using stable isotopes: modelling and results from a regional survey of Boreal lakes. *Journal of Hydrology*, 262(1-4), 128-144, doi: 10.1016/S0022-1694(02)00022-7.

Gibson JJ, Reid R, Spence C. 1998. A six-year isotopic record of lake evaporation at a mine site in the Canadian subarctic: results and validation. *Hydrological Processes*. 12(10-11):1779-92

Gillham RW. 1984. The capillary fringe and its effect on water-table response. *Journal of Hydrology*. 67(1-4):307-24, doi: 10.1016/0022-1694(84)90248-8.

Gleeson T, Marklund L, Smith L, and Manning AH. 2011. Classifying the water table at regional to continental scales. *Geophysical Research Letters*, 38(5), doi: 10.1029/2010GL046427.

Goderniaux P, Davy P, Bresciani E, de Dreuzy JR, and Le Borgne T. 2013. Partitioning a regional groundwater flow system into shallow local and deep regional flow compartments. *Water Resources Research*, 49(4), 2274-2286, doi: 10.1002/wrcr.20186.

Goodbrand A, Westbrook CJ, and van der Kamp G. 2019. Hydrological functions of a peatland in a Boreal Plains catchment. *Hydrological Processes*, 33(4), 562-574, doi: 10.1002/hyp.13343.

Government of Alberta. 2018. Environmental protection and enhancement act. Conservation and reclamation regulation. http://www.qp.alberta.ca/documents/Regs/1993_115.pdf. Accessed 10 October 2019

Gracz MB, Moffett MF, Siegel DI, and Glaser PH. 2015. Analyzing peatland discharge to streams in an Alaskan watershed: An integration of end-member mixing analysis and a water balance approach. *Journal of Hydrology*, 530, 667-676, doi: 10.1016/j.jhydrol.2015.09.072.

Gray DM, Landine PG, and Granger RJ. 1985. Simulating infiltration into frozen prairie soils in streamflow models. *Canadian Journal of Earth Sciences*. 22 (3): 464-72, doi: 10.1139/e85-045.

Gröning M, Lutz HO, Roller-Lutz Z, Kralik M, Gourcy L, Pöntenstein L. 2012. A simple rain collector preventing water re-evaporation dedicated for $\delta^{18}\text{O}$ and $\delta^2\text{H}$ analysis of cumulative precipitation samples. *Journal of hydrology*, 448, 195-200, doi: 10.1016/j.jhydrol.2012.04.041.

Gupta VK, Rodríguez-Iturbe I, and Wood EF. 2012. Scale problems in hydrology: runoff generation and basin response (Vol. 6). Springer Science and Business Media, doi: 10.1007/978-94-009-4678-1.

Haitjema HM, Mitchell-Bruker S. 2005. Are water tables a subdued replica of the topography? *Groundwater*, 43(6), 781-786, doi: 10.1111/j.1745-6584.2005.00090.x.

Haitjema HM. 1995. Analytic element modeling of groundwater flow. San Diego, California: Academic Press.

Hamon WR. 1963. Computation of direct runoff amounts from storm rainfall. *International Association of Scientific Hydrology Publication*, 63, pp.52-62.

Han J, Yang Y, Roderick ML, McVicar TR, Yang D, Zhang S, and Beck HE. 2020. Assessing the Steady-State Assumption in Water Balance Calculation Across Global Catchments. *Water Resources Research*, 56(7), p.e2020WR027392, doi: 10.1029/2020WR027392.

Han S, Yang Y, Lei Y, Tang C, and Moiwo JP. 2008. Seasonal groundwater storage anomaly and vadose zone soil moisture as indicators of precipitation recharge in the piedmont region of Taihang Mountain, North China Plain. *Hydrology Research*, 39(5-6), pp.479-495, doi: 10.2166/nh.2008.117.

Harbaugh AW. 2005. MODFLOW-2005, the US Geological Survey modular ground-water model: the ground-water flow process. Reston, VA: US Department of the Interior, US Geological Survey.

Hayashi M, Van der Kamp G. 2000. Simple equations to represent the volume–area–depth relations of shallow wetlands in small topographic depressions. *Journal of hydrology*, 237(1-2), 74-85, doi: 10.1016/S0022-1694(00)00300-0.

Healy RW. 2010. Estimating groundwater recharge. Cambridge University Press.

Heuperman A. 1999. Hydraulic gradient reversal by trees in shallow water table areas and repercussions for the sustainability of tree-growing systems. *Agricultural Water Management*, 39(2-3), 153-167, doi: 10.1016/S0378-3774(98)00076-6.

Hitchon B. 1969. Fluid flow in the Western Canada Sedimentary Basin: 1. effect of topography. *Water Resources Research*, 5(1), 186-195, doi: 10.1029/WR005i001p00186.

Holden J. 2006. Peatland hydrology. *Developments in Earth Surface Processes*, 9, 319-346, doi: 10.1016/S0928-2025(06)09014-6.

Hubbert MK. 1940. The theory of ground-water motion. *The Journal of Geology*, 48(8, Part 1), 785-944, doi: 10.1029/TR021i002p00648-1.

Hvorslev MJ. 1951. Time lag and soil permeability in ground-water observations, Waterways Experiment Station, Corps of Engineers. *US Army, Bulletin*, 36, 49.

Hwang HT, Park YJ, Sudicky EA, Berg SJ, McLaughlin R, and Jones JP. 2018. Understanding the water balance paradox in the Athabasca River Basin, Canada. *Hydrological Processes*, 32(6), pp.729-746.

Ireson AM, Barr AG, Johnstone JF, Mamet SD, van der Kamp G, Whitfield CJ, ... Sagin J. 2015. The changing water cycle: The Boreal Plains ecozone of Western Canada. *Wiley Interdisciplinary Reviews-Water*, 2, 505–521, doi: 10.1002/wat2.1098.

Jackson RB, Jobbágy EG, and Noretto MD. 2009. Ecohydrology in a human-dominated landscape. *Ecohydrology*, 2(3), 383-389, doi: 10.1002/wat2.1098.

Jaquet NG. 1976. Ground-water and surface-water relationships in the glacial province of northern Wisconsin—Snake Lake. *Groundwater*, 14(4), 194-199, doi: 10.1111/j.1745-6584.1976.tb03103.x.

Jeglum JK, Kershaw HM, Morris DA, and Cameron DA. 2003. Best forestry practices: a guide for the boreal forest in Ontario. Natural Resources Canada, Sault Ste. Marie, Ontario.

Jencso KG, McGlynn BL, Gooseff MN, Wondzell SM, Bencala KE, and Marshall LA. 2009. Hydrologic connectivity between landscapes and streams: Transferring reach-and plot-scale understanding to the catchment scale. *Water Resources Research*, 45(4), doi: 10.1029/2008WR007225.

Jobbágy EG and Jackson RB. 2004. Groundwater use and salinization with grassland afforestation. *Global Change Biology*, 10(8), 1299-1312, doi: 10.1111/j.1365-2486.2004.00806.x.

Jones MD, Imbers J. 2010. Modeling Mediterranean lake isotope variability. *Global and Planetary Change*, 71(3-4), 193-200, doi: 10.1016/j.gloplacha.2009.10.001.

Kalef, N. 2002. Interlinking hydrological behaviour and inorganic nitrogen cycling in a forested boreal wetland. MSc Thesis, Department Biological Sciences, University of Alberta. 83 pp.

Kenoyer GJ and Anderson MP. 1989. Groundwater's dynamic role in regulating acidity and chemistry in a precipitation-dominated lake. *Journal of Hydrology*, 109(3-4), 287-306, doi: 10.1016/0022-1694(89)90020-6.

Ketcheson SJ, Price JS, Carey SK, Petrone RM, Mendoza CA, and Devito KJ. 2016. Constructing fen peatlands in post-mining oil sands landscapes: challenges and opportunities from a hydrological perspective. *Earth-science Reviews*, 161, 130-139, doi: 10.1016/j.earscirev.2016.08.007.

Ketcheson SJ, Price JS, Sutton O, Sutherland G, Kessel E, and Petrone RM. 2017. The hydrological functioning of a constructed fen wetland watershed. *Science of the Total Environment*, 603, 593-605, doi: 10.1016/j.scitotenv.2017.06.101.

Kirkby MJ and Beven KJ. 1979. A physically based, variable contributing area model of basin hydrology. *Hydrological Sciences Journal*, 24(1), 43-69, doi: 10.1080/02626667909491834.

Knierim KJ, Kingsbury JA, Haugh CJ, Ransom KM. 2020. Using Boosted Regression Tree Models to Predict Salinity in Mississippi Embayment Aquifers, Central United States. *Journal of the American Water Resources Association*, doi: 10.1111/1752-1688.12879.

Kohavi R. 1995. August. A study of cross-validation and bootstrap for accuracy estimation and model selection. In *Ijcai* (Vol. 14, No. 2, pp. 1137-1145).

Krabbenhoft DP, Bowser CJ, Anderson MP, Valley JW. 1990. Estimating groundwater exchange with lakes: 1. The stable isotope mass balance method. *Water Resources Research*, 26(10), 2445-2453, doi: 10.1029/WR026i010p02445

Krabbenhoft DP, Bowser CJ, Kendall C, Gat J. 1994. Use of oxygen-18 and deuterium to assess the hydrology of groundwater-lake systems. *Environmental Chemistry of Lakes and Reservoirs*. L. Baker (Ed.), pp. 67-90.

Krabbenhoft DP, Webster KE. 1995. Transient hydrogeological controls on the chemistry of a seepage lake. *Water Resources Research*, 31(9), 2295-2305, doi: 10.1029/95WR01582.

Kratz T, Webster K, Bowser C, Maguson J, and Benson B. 1997. The influence of landscape position on lakes in northern Wisconsin. *Freshwater Biology*, 37(1), 209-217, doi: 10.1046/j.1365-2427.1997.00149.x.

LaBaugh JW, Rosenberry DO, Winter TC. 1995. Groundwater contribution to the water and chemical budgets of Williams Lake, Minnesota, 1980–1991. *Canadian Journal of Fisheries and Aquatic Sciences*, 52(4), 754-767, doi: 10.1139/f95-075.

LaBaugh JW, Winter TC, Rosenberry DO, Schuster PF, Reddy MM, and Aiken GR. 1997. Hydrological and chemical estimates of the water balance of a closed-basin lake in north central Minnesota. *Water Resources Research*, 33(12), 2799-2812, doi: 10.1029/97WR02427.

LaBaugh JW. 1986. Wetland Ecosystem Studies From A Hydrologic Perspective 1. *Journal of the American Water Resources Association*, 22(1), 1-10, doi: 10.1111/j.1752-1688.1986.tb01853.x.

Landwehr JM and Coplen TB. 2006. Line-conditioned excess: a new method for characterizing stable hydrogen and oxygen isotope ratios in hydrologic systems. In: *International conference on isotopes in environmental studies* (pp. 132-135). Vienna: IAEA.

Le PV, and Kumar P. 2014. Power law scaling of topographic depressions and their hydrologic connectivity, *Geophys. Res. Lett.*, 41, 1553–1559, doi: 10.1002/2013GL059114.

Lennox DH, Maathuis H, and Pederson D. 1988. Region 13, Western glaciated plains. *Hydrogeology*. The Geological Society of North America, Boulder Colorado. 1988. p 115-128.

Letts MG, Roulet NT, Comer NT, Skarupa MR, and Versegny DL. 2000. Parametrization of peatland hydraulic properties for the Canadian Land Surface Scheme. *Atmosphere-Ocean*, 38(1), pp.141-160, doi: 10.1080/07055900.2000.9649643.

Lieffers VJ and Rothwell RL. 1987. Rooting of peatland black spruce and tamarack in relation to depth of water table. *Canadian Journal of Botany*, 65(5), 817-821.

Lissey A. 1971. Depression-focused transient groundwater flow patterns in Manitoba. *Geological Association of Canada*, 9, 333–341.

Lou S, Li DH, Lam JC, and Chan WW. 2016. Prediction of diffuse solar irradiance using machine learning and multivariable regression. *Applied energy*, 181, pp.367-374.

Lukenbach MC, Hokanson KJ, Devito KJ, Kettridge N, Petrone RM, Mendoza CA, ... Waddington JM. 2017. Post-fire ecohydrological conditions at peatland margins in different

hydrogeological settings of the Boreal Plain. *Journal of Hydrology*, 548, 741-753, doi: 10.1016/j.jhydrol.2017.03.034.

Lukenbach MC, Spencer CJ, Mendoza CA, Devito KJ, Landhäusser SM, and Carey SK. 2019. Evaluating How Landform Design and Soil Covers Influence Groundwater Recharge in a Reclaimed Watershed. *Water Resources Research*, 55(8), 6464-6481, doi: 10.1029/2018WR024298.

Mack G and Morrison D (eds). 2006. *Waterfowl of the Boreal Forest*. Ducks Unlimited Canada, 108 pp., doi: 10.3390/rs11020161.

MacKenzie DD, and Renkema KN. 2013. In-situ oil sands extraction: Reclamation and restoration practices and opportunities compilation (p. 0-94, Rep.). Calgary, AB: Canada's Oil Sands Innovation Alliance.

Marshall IB, Schut P, and Ballard M. 1999. Canadian ecodistrict climate normals for Canada 1961–1990. A national ecological framework for Canada: attribute data. Environmental Quality Branch, Ecosystems Science Directorate, Environment Canada and Research Branch, Agriculture and Agri-Food Canada, Ottawa and Hull.

Meyboom P. 1966. Unsteady groundwater flow near a willow ring in hummocky moraine. *Journal of Hydrology*, 4, 38-62, doi: 10.1016/0022-1694(66)90066-7.

Moore KE, Fitzjarrald DR, Sakai RK, Freedman JM. 2000. Growing season water balance at a boreal jack pine forest. *Water Resources Research*. 36(2):483-93, doi: 10.1029/1999WR900275.

Montgomery J, Brisco B, Chasmer L, Devito K, Cobbaert D, Hopkinson C. 2019. SAR and LiDAR temporal data fusion approaches to boreal wetland ecosystem monitoring. *Remote Sensing*, 11(2), 161, doi: 10.3390/rs11020161.

Morris PJ, Belyea LR, and Baird AJ. 2011. Ecohydrological feedbacks in peatland development: a theoretical modelling study. *Journal of Ecology*, 99(5), 1190-1201, doi: 10.1111/j.1365-2745.2011.01842.x.

Mwale D, Gan TY, Devito K, Mendoza C, Silins U, Petrone R. 2009. Precipitation variability and its relationship to hydrologic variability in Alberta. *Hydrological Processes*, 23(21), 3040-3056, doi: 10.1002/hyp.7415.

National Resources Conservation Service (NRCS). 2004. *National engineering handbook, Part 630 hydrology*, USDA, Washington, DC.

National Wetlands Working Group. 1988. *Wetlands of Canada. Ecological land classification series, no. 24*. Sustainable Development Branch, Environment Canada, Ottawa, Ontario, and Polyscience Publications Inc., Montreal, Quebec, pp. 452.

Naylor S, Letsinger SL, Ficklin DL, Ellett KM, and Olyphant GA. 2016. A hydrogeological approach to quantifying groundwater recharge in various glacial settings of the mid-continent USA. *Hydrological Processes*, 30(10), pp.1594-1608, doi: 10.1002/hyp.10718.

Niswonger RG, Prudic DE, Regan RS. 2006. Documentation of the unsaturated-zone flow (UZF) package for modeling unsaturated flow between land surface and the water table with MODFLOW-2005. U.S. Geological Survey Techniques and Methods 6-A19. Reston, Virginia: USGS.

Nolan BT, Fienen MN, and Lorenz DL. 2015. A statistical learning framework for groundwater nitrate models of the Central Valley, California, USA. *Journal of Hydrology*, 531, pp.902-911, doi: 10.1016/j.jhydrol.2015.10.025.

NRCS U. 2004. National engineering handbook: Part 630—hydrology. USDA Soil Conservation Service: Washington, DC, USA, pp. 11-5

Nijssen B, Lettenmaier DP. 2002. Water balance dynamics of a boreal forest watershed: White Gull Creek basin, 1994–1996. *Water resources research*. 38(11):37-1, doi: 10.1029/2001WR000699.

Nwaishi F, Petrone RM, Price JS, and Andersen R. 2015. Towards developing a functional-based approach for constructed peatlands evaluation in the Alberta oil sands region, Canada. *Wetlands*, 35(2), 211-225, doi: 10.1007/s13157-014-0623-1.

Parlee BL, Geertsema K, Willier A. 2012. Social-ecological thresholds in a changing boreal landscape: insights from Cree knowledge of the Lesser Slave Lake region of Alberta, Canada. *Ecology and Society*, 17(2): 20, doi: 10.5751/ES-04410-170220.

Paulen RC, Fenton MM, and Pawlowicz JG. 2006. Map 269: Surficial Geology of the Peerless Lake Area, Alberta (NTS 84B). Alberta Geological Survey.

Paulsson O, Widerlund A. 2020. Pit lake oxygen and hydrogen isotopic composition in subarctic Sweden: A comparison to the local meteoric water line. *Applied Geochemistry*, 104611, doi: 10.1016/j.apgeochem.2020.104611.

Pawlowicz JG and Fenton MM. 2002a. Drift thickness of the Peerless Lake map area, NTS 84B. Map 253. Alberta Geological Survey, Edmonton, Alberta, Canada.

Pawlowicz JG and Fenton MM. 2002b. Drift Thickness of Alberta, 1:2,000,000 scale. Map 227. Alberta Geological Survey, Edmonton, Alberta, Canada.

Petermann E, Gibson JJ, Knöller K, Pannier T, Weiß H, Schubert M. 2018. Determination of groundwater discharge rates and water residence time of groundwater-fed lakes by stable isotopes of water (^{18}O , ^2H) and radon (^{222}Rn) mass balances. *Hydrological Processes*, 32(6), 805-816, doi: 10.1002/hyp.11456.

Petrone R, Devito KJ, and Mendoza C. 2016. Utikuma Region Study Area (URSA)—part 2: aspen harvest and recovery study. *The Forestry Chronicle*, 92(1), pp.62-65, doi: 10.5558/tfc2016-018.

Petrone RM, Silins U, and Devito KJ. 2007. Dynamics of evapotranspiration from a riparian pond complex in the Western Boreal Forest, Alberta, Canada. *Hydrological Processes: An International Journal*, 21(11), pp.1391-1401, doi: 10.1002/hyp.6298.

Plach JM, Ferone JM, Gibbons Z, Smerdon BD, Mertens A, Mendoza CA, Petrone R, Devito KJ. 2016. Influence of glacial landform hydrology on phosphorus budgets of shallow lakes on the Boreal Plain, Canada. *Journal of Hydrology*, 535, 191-203, doi: 10.1016/j.jhydrol.2016.01.041.

Pomeroy JW, Parviainen J, Hedstrom N, and Gray DM. 1998. Coupled modelling of forest snow interception and sublimation. *Hydrological processes*, 12(15), pp.2317-2337.

Prancevic JP, and Kirchner JW. 2019. Topographic controls on the extension and retraction of flowing streams. *Geophysical Research Letters*, 46(4), 2084-2092, doi: 10.1029/2018GL081799.

Prepas EE, Burke JM, Whitson IR, Putz G, and Smith DW. 2006. Associations between watershed characteristics, runoff, and stream water quality: hypothesis development for watershed disturbance experiments and modelling in the Forest Watershed and Riparian Disturbance (FORWARD) project. *Journal of Environmental Engineering and Science*, 5(S1), pp.S27-S37, doi: 10.1139/s05-033.

Price AG, Hendrie LK. 1983. Water motion in a deciduous forest during snowmelt. *Journal of Hydrology*. 64(1-4):339-56, doi: 10.1016/0022-1694(83)90076-8.

Price JS, Branfireun BA, Waddington JM, and Devito KJ. 2005. Advances in Canadian wetland hydrology, 1999–2003. *Hydrological Processes*, 19(1), 201-214, doi: 10.1002/hyp.5774.

Price JS, Edwards T, Yi Y, Whittington P. 2009. Physical and isotopic characterization of evaporation from Sphagnum moss. *Journal of Hydrology*, 369, 175-182, doi: 10.1016/j.jhydrol.2009.02.044.

Price JS, McLaren RG, and Rudolph DL. 2010. Landscape restoration after oil sands mining: conceptual design and hydrological modelling for fen reconstruction. *International Journal of Mining, Reclamation and Environment*, 24(2), 109-123, doi: 10.1080/17480930902955724.

Proulx S, Stein J. 1997. Classification of meteorological conditions to assess the potential for concrete frost formation in boreal forest floors. *Canadian Journal of Forest Research*. 27(6):953-8, doi:

Rawls WJ, Brakensiek DL, Saxton KE. 1982. Estimation of soil water properties. *Transactions of the ASAE*. 25(5):1316-20.

Redding TE and Devito K. 2011. Aspect and soil textural controls on snowmelt runoff on forested Boreal Plain hillslopes. *Hydrology Research*, 42(4), pp.250-267, doi: 10.2166/nh.2011.162.

Redding TE and Devito KJ. 2008. Lateral flow thresholds for aspen forested hillslopes on the Western Boreal Plain, Alberta, Canada. *Hydrological Processes*, 22(21), pp.4287-4300, doi: 10.1002/hyp.7038.

Redding TE. 2009. Hydrology of forested hillslopes on the Boreal Plain, Alberta, Canada. PhD Thesis, Department Biological Sciences, University of Alberta. 201 pp.

Reynolds W D. and Elrick DE. 1986. A method for simultaneous in situ measurement in the vadose zone of field-saturated hydraulic conductivity, sorptivity and the conductivity-pressure head relationship. *Groundwater Monitoring and Remediation*, 6(1), 84-95, doi: 10.1111/j.1745-6592.1986.tb01229.x.

Riddell JTF. 2008. Assessment of surface water-groundwater interaction at perched boreal wetlands, north-central Alberta. MSc Thesis, Department of Earth and Atmospheric Sciences, University of Alberta, 106 pp.

Ritchie JT. 1972. Model for predicting evaporation from a row crop with incomplete cover. *Water resources research*, 8(5), pp.1204-1213.

Rodriguez-Iturbe I. 2000. Ecohydrology: A hydrologic perspective of climate-soil-vegetation dynamics. *Water Resources Research*, 36(1), 3-9, doi: 10.1029/1999WR900210.

Rosenberry DO, Lewandowski J, Meinikmann K, Nützmann G. 2015. Groundwater-the disregarded component in lake water and nutrient budgets. Part 1: effects of groundwater on hydrology. *Hydrological Processes*, 29(13), 2895-2921, doi: 10.1002/hyp.10403

Sass GZ, Creed IF, Bayley SE, and Devito KJ. 2007. Understanding variation in trophic status of lakes on the Boreal Plain: A 20 year retrospective using Landsat TM imagery. *Remote Sensing of Environment*, 109(2), 127-141, doi: 10.1016/j.rse.2006.12.010

Schaap MG, Leij FJ, and Van Genuchten MT. 2001. ROSETTA: a computer program for estimating soil hydraulic parameters with hierarchical pedotransfer functions. *Journal of Hydrology*, 251, 163–176, doi: 10.1016/S0022-1694(01)00466-8.

Schaller MF and Fan Y. 2009. River basins as groundwater exporters and importers: Implications for water cycle and climate modeling. *Journal of Geophysical Research: Atmospheres*, 114(D4), doi: 10.1029/2008JD010636.

Schelig B, Tetzlaff D, Nuetzmann G, and Soulsby C. 2017. Groundwater isoscapes in a montane headwater catchment show dominance of well-mixed storage. *Hydrological Processes*, 31(20), 3504-3519, doi: 10.1002/hyp.11271.

Schindler DW. 1998. A dim future for boreal waters and landscapes. *BioScience*, 48(3), 157-164. doi: 10.2307/1313261.

Schuster PF, Reddy MM, LaBaugh JW, Parkhurst RS, Rosenberry DO, Winter TC, Antweiler C, Dean WE. 2003. Characterization of lake water and ground water movement in the littoral zone of Williams Lake, a closed-basin lake in north central Minnesota. *Hydrological Processes*, 17(4), 823-838, doi: 10.1002/hyp.1211.

Shaw RD, Prepas EE. 1990. Groundwater-lake interactions: II. Nearshore seepage patterns and the contribution of ground water to lakes in central Alberta. *Journal of Hydrology*, 119(1-4), 121-136, doi: 10.1016/0022-1694(90)90038-Y.

Shaw RD, Shaw JFH, Fricker H, and Prepas EE. 1990. An integrated approach to quantify groundwater transport of phosphorus to Narrow Lake, Alberta. *Limnology and Oceanography*, 35(4), 870-886, doi: 10.4319/lo.1990.35.4.0870.

Shi X, Pu T, He Y, Qi C, Zhang G, Xia D. 2017. Variability of stable isotope in lake water and its hydrological processes identification in Mt. Yulong region. *Water*, 9(9), 711, doi: 10.3390/w9090711.

Siegel DI, Winter TC. 1980. Hydrologic setting of Williams Lake, Hubbard County, Minnesota (No. 80-403). US Geological Survey, doi: <https://doi.org/10.3133/ofr80403>.

Šimůnek J, Van Genuchten MT, and Šejna M. 2006. The HYDRUS software package for simulating two-and three-dimensional movement of water, heat, and multiple solutes in variably-saturated media. Technical manual, version, 1, p.241.

Slattery SM, Morissette JL, Mack GG, Butterworth EW. 2011. Waterfowl Conservation Planning. *Boreal Birds of North America: A Hemispheric View of Their Conservation Links and Significance*, Published for the Cooper Ornithological Society, 41, 23.

Smail RA, Pruitt AH, Mitchell PD, and Colquhoun JB. 2019. Cumulative deviation from moving mean precipitation as a proxy for groundwater level variation in Wisconsin. *Journal of Hydrology X*, 5, p.100045, doi: 10.1016/j.hydroa.2019.100045.

Smerdon BD. 2007. The influence of climate on water cycling and lake-groundwater interaction in an outwash landscape on the Boreal Plains of Canada. PhD Thesis, Department of Earth and Atmospheric Sciences, University of Alberta, 152 pp.

Smerdon BD, Devito KJ, Mendoza CA. 2005. Interaction of groundwater and shallow lakes on outwash sediments in the sub-humid Boreal Plains of Canada. *Journal of Hydrology*, 314(1-4), 246-262, doi: 10.1016/j.jhydrol.2005.04.001.

Smerdon BD, Mendoza CA, and Devito KJ. 2007. Simulations of fully coupled lake-groundwater exchange in a subhumid climate with an integrated hydrologic model. *Water Resources Research*, 43(1), doi: 10.1029/2006WR005137.

Smerdon BD, Mendoza CA, Devito KJ. 2008. Influence of subhumid climate and water table depth on groundwater recharge in shallow outwash aquifers. *Water Resources Research*, 44(8) W08427, doi: 10.1029/2007WR005950.

Snedden JE. 2013. The root distribution, architecture, transpiration and root sapflow dynamics of mature trembling aspen (*Populus tremuloides*) growing along a hillslope. MSc Thesis, Department of Renewable Resources, University of Alberta, Edmonton, Canada, 103 pp.

Soil Classification Working Group. 1998 The Canadian System of Soil Classification (Third Edition). Ottawa, ON, Agriculture and Agri-Food Canada.

Sophocleous M. 2002. Interactions between groundwater and surface water: the state of the science. *Hydrogeology journal*, 10(1), 52-67, doi: 10.1007/s10040-001-0170-8.

Sprenger M, Tetzlaff D, Tunaley C, Dick J, Soulsby C. 2017. Evaporation fractionation in a peatland drainage network affects stream water isotope composition. *Water Resources Research*, 53(1), 851-866, doi: 10.1002/2016WR019258.

Strong WL and Roi GL. 1983. Rooting depths and successional development of selected boreal forest communities. *Canadian Journal of Forest Research*, 13(4), pp.577-588.

Sun F, Mejia A, and Che Y. 2019. Disentangling the contributions of climate and basin characteristics to water yield across spatial and temporal scales in the Yangtze River Basin: A combined hydrological model and boosted regression approach. *Water Resources Management*, 33(10), pp.3449-3468, doi: 10.1007/s11269-019-02310-y.

Sutton OF and Price JS. 2020. Soil moisture dynamics modelling of a reclaimed upland in the early post-construction period. *Science of the Total Environment*, 718, p.134628, doi: 10.1016/j.scitotenv.2019.134628.

Tammelin M and Kauppila T. 2018. Quaternary landforms and basin morphology control the natural eutrophy of boreal lakes and their sensitivity to anthropogenic forcing. *Frontiers in ecology and evolution*, 6:65, doi: 10.3389/fevo.2018.00065.

Thompson C. 2019. Hydrologic functioning of glacial moraine landscapes within Alberta's Boreal Plains. PhD Thesis, Department of Earth and Atmospheric Sciences, University of Alberta, 159 pp.

Thompson C, Devito KJ, and Mendoza CA. 2018. Hydrologic impact of aspen harvesting within the subhumid Boreal Plains of Alberta. *Hydrological Processes*, 32(26), pp.3924-3937, doi: 10.1002/hyp.13301.

Thompson C, Mendoza CA, Devito KJ, Petrone RM. 2015. Climatic controls on groundwater-surface water interactions within the Boreal Plains of Alberta: Field observations and numerical simulations. *Journal of Hydrology*, 527, 734-746, doi: 10.1016/j.jhydrol.2015.05.027.

Thompson C, Mendoza CA, Devito KJ. 2017. Potential influence of climate change on ecosystems within the Boreal Plains of Alberta. *Hydrological Processes*, 31(11), 2110-2124, doi: 10.1002/hyp.11183.

Thompson DK and Waddington JM. 2008. Sphagnum under pressure: towards an ecohydrological approach to examining Sphagnum productivity. *Ecohydrology*, 1(4), 299-308, doi: 10.1002/eco.31.

Thompson SE, Katul GG, and Porporato A. 2010. Role of microtopography in rainfall-runoff partitioning: An analysis using idealized geometry, *Water Resour. Res.*, 46, W07520, doi: 10.1029/2009WR008835.

Tóth J. 1962. A theory of groundwater motion in small drainage basins in central Alberta, Canada. *Journal of Geophysical Research*, 67(11), 4375-4388, doi: 10.1029/JZ067i011p04375.

Tóth J. 1963. A theoretical analysis of groundwater flow in small drainage basins. *Journal of Geophysical Research*, 68(16), pp.4795-4812.

Tóth J. 1970. A conceptual model of the groundwater regime and the hydrogeologic environment. *Journal of Hydrology*, 10(2), 164-176, doi: 10.1016/0022-1694(70)90186-1.

Tóth J. 1978. Gravity-induced cross-formational flow of formation fluids, red earth region, Alberta, Canada: Analysis, patterns, and evolution. *Water Resources Research*, 14(5), 805-843.

Tóth J. 1999. Groundwater as a geologic agent: an overview of the causes, processes, and manifestations. *Hydrogeology journal*, 7(1), 1-14, doi: 10.1007/s100400050176

Tóth J. 2009. *Gravitational systems of groundwater flow: theory, evaluation, utilization*. Cambridge University Press.

Tóth T, Balog K, Szabó A, Pásztor L, Jobbágy EG, Noretto MD, and Gribovszki Z. 2014. Influence of lowland forests on subsurface salt accumulation in shallow groundwater areas. *AoB Plants*, 6, doi: 10.1093/aobpla/plu054.

Townley LR, Davidson MR. 1988. Definition of a capture zone for shallow water table lakes. *Journal of Hydrology*, 104(1-4), 53-76, doi: 10.1016/0022-1694(88)90157-6.

Turkeltaub T, Kurtzman D, Bel G, and Dahan O. 2015. Examination of groundwater recharge with a calibrated/validated flow model of the deep vadose zone. *Journal of Hydrology*, 522, pp.618-627, doi: 10.1016/j.jhydrol.2015.01.026.

Van Der Velde Y, Lyon SW, and Destouni G. 2013. Data-driven regionalization of river discharges and emergent land cover–evapotranspiration relationships across Sweden. *Journal of Geophysical Research: Atmospheres*, 118(6), 2576-2587, doi: 10.1002/jgrd.50224.

Vogwill R. 1978. *Hydrogeological map of the Lesser Slave Lake Alberta, NTS 83O. Map 119*. Alberta Research Council, Edmonton, Alberta, Canada.

Waddington JM, Morris PJ, Kettridge N, Granath G, Thompson DK, and Moore PA. 2015. Hydrological feedbacks in northern peatlands. *Ecohydrology*, 8(1), 113-127, doi:10.1002/eco.1493.

Wang T, Franz TE and Zlotnik VA. 2015. Controls of soil hydraulic characteristics on modeling groundwater recharge under different climatic conditions. *Journal of Hydrology*, 521, pp.470-481, doi: 10.1016/j.jhydrol.2014.12.040.

Wang T, Zlotnik VA, Šimunek J, and Schaap MG. 2009. Using pedotransfer functions in vadose zone models for estimating groundwater recharge in semiarid regions. *Water Resources Research*, 45(4), doi: 10.1029/2008WR006903.

Wang Y, Hogg EH, Price DT, Edwards J, and Williamson T. 2014. Past and projected future changes in moisture conditions in the Canadian boreal forest. *The Forestry Chronicle*, 90(5), 678-691, doi: 10.5558/tfc2014-134.

Webster KE, Kratz TK, Bowser CJ, Magnuson JJ, Rose WJ. 1996. The influence of landscape position on lake chemical responses to drought in northern Wisconsin. *Limnology and Oceanography*, 41(5), 977-984, doi: 10.4319/lo.1996.41.5.0977.

Winter TC and Rosenberry DO. 1998. Hydrology of prairie pothole wetlands during drought and deluge: a 17-year study of the Cottonwood Lake wetland complex in North Dakota in the perspective of longer term measured and proxy hydrological records. *Climatic Change*, 40(2), 189-209, doi: 10.1023/A:1005448416571.

Winter TC, Rosenberry DO, LaBaugh JW. 2003. Where does the ground water in small watersheds come from? *Groundwater*, 41(7), 989-1000, doi: 10.1111/j.1745-6584.2003.tb02440.x.

Winter TC. 1986. Effect of ground-water recharge on configuration of the water table beneath sand dunes and on seepage in lakes in the sandhills of Nebraska, USA. *Journal of Hydrology*, 86(3-4), 221-237, doi: 10.1016/0022-1694(86)90166-6.

Winter TC. 1999. Relation of streams, lakes, and wetlands to groundwater flow systems. *Hydrogeology Journal*, 7(1), 28-45, doi: 10.1007/s100400050178.

Winter TC. 2001. The concept of hydrologic landscapes 1. *JAWRA Journal of the American Water Resources Association*, 37(2), 335-349, doi: 10.1111/j.1752-1688.2001.tb00973.x.

Winter TC. 2001. The concept of hydrologic landscapes 1. *JAWRA Journal of the American Water Resources Association*, 37(2), 335-349, doi: 10.1111/j.1752-1688.2001.tb00973.x.

Wossenyeleh BK, Verbeiren B, Diels J, and Huysmans M. 2020. Vadose zone lag time effect on groundwater drought in a temperate climate. *Water*, 12(8), p.2123, doi: 10.3390/w12082123.

Wu J, Kutzbach L, Jager D, Wille C, Wilmking M. 2010. Evapotranspiration dynamics in a boreal peatland and its impact on the water and energy balance. *Journal of Geophysical Research: Biogeosciences*. 115(G4). doi: 10.1029/2009JG001075.

Wytrykush C, Vitt D, McKenna G, and Vassov R. 2012. Designing landscapes to support peatland development on soft tailings deposits. *Restoration and Reclamation of Boreal Ecosystems: Attaining Sustainable Development*, 161-178.

Yang Y, Wu Q, Hou Y, Zhang P, Yun H, Jin H, Xu X, Jiang G. 2019. Using stable isotopes to illuminate thermokarst lake hydrology in permafrost regions on the Qinghai-Tibet plateau, China. *Permafrost and Periglacial Processes*, 30(1), 58-71, doi: 10.1002/ppp.1996.

Zuber A. 1983. On the environmental isotope method for determining the water balance components of some lakes. *Journal of Hydrology*, 61(4), 409-427, doi: 10.1016/0022-1694(83)90004-5.

Appendix A⁴

The three-year cumulative departure from the long-term mean precipitation as an appropriate indicator of landscape moisture state

This appendix documents the analysis used to justify the use of the three-year cumulative departure from the long-term mean P (CDM-3) as an indicator of landscape moisture state in Chapter 2. In the following analysis, the shallowest depth to water table (WT) observed at each well was compared against each of four climate indices for that year. A simple linear regression was fit to each WT-climate index pair (See Figure A-1 for examples). The specific indices are: the total precipitation for that hydrologic year (Pann); the two-year cumulative departure from the longterm mean P (CDM-2); the three-year cumulative departure from the long-term mean P (CDM-3); and, the four-year cumulative departure from the long-term mean P (CDM-4). Amongst Pann, CDM-2, CDM-3, and CDM-4, the best performing index, as determined by R^2 values from linear regressions between the climate index and WT positions, for URSA as a whole, was the CDM-3. It was also the best performing index for the CO, HM, and CP HRAs. However, the CDM-4 was the best for the CO-P wells (Table A-1).

⁴ A version of this appendix was published as supplementary material in: Hokanson K.J., Mendoza C.A., Devito K.J. Interactions between regional climate, surficial geology, and topography: Characterizing shallow groundwater systems in subhumid, low-relief landscapes. *Water Resources Research*. 2019; 55(1):284-97. doi: 10.1029/2018WR023934.

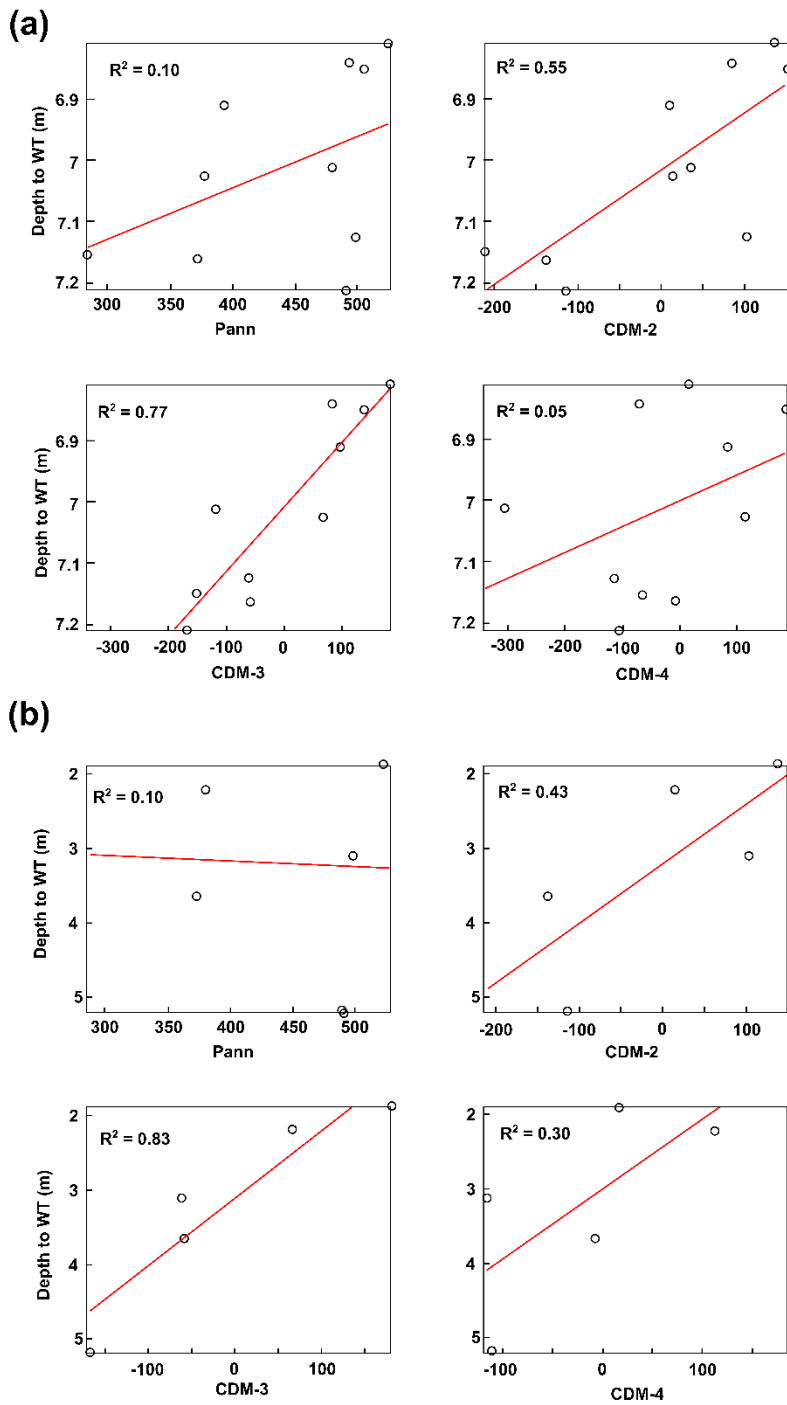


Figure A-1: An example showing the relative correlations between the annual minimum WT position for (a) well 85 in the CO HRA and (b) well 569 in the HM HRA and the total precipitation for that hydrologic year (Pann), the 2 year cumulative departure from the mean (CDM-2), the 3 year cumulative departure from the mean (CDM-3), and the 4 year cumulative departure from the mean (CDM-4). Linear regression R^2 values for each best-fit line are shown in bold above each subplot.

Table A-1: Regression coefficients (R^2) for linear correlations between the shallowest annual WT for each study well vs. climatic indices. Green cells indicate the highest R^2 value for that site.

HRA	Well	Pann	CDM-2	CDM-3	CDM-4
CO	66	0.18	0.37	0.55	0.01
CO	64	-0.08	-0.07	-0.07	-0.07
CO	63	-0.08	-0.08	0.01	0.10
CO	85	0.10	0.55	0.77	0.05
CO	10	0.19	0.77	0.81	0.10
CO	9	0.21	0.45	0.58	-0.07
CO	8	-0.06	0.04	0.14	-0.08
CO	3	-0.05	-0.01	-0.01	0.02
CO-P	73	0.14	0.06	0.16	0.02
CO-P	94	-0.06	-0.13	0.09	-0.14
CO-P	16	-0.06	-0.10	-0.06	0.32
CO-P	15	-0.09	-0.10	-0.10	0.32
CO-P	14	-0.06	-0.05	0.05	0.26
CO-P	13	-0.09	-0.07	-0.02	0.24
CO-P	11	-0.02	-0.08	0.02	-0.05
HM	220	-0.14	0.12	0.32	-0.19
HM	569	-0.33	0.43	0.83	0.30
HM	65	-0.06	0.08	0.37	0.66
HM	20	-0.14	0.10	0.43	-0.07
HM	19	0.63	0.14	0.02	-0.03
HM	17	0.21	0.29	0.25	-0.07
HM	4	0.37	0.62	0.50	-0.01
HM	1	0.07	0.29	0.36	-0.07
CP	32	0.18	0.62	0.70	-0.20
CP	26	0.18	0.27	0.29	-0.06
CP	12	0.44	0.34	0.11	-0.07
CP	7	-0.05	-0.07	0.12	0.02
CP	6	0.01	0.01	-0.06	-0.07
CP	5	0.42	0.67	0.06	0.03

Appendix B⁵

Complementary 1D model

This appendix documents the methodology used to estimate the van Genuchten-Mualem soil hydraulic parameters for the forest floor and upper soil layers in the model presented in Chapter 5. A one-dimensional model was constructed in HYDRUS 1-D (Šimůnek et al., 2008) to simulate measured volumetric water content (VWC) at a soil pit located near the WA well on the study hummock (Figure 5-2). This modelling was performed to assign appropriate van Genuchten-Mualem soil hydraulic parameters for the forest floor and upper soil layers in the 2D model of the primary text. The soil pit was instrumented with five soil water content probes (CSI model 616, Campbell Scientific Inc., Logan, Utah) at the following depths: 0.05 m (LFH - forest floor), 0.2 m, 0.4 m, 0.6 m, 0.95 m. The calibrated van Genuchten-Mualem (VGM) soil hydraulic parameters were then used in the 2D model for the forest floor and soil layers (Figure 5-2, Table 5-1).

The 1D model was constructed to be 10 m deep and discretized into 0.01 m layers, with a constant pressure head lower boundary condition, where $\Psi = 4.2$ m. This translates to a water table ($\Psi=0$) positioned 5.8 m below the soil pit, which was the highest water table elevation during the instrumented period. Soil layer thicknesses, saturated hydraulic conductivity (K), saturated soil water content (θ_s), bulk density, and soil texture (sand and clay %), for the forest floor and soil horizons were explored and quantified by Redding (2009) for this and nearby hummocks. These values were used both as a starting point and to constrain the calibrated VGM parameters. The VGM α and n parameters were initially informed by pedotransfer function values for soils with parameters similar to those reported in Redding (2008) for the forest floor and upper soil layers (ROSETTA; Schaap et al., 2001). The VGM parameters were then calibrated to best simulate the observed VWC for each soil layer corresponding to each sensor depth. The final calibrated suite of VGM parameters yielded simulated VWC that had an R-squared of 0.95 and a root mean square weighted error of 0.0059, when compared to the observed VWC. The model was fairly insensitive to the parameters attributed to the till, therefore they were not optimized in the 1D modelling exercise and were the focus of the calibration of the 2D model in the main manuscript.

The final calibrated VGM parameters for the 1D model can be seen in Table B-1. However, in the subsequent 2D model domain, the soil layers were generalized and are represented by 2 layers, the forest floor (0.1 m thick) and the combined A and B horizons (0.6 m thick).

⁵ A version of this appendix was published in:

Hokanson K.J., Thompson C., Devito K., Mendoza C.A. Hummock-scale controls on groundwater recharge rates and the potential for developing local groundwater flow systems in water-limited environments. *Journal of Hydrology*. 2021; 29 126894.

Table B-1: van Genuchten-Mualem soil hydraulic properties for 1D model

Material	θ_r	θ_s	α (1/m)	n	K (m/d)	Profile depth	Probe depth
						ranges (m)	(m)
Forest Floor	0.06	0.90	13.00	1.90	16.00	0 - 0.1	0.05
Soil 1	0.06	0.53	4.50	1.62	1.27	0.1 - 0.3	0.2
Soil 2	0.15	0.55	0.80	1.37	0.09	0.3 - 0.5	0.4
Soil 3	0.15	0.16	0.23	1.95	0.09	0.5 - 0.7	0.6
Soil 4	0.15	0.45	0.57	1.69	0.01	0.7 - 1.1	0.95
Till	0.19	0.45	0.50	1.11	0.01	1.1 - 10.0	--

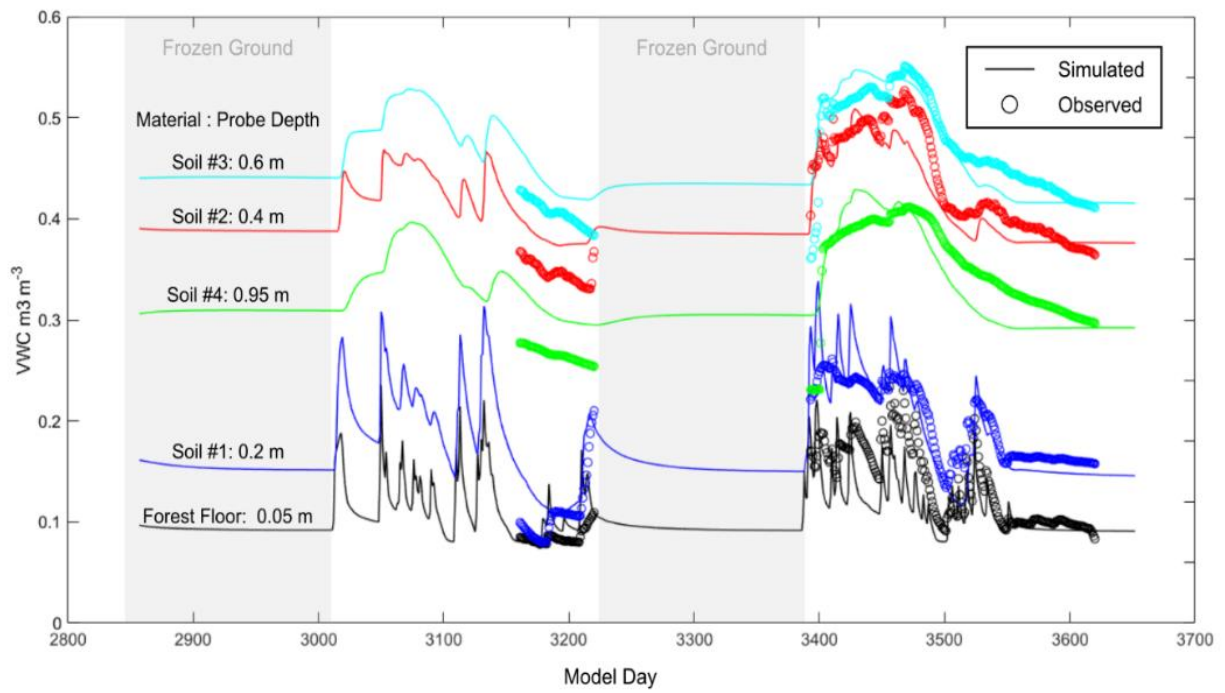


Figure B-1: Observed and simulated volumetric soil water content for the 1D model. Materials and probe depths are annotated on the graph and correspond to the materials and depths in Table B-1.

Appendix C⁶

Sensitivity analysis of 2D model

This appendix documents a sensitivity analysis of the 2D model in Chapter 5. This model serves as a natural outgrowth or continuation of the work conducted by Thompson et al. (2015, 2018), which contains a much more detailed sensitivity analysis and has more emphasis on the role of the peatland and atmospheric fluxes (i.e., ET and P). The scope of this work, however, is focused on the water table position in the mineral hummock. The subsequent sensitivity analysis, therefore, reflects this.

Several model parameters and boundary conditions were considered for the sensitivity analysis: soil thickness above the glacial till, the anisotropy ratio, the van Genuchten α and n parameters of the till, and the peatland water table elevation. The results of this analysis can be seen in Figure C-1. Changing the lower boundary condition, peatland VGM parameters, and the range between saturated and residual water content of the till was found to have minimal impacts on the model results and are therefore not reported here. Changing the soil thickness, the anisotropy ratio, and the till unsaturated flow parameters had disproportionate effects at the upper slope of the hummock (WA), where the vadose zone is thickest, compared to the mid-slope (WB) and toe of slope (WC) regions. However changing the elevation of the fixed water table in the peatland had a stronger effect on the water table position in the lower portions of the hummock and had a negligible effect in the upper slope.

The soil layer, which represents the weathered A and B horizons below the forest floor and above the parent material, has a large control over groundwater recharge (Lukenbach et al., 2019; Naylor et al., 2016). The soil layer acts to hold and retard infiltration from precipitation before it percolates to deeper regions beyond the aspen root zone. When the soil layer is thick (e.g., it extends to 1.0 m below the model surface), groundwater recharge is reduced, thereby reducing and delaying the spring peak in the groundwater mound elevation. Contrastingly, reducing the soil thickness (e.g., it extends to 0.3 m below the model surface) has the opposite effect, where the spring groundwater mound elevation peak is increased by approximately 2.5m and advanced by approximately 20 days. This has been explored thoroughly in both Lukenbach et al. (2019), who found similar results in a reclamation setting.

Anisotropy in the model was adjusted by holding the vertical hydraulic conductivity constant and increasing the horizontal hydraulic conductivity by applying a multiplier. For all scenarios, the forest floor was kept isotropic. As the anisotropy ratio ($K_x:K_z$) increased from the base case (30:1) to 100:1, the groundwater mound elevation decreased and seasonal water table fluctuations were dampened as

⁶ A version of this appendix was published in:

Hokanson K.J., Thompson C., Devito K., Mendoza C.A. Hummock-scale controls on groundwater recharge rates and the potential for developing local groundwater flow systems in water-limited environments. *Journal of Hydrology*. 2021; 29 126894.

the resistance to lateral flow decreased. Conversely, under isotropic conditions (1:1), groundwater mounding was increased and seasonal water table fluctuations were amplified.

There were discrepancies in some years in the form of late season precipitation events. For example, in 2011, 2013 and 2016, it is evident that significant mid and late summer precipitation events caused rises in the water table at WA, however they were not present in the simulated water tables (Figure 4a). This is most likely due to the presence of dual permeability, perhaps in the form of macropore or fracture flow in the till that is not captured in the model. If a high enough K_z value (5×10^{-2} m/d) was used, the late season hydrograph peaks could be seen; however, the overall timing and magnitude of the hydrographs were too early and low, respectively (Figure C-1e). The van Genuchten α and n parameters were therefore calibrated in conjunction with hydraulic conductivity holistically to best represent the system as a whole, again as a means of avoiding over-parameterizing the model so as to increase its applicability elsewhere. The effects of changing the VGM parameters α and n can be shown in Figure C-1d and C-1e. Higher values of α and n parameters result in greater groundwater recharge, and therefore higher water tables (Figure C-1e), consistent with previous findings (Wang et al., 2009).

In the model, the upper boundary condition in the peatland is a specified pressure head (Ψ) of -0.3 m, in other words the water table is fixed at a depth of 0.3 m below the peat surface. For this sensitivity analysis, the water table elevation was increased to be equal to the peat surface ($\Psi = 0$) and decreased to depth of 1 m ($\Psi = -1.0$ m) to show the effects that a high and low water table configuration in the peatland would have on the adjacent hillslope. The change in peatland water table position had negligible effects on the water table behaviour in the upper slope of the hummock; however, areas closer to the peatland had more amplified effects (Figure C-1c). At the toe of the slope (WC), adjacent to the peatland margin, the decrease in peatland water table position caused a corresponding decrease in the fall hillslope water table of approximately 0.3 to 0.4 m. In the mid-slope region, the water tables showed lower positions in the fall, but the spring peaks area similar (within 0.2 m of the base case).

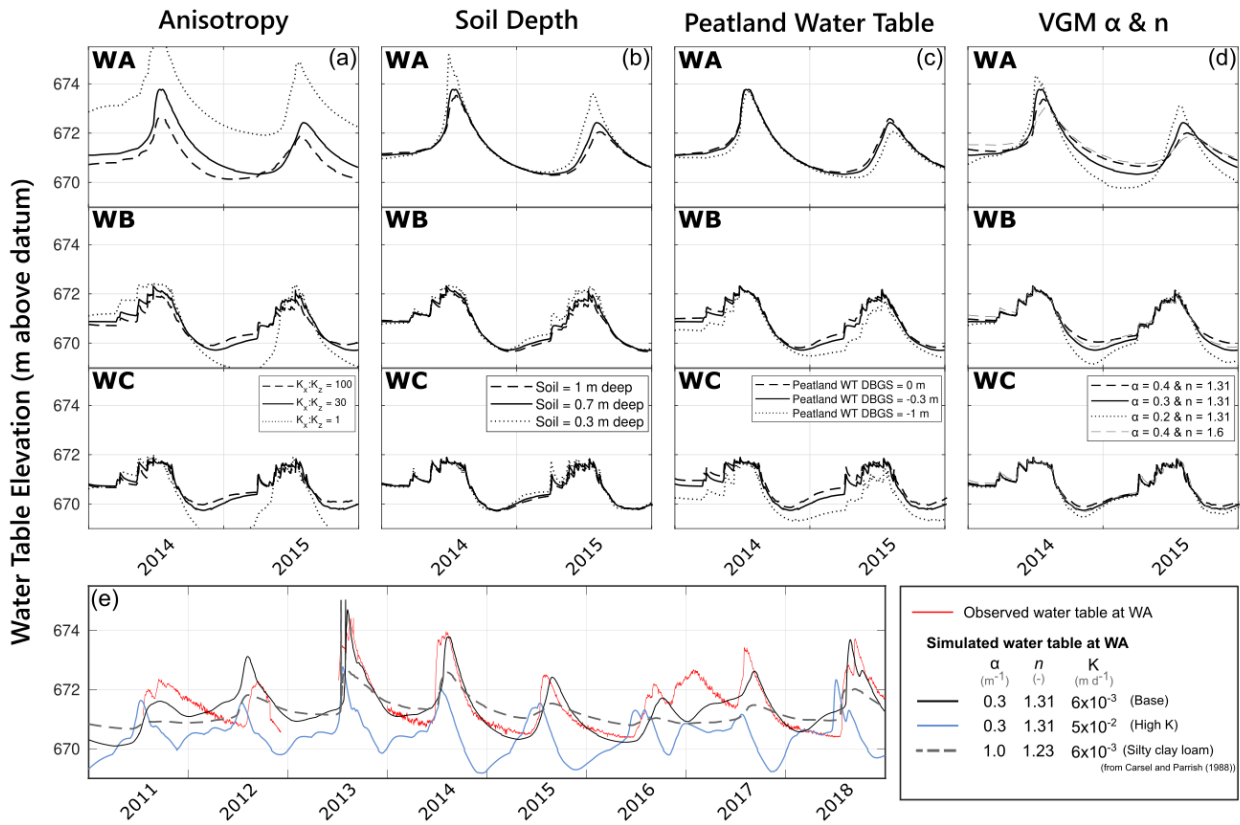


Figure C-1: Results from the sensitivity analysis of major model parameters for the detailed study hummock model showing the effects of (a) anisotropy ratio, (b) soil depth, (c) peatland water table elevation, (d) van Genuchten-Mualem α and n parameters. The lower panel shows the probable dual permeability of the glacial till and the effects of α , n , and K in that context.